# Synthetic strategies towards multivalent lectin ligand mimics

*By*

**Lydia Joanne Kriticos, MSci**

*Being a thesis submitted for the degree of*

**Master of Philosophy**

*To*

The University of East Anglia

School of Pharmacy

Feburary 2017

*Based on research carried out under the supervision of*

Dr Chris J Hamilton

School of Pharmacy, University of East Anglia

# Abstract

Lectins are a class of sugar-binding proteins of interest to pharmaceutical research due to their varied roles in diseases and specific presentation on different tissue types. Compounds that bind strongly to specific lectins may have potential both as drugs and targeting agents. The synthesis of multivalent scaffolds designed as lectin ligand mimics are presented in this work. Two different core scaffolds, calix(4)arene and Trizma base were used along with two sugar ligation strategies, Huisgen-Sharpless cycloaddition (giving *O*-glycosides) and aminooxy based chemoselective ligation (giving *N*-glycosides).

Three *O*-glycosidic tri-substituted ligand mimics using Trizma base as the central scaffold were synthesised using Huisgen-Sharpless cycloaddition. Similarly sized tri-substituted aminooxy Trizma centred scaffolds were synthesised with the intention of comparing the effects of ligation strategy on lectin binding.

Progress was made towards synthesising sugar-substituted calixarenes using both ligation strategies.

# Contents

# List of Illustrations

# Acknowledgements

First and foremost my thanks to Dr Chris Hamilton for his support, guidance and encouragement throughout this project, without which it couldn't have been completed. Thanks also to Dr Lesley Howell for her support, assistance and constructive criticism.

Thank you to Colin Macdonald for all his help with NMR spectra and Rebecca Baldwin for hers with the mass spectrometry equipment. Additionally thanks must go to the EPSRC National Mass Spectrometry Service Centre in Swansea for high resolution mass spectra.

Thanks to my lab colleagues, past and present, firstly to those in Dr Hamilton's group particularly Sunil Sharma, Alex Roberts, Miriam Arbach, Dominic Rodrigues and Emma Gould. Also thanks to members of other labs in which this research was conducted for their patience, assistance and support, Richard Steel, Michael Austin and Sarah Goffin.

Thank you to my friends and family for their encouragement and showing an interest in my work.

Finally thank you to my partner. I couldn't have done it without you.

# 1. Introduction

## 1.1 Lectins and Multivalency

Complex glycolipids and glycoproteins cover the surfaces of mammalian cells, controlling a wide variety of physiological processes via their interaction with and recognition by complementary proteins called lectins.[1] Carbohydrate-lectin interactions mediate a host of processes such as cell adhesion and transport, the inflammatory response, recognition of pathogens and key stages of many diseases, eg attachment of bacterial toxins, bacterial and viral attachment to host cell membranes, and cancer metastasis.

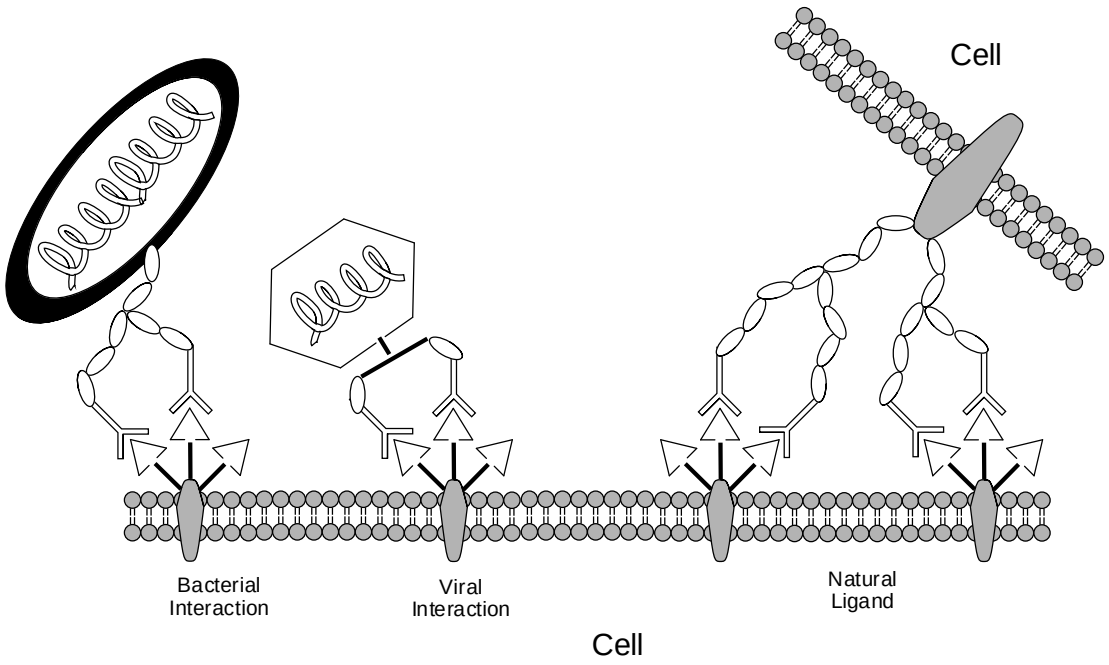


**Figure 1:** Representation of some lectin-carbohydrate interactions at the cell surface, showing first stages of bacterial and viral invasion of cells and cell-cell adhesion. With oligosaccharides represented by triangles shown binding to lectin receptors sites.

Protein-carbohydrate interactions are non-covalent and individual interactions usually display weak binding, with $K_d$ values ranging from mM to μM.[2] Multivalent display, both of the carbohydrate ligand and the carbohydrate recognition domain or

the entire lectin, causes a marked increase in the observed affinity, which is known as the glycoside cluster effect. This increase in affinity is greater than would be expected if it was caused by increased ligand concentration alone. The individual interactions enhance each other via two mechanisms: a chelate effect in which binding sites either on the same or adjacent receptors are crosslinked by multivalent ligands and a statistical effect where the local concentration of the ligand at a binding site is increased by its multivalent presentation.[3] These effects are illustrated in **Figure 2** below.

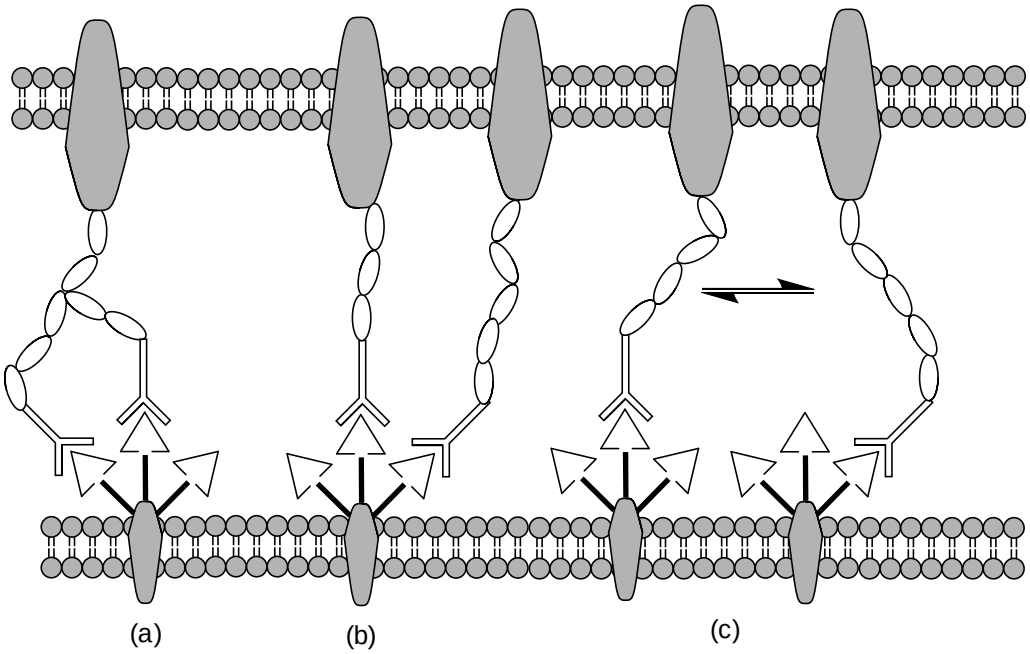


**Figure 2:** Illustration of the glycoside cluster effect, (a) cross linking of carbohydrate ligand by a lectin with multiple binding sites, (b) multiple monovalent lectins cross linked by a carbohydrate ligand, (c) statistical effect whereby array of displayed saccharides provides a higher local concentration of the ligand. With oligosaccharides represented by triangles shown binding to lectin receptors sites.

As multiple ligands and binding sites are often displayed in a repeated fashion across cell surfaces chelation can occur between a single ligand and receptor or across multiple ligands or receptors, as illustrated below. These maxi and mini clustering effects can be seen separately or within the same system.[3]

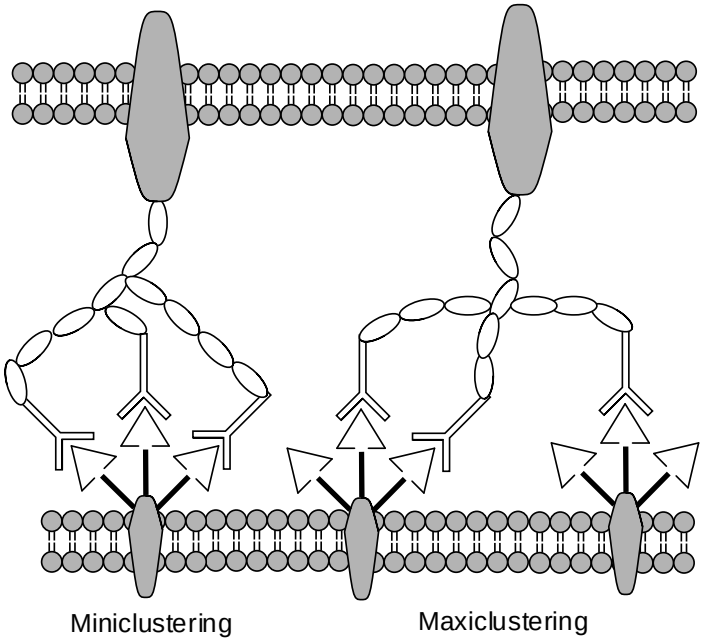


**Figure 3:** Mini and maxi clustering effects, possible forms of chelation between multivalent ligands and receptors. With oligosaccharides represented by triangles shown binding to lectin receptors sites.

These cross linking binding mechanisms are behind the glycoside cluster effect, with the potential for exponential increases in binding affinity in systems that encourage chelation. As a result lectin ligand mimics almost invariably include multiple copies of the recognised saccharide to encourage a greater binding affinity with the target. But simply increasing the number of displayed sugars doesn't always lead to increased affinity, especially in larger ligand mimics.[4] Directly comparing binding results across different scaffolds can also be difficult, differing numbers of sugars and possible cooperative effects (when a binding event effects the likelihood of subsequent binding events, making them either more or less favourable) need to be taken into account.[5] It is now generally accepted that the underlying scaffold has a substantial effect on binding affinity both by influencing the display and presentation of binding residues and by interacting directly with the lectin.[6]

A variety of different synthetic approaches to lectin ligand mimics have been used and developed. Structures based on polymers, proteins, lipids and nanoparticles have all been used with some success but these approaches often result in poorly defined structures, where the exact location and number of sugar residues may be in doubt.[3] In this small molecules, glycoclusters and dendrimers have an advantage: smaller

clusters can usually be characterised by conventional methods while systematic approaches to dendrimer synthesis generally result in well defined and homogenous structures. Groups such as Roy *et al* showcase some of the variety of dendrimers now available using orthogonal building blocks and convergent synthesis.[7]

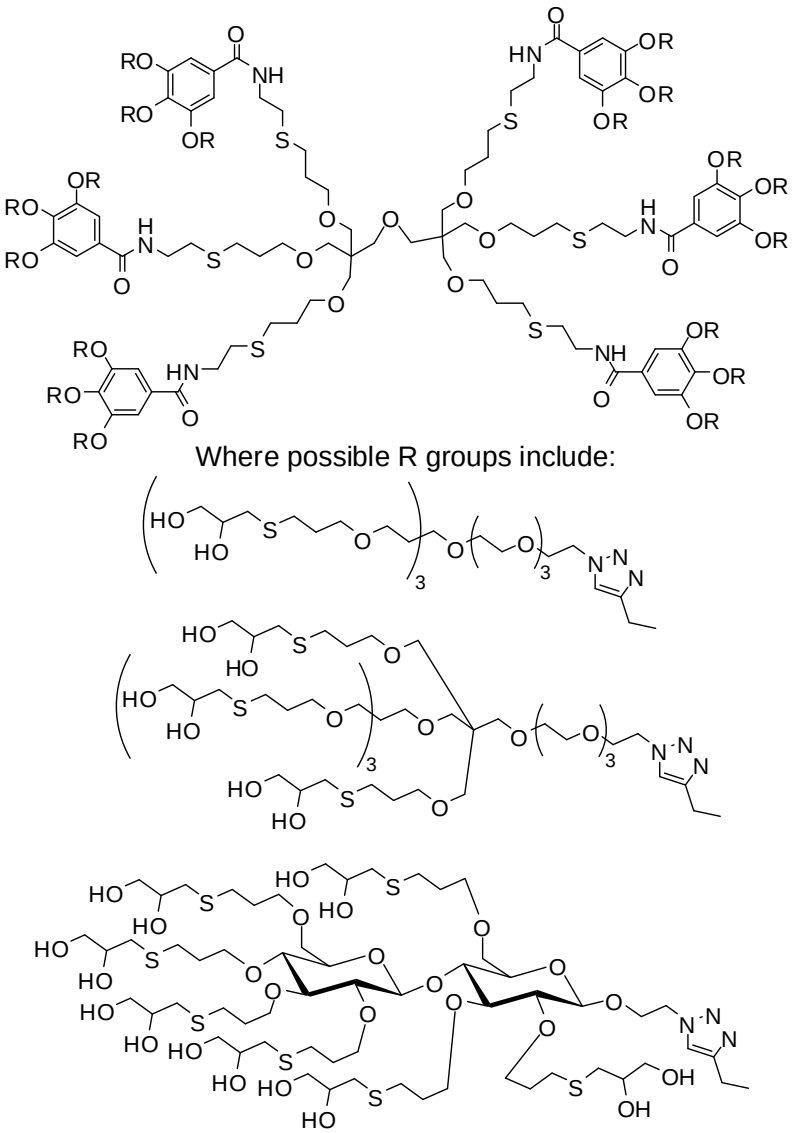


**Figure 4:** Examples of dendrimer structures developed by Roy *et al* using their 'onion peel approach'[7]

In addition to homogeneity and relative ease of characterisation small molecules and glycoclusters may be incorporated into larger glycodendrimers at a later stage as in **Scheme 1.**

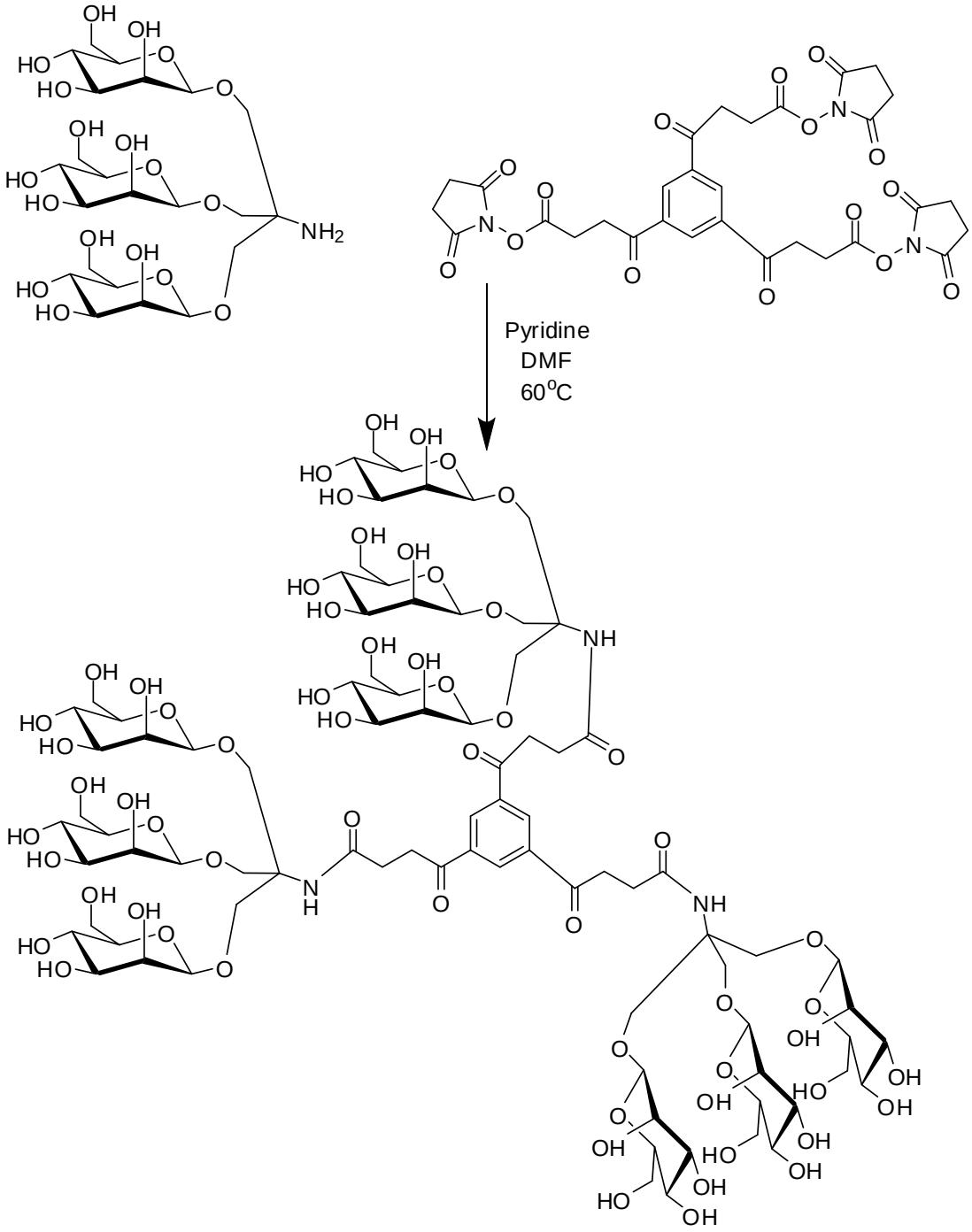


**Scheme 1:** Glycodendrimers can be built up of smaller clusters, as with this dendrimer with peripheral tri-mannosyl Tris clusters.[3]

This project concentrates on producing small glycoclusters based around two different scaffolds giving small molecules with differing topologies and display of monosaccharides. The following sections discuss previous work in the field,

successful lectin ligand mimics based on a variety of scaffolds and a selection of medically relevant lectin targets.

## 1.2 Lectins in Infection

Adherence of lectins on the surface of bacterial cells and viral capsules to carbohydrates on host cell membranes (or vice versa) is the first stage of infection for many diseases, with lectins playing a role in *E. coli*,[8] HIV[9], Ebola virus[10] and *P. aeruginosa* infections.[11]

Additionally several species of bacteria utilise lectins as a way of delivering bacterial toxins to host cells. These include the cholera, *E. coli* heat labile and shiga toxins, all of which have the same basic $AB_5$ structure, where B is a lectin and A is an enzyme responsible for the observed toxicity. The lectin portion binds to specific glycolipids present on the surface of intestinal cells (GM1 in the case of cholera and *E. coli* heat labile toxins, $Gb_3$ in the case of shiga and shiga-like toxins, **Figure 5**). The toxin is then internalised via endocytosis and transported to the endoplasmic reticulum where it is broken down and the toxic subunit A is released into the cytosol.

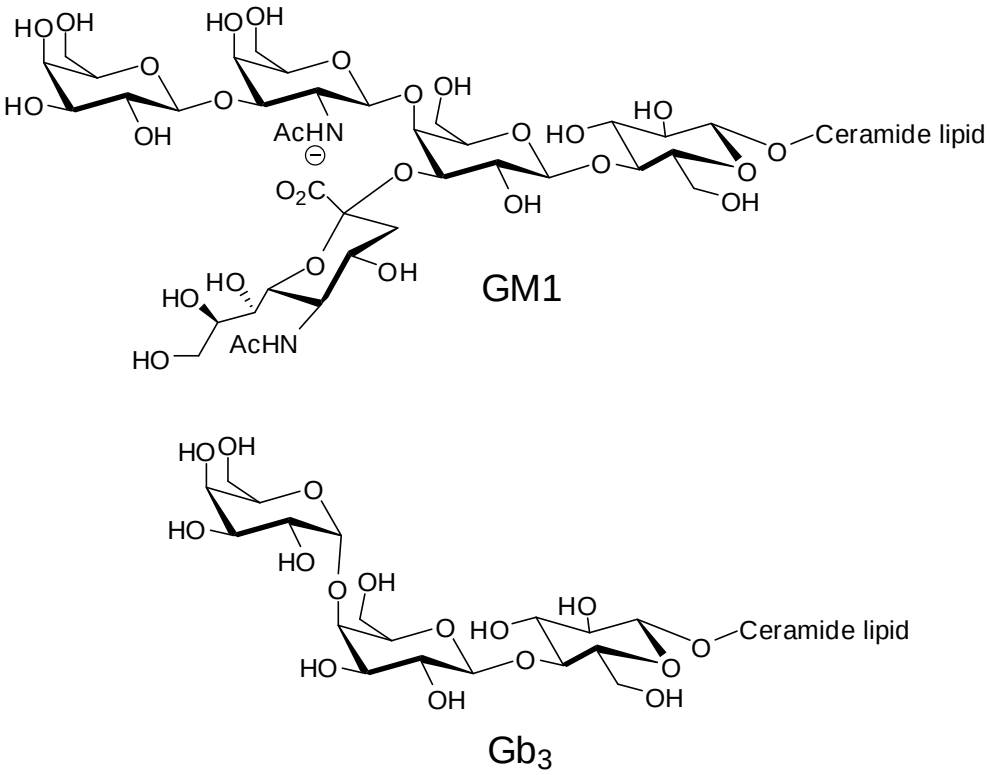





**Figure 5:** Oligosaccharide portions of natural cholera and shiga-like toxin ligands, GM1 and $Gb_3$.

The diarrhoeal diseases caused by these toxins are a serious threat to human health and it has been suggested that suitable ligand mimics could prevent toxins entering host cells, avoiding or reducing serious symptoms. The affinity of monovalent GM1 for cholera and *E. coli* toxins is unusually large for lectin-carbohydrate interactions ($K_d$ = 10-40 nM).[12] Despite this ligand mimics often rely on multivalency due to GM1's complexity and the synthetic difficulty producing the carbohydrate portion. Simplified monovalent galactose based inhibitors that are commonly used are shown below with their dissociation constants.

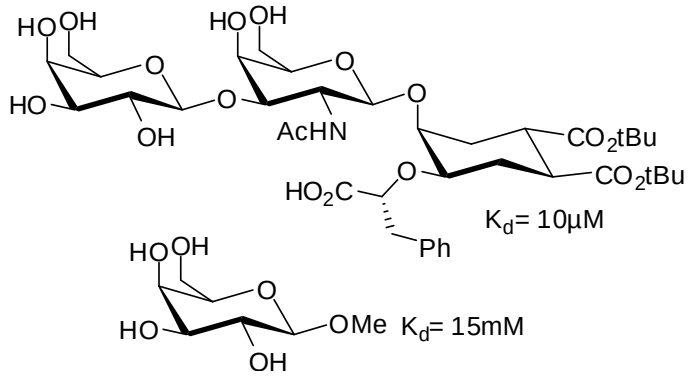


**Figure 6:** Common monovalent ligand mimics for cholera toxin with dissociation constants.[12, 13]

In contrast shiga toxin binds individual $Gb_3$ molecules with a $K_D$ = 1 mM, within the usual range of monovalent lectin-carbohydrate affinities, relying on the glycoside cluster effect to function and bind strongly to cell surfaces. Shiga toxin has 15 binding sites, all capable of simultaneous interaction with $Gb_3$, its binding to whole cells is comparable to cholera toxin.[14]

Several inhibitors of shiga and shiga-like toxins have been produced; the Starfish dendrimer created by Bundle *et al* (**Figure 7**) is a notable example.[15]

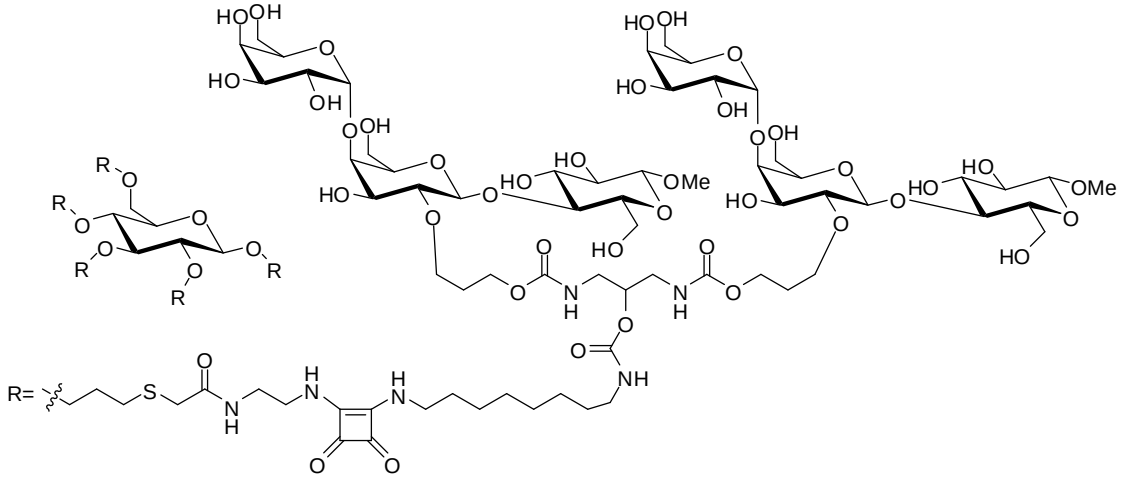


**Figure 7:** Starfish dendrimer, a lectin ligand mimic for shiga-like toxins I and II.[15]

The ligand was designed with reference to the target protein structure: as multiple binding sites are present per B subunit the shiga and shiga-like toxins have a range of inter-binding site distances from ~9 Å (within a B subunit) to ~50 Å (between B

subunits).[16] Branching at the end of each linker unit was intended to allow binding to two sites per B subunit (specifically binding sites 1 and 2 which were thought to be the highest affinity sites[15]), with each linker arm interacting with one of the five B subunits. However crystal structure of the complex revealed that Starfish crosslinks two proteins, one trisaccharide per linker binds a site on one B subunit creating a stable complex.[15]

The Starfish dendrimer showed an impressive 1-10 million fold increase in inhibition over monomeric $Gb_3$ against shiga-like toxins I and II (Stx1 and Stx2).[15] The ligand's $IC_{50,}$ in a solid phase binding-inhibition assay with Stx2 was 6.0 nM, sufficient for Starfish's therapeutic potential to be tested in vivo.[17] Starfish can prevent mouse mortality when co-injected with a lethal dose of Stx1 (at 25 µg/g and 2.5 µg/g Starfish) but despite strong in vitro binding was ineffective against Stx2.[17] Further investigation with radio-labelled toxins showed that Starfish altered the distribution of Stx1 in mouse tissues, substantially reducing toxin accumulation in the main target organs, brain and kidneys.[17] This effect wasn't evident in Stx2 tests.

The group developed a second shiga-like toxin inhibitor, dubbed Daisy (**Figure 8**), with the same glucose core, but extended linker arms and $Gb_3$ attached at the reducing position as it is in the natural ligand.[17]

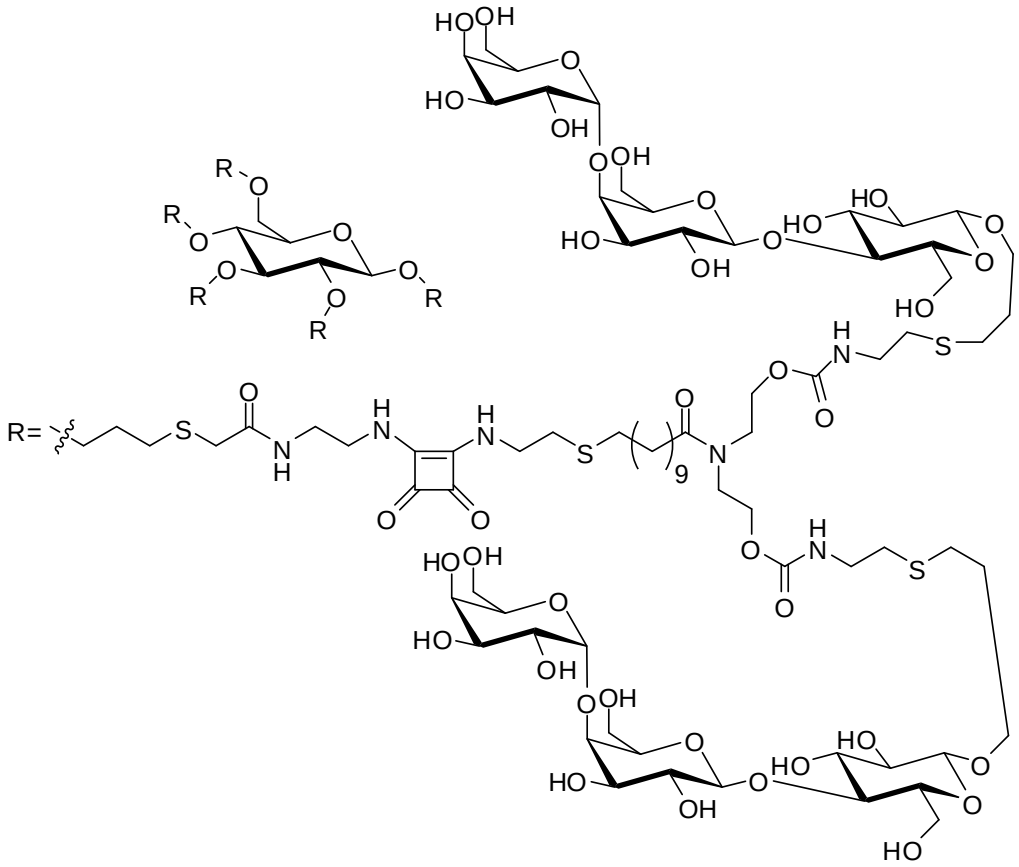

**Figure 8:** Daisy dendrimer, a lectin ligand mimic for shiga-like toxins.[17]

Daisy was developed in an attempt to create a lectin ligand mimic that provided protection against Stx2. The group chose to lengthen the dendrimer linker arms in part because Stx2 has bulkier residues between binding sites 1 and 2 than the Stx1 equivalent, they theorised that longer linkers might encourage binding to both sites.[17]

Initial results were discouraging with Daisy showing a substantial increase in $IC_{50}$ for solid phase Stx2 binding inhibition assays (296 nM compared to 6 nM for Starfish).[17] Daisy also had a higher $IC_{50}$ in Stx2 cytotoxicity assays using Vero cells although the increase was less dramatic than in the solid phase assays (11 µM compared to 1.6 µM for Starfish).[17] Despite this Daisy protected mice from lethal doses of both Stx1 and Stx2 when administered with the toxin, and also increased survival in mice that were orally infected with Stx2 producing *E. coli*.[17]

Other groups have also successfully attempted to target shiga-like toxins. Nishikawa *et al* synthesised a series of carbosilane dendrimers that were also targeting Stx1 and Stx2, the Supertwigs (**Figure 9**).[18]

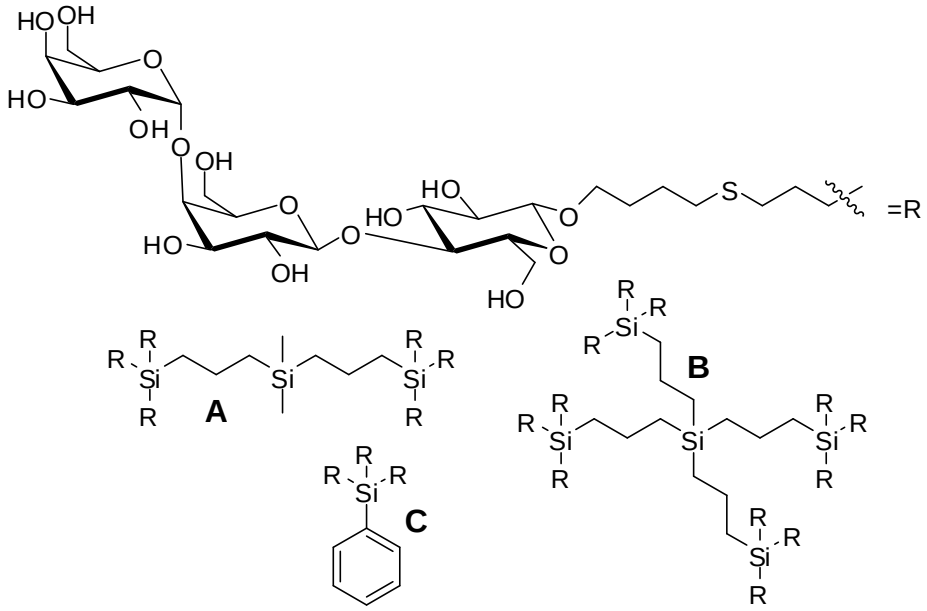


**Figure 9:** Supertwig dendrimers, lectin ligand mimics for shiga-like toxins I and II.[18]

Supertwigs **A** and **B** were designed so that the binding trisaccharides would be ~30 Å from the central silicone in order to access as many binding sites as possible on the toxins. Both showed stronger binding affinity towards immobilised Stx1 then the shorter **C**, ($K_D$ values of 1 µM, 0.2 µM and 22 µM respectively).[18] Binding inhibition assays using Vero cells also showed promising results; Supertwig **A** had an $IC_{50}$ of 0.33 µM against Stx1 and 3.5 µM against Stx2 while Supertwig **B** had $IC_{50}$s of 0.16 µM against Stx2 and 2.0 nM against Stx1.[18, 19] In contrast **C** had an $IC_{50}$ 270 times higher. Cell viability was also tested, none of the Supertwig compounds caused cell mortality but both Supertwigs **A** and **B** inhibited the cytotoxic effect of Stx1 ($IC_{50}$ of 30 nM and 25 nM respectively) and Stx 2 ($IC_{50}$ of 43 nM and 29 nM respectively) in Vero cells.[18] Like Starfish the Supertwig dendrimers were then used in in vivo mouse models.

Rather than testing both toxins Nishikawa *et al* focused on Stx2, due to its greater clinical significance and toxicity. When intravenously administered to mice with a lethal dose of Stx2, Supertwig **C** showed no inhibitory effect, as might be expected since **C** didn't inhibit cytotoxicity in cells. However results for Supertwigs **A** and **B** were markedly different, despite giving similar protection against cytotoxicity in vitro. Supertwig **B** lengthened the average survival time of infected mice to 4 days

(compared to 3 in the control) but failed to counteract the lethal effect of Stx2.[18] Despite being the weaker Stx2 inhibitor Supertwig **A** showed greater therapeutic potential. Mice treated with Supertwig **A** (at 5µg/g) survived over 2 months with no symptoms and the compound was also found to be effective at treating infection by Stx-producing *E. coli*.[18] Intravenous administration of Supertwig **A** to orally infected mice almost abolished mortality, with six of the seven treated mice surviving without neurological symptoms for 40 days, while the entire control group died within 14 days.[18] Further investigation revealed that, similarly to Starfish with Stx1, Supertwig **A** dramatically changed accumulation of labelled Stx2. Treated mice had 3.8 times less toxin in their brains and 1.7 times less toxin in their kidneys than controls, indicating a degree of protection for the toxin's target organs.[18] Follow up investigations using labelled Stx2 in Vero cells suggested that Supertwig **A** triggered uptake and degradation of the Stx2 toxin by cells though the mechanism was unclear. Supertwig **B** showed a similar effect, though much reduced compared to **A**.[18]

The group expanded on their series of dendrimers with a second generation of larger carbosilanes, with 18 and 36 sugar-bearing linkers, shown below (**Figure 10**).[19]

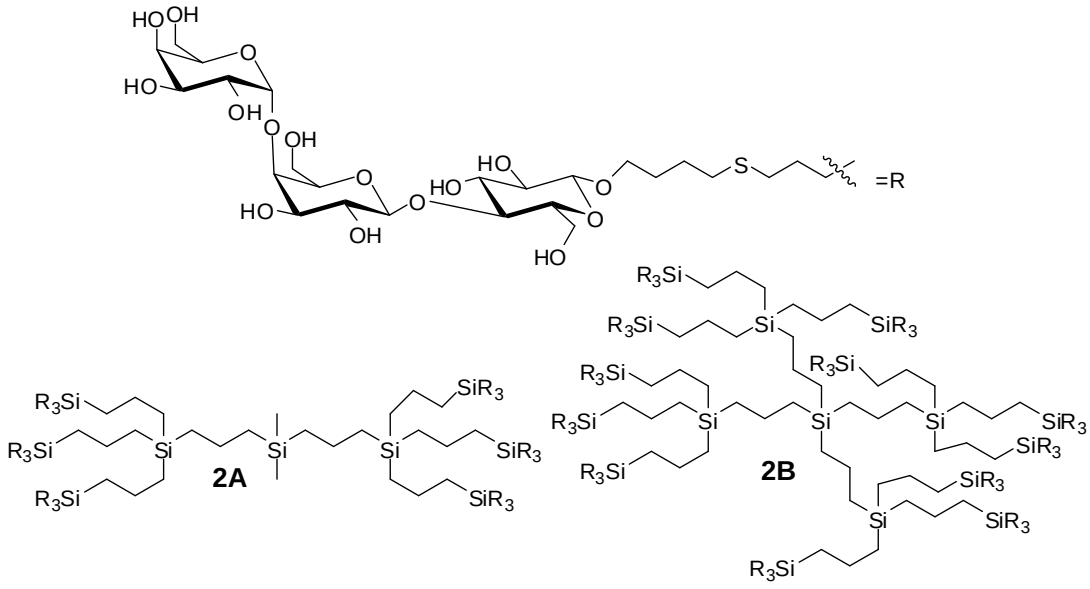


**Figure 10:** Second generation Supertwig dendrimers[19]

Supertwigs **2A** and **2B** showed broadly similar dissociation constants with immobilised shiga-like toxins, 0.45 and 0.2 µM with Stx1 and 0.57 and 0.23 µM

with Stx2. Binding inhibition assays using Vero cells gave identical $IC_{50}$s of 0.21 μM against Stx1 and $IC_{50}$s of 2.1 and 9.5 μM for Stx2 with **2A** and **2B** respectively, values that were not a substantial improvement on first generation Supertwig **A**.[19] Differences between Supertwigs **2A** and **2B** were observed in cytotoxicity assays with **2A** giving lower $IC_{50}$s against both Stx1 and Stx2 (0.18 and 0.26 μM respectively) compared to **2B** (17 and 19 μM respectively).[19]

As with the first generation structures **A** and **B** a dramatic difference was observed between Supertwigs **2A** and **2B** in vivo. When coadministered to mice with a lethal dose of Stx2, Supertwig **2A** prevented mouse mortality, while **2B** only resulted in a slight increase in average survival, with all mice dead within 4 days (control mice died within 3).[19] The group repeated investigations into induced cellular uptake of labelled Stx2, using U937 rather than Vero cells. As previously observed first generation Supertwig **A** triggered uptake of Stx2. Supertwig **2A** also triggered uptake of the toxin, to an even greater extent than the first generation compound, while Supertwig **2B** had a much smaller effect, further supporting the groups' conclusion that induced uptake of the toxin was crucial in protecting mice from Stx2.[19]

Several crucial elements of the structures were identified: the hydrophobic central core Supertwigs **A** and **2A** share, with at least six total trisaccharides, arranged in clusters at each end.[19] This combination of characteristics seemed to be essential for enhancing binding and uptake of shiga-like toxins.

Nishikawa *et al* also attempted to extend their dendrimer series using a simpler, more easily synthesised disaccharide in an attempt to see whether similar binding affinities and biological effects could be obtained with a shorter oligosaccharide (**Figure 11**).[20]

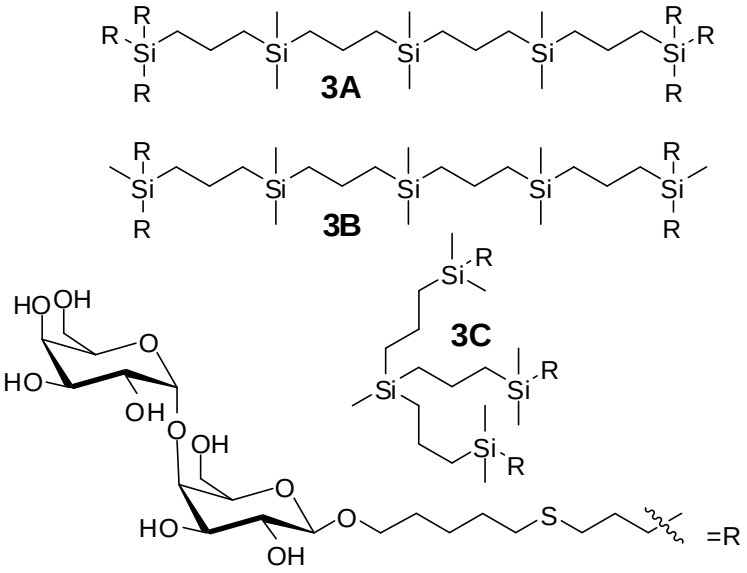


**Figure 11:** Third generation Supertwig dendrimers[20]

Unfortunately the third generation Supertwigs generally showed lower binding when screened against immobilised and labelled shiga-like toxins.[20] Supertwigs **3A** and **3B** had $K_D$s roughly 10 and 50-100 times higher than the first generation Supertwig **A**. Supertwigs **3A** and **3B** were also less effective than Supertwig **A** at inhibiting Stx1 and Stx2 binding to Vero cells.[20] Supertwig **3C** showed broadly similar activity to the less active Supertwig **C**.

While both groups produced ligand mimics with high affinity to isolated lectins these results didn't immediately translate to success in vivo. Starfish, Daisy and the Supertwigs were all effective lectin ligand mimics designed with knowledge of the protein structure, lectin binding sites and the natural ligand. The different series of dendrimers appear to target different binding sites on the toxins, with sites 1 and 2 acting as the main targets for Starfish and Daisy, while for successful Supertwigs **A** and **2A** site 3 was essential.[15, 19] Despite having higher in vitro $IC_{50}$s for shiga-like toxins, Supertwig **A** proved to be more effective than Starfish in vivo. Daisy also had poor in vitro results but showed substantial improvement protecting mice from Stx2. While Supertwig **2A** showed many of the same properties as the first generation Supertwig **A**, but in vivo experiments used a higher dosage (50 µg/g of Supertwig **2A** was required while Supertwig **A** gave the same results with 5 µg/g).[19] Additionally Nishikawa *et al* didn't use Stx1 in any in vivo tests; while both Starfish

and Daisy were screened with both shiga-like toxins the Supertwigs ability to combat Stx1 is unknown.

Although there were some differences in the binding residues used by both groups (trisaccharides in Starfish are not attached via the reducing end) differences in selectivity and in vivo activity seem to be largely due to the underlying scaffold and linkers, controlling the topography and clustering of sugar residues and hence their ability to interact with their target. The work of these two groups highlights both the effectiveness and complexity of targeting therapeutically relevant lectins. Their ability to understand the target and optimise the ligand structures was key to their eventual success.

## 1.3 Galectins

Galectins are a family of lectins recognising β-galactose with a wide variety of functions and expression. Fifteen galectins are known to be expressed in mammals affecting an array of biological processes including the activation and selection of T cells, transport of cell membrane glycolipids and glycoproteins and receptor kinase signalling.[21] They're also known to play a role in cancer metastasis and HIV infection.[9, 22]

The eleven human galectins are classified according to their structures into prototypical, tandem-repeat and chimeric, shown below (**Figure 12**). Prototypical galectins contain one binding domain, with proteins associating to form homodimers. Tandem repeat galectins contain at least two distinct binding domains, linked by a short peptide (5-50 amino acids). Chimeric galectins, only galectin-3 in humans, have a single binding domain and a large amino terminal domain which enables the proteins to aggregate, commonly forming pentamers.[23]

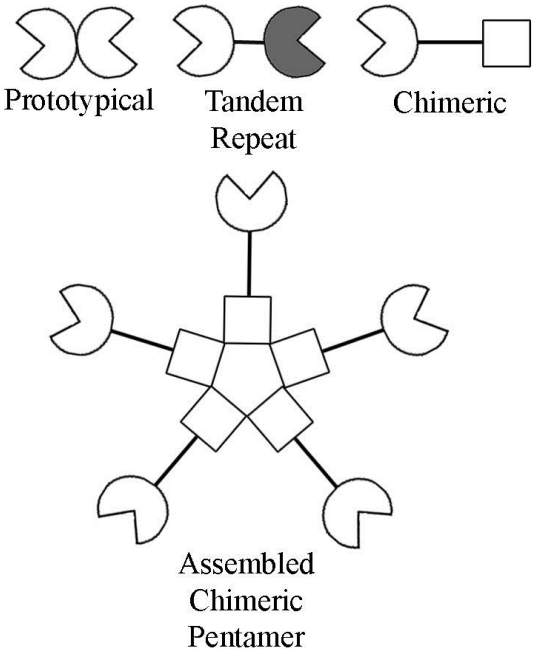


**Figure 12:** Representation of the structures of human galectins. Galectins 1, 2, 7, 10, 13 and 14 are prototypical. Galectins 4, 8, 9 and 12 are tandem repeat. Galectin 3 is the only chimeric galectin in humans.[23]

A variety of lectin ligand mimics targeting galectins have been developed, many of which focus on galectin 1 (Gal-1) and galectin 3 (Gal-3). Both galectins are known to play important roles in cancer progression and the inflammatory response. Gal-1 is thought to reduce inflammatory responses, it can inhibit production of some pro-inflammatory cytokines (such as interferon-γ and interleukin-2) and induce production of anti-inflammatory cytokines (interleukin-10, interleukin-5 and transforming growth factor-β).[23] In contrast Gal-3 can inhibit production of interleukin-5 in some cells and activate mast cells and neutrophils (both of which can be involved in inflammation).[23]

In addition to being upregulated in many cancers Gal-3 can promote metastasis by binding to cadherins, transmembrane proteins responsible for cell-cell adhesion. By binding to N-glycans on these proteins Gal-3 reduces homotypic adhesion, causing tumour cells to detach and promoting metastasis.[21] High serum levels of Gal-3 have been linked to higher instances of metastasis in cancer patients.[22] Gal-1 has been shown to contribute to tumour cell survival and experiments with knockout cells showed it to be essential for angiogenesis.[23] Natural ligands for Gal-1 and Gal-3

have also been linked to poor cancer prognosis. High serum levels of LGalS3BP, a glycoprotein ligand for both galectins which is known to be capable of bridging galectins on tumour cell surfaces, has been linked to metastasis.[22] As a result Gal-1 and Gal-3 have been suggested as possible therapeutic targets in a range of conditions, with several groups aiming to create selective inhibitors of one or both of these galectins.[22, 24]

Pieters *et al* produced several effective monovalent ligand mimics for Gal-1 and Gal-3, such as those shown in **Figure 13**.

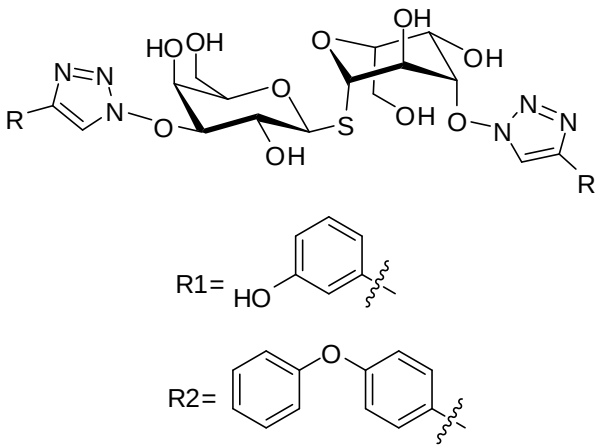


**Figure 13:** Thiodigalactoside derivative, ligand mimics for Gal-1 and Gal-3. R2 shows a preference for Gal-3.[24]

The monovalent compound R1 above was developed by Pieters *et al* in an attempt to create a ligand specific for Gal-3, showing impressive affinity for both Gal-1 and Gal-3 ($K_D$s of 0.013 and 0.022 μM respectively, determined using fluorescence polarisation assay).[24] While this was the best overall binding affinity for both galectins the group did achieve better specificity with related compound R2. R2 showed a markedly greater affinity for Gal-3 than Gal-1, with $K_D$s of 0.36 and 84 μM respectively.[24] All the compounds produced by Pieters *et al* for this study were monovalent and (as discussed in previous sections) multivalent display of binding sugars can result in considerable enhancements in binding affinity and specificity.[3]

Aiming to produce effective inhibitors using systematic synthetic modifications Yao *et al* created a series of simple structurally diverse glycoclusters as Gal-3 ligand

mimics. Using small generic scaffolds and C-lactose as the binding moiety, they synthesised mono, di, tri and tetra valent glycoclusters with a variety of linker lengths and topologies. Surface plasmon resonance (SPR) was then used to determine $K_D$ values with Gal-3. The group used lactose as a comparison, and measured its $K_D$ as 342 µM, the monovalent compounds produced had significantly higher $K_D$s (most could not be measured accurately) which the group suggested was due to the lack of an anomeric oxygen.[25] The divalent examples are shown (**Figure 14**).

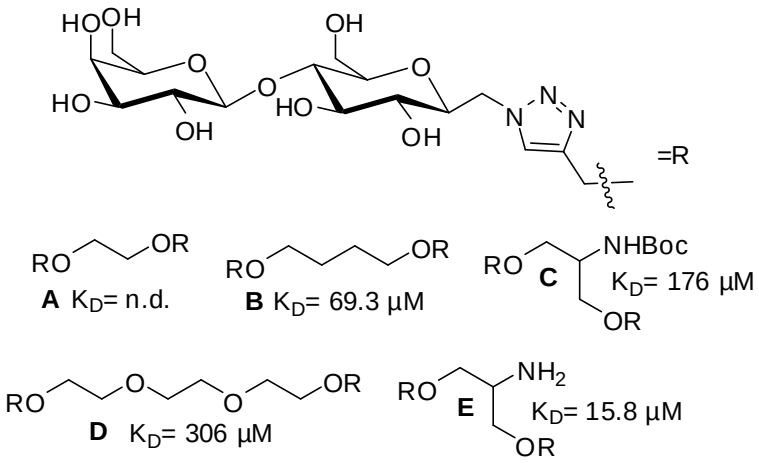


**Figure 14:** A selection of divalent Gal-3 ligands with $K_D$ values.[25]

The divalent compounds gave a wide range of binding affinities, even when the scaffold backbones are similar lengths. The higher affinity of compound **E,** compared to **C** and **B** which have similarly spaced sugar groups, could be due to favourable interactions between the scaffold free amine and the lectin but further investigation into the binding mode of these compounds wasn't carried out. A large range of $K_D$s was also seen for the trivalent compounds (**Figure 15**).

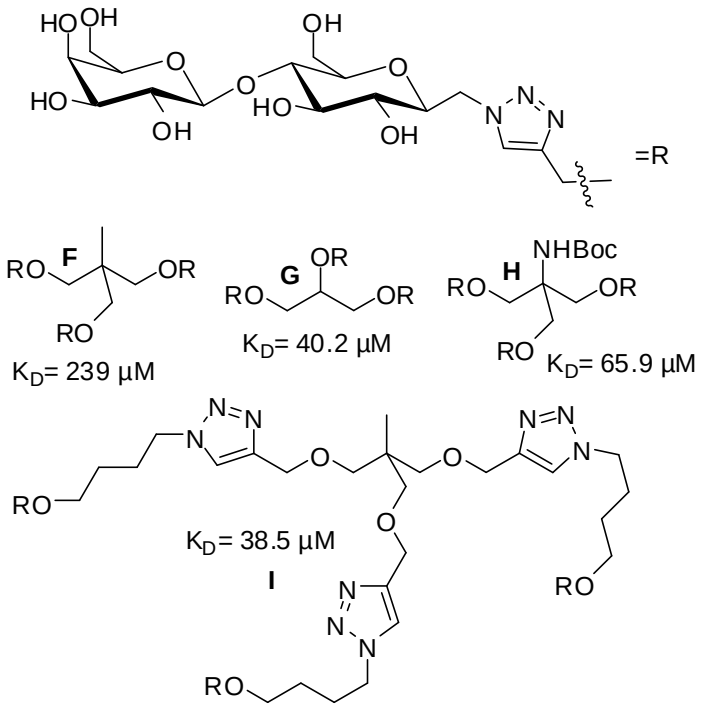


**Figure 15:** Trivalent Gal-3 ligands with $K_D$ values shown.[25]

Although compounds **F**, **G** and **H** are structurally similar they showed significant differences in $K_D$ values and while **G** and **I** have very different structures and spacing between sugar groups their $K_D$s were similar.

Without further study (for example using xray crystallography or computational modelling) the precise cause of these differences in affinity is unclear. None of the compounds produced showed particularly impressive binding affinities, with $K_D$s ranging from 1970-15.8 µM.[25] But the study neatly demonstrates how much the underlying scaffold, linkers and display of sugar residues effects interaction with lectins.

While Yao *et al*'s choice to use simpler sugar units made the synthesis of their library quicker and easier than it would have been with a more complex glycoside it also resulted in less potent products despite the glycoside cluster effect. Their ligation strategy (Huisgen-Sharpless cycloaddition) also allows attachment of more complex saccharides. The potential to vary and improve the inhibitors was considered when the synthesis was planned, results from the C-lactosyl substituted

scaffolds could be used to identify the most effective display of saccharides, concentrating later synthetic efforts.

## 1.4 Ficolins

Several classes of lectins are involved in activating the complement system as part of innate immunity; the three human ficolins are one of them. Ficolins and mannose binding lectin (MBL) both activate the complement system via the lectin pathway. The lectins act as pattern recognition molecules triggering the activation of MASPs (mannose binding lectin associated serum proteases). A lectin-MASP complex binds to carbohydrates on pathogens, which allows MASP-2 to convert into an active form. Activated MASP-2 then cleaves C4 and C2 (similarly to activated C1s in the classical pathway) eventually forming C4b2a which cleaves C3. The fragment C3b then triggers formation of a membrane attack complex, forming a hole in the target membrane.[26] MBL and ficolins play an essential role in innate immunity by activating the complement system in this way.

Ficolins are GlcNAc binding oligomeric lectins made up of fibrinogen-like and collegen-like domains.[27] The human ficolins (L, M and H) are made of several units arranged in a 'bouquet-like' structure, with each unit formed of a trimer.

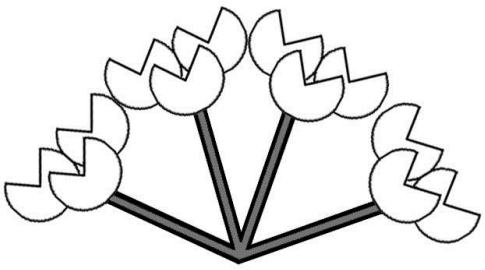

**Figure 16:** Bouquet-like 12-mer structure typical of ficolin-L.[27]

The triple helix collagen-like stalk domains form disulfide crosslinkages which allow assembly of the oligomers, and also contain the binding site for MASPs essential for triggering the lectin complement cascade.[28] The globular fibrinogen-like domains contain multiple binding sites which are repeated structures in ficolins H and M, while ficolin-L has three distinct binding sites per subunit.[28]

Binding is centred on the acetyl group but most ficolins and all human ficolins show a preference for GlcNAc with ficolin-L showing a $K_D$ of 2.3 nM (measured by surface plasmon resonance using immobilised GlcNAc on bovine serum albumin).[27] While GlcNAc is their main ligand human ficolins are promiscuous, recognising a variety of acetylated ligands summarised in **Table 1** below.

| Ficolin | Known Ligands | Known Functions | Protein Expression |
|---|---|---|---|
| L | GlcNAc, galactose, β (1-3) D-glucans,[28] lipoteichoic acid,[27] DNA[29] | Opsonin and complement activation | Serum and plasma |
| M | GlcNAc, GalNAc, sialic acid[28] | Complement activation and phagocytic receptor | Plasma, monocytes, alveolar epithelial cells, neutrophils |
| H | GlcNAc, GalNAc, acetylsalicylic acid,[30] fucose,[28] polysaccharide preparations from *S. typhimurium,*[30] *E. coli,*[31] *A. viridans.*[30] | Opsonin and complement activation | Serum, plasma, bronchus, alveolus, bile duct |

**Table 1:** Human ficolin ligands and functions

As they were discovered fairly recently (1996) the full scope of ficolin activity isn't known.[32] Ficolin-L is known to bind several capsulated bacteria (including *Salmonella typhimurium, E. coli, Staphylococcus aureus* and *Staphylococcus pneumoniae*) and activate the lectin pathway in response to binding.[26, 33] Ficolin-L can bind to influenza A virus, inhibiting infection in vitro and in mouse models, possibly by binding to hemagglutinin and neuraminidase, viral glycoproteins common on influenza strains.[34] It can also interact with hepatitis C virus, binding glycoproteins E1 and E2 and activating the lectin pathway pf complement.[35] Binding

to a saprophytic mould responsible for fungal infections (*Aspergillus fumigatus*, live and fixed conidia) has also been demonstrated.[36] Ficolin-H binds *Aerococcus viridans* cells and influenza A virus strains inhibiting viral infectivity in vitro.[37, 38] Ficolin-M has been shown to bind *S. aureus* and some *S. typhimurium* strains but it has also known to bind Ebola virus glycoproteins with high affinity, enhancing Ebola infection.[39, 40]

Despite the potential therapeutic benefits to date there have been no attempts to use glycodendrimers to target ficolins.

## 1.5 Proposed Lectin Ligand Mimics

This project focuses on the synthesis of small glycoclusters intended to be lectin ligand mimics. Three monosaccharides were chosen, galactose and GlcNAc as they could potentially be used to target therapeutically relevant lectins (such as human galectins and ficolins) and glucose as a negative control. As the small selection of lectin ligand mimics discussed shows a wide variety of scaffolds, linkers and ligation strategies have been successfully employed in the past. Two core scaffolds and two ligation strategies were chosen as the synthetic focus: tris(hydroxylmethyl)aminomethane (Tris) and calix(4)arene cores with Huisgen-Sharpless azide-alkyne cycloaddition and secondary aminnoxy ligation.

By utilising two concurrent ligation strategies (aminooxy ligation and azide-alkyne cycloaddition, both of which are discussed further in subsequent chapters) it was hoped that some of the synthetic challenges associated with saccharides, such as complex protecting group strategies, low yields and long synthetic routes, could be circumvented. The planned synthetic routes, especially in Tris scaffolds, allow for systematic variation of the eventual structure. Varying the length and flexibility of linker arms would permit the scaffolds to be tailored to individual lectins, giving a synthetically straightforward starting point for development of high affinity ligands.

Proposed structures are for both scaffolds and ligation methods are shown below (**Figure 17-18**), tri valent Tris compounds and di valent calixarenes were chosen for synthetic expediency.

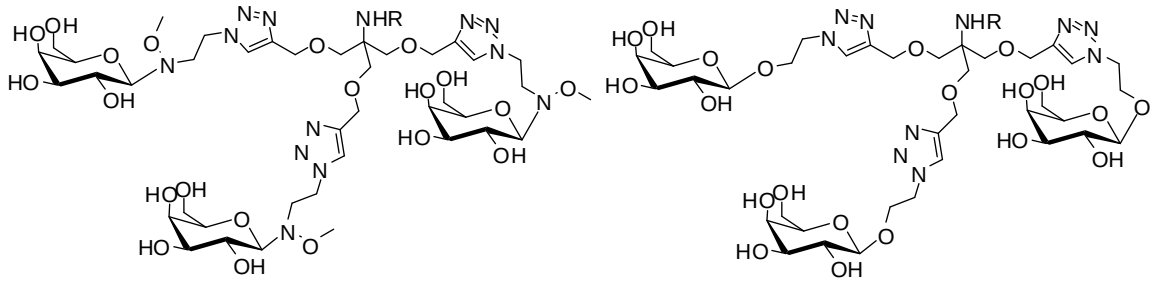

**Figure 17:** Proposed glycoclusters with central Tris scaffold, secondary aminooxy ligation of galactose is shown on the left and Husigen-Sharpless cycloaddition on the right. R is any suitable chromophore or fluorophore.

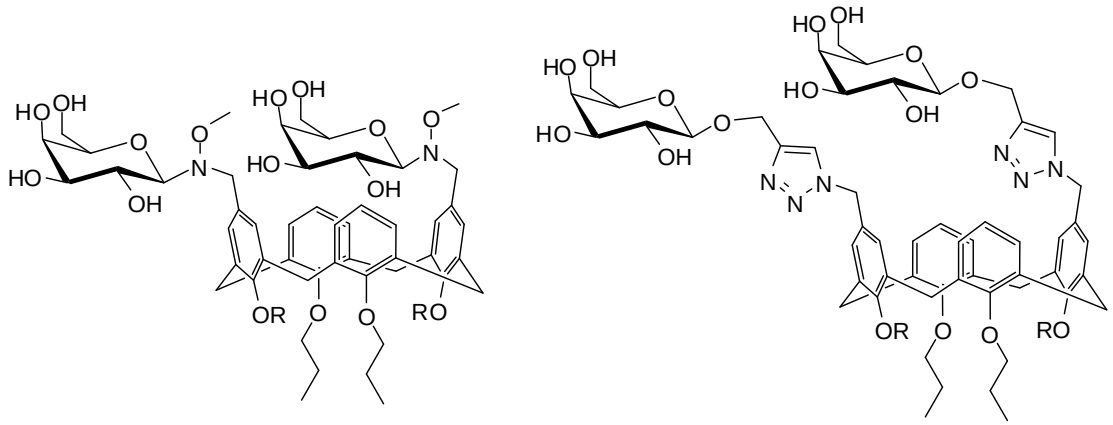

**Figure 18:** Proposed glycoclusters with central calix(4)arene scaffold, secondary aminooxy ligation of galactose is shown on the left and Husigen-Sharpless cycloaddition on the right. R is any suitable chromophore or fluorophore and a suitable linker.

The following chapters detail synthetic routes aimed at producing lectin ligand mimics bearing fluorophores or chromophores.

# 2. Synthesis of Tris based glycodendrimers

## 2.1 An overview of Trizma

Trizma base (Tris) is a well known and widely used biological buffer with an effective buffering range of pH 7-9. The compound is readily available, cheap and known to be non-toxic. Its structure, shown in **Figure 19,** is simple and flexible with easily distinguished functional handles. This combination of properties makes it an attractive starting point for biological scaffolds especially when the precise structure of the target binding site is unknown.

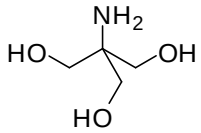


**Figure 19:** Molecular structure of Trizma buffer

If the primary amine is first protected a wide variety of structures can be coupled to the available alcohols allowing the construction of moderately sized scaffolds or clusters displaying one type of moiety at the alcohols and another at the amine.[41, 42] The choice of lectins as a target and their improved binding to multiple carbohydrate groups makes the alcohols the obvious choice for attachment of these sugar residues. This would leave the amine available for attachment of fluorophores or chromophores resulting in small probes, which could be easily varied via relatively short and straight forward synthesis. An example of the type of structure proposed is illustrated below in **Figure 20**.

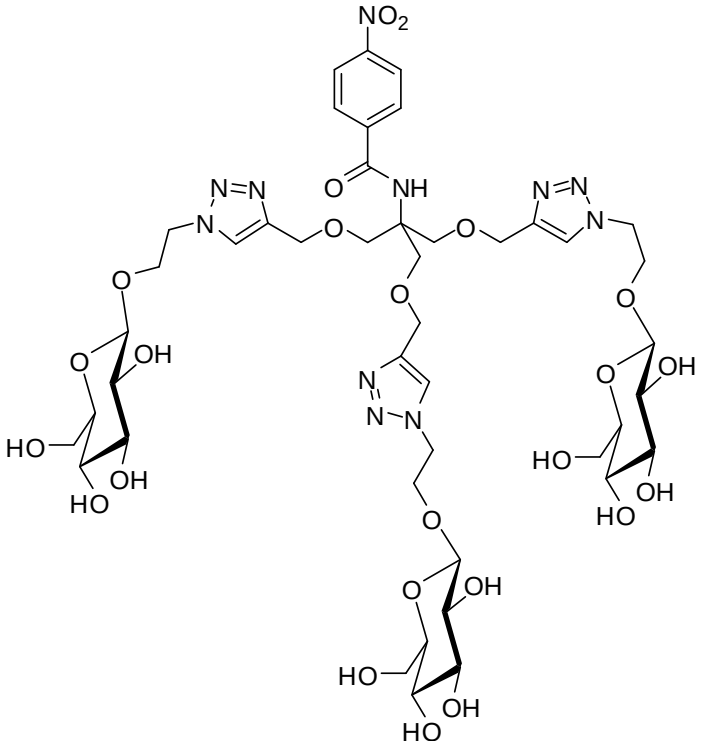


**Figure 20:** A proposed structure for a Tris based lectin ligand mimic and probe. Made up of a central Tris core, simple chromophore coupled to the amine and linkers bearing terminal sugar residues coupled to the alcohols.

By utilising linkers to attach the desired carbohydrate residues the properties of the scaffold can be fine-tuned to a far greater extent before any sugars are introduced. This reduces the number of synthetic steps carried out on the carbohydrate, an important consideration when simple di and tri saccharides are often expensive or difficult to synthesise, reducing the loss of precious material. Such an approach would also increase the variety of the ligand mimics. Control of linker functionality could be used to adjust the solubility of the scaffold. Introducing branching to the linkers also allows alteration of the number and arrangement of displayed sugar groups while adjusting the length and flexibility sufficiently can dramatically alter interaction with lectins.[43, 44, 45]

Our synthetic route was intended to allow linkers to be changed and adjusted as necessary, to improve a scaffold's interaction with specific targets or physical properties. It seemed reasonable to use a flexible core and linkers as a starting point. Binding to a specific target might be improved by adjusting the linkers to change the length, flexibility or number of sugars displayed on a Tris core. Linkers coupled to

the Tris alcohols can be varied easily, allowing straightforward investigation of these effects.

Direct attachment of galactose to the Tris alcohols (illustrated in **Figure 21**) was previously performed by Biessen *et al*, as part of a series of Tris-based ligands aimed at targeting the hepatic asialoglycoprotein receptor, a liver cell-surface lectin.[46]

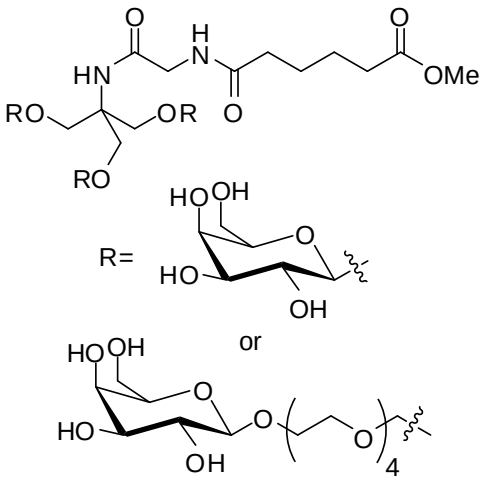


**Figure 21:** An example of a Tris based scaffold with galactose directly coupled to alcohol groups (Ki = 390 μM) and a Tris based scaffold with galactose attached using a polyethylene glycol linker (Ki = 0.2 μM).[46]

The compound shown above (**Figure 21**) with galactose directly attached to the Tris scaffold was a poor binder and could not displace the chosen control, indicating a Ki greater than 390 μM.[46] For comparison the best binder in the series (with galactose attached via a flexible polyethylene glycol linker) had a Ki of 0.2 μM, providing another example of the importance of linker length and the display of binding sugars in creating a successful ligand. Yields varied throughout the series from 67-24%, direct attachment of galactose to the Tris scaffold was low yielding (36%).[46] The combination of low yield and poor binding in previous studies made it seem likely direct attachment of sugars to Tris was not worth pursuing.

A small Tris based cluster, similar to our intended targets, has been made previously as part of a series by Yao *et al* aimed at producing galectin-3 ligands (**Figure 22**).[25]

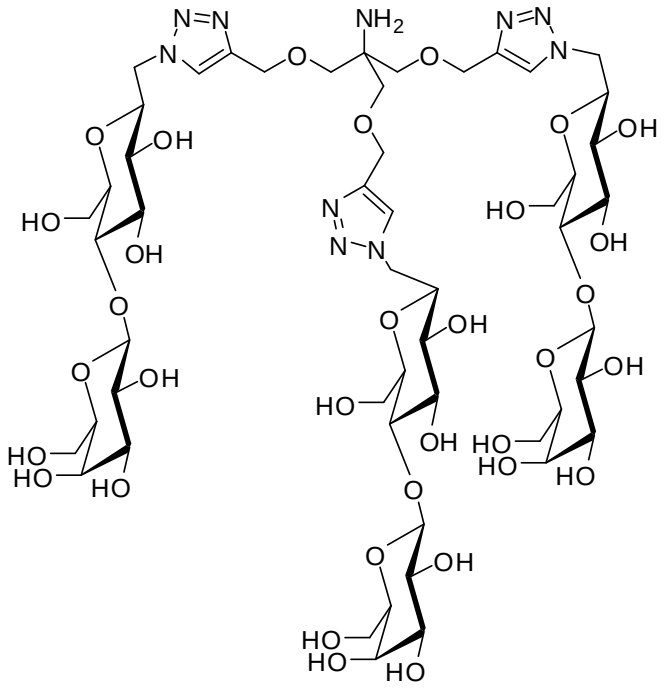

**Figure 22:** Tris based C-lactosyl glycocluster produced by Yao *et al*.[25]

Designed by Yao *et al* as part of a series of small, flexible click-coupled compounds, it showed reasonable binding affinity towards galectin-3, with a $K_D$ of 65.9μM which compared favourably with the other tri-glycosylated compounds tested ($K_D$s ranged from 239 to 38.5 μM).[25]

The choice of click chemistry allowed a series of 16 scaffolds to be created in a relatively straight forward manner: an azide appended C-lactosyl derivative was synthesised and reacted with small, propargyl containing molecules. The group also took advantage of click chemistry to extend the linkers on one of their core scaffolds, improving the $K_D$ considerably (from 239 μM on the original scaffold to 38.5 μM with extended linkers).[25] While their use of click chemistry allowed simple production and refinement of the small clusters investigated removing the anomeric oxygen from the binding residues has potential disadvantages. The anomeric oxygen can be essential for recognition: removing it may reduce enzymatic degradation of the scaffolds but it may also hinder lectin binding. We chose to use azido-sugar derivatives with the anomeric oxygen intact.

Tris has also been used to build up glycodendrimers, often either as a branching unit close to the core or as a glycocluster controlling display of sugar units at the periphery.[3, 45, 47, 48]

A 2002 review by Turnbull *et al* provides multiple examples of glycodendrimers using Tris based glycoclusters as their peripheral layer.[3] A prominent example is a series of dendrimers synthesised by Ashton *et al*, using a trisubstituted Tris glycocluster to build up 9-, 18- and 36-mer dendrimers, the 9-mer is shown below (**Figure 23**).[49]

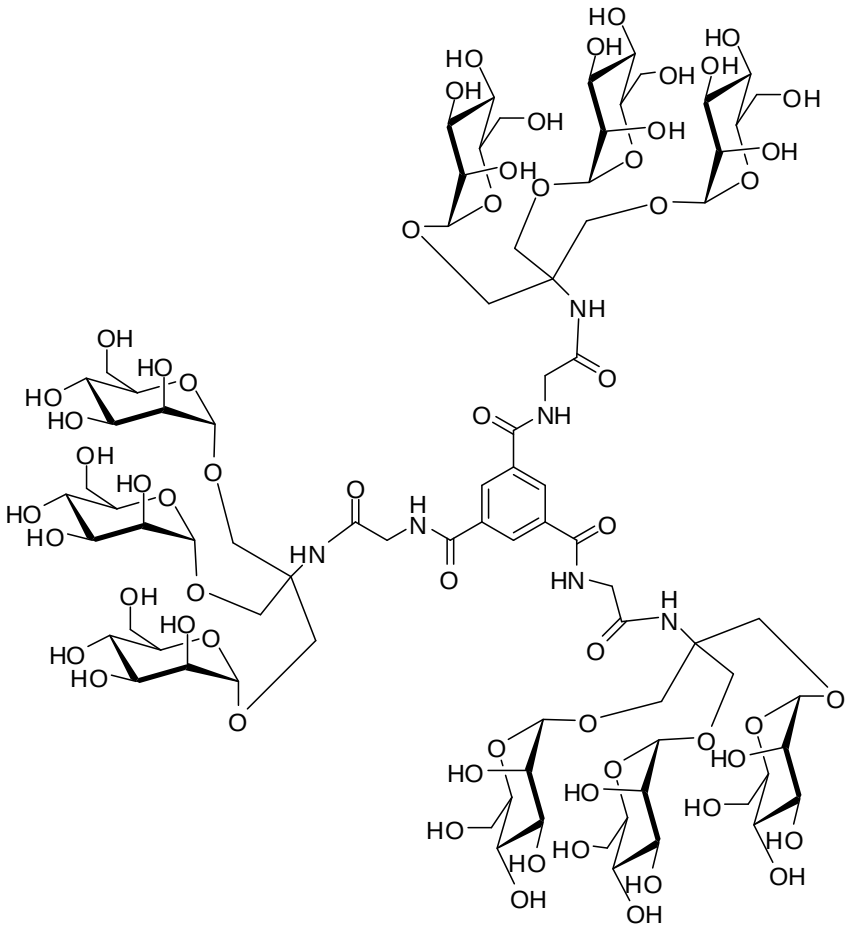

**Figure 23:** 9-mer mannose glycodendrimer, using Tris to display the monosaccharides.[49]

As expected the dendrimers all showed greater inhibition of lectin Concanavalin A than the trisubstituted glycocluster in an Enzyme Linked Lectin Assay (ELLA), with the 9-mer exhibiting a reasonable $IC_{50}$ of 0.65 mM, four times greater than the Tris

cluster.[49] However differences between the 9- and 18-mer were small and the activity of the 18- and 36-mer were similar.[49] This effect has been seen previously in high valence compounds with binding plateauing in high valency compounds and it has been suggested that the origin is steric.[3] A high number of tightly packed ligands may not be able to interact well with lectin binding sites simply because the ligands are too crowded, an effect that might be mitigated by the structure of the underlying scaffold or by using linkers at the branching points of the dendrimer, increasing the distance between ligands.

Some approaches have utilised click chemistry in combination with Tris to quickly build up large, branched dendrimers such as that illustrated in **Figure 24**.[50, 51, 52, 53]

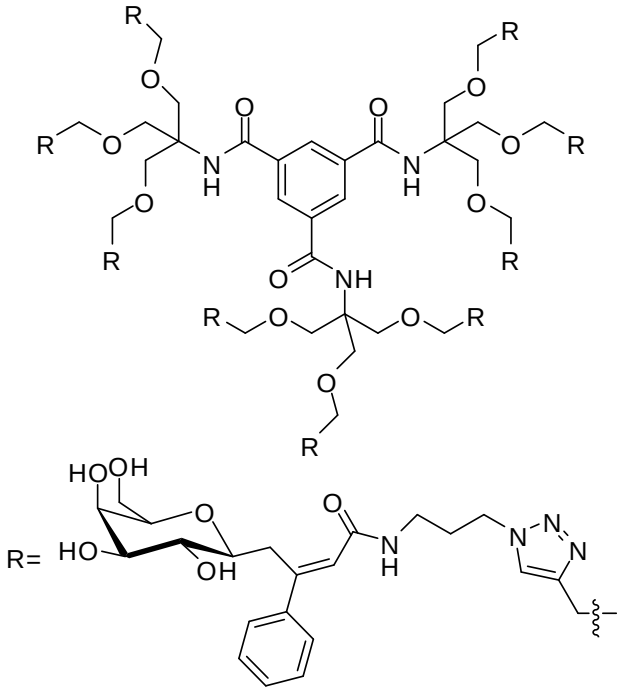


**Figure 24:** A dendrimer produced by Chabre *et al* utilising Tris cores and click chemistry.[50]

The structure shown in **Figure 24** was synthesised by Chabre *et al* as part of a series aimed at targeting LecA of *P. aeruginosa*, a known virulence factor associated with infections by this opportunistic bacteria. The series contained dendrimers of varying sizes with 3-36 C-galactose residues, although several of the larger compounds were too hydrophobic to dissolve readily in water preventing ELLA analysis of the entire series. In this case dendrimer design was aided by crystal structures of the target

lectin and computational docking studies. The results confirmed that in this lectin binding site the anomeric oxygen is exposed to the solvent leading the group to suggest that C-galactose residues could be employed without negatively affecting the binding interaction.[50] The group synthesised and screened several potential monomers before choosing to use azido and propargyl substituted derivatives, allowing them to build up their dendrimers in a straight forward manner via click chemistry. 3- and 6-mer derivatives were designed around the same aromatic core as the Tris based 9-mer and a 3-mer Tris based cluster was also synthesised. Of the dendrimers tested, the Tris based compound in **Figure 24** had the best binding to LecA, with an impressive $K_d$ value of 230 nM.[50]

As a small scaffold Tris appeared to meet our requirements, being flexible, nontoxic, soluble and easy to synthetically manipulate. As discussed it has previously been used to create successful lectin ligand mimics both as small clusters and as a display or branching agent in larger dendrimers. We anticipated that it could be used to create compounds suitable for use as probes or for screening. With careful choice of linking strategy these could later be optimised for more specific interactions by manipulating the length, rigidity and functionality of the linker arms. With this in mind we began to look at using azide alkyne click chemistry the uses and advantages of which are discussed in the following section.

## 2.2 An overview of click chemistry

The term ‘click chemistry’ refers to a variety of procedures which aim to meet the same set of exacting criteria, originally defined by Sharpless. Click reactions should be stereospecific, high yielding, tolerant of a wide range of functionality, simple to perform, conducted in benign or easily removed solvents, have high atom efficiency and result in high purity products without chromatography.[54]

Several synthetic procedures meet all or most of these conditions. Nucleophilic attack on aziridines and epoxides, radical reactions between thiols and alkenes, the Diels-Alder reaction, non-aldol carbonyl reactions such as urea or oxime formation and some cycloaddition reactions have all been described as click chemistry.[54] Our

synthetic strategy focused on one particular click reaction, formation of triazoles from the cycloaddition of azides and alkynes.

Huisgen-Sharpless azide alkyne 1,3-dipolar cycloaddition, one of the most common reactions referred to as click chemistry, is a well-known and robust procedure which has been used on a diverse array of compounds. Examples include proteins, mono and polysaccharides (functionalised at several positions), nucleic acids, biomacromolecules, dendrimers, aromatic heterocycles, spiropyrans, porphyrins, resins and small molecules.[55, 56, 57] The reaction is extremely orthogonal, most other functional groups are stable to the reaction conditions and protecting groups are generally unnecessary adding to its popularity. Usually copper(I) catalysed (although a ruthenium catalysed method has been developed giving the opposite regioselectivity) the method is generally fast, high yielding, regioselective and tolerant of a broad range of functional groups.[58]

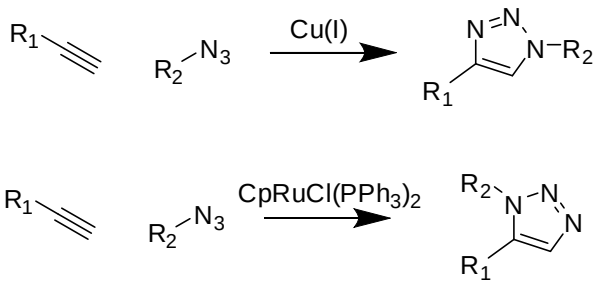


**Scheme 2:** Summary of the two common metal catalysed azide-alkyne click procedures, each producing a majority of one of the two possible regioisomers.

The triazole linkage formed is known to be chemically and enzymatically stable as well as nontoxic.[59] The reactive species themselves rarely occur in nature and typically react specifically with each other.[59] This combination of properties makes the azide-alkyne click reaction an extremely attractive method for coupling diverse components, especially when the eventual aim is to produce molecules for biological testing. The two common metal catalysed azide-alkyne click reactions (hereafter simply click reactions) are illustrated above in **Scheme 2.** Since Cu(I) is essential for copper catalysis a reducing agent such as sodium ascorbate is often present in the copper catalysed reaction to maintain Cu(I) in the mixture. The mechanism for the copper catalysed procedure is shown below in **Scheme 3**.[60]

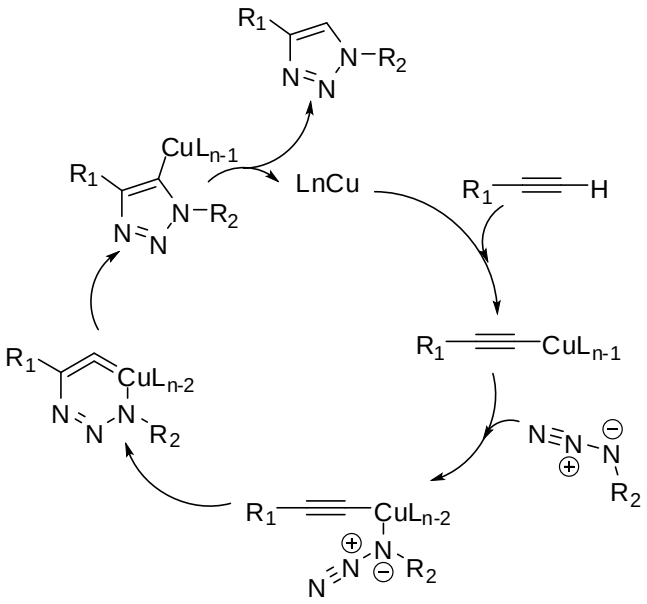

**Scheme 3:** Mechanism proposed by Sharpless *et al* for the copper(1) catalysed click reaction.[60]

The click reactions tolerance of varying functionalities allows the synthesis of a single base scaffold that can be coupled to multiple sets of linkers and saccharides, cutting out the need to synthetically tweak each scaffold to a particular ligand monomer. An initial set of flexible lectin ligand mimics could be synthesised relatively straightforwardly and then adjusted giving several generations of ligand mimics with a consistent coupling strategy throughout. With this in mind we planned an initial set of Tris based, click coupled scaffolds bearing three distinct monosaccharides.

## 2.3 Synthesis of Tris based scaffolds

Inspired by the numerous uses of click chemistry to build up Tris based dendrimers we planned to begin with small, simple and flexible tri-substituted Tris scaffolds, with monosaccharides coupled through short linkers via click chemistry. The proposed synthetic route is shown below in **Scheme 4**.

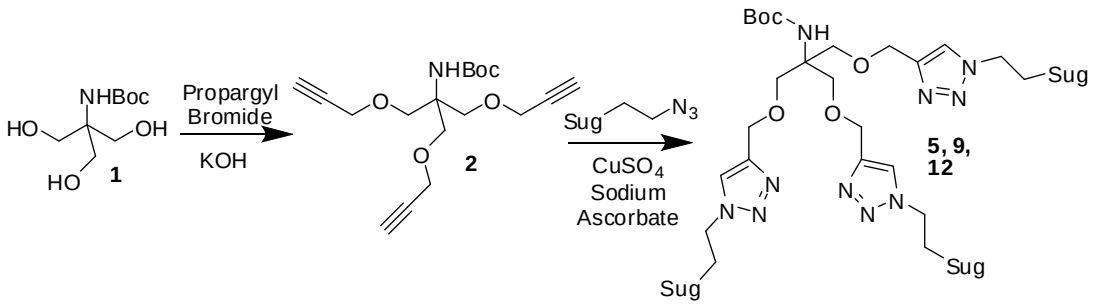


**Scheme 4:** Proposed synthetic route to initial small, simple Tris based lectin ligands.

The tri-propargyl substituted Tris scaffold (**2**) was produced in reasonable yield (69%) following literature procedures which are shown below in **Scheme 5**.[47] With a suitable starting scaffold in hand attention turned to choice of monosaccharides and the remaining portion of the linker.

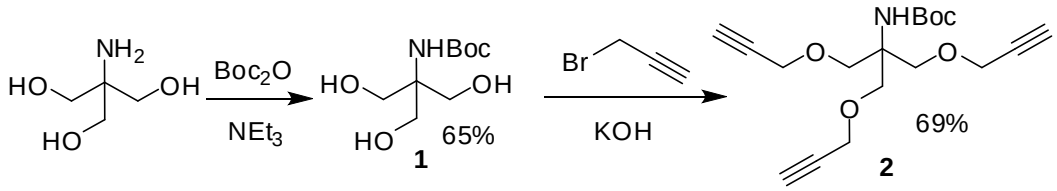


**Scheme 5:** Synthesis of tripropargyl Tris scaffold (**2**)

D-Galactose, D-glucose and N-acetyl D-glucosamine (GlcNAc) were chosen as initial monosaccharides of interest: galactose has a high presentation in biological systems and the large number of lectins recognise and interact with galactose. GlcNAc was selected as the ligand of choice for ficolins, a family of lectins which activate the complement pathway, and as the preferred ligand of a plant lectin stored in house (wheat germ agglutinin). Glucose was chosen as a negative control.

Although there are lectin ligand mimics using sugars that lack an anomeric oxygen it was felt that since this position is important for recognition by some lectins our first generation scaffolds should include it.[61, 62] With this in mind, simple 2-azidoethanol (**3**) was chosen as an initial linker component, this was also synthesised according to literature procedures.[63] **3** was then coupled at the anomeric position to D-galactose pentaacetate using boron triflouride etherate as an activator as illustrated in **Scheme 6**.[64]

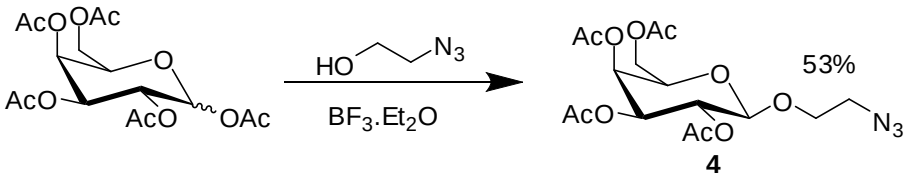


**Scheme 6:** Synthesis of azido-coupled galactose (**4**)

The β anomer (**4**) was isolated in 53% yield and reaction with tripropargyl Tris (**2**), catalysed by copper (I) formed in situ by copper sulfate and sodium ascorbate, gave the fully protected tri-galactose Tris scaffold (**5**) illustrated in **Figure 25.** Unusually for click reactions it was necessary to purify **5** by flash column chromatography and the product was isolated in 66% yield. Due to the reaction taking place at multiple sites a slight excess of the azide (**4**) was used; the product was purified to ensure its complete removal and that any residual azide would not interfere with planned binding experiments. A small amount of **4** (11mg) was recovered during chromatography.

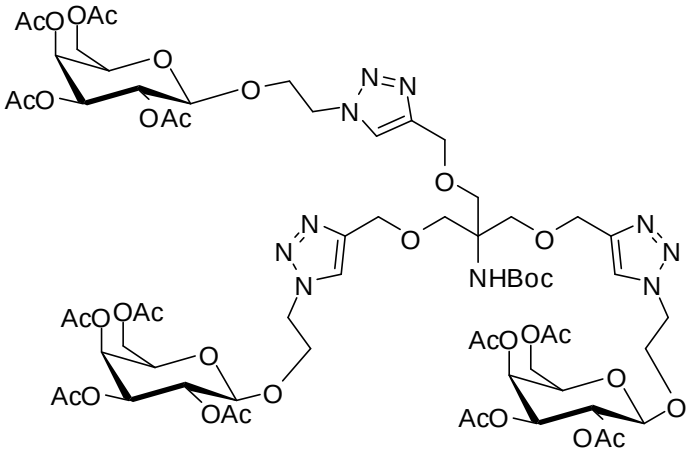


**Figure 25:** Tri substituted galactose bearing Tris scaffold (**5**)

Product formation was suggested by IR, with the absence of characteristic strong absorption for both terminal alkynes (3291 $cm^{-1}$ in Tris core **2**) and azides (2103 $cm^{-1}$ in azido-galactose compound **4**). Further confirmation came from NMR (fully assigned with the aid of COSY and HSQC) and mass spec experiments.

Peaks associated with the terminal alkyne groups of **2** at 2.42 ppm in the proton spectrum and at 79.7 and 74.7 ppm in the carbon spectrum disappeared while peaks

associated with the ethyl linker in **4** between the azide and galactose shifted significantly. Both $CH_2$ groups were shifted downfield on reaction: from 3.49-3.43 and 3.29-3.23 ppm to 4.64-4.61 and 4.54 ppm for the environments adjacent to the azide or triazole respectively while for the environments next to the anomeric position shifts were from 4.09-4.04 and 3.68-3.62 ppm to 4.26 and 3.96-3.90 ppm. This together with the appearance of peaks consistent with a triazole ring at 7.62 ppm in the proton and 144.7 and 124.3 ppm carbon spectra (carbon peaks assigned as the quaternary and protonated carbons of the ring respectively) strongly suggested that the click reaction had occurred, linking the Tris scaffold and galactose.

Regioselectivity of the tri-galactose product (**5**) was confirmed by the NMR. Proton shifts for the 1,4 triazole are significantly higher than for the equivalent 1,5 triazole, generally coming at 7.50 ppm or higher while the 1,5 triazole would be expected at around 7.30 ppm. A difference in expected shifts is also observed in the carbons of the triazole ring, with the protonated environment of the 1,4 triazole usually coming upfield of its 1,5 equivalent, at around 120 ppm rather than 130 ppm.

Final confirmation came from high resolution mass spec results, with a prominent positive mass ion observed at 1587.5954 m/z, in good agreement with the predicted value of 1587.5956 for the product.

Encouraged by this initial success an attempt was made to synthesise the GlcNAc equivalent using the same boron triflouride etherate based procedure. However this was unsuccessful, probably due to the stability of the α starting material **6**, which was used as it was the major product of reactions to acetate protect GlcNAc. The α starting material was recovered.

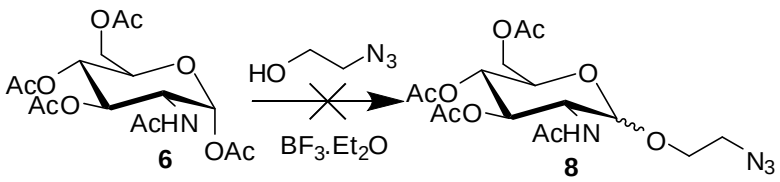


**Scheme 7:** Initial unsuccessful attempt to synthesise azide linked GlcNAc (**8)**

In order to encourage reaction with 2-azidoethanol (**3**) the acetylated GlcNAc starting material was activated by acid induced cyclisation, creating the oxazoline, using trimethylsilyl trifluoromethanesulfonate (TMSOTf).[65] This neighbouring group participation is known to increase the selectivity at the anomeric position.[66]

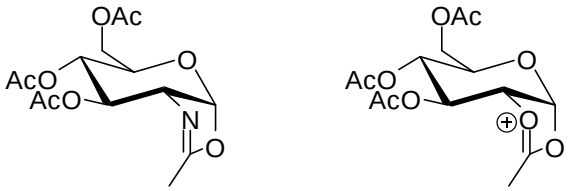


**Figure 26:** Oxazoline **7** compared to the oxonium ion equivalent formed when an ester protected hydroxyl is present at the 2 position

This cyclisation also occurs with ester protection of a hydroxyl at the 2 position, however this oxonium ion is considerably less stable and so unlike the oxazoline (**7**) it cannot generally be isolated. Both derivatives are illustrated in **Figure 26.**

Due to its reactive nature **7** was used as a crude however full characterisation was still possible. Comparison of mass spec data for acetate protected GlcNAc **6** and oxazoline **7** suggested that cyclisation had occurred. The most prominent mass ion for **7** was at 330.1 m/z, matching well with the predicted value for $MH^+$ (330.3). Compared to the observed ions in the spectra of **6**, which showed a prominent ion at 412.1 m/z ($MNa^+$), this suggested a mass loss consistent with formation of the oxazoline product.

Large differences in specific rotation between **6** and **7** also supported the idea of product formation. At similar temperatures and concentrations the specific rotation for **6** was recorded as $+89.4^o$ in methanol, while **7** was recorded as $+6.0^o$ in the same solvent. Literature values (taken in chloroform) showed a similarly large change in specific rotation going from the acetate protected GlcNAc (+94, 21$^o$C)[67] to the desired oxazoline (+12.2, 18$^o$C)[68], suggesting that the product had been successfully synthesised.

Product formation was confirmed by NMR. Loss of acetate peaks in both the proton and carbon spectra of **7** (characteristically at ~2.10 ppm in the proton and ~170 ppm

and ~20 ppm in the carbon) strongly suggested loss of an acetate group, consistent with the intended cyclisation. Further assignment, assisted by COSY and HSQC of both starting material **6** and product **7**, revealed large shifts for the anomeric and 2 position in both proton and carbon spectra. The anomeric proton was observed at 6.17 ppm with a J coupling of 3.6 Hz in **6** whereas for the product **7** it was shifted upfield to 5.96 ppm with a much higher J value of 7.2 Hz. In contrast the anomeric carbon shifted downfield from 90.8 ppm in **6** to 99.5 ppm in **7**. More dramatic shifts were observed at the 2 position, with the proton signal moving from 4.48 ppm to 4.13 ppm on reaction and the carbon from 51.2 ppm to 65.1 ppm.

Subtler difference in the NMR spectra of **6** and **7** also supported formation of the oxazoline: no proton signal for N-H was observed in **7** and two signals in the carbon spectrum of **7** came close to, but upfield from, characteristic acetate peaks suggesting imine formation. These peaks came at 166.8 ppm for C=N (compared to 168.7 ppm for the most shielded C=O group in starting material **6**) and 14.1 ppm for the associated methyl (compared to 20.7 ppm for the most shielded methyl carbon in **6**).

Having obtained **7,** reaction with 2-azidoethanol (**3**) was attempted again. Several different methods were trialled, each conducted under dry conditions in DCM or dichloroethane using an acid catalyst. Previously established literature procedures were followed or used as starting points in each case, using TMSOTf, concentrated sulfuric acid and copper (II) chloride.[65, 69, 70]

A significant mass loss was recorded for reaction with sulfuric acid, 28 mg of crude material were recovered from a 100 mg scale reaction. The material recovered was a mixture of starting material and product (~ratio of 1:1.5) which was not purified further.

Reaction with TMSOTf was conducted over two days as TLC consistently showed that the starting material **7** had not been consumed. Purification did give the azide-linked product **8** but with an extremely low yield of 7%. Use of copper (II) chloride increased the yield slightly to 16% over the same time period allowing the production of the azide-linked GlcNAc **8** as illustrated in **Scheme 8**.

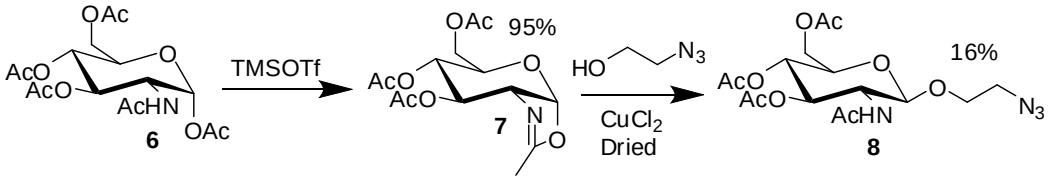


**Scheme 8:** Synthetic route to azide linked GlcNAc **8** via oxazoline **7**.

IR and mass spec both suggested azide **8** had been successfully synthesised: with a characteristic azide peak recorded at 2111 $cm^{-1}$ and a mass ion at 417.1 m/z comparing well to the predicted value for $MH^+$ (417.16 m/z). NMR spectra confirmed both the formation of the azide **8** and the anomeric form; J coupling for the anomeric proton was 8.4 Hz which strongly suggests the β form. Additional peaks were observed in the carbon (at 68.6 and 50.6 ppm) and proton spectra (at 4.07-4.02, 3.75-3.68, 3.54-3.45 and 3.29-3.23 ppm) associated with the ethyl linker and were positively identified with reference to COSY and HSQC. Large shifts in the proton and carbon spectra were observed for position 2, going from oxazoline **7** to azide **8**. Proton peaks shifted from 4.13 ppm to 3.81 ppm on reaction and those for the carbon from 65.1 ppm to 55.0 ppm. This along with the appearance of an N-H signal in the proton spectra of **8** (at 5.58 ppm) established that the oxazoline ring of **7** was no longer present, confirming that the azide **8** had been synthesised as intended.

Reaction of the β anomer (**8**) with tripropargyl Tris scaffold (**2**) catalysed by copper (I) successfully produced the protected tri substituted GlcNAc scaffold (**9**) shown in **Figure 27** but the yield was extremely low (5%). Several impurities were isolated along with a significant portion of the azide starting material **8** suggesting that despite a reaction time of 22 hrs the reaction had not gone to completion. This coupled with the similar Rf values of the product and impurities meant that very little pure **9** was isolated from the initial reaction although it is likely that by adjusting the reaction and purification conditions the yield could be significantly improved.

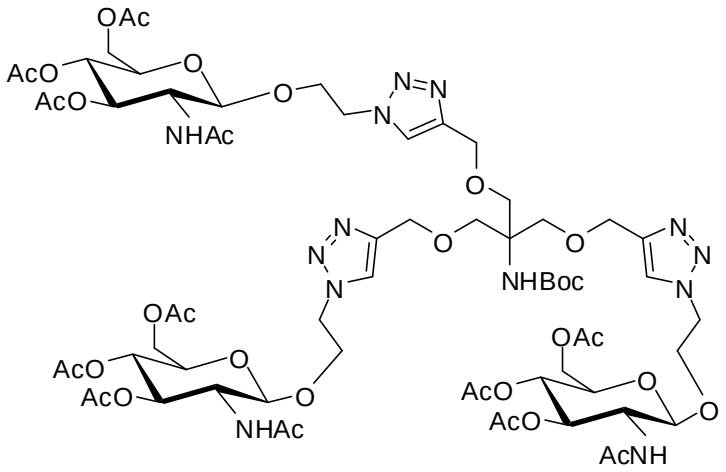


**Figure 27:** Tri substituted GlcNAc bearing Tris scaffold (**9**)

Both IR and initial mass spec suggested product formation. The IR spectra of **9** lacked the characteristic azide peak (observed at 2111 $cm^{-1}$ in **8**) and the C-H signal characteristic of terminal alkynes (seen at 3291 $cm^{-1}$ in propargyl Tris scaffold **2**). The lack of these functional groups suggested that the click reaction had occurred. Prominent mass ions were observed at 1486.8 m/z and 1609.0 m/z, corresponding well to predicted values for ($M^+$ -Boc) and $MNa^+$ (predicted to be 1484.4 m/z and 1607.5 m/z) strongly suggesting product formation. Due to the size of the intended product MALDI was used in preference to ESI, so lower weight mass ions associated with the starting materials **2** and **8** were not easily detectable. Confirmation of the product mass ion came from high resolution mass spec, with a clear ion at 1584.6428 m/z (matching well with the predicted value for $M^+$ of 1584.6430).

Further confirmation came from proton and carbon NMR spectra (fully assigned with the aid of COSY and HSQC). In the proton spectrum the triplet associated with the terminal alkyne of the Tris starting material **2** (at 2.42 ppm) was absent, while a prominent singlet at 7.70 ppm suggested the presence of a 1,4 triazole ring. The presence and regioselectivity of the triazole was further supported by peaks in the carbon NMR spectrum at 144.4 ppm (the quaternary carbon) and 124.5 ppm (the protonated carbon). Large shifts were observed in both the proton and carbon spectra for the ethyl linker. In the azide linked GlcNAc **8** protons from the linker, adjacent to the anomeric position, were observed at 4.07-4.02 ppm and 3.75-3.68 ppm. In **9** they appeared at 4.67-4.61 ppm and 4.50-4.44 ppm, suggesting a significant change in the local magnetic (and hence chemical) environment. A similar large downfield shift

was seen for the protons adjacent to the azide in **8** and the triazole in **9**, going from 3.54-3.45 ppm and 3.29-3.23 ppm in **8** to 4.32-4.23 ppm and 3.86 ppm in **9**. The attached carbon shifted from 50.8 ppm in **8** to 64.3 ppm in **9,** while the carbon adjacent to the anomeric position moved from 68.6 ppm to 50.2 ppm on reaction. Together the spectroscopic data confirms that **9** was synthesised as intended and the lack of peaks that can not be assigned to the product in the mass spec, proton and carbon NMR strongly suggests a high purity for isolated **9**.

Attention then turned to creating the final glucose bearing scaffold. Initial attempts to synthesise the azide linked glucose derivative **11** directly by coupling with 2-azidoethanol (**3)** were unsuccessful. **Scheme 9** shows the general strategy attempted.

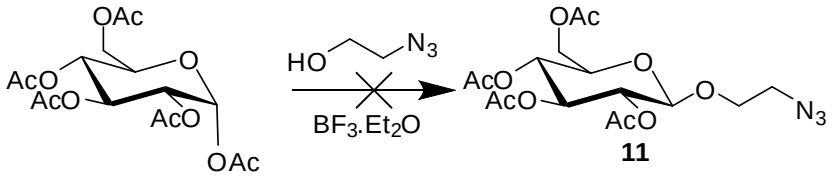


**Scheme 9:** Attempts to synthesise azide-linked glucose derivative **11** directly using 2-azidoethanol (**3**) were unsuccessful

Crude NMRs from the reaction shown in **Scheme 9** showed that product was formed, but after 2 days the starting penta-acetyl glucose still predominated. This was determined by comparing integral values for the anomeric protons of azide linked glucose **11** (at 4.60 ppm) and the penta-acetyl starting material (at 6.33 ppm) in the crude NMRs after 1 and 2 days. The integrals showed that after two days approximately 60% of the starting material is still present.

As a result an alternative strategy was attempted and found to be successful. Penta-acetyl glucose was coupled with bromoethanol using boron trifluoride etherate and the bromide **10** subsequently converted to the azide **11** as illustrated in **Scheme 10**.[71]

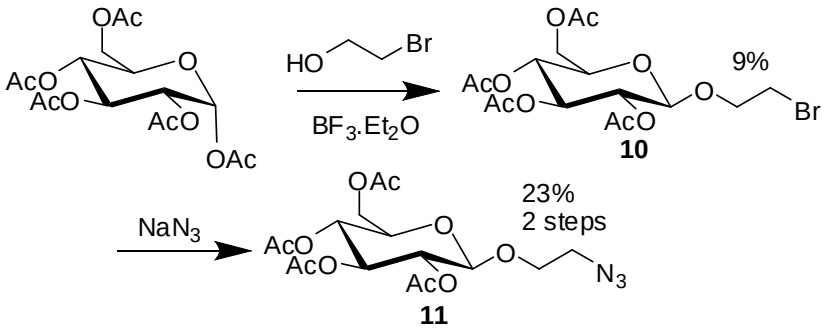


**Scheme 10:** Synthesis of azide-linked glucose derivative **11** via bromide derivative **10**

Low recorded yields of the bromide derivative **10** (9%) were due to purification difficulties; in the solvent systems used for column chromatography **10** co-eluted with a small amount of penta-acetyl glucose starting material which was removed by successive recrystalisation. This drastically reduced the initial overall yield from approximately 65% (estimated using integration of anomeric peaks in proton NMR).

Since the sodium azide in the subsequent step could only be expected to react with bromide **10** the reaction was conducted using crude **10**. This gave the desired azide linked glucose derivative **11** in low to moderate yield of 23% over two steps (from the penta-acetyl glucose), suggesting an average yield of approximately 35% for the second step. The bromide derivative **10** was not recovered from the reaction mixture, though significant proportions of penta-acetyl glucose were.

Successful azide formation was strongly suggested by the IR, showing a characteristic azide peak at 2105 $cm^{-1}$. This was supported by mass spec, with the azide **11** showing a prominent ion at 440.1 m/z, consistent with predicted values for $MNa^+$, while the most intense ion peak in spectra of bromide **10** was at 476.9 m/z (assigned as $MNa^+$), consistent with the heavier bromide isotope.

Confirmation came from the proton and carbon NMR (fully assigned with the aid of COSY and HSQC). Proton environments adjacent to the bromide in **10** were extremely close together, effectively forming one multiplet at 3.48-3.44 ppm. In azide **11** the environments had shifted enough to be distinct and were observed at 3.52-3.46 ppm and 3.29 ppm. Success of the reaction was further confirmed by shifts

in the carbon spectra, going from 30.0 ppm in starting material **10** to 50.7 ppm in azide **11**. The β anomeric form was confirmed by the shift and J coupling values of the anomeric proton in **11** (4.59 ppm, 8 Hz) and to a lesser extent by the optical rotation, which was similar to literature values although the concentration and solvent differed ($[\alpha]_D^{25.0}$ -48.4 (*c* 1.96, MeOH) (lit.,[72] $[\alpha]_D^{20}$ -31.2 (*c* 1.14, $CH_2Cl_2$)).

The click reaction between the β azide linked glucose **11** and the tri propargyl Tris scaffold **2** was copper (I) catalysed as for the previous derivatives. Following the low yield and partial completion of the reaction with the GlcNAc derivative **9,** (which had extremely similar Rf values to the azide starting material **8** and mono or di substituted scaffolds) the reaction was left for five days instead of overnight. The expected tri substituted glucose scaffold (**12** shown in **Figure 28**) was successfully synthesised and isolated in moderate 36% yield. A small amount of partially reacted material was recovered, suggesting that once again the reaction had failed to go to completion.

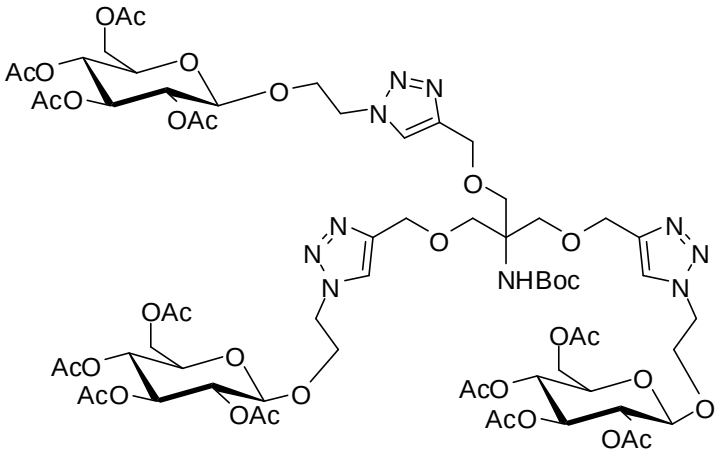


**Figure 28:** Tri substituted glucose bearing Tris scaffold (**12**) isolated in 36% yield

Both IR and initial mass spec results suggested **12** had been successfully synthesised. As in the previous examples (compounds **5** and **9**) characteristic peaks in the IR associated with azide (2105 $cm^{-1}$ for starting material **11**) and terminal alkynes (3291 $cm^{-1}$ in tri propargyl Tris core **2**) were absent. MALDI showed a prominent peak at 1611.31 m/z, consistent with $MNa^+$ which combined with the IR strongly suggested that the click reaction had occurred. Further support came from the high resolution mass spec, with a peak at 1587.5938 m/z corresponding well with the calculated

value for $M^+$ (1587.5937 m/z), strongly suggesting that the intended tri-glucose substituted Tris scaffold **12** had been synthesised as intended.

Confirmation of the structure of **12** came from the proton and carbon NMR, fully assigned with the aid of COSY and HSQC. A prominent singlet in the proton spectrum of **12** at 7.60 ppm, characteristic of the 1,4 triazole, along with the absence of a triplet at 2.42 ppm (assigned to the terminal alkyne in Tris core **2**) strongly suggested the formation of the 1,4 triazole. Peaks in the carbon spectrum at 145.0 ppm (assigned as the quanternary triazole carbon) and 124.0 ppm (assigned to the protonated triazole carbon) also supported this. Large shifts in the protons of the ethyl linker also strongly suggested the click reaction had occurred, although unlike the previous sugar bearing scaffolds (tri galactose **5** and tri GlcNAc **9**) shifts in the carbons were small. The carbon adjacent to the azide in **11** was observed at 50.7 ppm, and shifted to 50.0 ppm on reaction, with a similarly small shift from 68.5 ppm to 67.9 ppm for the carbon adjacent to the anomeric position. However the attached protons (adjacent to the anomeric position) shifted from 4.03 ppm and 3.73-3.66 ppm in the azide starting material **11** to 4.27-4.21 ppm and 3.97-3.91 ppm in the product **12**. The proton environments adjacent to the azide in **11** and the triazole in **12** showed larger downfield shifts, from 3.52-3.46 ppm and 3.29 ppm in **11** to 4.62-4.56 ppm and 4.74-4.54 ppm in **12**.

Together the spectroscopic data supported that the tri-glucose bearing Tris scaffold **12** had been synthesised as intended, with the region and anomeric selectivity shown, as with the previous scaffolds tri-galactose **5** and tri-GlcNAc **9.** Purity of the isolated tri-substituted scaffolds was strongly supported by the lack of unassigned peaks in mass spec, proton and carbon NMR in all cases.

Despite multiple issues with low yields the three simple target scaffolds **5, 9,** and **12** were all successfully synthesised and purified. The scaffolds were stored at -18$^{o}$C as the acetate-protected structures.

## 2.4 Chapter Summary

To begin with a simple tri-propargyl Tris core **2** was synthesised, along with a short azide linker **3**. D-galactose derivative **4** was then synthesised using azidoethanol **3**. By using copper catalysed click reaction **4** was linked to Tris core **2,** creating tri-galactose bearing scaffold **5** (**Scheme 11).**

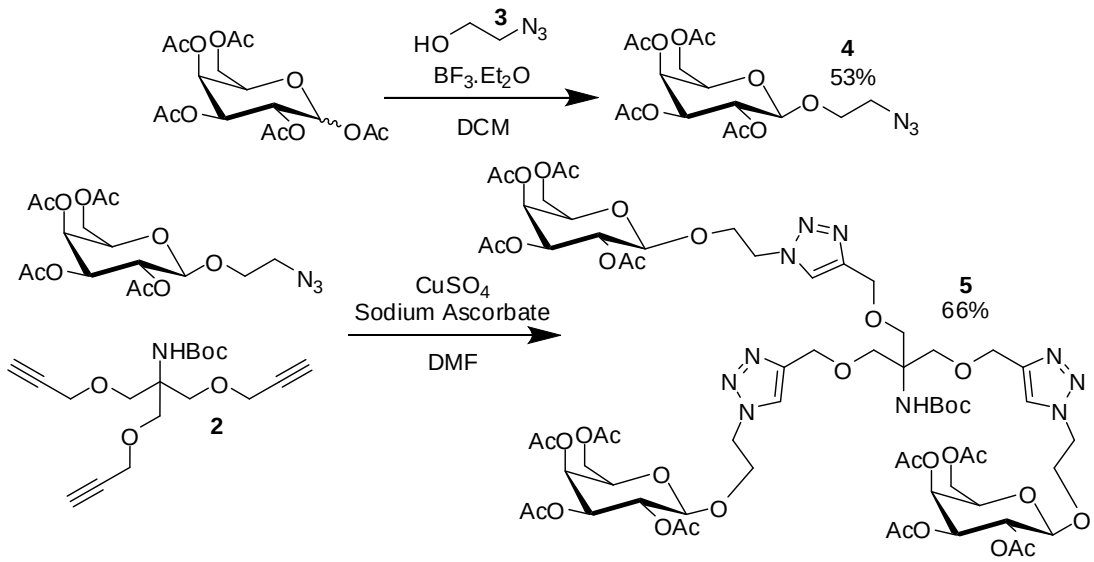


**Scheme 11:** Synthetic route to azide-linked D-galactose **4** and hence tri-galactose bearing Tris scaffold **5**

The azide-linked GlcNAc derivative **8** was also produced using azidoethanol **3**, via the oxazoline **7**. **8** was then clicked to the Tris core **2** giving the tri substituted GlcNAc bearing scaffold **9** (**Scheme 12)**.

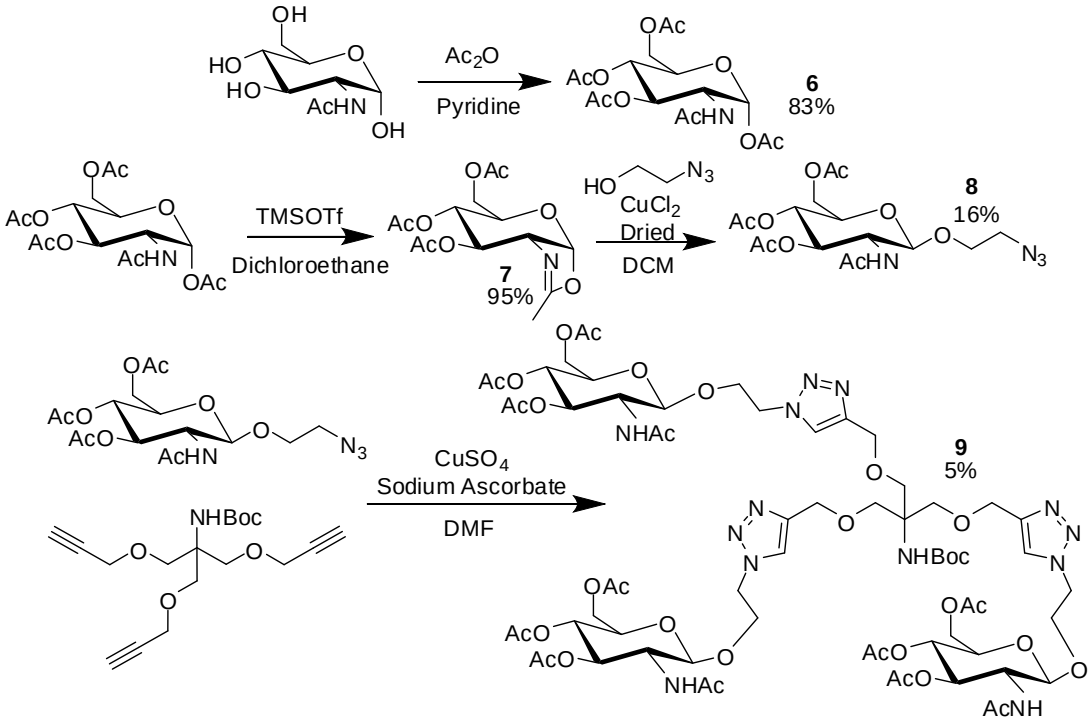


**Scheme 12:** Synthetic route to azide-linked GlcNAc derivative **8** and hence tri substituted GlcNAc bearing scaffold **9**

The glucose equivalent, **11**, was synthesised via bromoethanol rather than azidoethanol as shown below in **Scheme 13**, before reacting with tri propargyl Tris core **2** as previously. This gave the final scaffold, tri substituted glucose scaffold **12**, in moderate yield (35%).

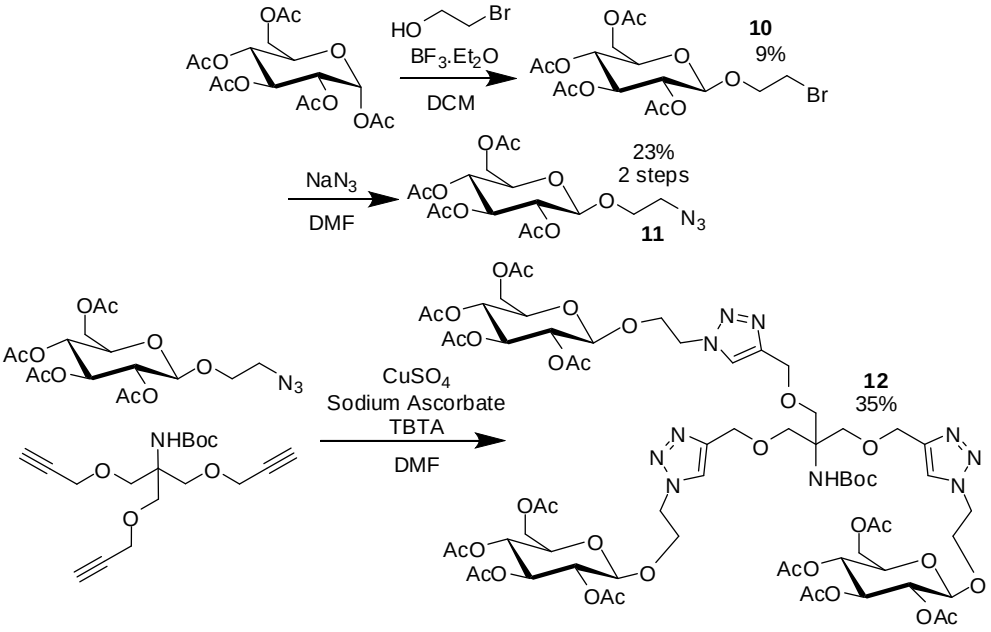


**Scheme 13:** Synthesis of azide-linked glucose derivative **11** and tri substituted glucose bearing scaffold **12**.

In order to expand on the scaffold series we next turned to alternative ligation methods and began to investigate methods for synthesising aminooxy bearing Tris scaffolds described in the following chapter. It was hoped that the lectin binding ability of these scaffolds could be directly compared at a later date.

# 3. Synthetic approaches to Aminooxy substituted Tris scaffolds

## 3.1 An overview of aminooxy coupling

A pure unprotected hexose in solution spontaneously converts to a minority of the ring opened aldehyde form, which can then interconvert between the ring closed alpha or beta pyranose or furanose forms with the exact proportions of each dependent on the conditions and the hexose used.[66] This is illustrated below in **Scheme 14.**

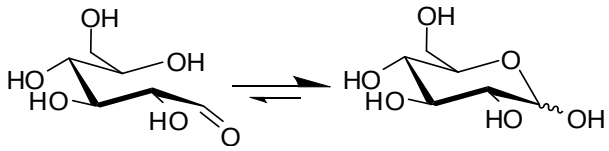


**Scheme 14**: Interconversion between pyranose ring-closed and ring-opened forms of glucose

Aminooxy groups rely on this interconversion as they react with the aldehyde of the ring opened sugar under acidic conditions.[73] Reaction occurs via a mechanism similar to imine formation; it is unusual in that it proceeds with unprotected sugars, giving addition specifically at the anomeric position, with a marked preference for the beta pyranose form.[73, 74] Primary aminooxy functionality traps the ring opened form but secondary aminooxy groups tend to give a single pyranose form as the major product. In most cases the β anomer is formed almost exclusively although there are some exceptions; mannose tends to give almost equal proportions of alpha and beta pyranose forms.[75] The mechanism for this reaction is shown below in **Scheme 15.**

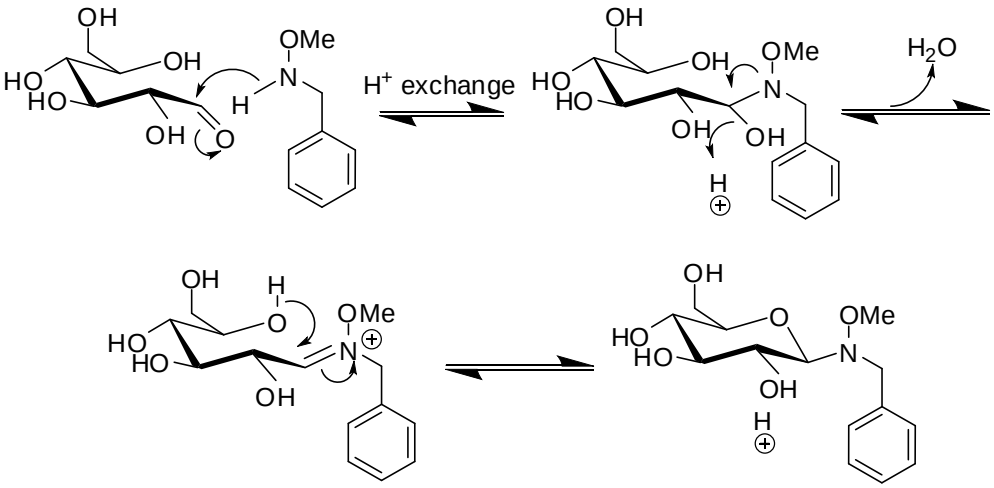


**Scheme 15:** Mechanism for the reaction between a secondary aminooxy compound and glucose.

This strategy has several synthetic advantages: reactions can be performed in water or buffers, are often high yielding and enantioselective, with no activating or protecting groups necessary.[76] This combination of properties can result in a shorter synthetic route to the desired compound, compared to the *O*-glycoside equivalent and usually requires less synthetic steps on the saccharide itself, increasing overall yields.[76] There are some disadvantages. As illustrated in **Scheme 15** the reaction is reversible at low pH (although products are stable at neutral and high pH) which can lead to product decomposition or mixtures of products and starting material.[77] These mixtures can have low solubility in organic solvents and so can be difficult to purify by flash column chromatography on silica.

Aminooxy linked sugars are not always recognised by their biological target, especially when bulky R groups are present on the starting secondary aminooxy and when tested alongside *O*-glycoside equivalents aminooxy linked compounds are sometimes less active.[76, 78] However activity and selectivity trends observed in secondary aminooxy linked compounds are often mirrored in their *O*-glycoside equivalents.[76] Along with the simpler synthetic process this can make aminooxy compounds useful for screening, identifying the most interesting saccharides without the complex synthesis of an *O*-glycoside library.[79]

While the reaction between hexoses and secondary aminooxy functionality produces almost exclusively pyranose structures (as shown above in **Scheme 15**) using primary aminooxy functionality results in an equilibrium mixture of two linear and one ring closed product, illustrated below in **Scheme 16.**

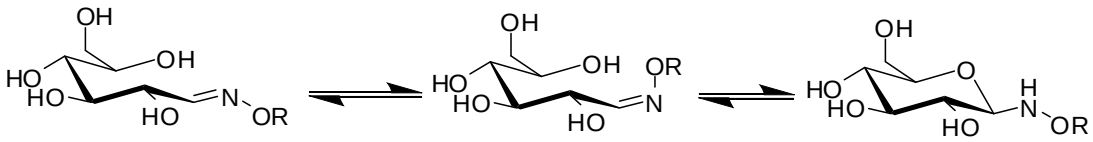

**Scheme 16:** Interconversion between glyco-oxime isomers

Although preservation of the pyranose structure is often thought to be essential for lectin recognition[80, 81] several groups have found primary aminooxy functionality advantageous. The presence of a minority ring-closed saccharide allows recognition with less risk of false negatives from aminooxy R groups interfering with binding.[82] A single ring opened sugar can function almost as part of a linker, displaying terminal residues, so long as the saccharide is large enough that the ring-opened unit doesn't have a significant effect on binding.[83, 84]

Feizi *et al* developed primary aminooxy compounds for use in microarray analysis to further assign oligosaccharide-protein interactions, an example in shown below in **Figure 29**.

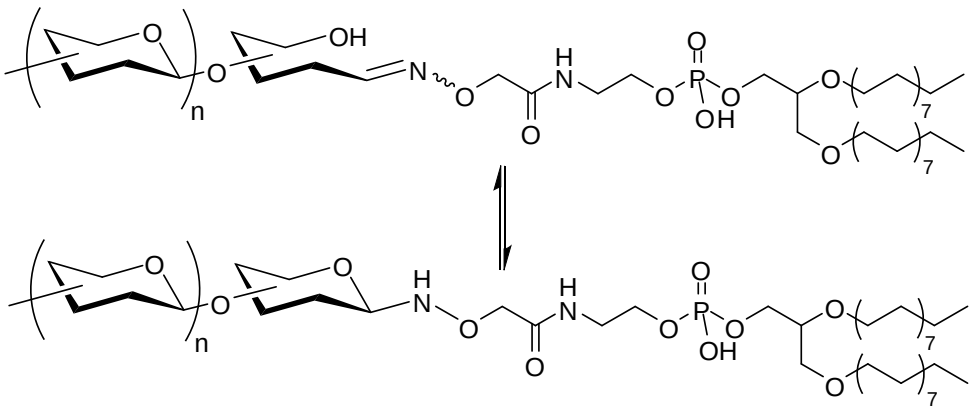

**Figure 29:** Primary aminooxy compound used to immobilise oligosaccharides for microarray analysis by Feizi *et al*[82]

The attraction of an aminooxy based compound for Feizi *et al* was the minority of ring closed oligosaccharide in the equilibrium mixture formed. Previous immobilisation techniques either required chemical synthesis of the ligand, limiting the number of compounds available compared to isolated natural products, or relied on reductive amination as a method of choice, a process that leaves core monosaccharides in a ring opened state (example compound shown in **Figure 30**).

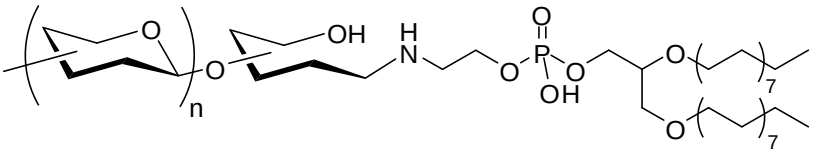


**Figure 30:** Immobilisation of oligosaccharides using reductive amination[82]

An aminooxy based approach makes up for many of the shortcomings of reductive amination, which can be unsuitable for smaller saccharides or systems where the core saccharides contribute to strong binding because of the ring opened structure of the resulting ligand.

Feizi *et al* produced a series of primary aminooxy based neoglycolipids to investigate any differences in lectin binding compared to equivalent neoglycolipids produced via reductive amination.[82] They first conducted an NMR study using a primary aminooxy based test compound (shown below **Figure 31**) to confirm that ring closed saccharides would be present. Their results, that 15% of the mixture was ring closed in solution, are supported by Thygesen *et al* who found up to 20% of the equilibrium mixture was ring closed in their previous NMR studies using a variety of mono, di and trisaccharides.[82, 85]

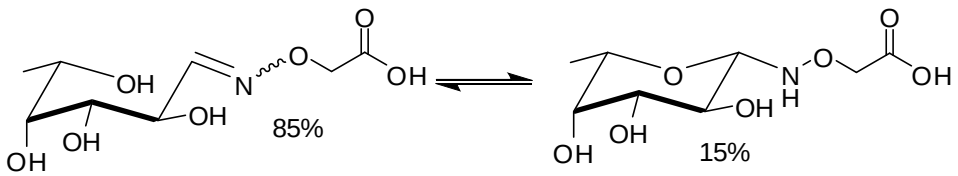


**Figure 31:** Compound used by Feizi *et al* to investigate the proportion of ring closed sugar at equilibrium[82]

Feizi *et al* then produced $Le^x$ trisaccharide probes using primary aminooxy ligation, secondary aminooxy ligation and reductive amination (**Figure 32**).

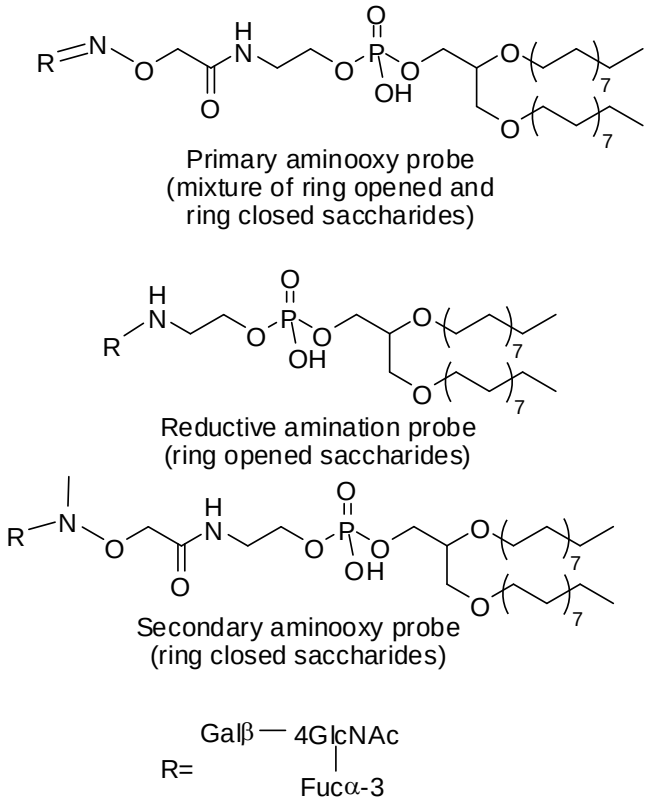


**Figure 32:** Neoglycolipid probes used by Feizi *et al* in microarrays[82]

Their binding to anti-L5 and anti-SSEA-1 antibodies was compared in a microarray format. These antibodies were chosen because previous work showed they require intact core monosaccharides for binding.[86] Neither antibody bound the ring opened, reductive amination based probes and both bound with primary aminooxy based probes.[82] Results from secondary aminooxy probes were more complex, with no binding to anti-SSEA-1 observed but significant binding to anti-L5, with the fluorescence three times that of the primary aminooxy probe (~30,000 and ~10,000 flourescence units respectively at 7 fmol, possibly due to the greater proportion of ring closed sugar in secondary aminooxy compounds).[82] The group suggested that having a methyl group close to the anomeric position might interfere with anti-SSEA-1 recognition.[82]

As a result Feizi *et al* decided to concentrate on primary aminooxy probes, contrasting them with reductive amination based probes for a wide range of lectins

and ligands. Results for the three siglecs tested broadly supported the suggestion that siglecs interact with monosaccharides distant from the primary binding site.[82, 87] All siglecs (hSiglec-7, hSiglec-9 and mSiglec-E) exhibited differences in binding to primary aminooxy and reductive amination probes bearing the same ligand. Each siglec tested showed markedly stronger binding to a primary aminooxy probe bearing trisaccharides NeuAcβ-3Galβ-4Glc, compared to the ring opened equivalent. hSiglec-7 showed little appreciable binding to other primary aminooxy or reductive animation based probes but hSiglec-9 and mSiglec-E both showed preferences for two other carbohydrate ligands in the series, both primary aminooxy probes.[82]

These results underline the importance of the pyranose form to binding interactions with a variety of lectins. While primary aminooxy ligation allows the possibility of a pyranose structure the majority is in the ring open form, potentially reducing binding interaction compared to a linkage that traps the glucoside in a pyranose form. When larger or longer polysaccharide chains are employed primary aminooxy groups can be effective and the minority of ring closed saccharide in solution allows some binding even in smaller ligands. However when monosaccharides are employed the pyranose form is highly desirable, which contributed to the choice of secondary aminooxy functionality as a ligation strategy in this project.

So far the majority of secondary aminooxy linked therapeutics have shown moderate to low activity. [75, 79, 88] Some of the most detailed studies have focused on digitoxin, aiming to improve the drug's anticancer properties.[76] Digitoxin's target, $Na^+$, $K^+$-ATPase, is unregulated in several cancers and previous studies have shown replacing the molecule's natural trisaccharide with certain monosaccharides improves the drugs performance against several cell lines.[79]

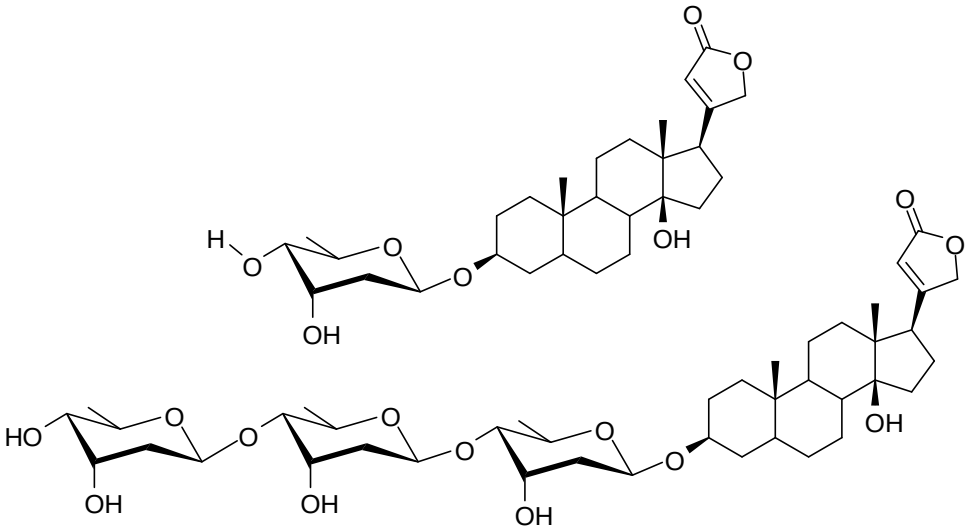


**Figure 33:** Mono and trisaccharides digitoxin analogues[79]

Iyer *et al* screened the mono and tri saccharide analogues shown above in **Figure 33**, against a library of 58 cancer cell lines which consistently showed lower $GI_{50}$ concentrations for the monosaccharide. The improvement against colon cancer line HCT-116 and melanoma line SK-MEL-5 was particularly marked, going from 5.4 nM in the monosaccharide to 25 nM in the trisaccharide for HCT-116 and from 5.5 nM to 37.1 nM for SK-MEL-5.[79]

Work on digitoxin analogues by Iyer *et al* went on to directly compare the cytotoxic effects of aminooxy linked variants of these *O*-glycosidic compounds (**Figure 34)**.

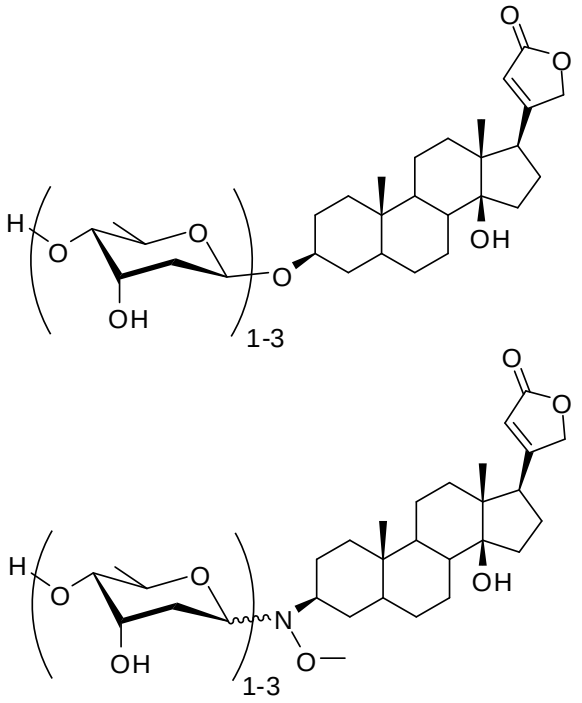


**Figure 34:** *O*-glycosidic and aminooxy linked digitoxin analogues.[79]

Aminooxy compounds showed lower anti-cancer activity in all cell lines screened, but patterns of selectivity and relative potency seemed to be retained.[79] In apoptosis assays against NCI-H460 cells the monosaccharide analogues for both *O*-glycosidic and aminooxy compounds were consistently more potent, followed by the di and trisaccharides. But the difference in potency between *O*-glycosidic and aminooxy analogues was marked, with the *O*-glycosidic monosaccharide inducing apoptosis in 72% of cells at the highest concentration while the aminooxy equivalent only induced apoptosis in 30%.[79] Screening against four cancer cell lines with both sets of compounds showed broadly similar selectivity patterns, with the two monosaccharide analogues both having their lowest $IC_{50}$ concentrations against NCI-H460 cells (11 nM and 24 nM for the *O*-glycosidic and aminooxy analogues respectively).[79] However there were some exceptions: the aminooxy trisaccharide analogue showed much greater potency than expected against SK-OV-3 cells, with an $IC_{50}$ similar to the aminooxy monosaccharide (0.86 µM and 0.98 µM respectively).[79] In contrast the *O*-glycosidic trisaccharide had lower activity against SK-OV-3 than the *O*-glycosidic monosaccharide (0.097 µM and 0.05 µM respectively), demonstrating that while useful aminooxy compounds do not perfectly predict their *O*-glycosidic equivalents.[79]

Given the synthetic difficulty involved in preparing *O*-glycoside analogues of complex pharmaceuticals the similar selectivity and potency patterns of aminooxy analogues, coupled with the discovery that both sets of analogues had a similar mechanism of action, is a significant find.[79] It suggests screening libraries of aminooxy based compounds could be used to confidently predict the properties, potency and mechanism of action of *O*-glycosidic therapeutics.

Producing secondary aminooxy Tris scaffolds would enable us to compare their ligand properties with the click-coupled *O*-glycosides described earlier (**Chapter 2**) and investigate whether the aminooxy scaffold patterns of activity and selectivity are similarly predictive of *O*-glycoside properties.

## 3.2 Attempts to synthesise tri-aldehyde bearing scaffolds

One of the most common synthetic strategies for producing aminooxy functionalised molecules is to reduce oximes previously produced by reacting aminooxy salts with aldehydes. As a result a tri-aldehyde Tris scaffold was thought to be the most convenient route to the tri-aminooxy. The intended route is shown in **Scheme 17**.

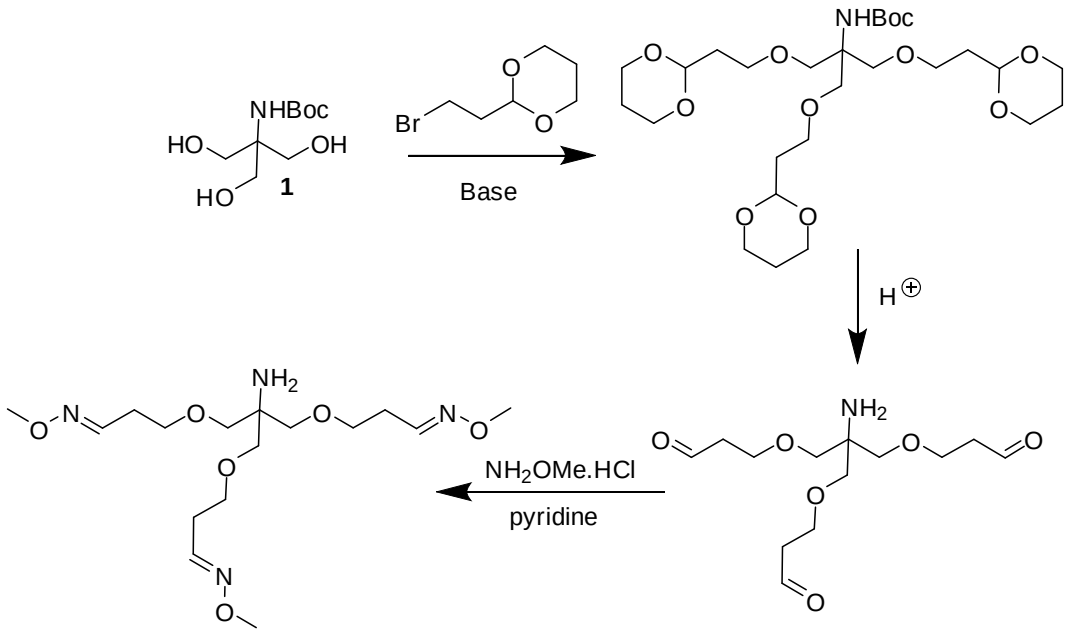


**Scheme 17:** Proposed route to tri-oxime scaffold

Direct coupling of aldehydes seemed likely to be problematic: formation of hydrates can occur under the basic conditions used in the substitution reaction, suitable short linkers are not readily commercially available and common synthetic routes involve forcing conditions heating in strong acid.[89] Synthetically, 3-bromopropanal is commonly used to introduce bromide functionality[90, 91] while 2-bromoethanal is generally used to create fused ring systems.[92, 93] Both applications suggest that the aldehydes are reasonably reactive and that protection would be a sensible precaution to prevent side reactions.

2-bromoethyl-1, 3-dioxane was chosen as a simple, commercially available molecule with masked aldehyde functionality. The dioxane protecting group can be easily removed with acid and the subsequent steps, shown on benzaldehyde in **Scheme 18**, which proceed in good yield on a wide variety of scaffolds are a common route to the desired aminooxy functionality. [94, 95, 96]

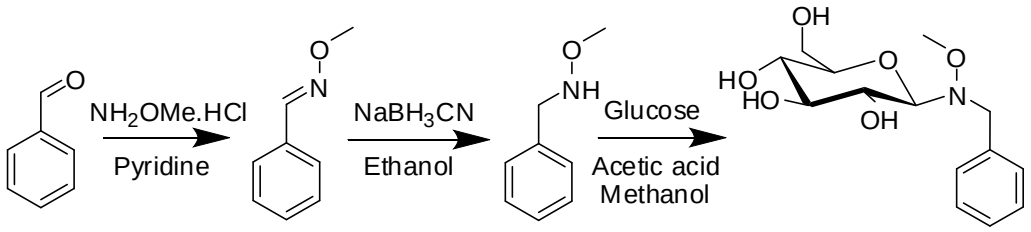


**Scheme 18:** Common synthetic route to aminooxy functionality and neoglycoside equivalent.[77, 97, 98]

The reaction shown in **Scheme 19** was attempted under a variety of conditions, using different bases, additives, and equivalents of reagents (**Table 2**). Where a mixture of water and THF was used, the hydroxides were added as an aqueous solution, in dry solvent they were added as a finely ground powder. In each case the Tris scaffold was mixed with the base then the dioxane was added. All reactions were carried out overnight.

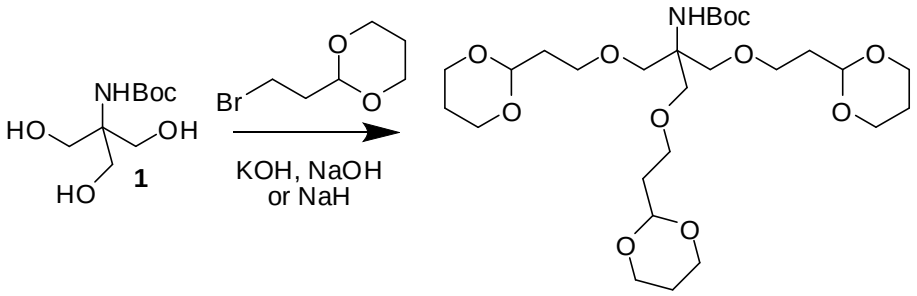


**Scheme 19:** Proposed method to couple Tris and 2-bromoethyl-1, 3-dioxane

| Equiv Dioxane | Base | Equiv Base | Solvent | Temp | Additives |
|---|---|---|---|---|---|
| 5 | KOH | 4 | THF:water | RT | NA |
| 5 | NaOH | 4 | THF:water | RT | NA |
| 5 | NaH | 4 | dry DMF | RT | NA |
| 5 | NaH | 4 | dry THF | RT | NA |
| 5 | KOH | 4 | dry DMF | RT | NaI |
| 5 | NaH | 4 | dry DMF | RT | NaI |
| 5 | KOH | 6 | dry DMF | RT | NA |
| 6 | KOH | 6 | dry DMF | 50$^{o}$C | NA |

**Table 2:** Conditions for coupling attempts

Under the conditions tested coupling to the Tris scaffold was not detected by proton or carbon NMR. 2-Bromoethyl-1, 3-dioxane was recovered in all cases, often as a mixture with 2-vinyl-1,3 dioxane which was produced by decomposition of the starting material under basic conditions. The Tris starting material was detected but not recovered as its high aqueous solubility meant it was removed during the work up.

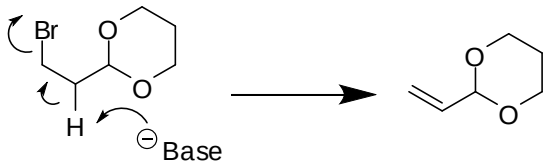


**Scheme 20:** Decomposition of 2-bromoethyl-1,3 dioxane via E2 elimination.

A greater proportion of the alkene side product was observed when sodium hydride was used as the base. Since the electrophile used in this case is a primary alkyl halide the elimination mechanism is likely to be E2 and the desired substitution is likely to be $S_N2$. E2 elimination is encouraged by stronger, less hindered bases, so recovering a greater proportion of the elimination product with sodium hydride is not surprising. The mechanism for this decomposition is shown above in **Scheme 20**.

Generally the vinyl-1,3 dioxane was recovered and no coupling with the Tris was detected. Since no coupling was observed it was concluded that the Tris scaffold was unreactive towards the dioxane.

An alternative strategy was envisioned using tri-nitrile substituted Tris and followed by conversion to the tri-aldehyde. The tri-nitriles shown below in **Scheme 21** had been previously synthesised in good yield and was chosen partly on this basis.[99]

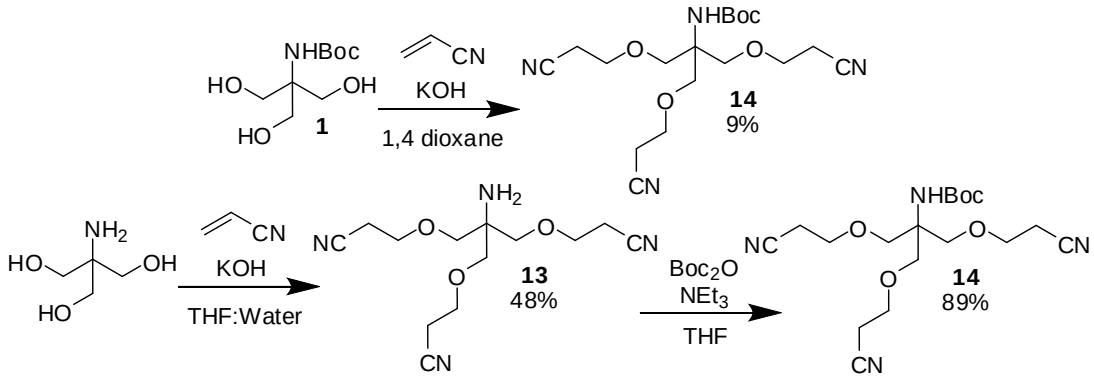


**Scheme 21:** Synthesis of tri-nitrile Tris compounds **13** and **14**.

Compound **14** was originally synthesised from Boc protected Tris **1,** however the yield using this method was much lower (9%) and as a result the procedure illustrated above in **Scheme 21** was preferred.

Presence of the Boc group in **14** was suggested by a prominent carbonyl peak in the IR at 1708 $cm^{-1}$ and confirmed by strong, characteristic peaks in the proton and carbon NMR. Strong peaks for Boc methyl groups were found at 1.42 ppm in the proton and 28.4 ppm in the carbon NMR, while the carbonyl was present at 154.9 ppm.

The presence of the nitrile groups was supported by IR with signals in at 2251 $cm^{-1}$ for both **13** and **14** characteristic of aliphatic nitriles. Further support came from the carbon NMR with the nitrile carbon present at 118.1 ppm for **13** and at 118.0 ppm for **14**. Structures of both compounds were confirmed by mass spec, $MNa^+$ ions were found for both **13** and **14** at 302.9 m/z and 403.0 m/z.

Although multiple reagents are used for conversion of nitriles to aldehydes in the literature more reactive reducing agents, such as diisobutylaluminum hydride (DIBAL) and lithium aluminium hydride are necessary for the reaction to proceed in aliphatic nitriles.[100] Reaction with lithium aluminium hydride and metal hydrogenation catalysts can risk reducing nitriles too far. DIBAL is known to reliably produce the aldehyde. It was thought that using DIBAL would prevent the formation of mixed products, with a combination of terminal aldehyde, alcohol and possibly amine functionalities on the scaffold.

Conversion was attempted both with the Boc protected (**14**) and unprotected tri-nitrile scaffold **(13)**. Different reaction times, temperatures and quenches were used (**Table 3)**. Dry solvents and glassware were used throughout and 4.5 equivalents of DIBAL were added over at least five minutes in each case. The initial test reaction was conducted using DIBAL that was over a year old and the starting material was recovered which led to replacement of the DIBAL stock. The DIBAL used subsequently had been open for less than a month, ensuring that degradation of this reagent was not a factor.

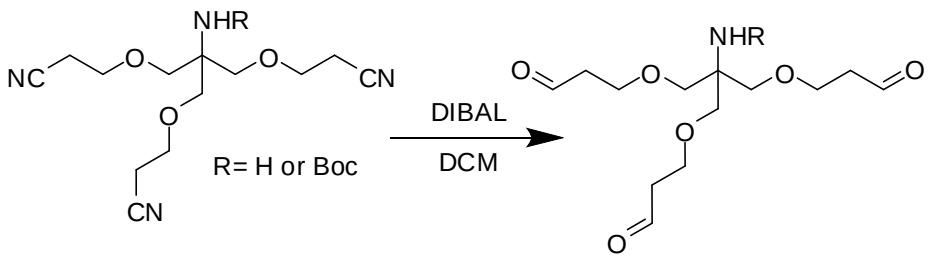


**Scheme 22:** Proposed route to tri-aldehyde via nitrile, from compounds **13** (unprotected) and **14** (Boc protected).

| Starting Material | Time | Quench | Temp $^{o}C$ |
|---|---|---|---|
| **13** | 20min | water | -5 |
| **13** | 1 hr | water | -5 |
| **13** | 2 hr | water | -5 |
| **13** | 3 hr | water | -5 |
| **14** | 1 hr | water | -5 |
| **14** | 2 hr | water | -78 |
| **14** | 2 hr | methanol | -78 |

**Table 3:** Conditions for attempted nitrile conversion

Unfortunately no aldehyde conversion was detected under the reaction conditions used. Use of active DIBAL resulted in significant mass loss with only the starting material and solvents readily identifiable in the crude. A greater proportion of starting material was recovered when shorter reaction times were used and when the Boc protected **14** was used under comparable conditions. Conducting the reaction at lower temperature and varying the quench in an attempt to reduce decomposition did not improve the reaction.

Typical proton NMRs of the crudes produced showed strong peaks corresponding to the starting material and DCM. Experiments using **13** showed multiple broad peaks in the region 1-2 ppm, likely decomposition products, and multiple small peaks at approximately 9.8 ppm which could be residual aldehyde containing compounds. Any aldehyde present was in minority, with integration of the collected peaks having a ratio of approximately 1:18 compared to one proton from the starting material. Experiments using **14** showed less of the broad decomposition peaks upfield and a higher proportion of possible aldehyde peaks at 9.8 ppm (ratio of approximately 1:9 compared to one starting material proton). Formation of some aldehyde was supported by carbon NMR, showing a small peak at 201.15 ppm. Longer reaction times at lower temperature, in an attempt to assure conversion while reducing decomposition, resulted in greater mass loss and the absence of even small quantities of aldehyde from the crude.

It was concluded that either the aldehyde was formed but unstable or the starting materials used decomposed under the reaction conditions more quickly than the aldehyde was formed.

Finally, inspired by Willand-Charnley *et al*, a strategy was developed based on ozonolysis. Work by this group suggests that pyridine catalyses ozonolysis reactions.[101] This was of interest since the standard conditions used to convert aldehydes to oximes are stirring with an aminooxy salt in the presence of a tertiary amine base such as pyridine.[98, 102] A one-pot, two step conversion directly to the desired tri-oxime was envisioned (**Scheme 23**).

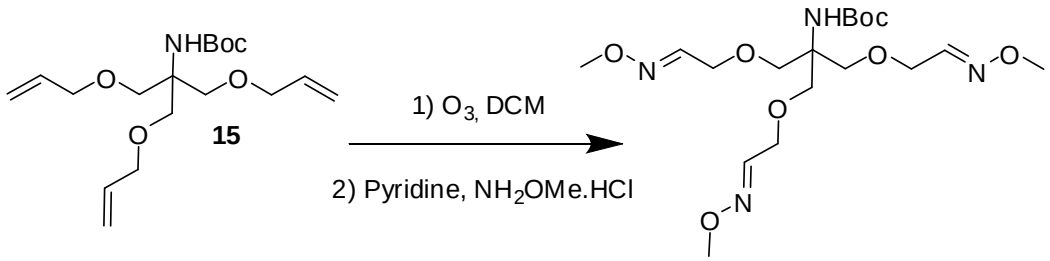


**Scheme 23:** Proposed one-pot ozonolysis conversion

In order to confirm that conversion to the oxime was possible under ozonolysis conditions, a test reaction was carried out using styrene. The reaction was carried out under standard ozonolysis conditions, all reagents and solvents were dried and a mixture of pyridine and dichloromethane used as solvent (1.1:1). 2.5 equivalents of O-methylhydroxyamine hydrochloride was added, the mixture cooled to -78$^{o}$C and ozone bubbled through for 45 minutes. The reaction was then purged with oxygen and quenched with dimethylsulfide. The mixture was extracted and washed with water repeatedly to reduce the presence of pyridine before investigation of the crude mixture by proton and carbon NMR.

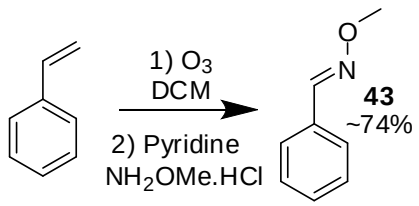


**Scheme 24:** One-pot conversion of alkene to oxime

Styrene was completely consumed. Formation of both benzaldehyde and O-methylbenzaldehyde oxime **43** was observed by NMR but the mixture was not purified and the oxime not isolated. Characteristic peaks for both compounds were clearly visible in the proton spectrum, the initial mixture was estimated to be 7:3 oxime to aldehyde with pyridine also present. The presence of both compounds was further confirmed by carbon NMR. The mixture was then left to stir overnight, since oxime formation was expected to be the slower reaction. The proportion of oxime compared to aldehyde was indeed seen to increase, though only slightly. The conversion under these conditions was estimated at 74% by integration of proton NMR peaks.

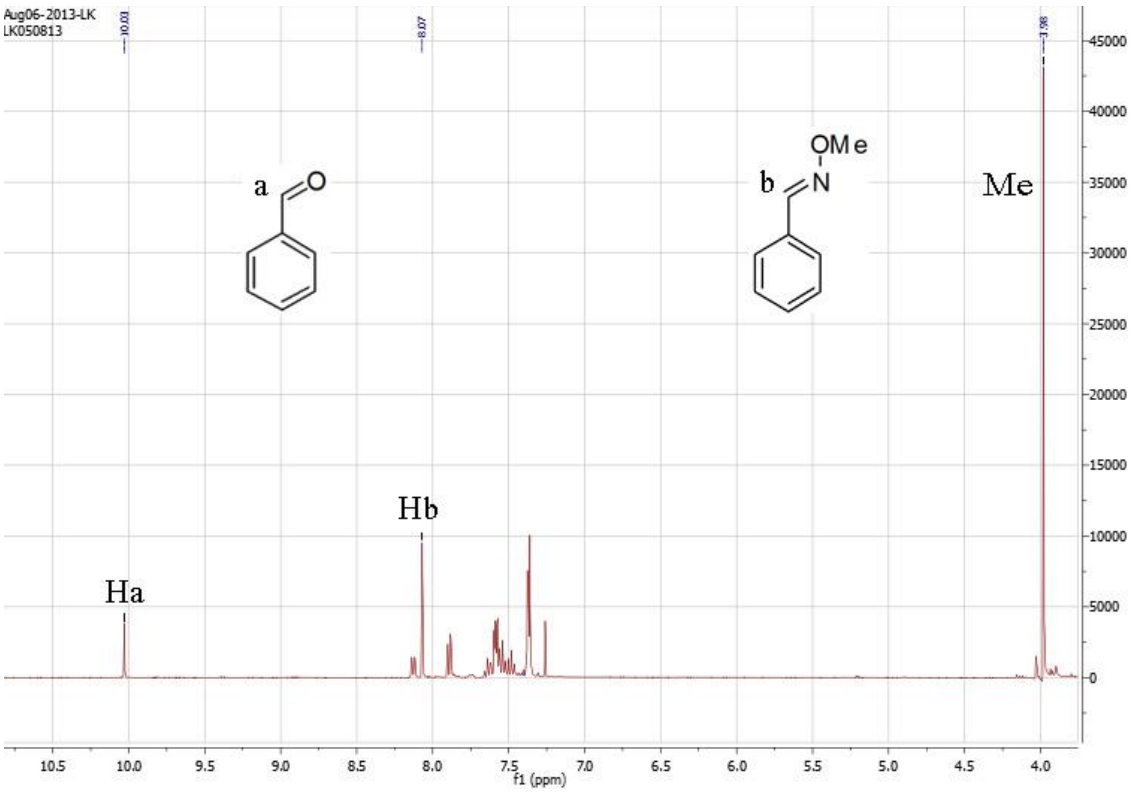


**Figure 35:** Proton NMR of one pot ozonolysis reaction in the presence of O-methylhydroxylamine hydrochloride ($H_2NOMe.HCl$) with styrene in $CDCl_3$.

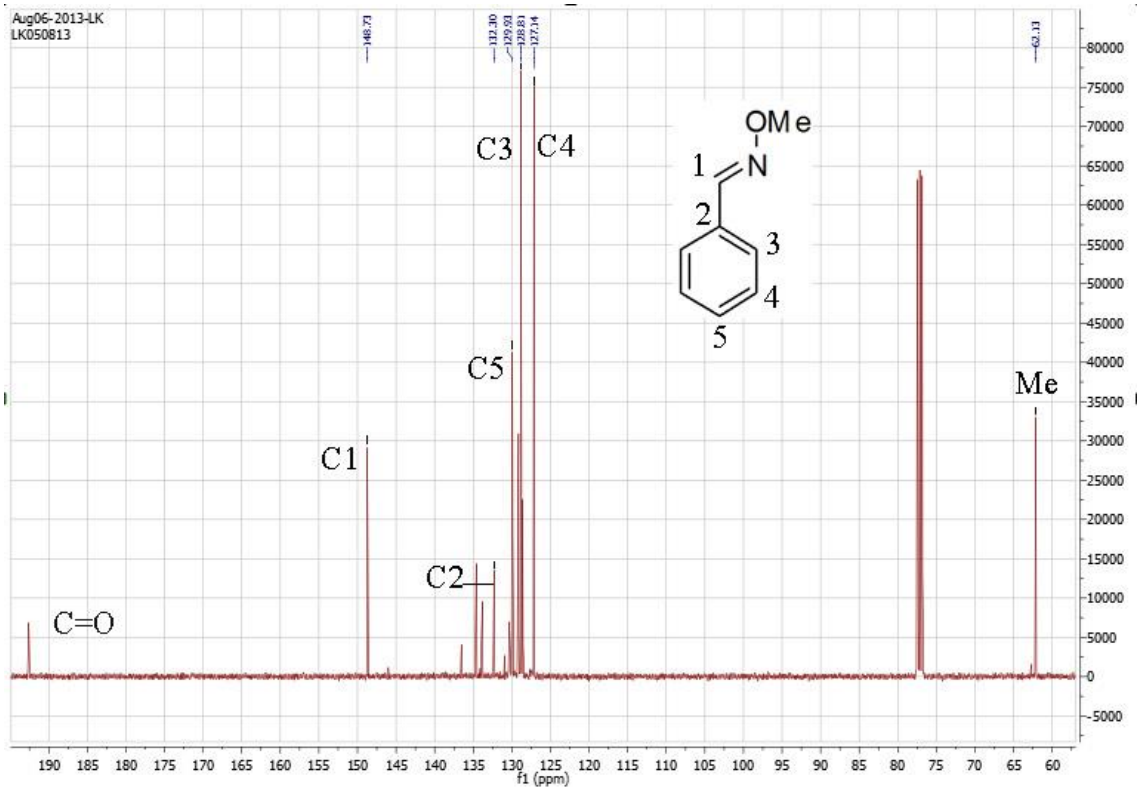


**Figure 36:** Carbon NMR of one pot ozonolysis reaction in the presence of O-methylhydroxylamine hydrochloride ($H_2NOMe.HCl$) with styrene in $CDCl_3$. Aldehyde peak and O-methylbenzaldhye oxime peaks highlighted. Allyl peaks absent.

Encouraged by this result tri-allyl Tris compound **15** was synthesised as shown below in **Scheme 25**.

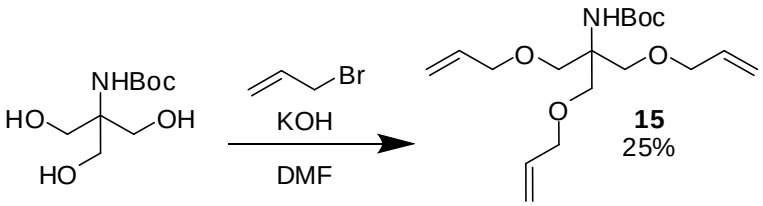


**Scheme 25:** Synthesis of tri-allyl Tris **15**

Proton and carbon NMR both strongly suggested the reaction had been successful. The allyl CH was observed at 5.93-5.83 ppm in the proton and at 134.9 ppm in the carbon while the terminal $CH_2$ carbon was seen at 116.9 ppm with proton peaks at 5.28-5.14 ppm, consistent with the product. The structure was confirmed by mass spec with a significant mass ion at 364.0 m/z, consistent with $MNa^+$.

Once satisfied that **15** had been synthesised the one pot ozonolysis reaction was attempted. Conditions used were similar to the conditions used in the styrene test reaction (three equivalents of aminooxy salt per allyl group were used in reaction with **15**). Unfortunately neither aldehyde nor oxime were detected by NMR.

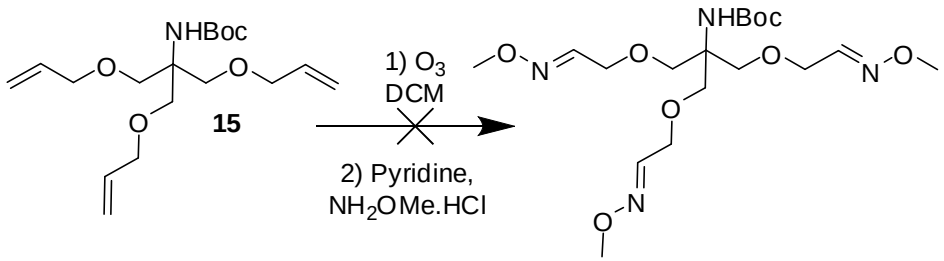


**Scheme 26:** One pot ozonolysis reaction attempted with tri allyl Tris compound **15**

The crude was subjected to two different work up conditions in order to ensure that aldehyde or oxime containing products were not being removed by, or reacting with, aqueous washes. Aqueous organic extraction resulted in an NMR spectrum that mostly showed solvent peaks. A group of broad peaks at 1.57-1.41 ppm might have represented the Boc group but other characteristic peaks relating to the scaffold, including methylenes, methoxy and allyl peaks were absent.

Alternately, concentrating the crude and washing with small volumes of hexane did not entirely remove pyridine or the DMSO side product caused by quenching the ozonolysis reaction. No obvious aldehyde or oxime peaks were observed. Small peaks were seen at 1.32, 1.26, 3.97 and 3.70 ppm. These did not seem to correlate to peaks on the intact Tris scaffold.

A carbon NMR was taken of this sample in an attempt to understand what the mixture was decomposing in to and confirm that mixed allyl, aldehyde and oxime substituted scaffolds were not present. DMSO was clearly visible and although at first glance it appeared to contain pyridine the expected peak at 136.0 ppm was absent. The loss of peaks at 134.9 ppm and 116.9 ppm confirmed that the allyl functionality had been completely consumed during the reaction. Unidentified peaks were observed at 163.3, 143.4, 143.3, 126.3 and 28.0 ppm. The minor peak at 28.0

ppm suggested Boc methyl groups but the corresponding carbonyl peak at approximately 155 ppm was not visible. The peak at 163.3 ppm was too low to represent aldehyde formation and higher than usual for an oxime, which generally occur at 155-145 ppm[103, 104] although they can come in the mid to high 160s when electron withdrawing groups are present.[105] The two prominent peaks at 143 ppm were also within the range of possible oxime shifts but the absence of a peak at approximately 62 ppm showed the expected methoxy was not present. The lack of peaks at approximately 75-70 ppm suggested both methylene groups associated with the scaffold were absent.

It was concluded that the starting material was completely decomposing into an unidentifiable mixture, possibly on warming the ozonolysis mixture to room temperature. As oxime formation is probably the slow step and allyl groups were consumed during the reaction, it seemed likely that the aldehyde was formed and decomposed.

It seemed reasonable at this point to assume that any aldehyde containing Tris scaffold formed was unstable. The mass loss observed during attempted nitrile conversions, combined with the lack of intact Tris in the ozonolysis mixture, supported this conclusion.

Common alternative approaches to the desired aminooxy include substitution and conversion of phthalimide, which is cleaved with hydrazine, converted to an oxime and then reduced giving an R-O-N structure that links the aminooxy to the desired scaffold. An example is shown in the scheme below.

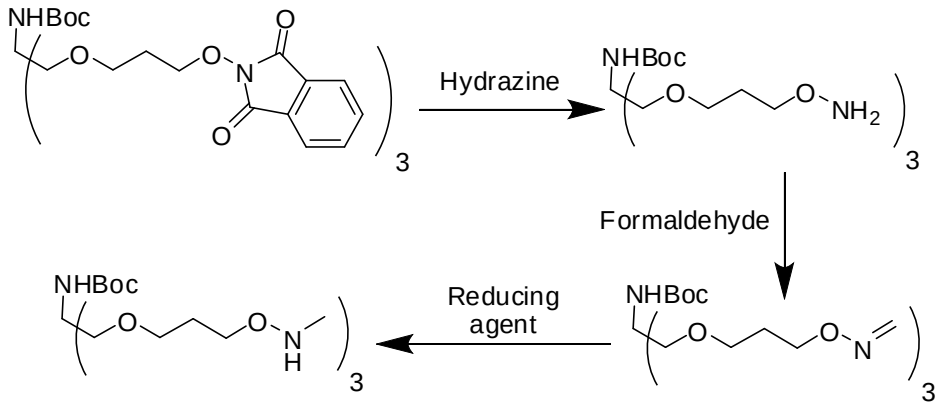


**Scheme 27:** An alternative strategy for introducing aminooxy groups

Although it was considered, this standard route required multiple synthetic steps on the scaffold and multiple purifications also seemed likely. A shorter, or convergent, route was thought to be more convenient. With this in mind we began to consider click chemistry as a method for introducing aminooxy functionality.

## 3.3 Using click chemistry to attach aminooxy functionality

As synthesising the tri-aldehyde scaffold had so far failed, with degradation under relatively mild conditions, an alternative approach seemed necessary. Propargyl groups had previously been coupled to Tris scaffolds as part of the project (see **Chapter 2**) and click reactions with azide linked monosaccharides had been carried out successfully, though yields varied. Using click chemistry to attach aminooxy functionality directly therefore seemed like a reasonable route to the target scaffold shown below.

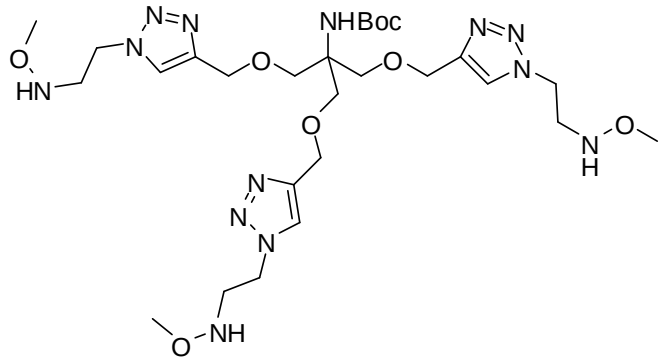


**Figure 37:** Target tri-aminooxy Tris scaffold

Attention shifted to producing a small linker containing both aminooxy and azide functionality. Ideally the link between them would be an ethyl chain since this would give any sugar substituted aminooxy scaffolds the same size and spacing between sugars as equivalents synthesised by directly clicking azide linked sugars to the tri-propargyl scaffold **2**. Any difference in lectin binding between them would then be due to the differing functionality at the anomeric position or the labile nature of the aminooxy bond.

The previously synthesised azido-ethanol **3** seemed a reasonable starting point. It was proposed that the alcohol group could be replaced with the target aminooxy via a simple substitution by first converting the alcohol to a tosyl group (**Scheme 28**).

Concurrently a route starting from bromoethanol was investigated since direct conversion from alcohol to azide groups is known (**Scheme 28**).[106, 107]

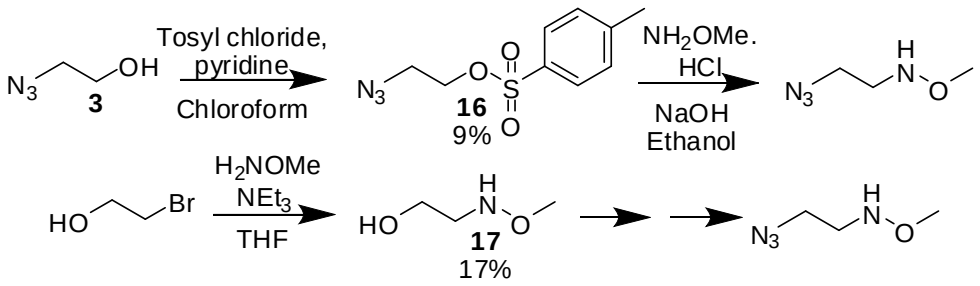


**Scheme 28:** Proposed routes to azide, aminooxy linker

Synthesis of 2-azidoethyl tosylate **16** was straightforward but low yielding (9%). The tosylate **16** was refluxed in ethanol with three equivalents of the aminooxy salt and sodium hydroxide was added (to produce the neutral O-methylhydroxylamine *in situ*). The mixture was monitored by periodic NMR of samples taken from the reaction. Over three days the observed tosylate **16** decreased but product formation was not observed. As a result this route was abandoned.

The alternative route, starting from bromoethanol, to give of 2-methoxyamino ethanol **17** was similarly low yielding although it was improved by using a solution of the free O-methylhydroxylamine rather than the equivalent hydrochloric salt (from 4% to 17%). An attempt was made to convert **17** directly to the desired azide using conditions similar to those suggested by Rokhum *et al* illustrated below in **Scheme 29**.[107] This paper theorised that by adding sodium azide to a mixture classically used to convert alcohols to iodides the desired azide might be isolated in a one-pot process, they successfully applied the method to a variety of alcohols. The reported reactions were fast and high yielding.[107]

A solution of the alcohol **17**, sodium azide and imidazole was mixed with a solution of triphenylphosphine and iodine. The mixture was monitored by periodic proton

NMR, with samples removed, quenched with sodium thiosulfate solution, extracted with ethyl acetate and subjected to a small-scale aqueous work up. Neither the desired product nor the alcohol starting material were detected by NMR, although triphenylphosphine and imidazole were both visibly present. Absence of the expected triplets was especially troubling as it indicated that the ethyl chain was missing.

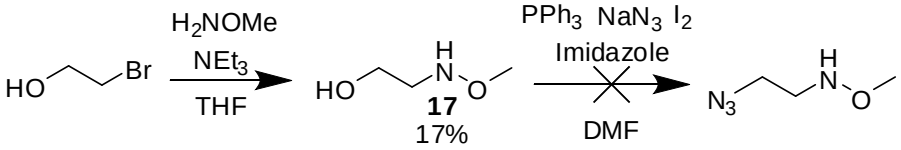


**Scheme 29:** Direct conversion of 2-methoxyamino ethanol to N-(2-azidoethyl)methylhydroxyamine failed

Given the disappearance of the starting materials in both reactions and the absence of obvious side products it seemed reasonable to conclude that the product was forming and either unstable or difficult to isolate. In both cases only the reaction solvent and additives such as triphenyl phosphine were observed by NMR after aqueous work up. High aqueous solubility or low boiling point were both possible and would have made the product extremely difficult to isolate with the work up conditions employed.

To reduce any instability and avoid complicated work up procedures, O-methylhydroxylamine was Boc protected, which should limit the possibility of side reactions, raise the boiling point and lower the aqueous solubility of the resulting linker. Boc groups could be removed once the azide linker had been coupled to the desired scaffold, giving the free aminooxy as planned.

Initially reaction directly with bromoethanol was attempted, as shown in **Scheme 30** and detailed in **Table 4**, in the hope of avoiding further protection and deprotection steps. Reactions using triethylamine as the base also used it as the reaction solvent, while reactions with sodium hydride used dry THF. Initial reactions with triethylamine, using two equivalents, were conducted in the dark although subsequent reactions were carried out allowing exposure to light with no difference

in results. In each case the expected product was not detected though both starting materials were present. The reactions were monitored by periodic NMR of samples but later synthesis and characterisation of the target compound **21** confirmed that the product was not present.

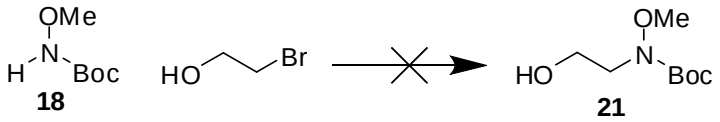


**Scheme 30:** Attempted coupling of bromo ethanol and Boc-protected aminooxy

| Base | Time | Temperature $^{o}C$ | Equiv Base |
|---|---|---|---|
| $NEt_3$ | 2 days | RT | 2 |
| $NEt_3$ | 3hr | 50 | 2 |
| $NEt_3$ | 5hr | 50 | 2 |
| $NEt_3$ | 5hr | 50 | 3 |
| $NEt_3$ | overnight | 50 | 2 |
| NaH | 1hr | RT | 1.1 |
| NaH | overnight | RT | 1.1 |

**Table 4:** Conditions used for attempting reaction of bromoethanol and Boc protected aminooxy **18**

Triethylamine was initially used as the base since it was expected that the pKa of the aminooxy based material would be much lower than the pKa of bromoethanol which is thought to have a pKa of 13-14. The pKa of O-methylhydroxylamine and N,O dimethylhydroxylamine are known to be approximately 4.60 and 4.75 respectively, the Boc protected aminooxy derivative was expected have a similar pKa or lower due to the conjugating effect of the Boc carbonyl.[108] It was therefore expected that even an excess of triethylamine would deprotonate the aminooxy group in preference to the alcohol.

Use of a stronger base such as sodium hydride would have ensured deprotonation of the aminooxy starting material **18** but even under these conditions no product formation was observed. Before NMR monitoring, sodium hydride reactions were

quenched with methanol and concentrated while the concentrated triethylamine reactions were diluted with deuterated solvent. Under these conditions previous issues due to possible water solubility or low boiling points seemed unlikely to be the problem. The most likely explanation for the lack of observed product was that the reaction was simply not occurring.

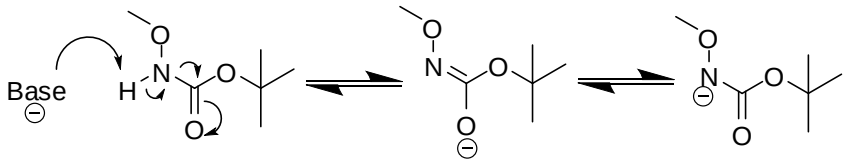


**Scheme 31:** Possible resonance structures of the deprotonated aminooxy starting material, **18**

This could be due to the presence of the Boc group which stabilises the conjugate base as shown by the resonance structures in **Scheme 31**. If sufficiently stabilised the anion may not react with bromoethanol. Alternative protecting groups would prevent this problem but the use of Boc was particularly attractive as it would allow aminooxy groups and the amine of the eventual scaffold to be deprotected simultaneously.

More forcing conditions could have been applied in an attempt to drive the reaction but it seemed likely to result in the degradation of the starting materials and result in the alcohol group participating in side reactions.

Instead bromoethanol was acetate protected, giving **19**, to prevent the alcohol participating in the reaction. Since the aminooxy starting material **18** was thought to be stable the reaction was originally conducted using an excess of sodium hydride (3 equivalents) to ensure deprotonation of **18**, while a small amount of iodine (0.1 equivalents) was mixed with the acetate protected starting material **19** in order to produce the more reactive 2-iodoethyl acetate *in situ*. Product was detected by proton NMR of the crude mixture when the procedure was performed using dry solvents, in the dark, overnight with a two-fold excess of 2-bromoethyl acetate, **19**.

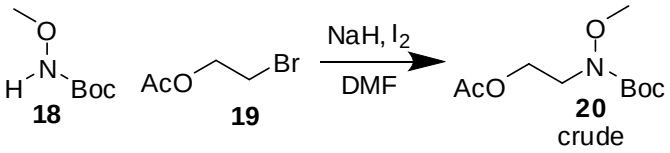


**Scheme 32:** Initial coupling conditions for production of **20**

Shifts in the suspected $CH_2$ signals adjacent to the bromine or aminooxy group from 3.50 ppm to 3.72 ppm strongly suggested product formation, but this put the $CH_2$ signal in the same region as the expected methoxy signal. COSY experiments confirmed that the signal at 3.71-3.68 ppm was interacting with a signal at 4.23 ppm, suggesting that these were the ethyl protons. HSQC showed that the signal at 3.71-3.68 ppm was made up of two environments, with carbons at 62.5 ppm and 47.9 ppm consistent with the expected ethyl and methoxy groups rather than impurities. This confirmed the idea that the multiplet represented overlapping ethyl and methoxy peaks. Successful synthesis was further confirmed by carbon NMR and mass spectrum.

However the product could not be isolated. Attempts at column chromatography on silica resulted in significant loss of material with proton NMRs of isolated fractions showing more peaks, especially those associated with degradation, than the original crude. After several unsuccessful attempts it was theorised that the product **20** was either reacting with, or sticking to, the silica column. Adding clean, dry silica to NMR samples of the crude material caused a loss of the product signals. Attention therefore shifted from purification method to the reaction procedure in the hope that a higher quality crude could be produced and used without further purification.

Replacing iodine with sodium iodide, which is a better source of iodide in solution, resulted in reduced observable side products. The major impurities in the crude when this method was used were DMF (the chosen solvent) and 2-bromoethyl acetate **19,** which could both be significantly reduced by repeated aqueous washes and long periods under vacuum.

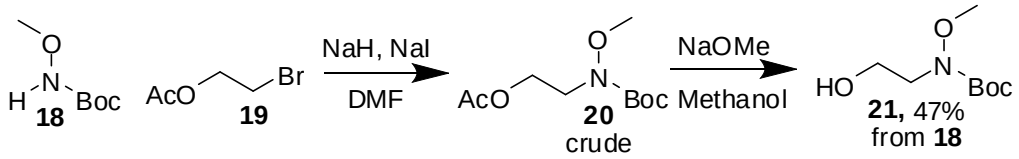


**Scheme 33:** Synthetic route to tert-butyl 2 hydroxyethyl(methoxy)carbamate

Following these adjustments to the procedure acetate deprotection was attempted on crude **20**. This was successful under Zemplén conditions as shown in **Scheme 33**. Aqueous work up was avoided in case the product was water soluble, the mixture was instead filtered through activated protonated cation exchange resin and solvent removed giving the expected alcohol **21** in reasonable yield (47% over two steps from **18**) and good purity.

Once isolated direct conversion of the alcohol to an azide was attempted again. Initially the conditions favoured by Rokhum *et al* were used and the reaction progress investigated by NMR.[107] Samples were quenched with sodium thiosulfate solution, extracted with chloroform, subjected to aqueous washed and dried over magnesium sulfate before the residual solvent was removed. A sample was taken after an hour, as there was a rapid loss of colour in the mixture over this period, but the NMR showed only starting materials. Further samples were taken after leaving the mixture overnight with the same result.

A similar strategy was then attempted, using a mixture of triphenyl phosphine, tetrabromomethane and sodium azide in dry DMF as shown below in **Scheme 34**. As with the previous method the reagents facilitate the conversion of an alcohol to a halide, which is then converted *in situ* to the desired azide. After stirring overnight only the starting materials were detected by NMR.

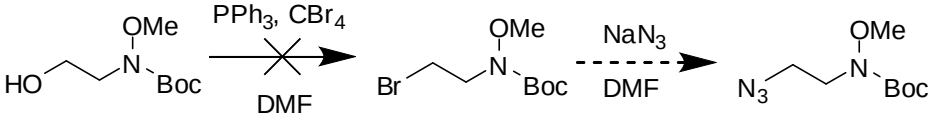


**Scheme 34:** One pot conversion of alcohol to azide via halides was unsuccessful

As the starting materials were recovered it seemed reasonable to assume that conversion to the halide was not taking place under the conditions employed. An

alternative strategy utilising a combination of DPPA, DBU and sodium azide was next attempted. This method produces an activated phosphate compound which then reacts to form the desired azide.

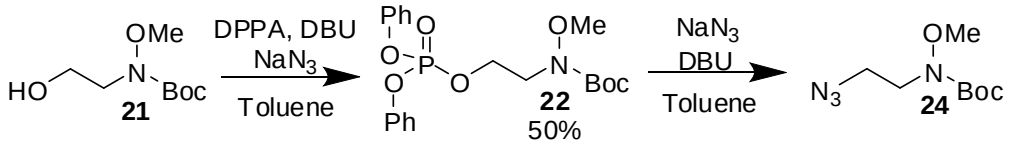


**Scheme 35:** Proposed one-pot route to azide linker, **24**

The reaction was conducted under anhydrous conditions and stirred overnight before quenching with dilute acid and extracting with chloroform. As proton NMR of the crude showed a combination of starting materials and possible products the mixture was purified by column chromatography on silica.

The isolated product was originally thought to be a mixture of the desired azide co-eluting with a phenyl phosphate as there was a clear shift in ethyl triplets in the proton NMR but aromatic peaks were also still present. Purification by column chromatography was attempted a second time but the mixture appeared no purer which prompted further characterisation to confirm that the mixture contained azide.

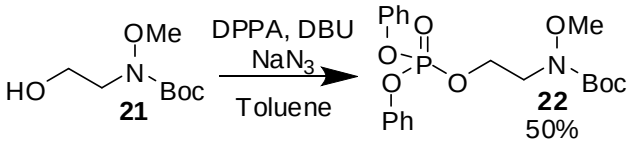


**Scheme 36:** Synthesis of phosphate **22**

IR spectroscopy was deemed unsuitable: excess DPPA had been used and if the observed phenyl peaks were due to DPPA an azide peak would be visible at approximately 2100 $cm^{-1}$ even if the desired product was not present. Phosphorous NMR confirmed that a single phosphate environment was present in the mixture. Close examination of the carbon NMR revealed splitting in both the aromatic and $CH_2$ environments of the linker. This indicated that the phosphorous was in close proximity to the ethyl chain. Both $CH_2$ peaks appeared as doublets: at 65.23 ppm with a coupling constant of 6.2 Hz and at 49.66 ppm with a coupling constant of 8 Hz. This suggested that the pure phosphate **22** had been isolated rather than a

mixture of azide and phosphate containing components. Mass spectra confirmed that **22** had been synthesised.

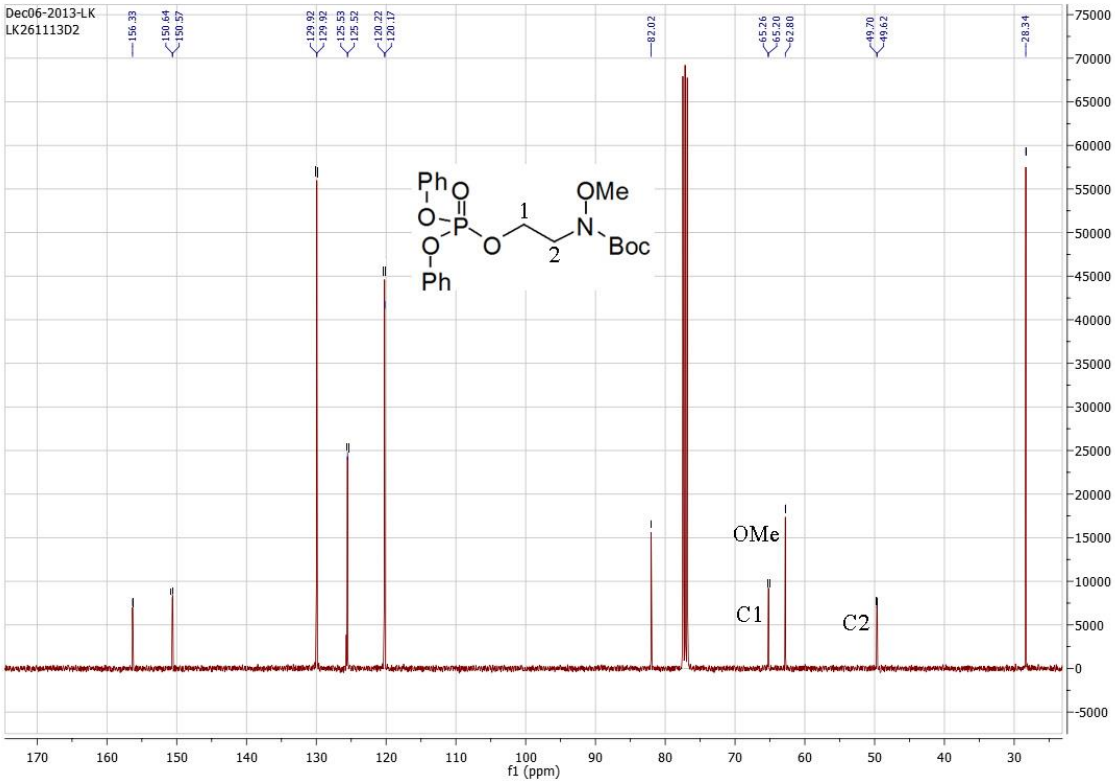


**Figure 38**: Carbon NMR of phosphate **22** with splitting in the aromatic and ethyl carbons shown.

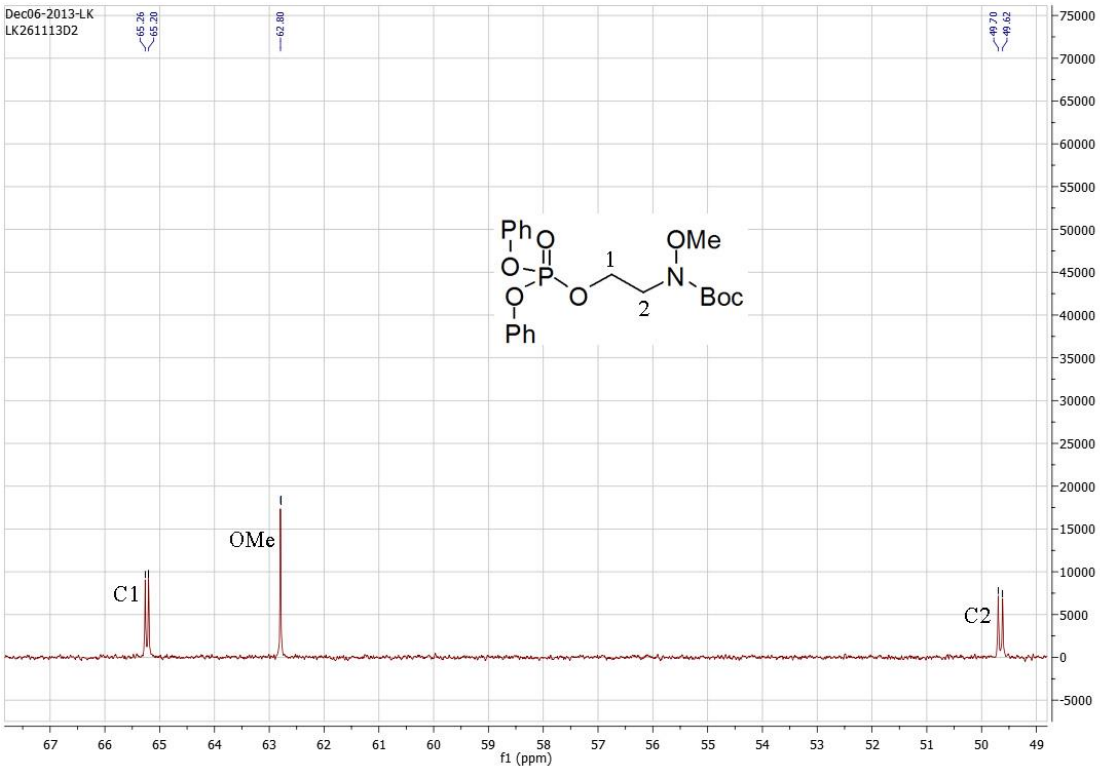


**Figure 39:** Carbon NMR of phosphate **22** with O-$CH_2$ and methoxy carbons shown, splitting in O-$CH_2$ present.

Several attempts were then made to convert the phosphate **22** to the desired azide (**Scheme 37**). The progress of the reaction was monitored by phosphorous NMR, if conversion to the azide occurred then new phosphorous peaks were expected to appear. The phosphate was dissolved in 1,4 dioxane, a large excess of sodium azide added and heated to 50$^{o}$C. NMRs were taken after three hours and after leaving overnight but the phosphate starting material still visible in each. The mixture was then heated to reflux. After stirring overnight the results were investigated by NMR and once again only the starting material was observed. Finally an excess of DBU was added to the refluxing mixture in order to further solubilise the sodium azide. After refluxing overnight the mixture was then extracted with chloroform, washed with brine, dried over magnesium sulfate and the solvent removed. This gave a pale oil which appeared to be a mixture of DBU, starting material and degradation products by NMR.

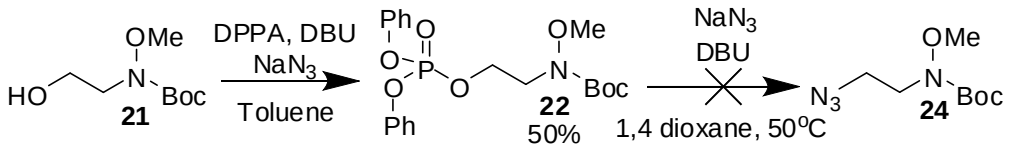


**Scheme 37:** Isolated phosphate could not be converted to azide

Following failure to produce the azide from the isolated phosphate the idea of a one-pot conversion directly from alcohol **21** was abandoned in favour of a traditional two step procedure. Mesylate **23** was synthesised in reasonable yield with no further purification necessary as shown in **Scheme 38**.

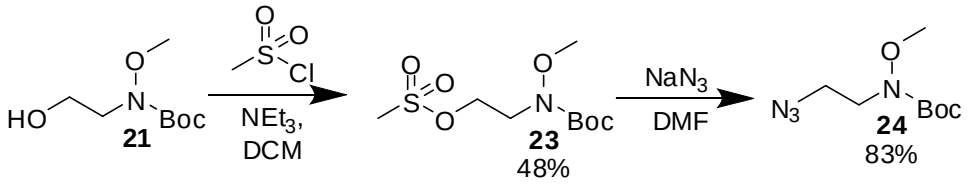


**Scheme 38:** Proposed synthetic route to the azide **24** via mesylate substituted linker **23**

The mesylate was originally identified by proton and carbon NMR. As expected the O-$CH_2$ triplet shifted from 3.77 ppm to 4.36 ppm, shift in the N-$CH_2$ triplet from 3.60 ppm to 3.78 ppm was also observed along with a characteristic singlet at 3.02 ppm for the sulfonate methyl group. The sulfonate methyl was also observed in the carbon NMR at 37.7 ppm. Its identity was confirmed by IR spectroscopy, which showed strong peaks at 1350 $cm^{-1}$ and 1171 $cm^{-1}$, consistent with sulfonate groups, along with a lack of the distinctive peak at 3435 $cm^{-1}$ showing that the alcohol was no longer present. The assignment was further supported by mass spectroscopy, with a mass ion 292.1 m/z found in positive ion electrospray, consistent with $MNa^+$.

Conversion to the azide (**24**) was successful though slow but yields were improved by warming the mixture to 50°C. However full characterisation proved problematic. Characteristic IR peaks suggested the product had been synthesised and changes of shift in the proton and carbon NMR confirmed this. Sulfonate peaks were absent from the IR while a strong peak at 2100 $cm^{-1}$ indicated the presence of azide. Likewise proton and carbon NMR strongly suggested the synthesis was successful.

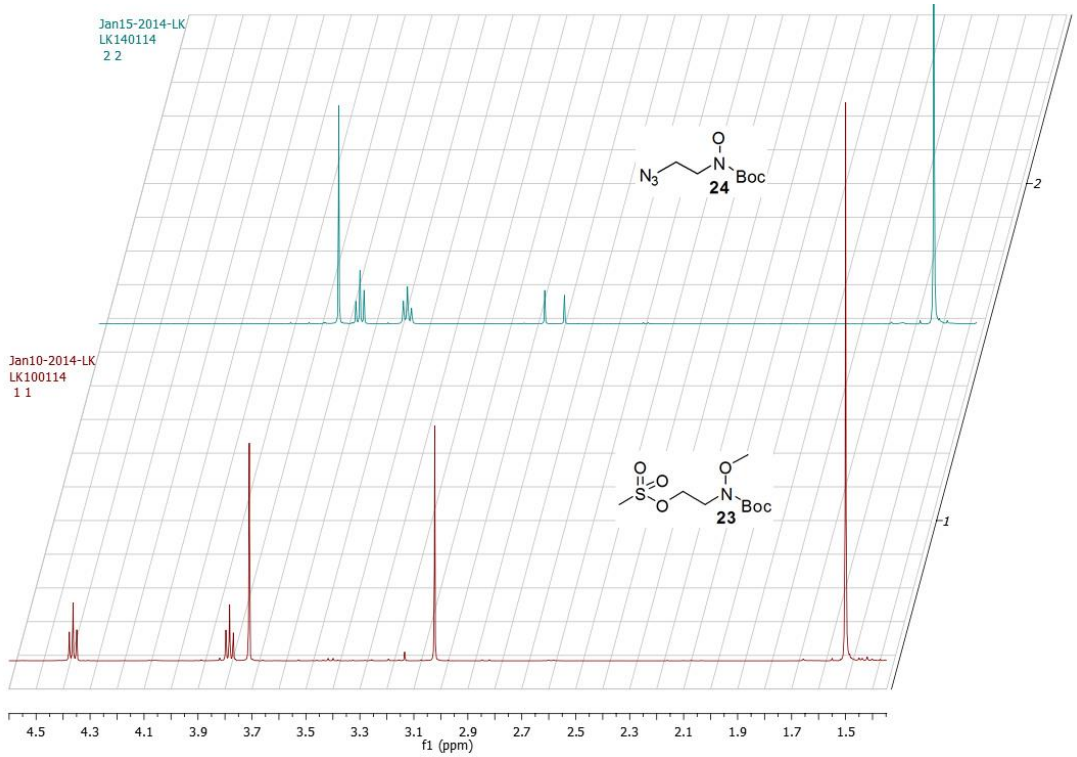


**Figure 40:** Comparison of proton NMRs for mesylate **23** and azide **24**

Sulfonate associated peaks were absent from the proton and carbon while large shifts were observed for both $CH_2$ groups in the proton and for the azide bound carbon in the $C^{13}$ spectrum. Triplets associated with $CH_2$ were detected at 3.63 ppm and 3.46 ppm, consistent with displacement of the sulfonate in favour of a less electronegative group. A similar result was seen in the carbon spectrum, with both $CH_2$ carbons appearing upfield compared to the methoxy; the alpha carbon underwent a shift from 62.7 ppm in the mesylate to 48.5 ppm in the azide. Despite this evidence strongly suggesting the presence of product, confirmation by mass spectroscopy was not possible. Multiple attempts to obtain spectra using electrospray were made and a sample was submitted for accurate mass but in all cases the mass ion was not detected.

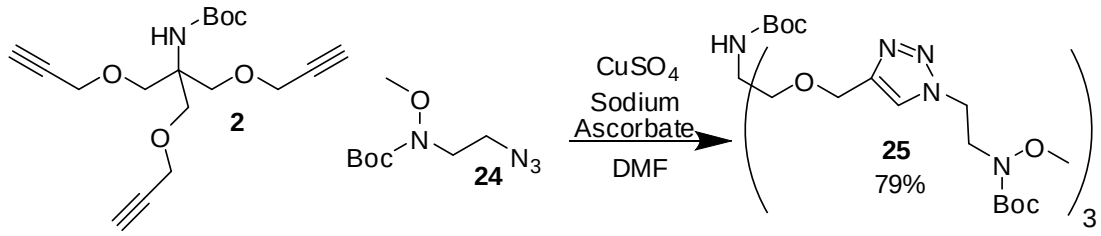


**Scheme 39:** Click reaction to produce Tris-based aminooxy scaffold **25**

Since the azide product **24** was clearly detected by the majority of spectroscopic methods available, the reaction was deemed successful and the material carried through. Click reaction was successful giving scaffold **25** in 79% yield (**Scheme 36).** Removal of copper salts was difficult in some cases, aqueous washes were occasionally sufficient although efficiency was improved by adding small amounts of EDTA to the aqueous wash. Column chromatography on silica also appeared to be successful.

IR spectra strongly suggested that the click reaction between azide **24** and tri propargyl Tris core **2** was successful. Peaks at 2100 $cm^{-1}$ and 3291 $cm^{-1}$ characteristic of azides and terminal alkynes weren't present in the spectrum for the product **25**, suggesting neither functional group was present in **25**.

Mass spec provided further confirmation with MALDI showing a prominent peak at 1007.22 m/z, corresponding well with $MNa^+$. High resolution mass spec also supported successful synthesis of the scaffold **25**, with an intense peak at 984.5460 m/z, comparing well with the predicted value for $MH^+$ of 984.5473 m/z.

Proton and carbon NMR (fully assigned with the aid of COSY and HSQC) confirmed that **25** had been synthesised as intended. Peaks associated with the terminal alkyne of Tris core **2** (a triplet at 2.42 ppm in the proton and carbons at 79.7 ppm and 74.7 ppm) were absent. The presence of the triazole was supported by observation of characteristic peaks at 7.60 ppm in the proton and in the carbon at 145.1 ppm (for the quaternary carbon) and 123.5 ppm (for the protonated carbon). As discussed in **Chapter 2** shifts in this range strongly suggest the expected 1,4 triazole as opposed to the 1,5 triazole.

Protons associated with the ethyl linker shifted downfield on reaction. Protons adjacent to the Boc protected aminooxy group came at 3.63 ppm in the azide starting material **24** but were visible at 3.94 ppm in the product **25**. Larger shifts were observed for the protons next to the azide in **24** and the triazole in **25,** which shifted from 3.46 ppm to 4.59-4.56 ppm on reaction. Shifts in the carbon environments were smaller: the azide linked carbon was observed at 48.5 ppm in **24** and the triazole linked carbon at 47.3 ppm in **25**. The carbon adjacent to the aminooxy environment in the linker also shifted slight, from 48.3 ppm in starting material **24** to 49.1 ppm in the product scaffold **25.** Taken together the spectroscopic data confirms the synthesis of Tris based scaffold **25** illustrated below in **Figure 41.**

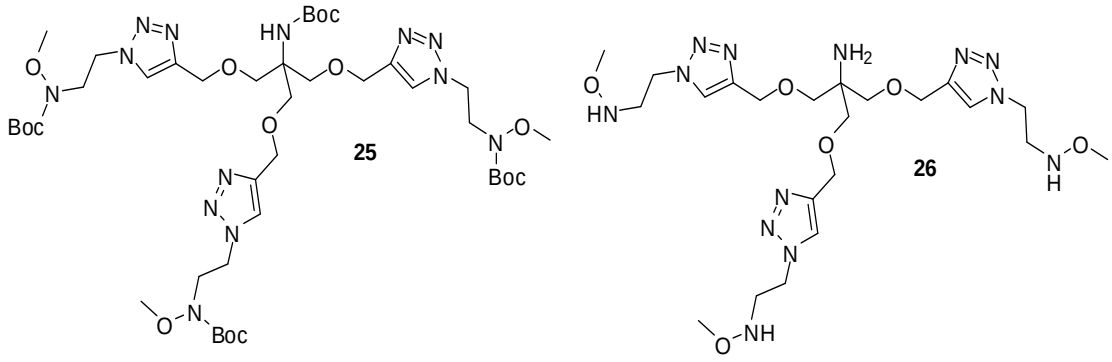


**Figure 41:** Boc protected Tris-based aminooxy scaffold **25,** and deprotected scaffold **26**

The final scaffold **25**, was subjected to global Boc-deprotection. This was initially carried out using TFA but this caused degradation of the product in larger scale reactions. Hydrochloric methanol was found to give the best results.

The deprotected scaffold **26**, shown above in **Figure 41**, was isolated as a crude and not purified further. Estimation by NMR integration suggested impurities were minor and impurity peaks in the mass spec were significantly less intense than peaks consistent with $MH^+$ and $MNa^+$ supporting the idea that impurities were present as traces.

Appearance of a broad peak at 2439 $cm^{-1}$ in the IR (characteristic of N-H in ammonium ions) suggested the deprotection reaction was successful which was supported by intense peaks in the mass spec at 584.3 m/z ($MH^+$) and 606.3 m/z ($MNa^+$).

Confirmation was provided by the NMR. Scaffold **26** was not soluble in chloroform, suggesting a more polar compound than the starting material **25** which supported the idea that a salt had been created. The change of solvent and pH for the NMR makes direct comparison of the shifts in spectra for Boc protected starting material **25** and deprotected scaffold **26** problematic as changes to both are known to effect chemical shift. However Boc protecting groups tend to show intense, characteristic peaks in both the proton and carbon spectra, which were present in spectra of **25** and absent in spectra of **26.** Proton spectra of **25** showed two strong peaks at 1.40 ppm, associated with the methyls of the Boc protecting groups. Additionally **25** showed strong peaks in the carbon NMR at 155.7 ppm and 154.9 ppm, consistent with Boc carbonyl groups, as well as at 28.5 ppm and 28.2 ppm, consistent with the methyl carbons. Less intense peaks were observed in the carbon spectrum of **25** both at 82.2 ppm which were identified as the quaternary carbons of the Boc groups. All of these characteristic peaks were absent from spectra of product **26**, confirming that the Boc groups had been removed.

With a successful route to the secondary aminooxy substituted Tris scaffold **26**, (**Figure 41)**, available the focus shifted to reaction with free sugars. The results of these experiments are discussed in the following chapter.

## 3.4 Chapter Summary

Initially attempts to produce an aminooxy functionalised scaffold focused on introducing aldehydes to the Tris scaffold as these could be easily converted to the oxime by reaction with aminooxy salts. This was unsuccessful, attempts are summarised below (**Scheme 40**).

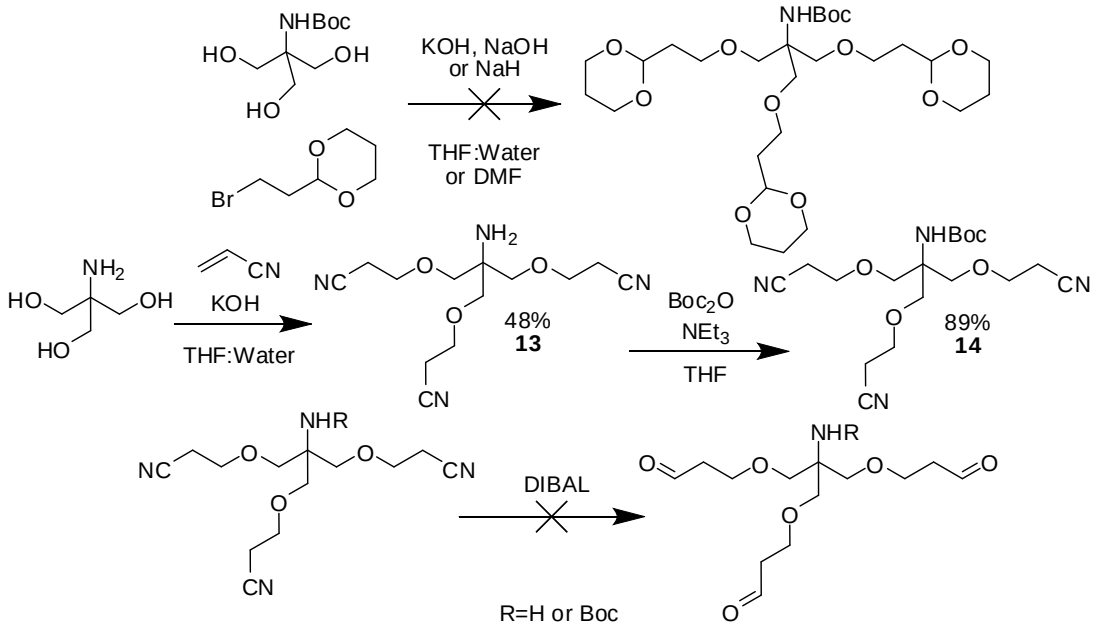


**Scheme 40:** Attempts to synthesis Tris scaffold with attached aldehydes failed

Conversion was attempted via the alkene using a one pot procedure: ozonolysis in the presence of pyridine and O-methylhydroxylammonium chloride. Test reaction with styrene was successful, however reaction with allyl substituted Tris scaffold **15** was not. Under the reaction conditions **15** appeared to decompose.

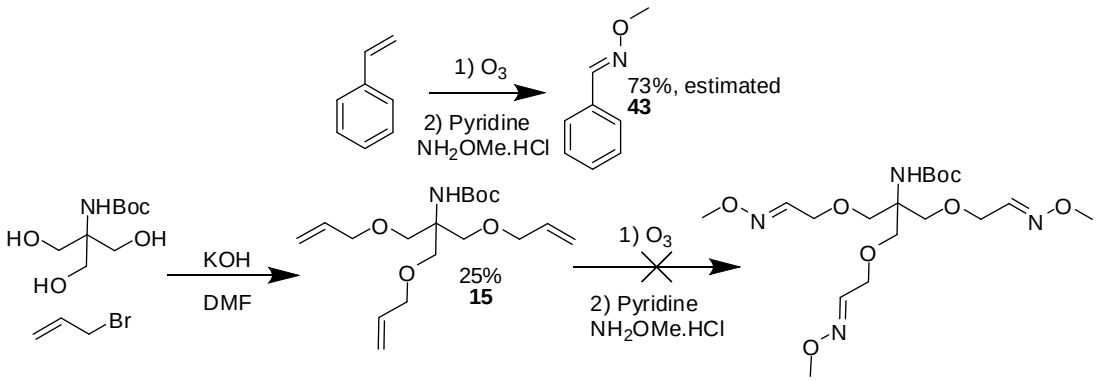


**Scheme 41:** One pot ozonolysis conversion of allyl groups to oximes was successful in test reactions but not using Tris compound **15**

Next we attempted to produce aminooxy substituted Tris scaffolds using click chemistry to introduce aminooxy groups to the scaffold. A suitable azide linker with a Boc protected aminooxy group was synthesised using the route shown below in **Scheme 42**.

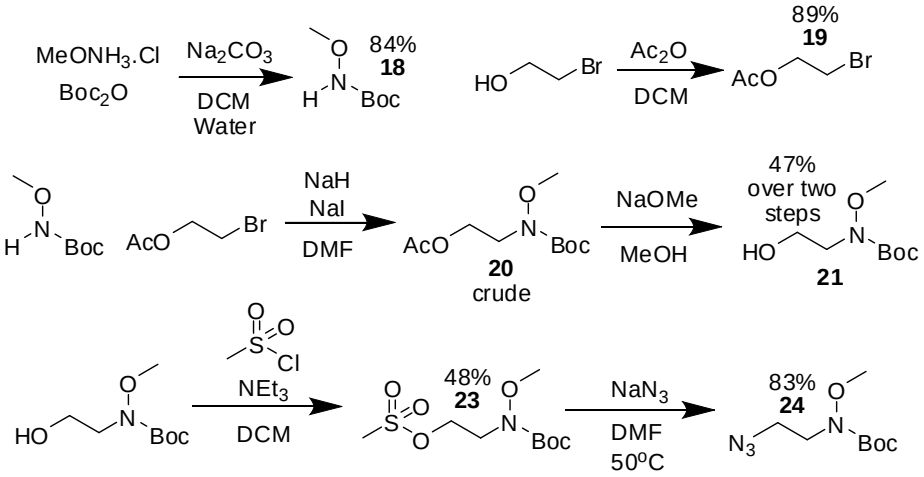


**Scheme 42:** Synthetic route to short linker with aminooxy and azide functionality

Click reaction between propargyl Tris **2** and azide linker **24** proceeded in good yield (79%) as shown below in **Scheme 43.**

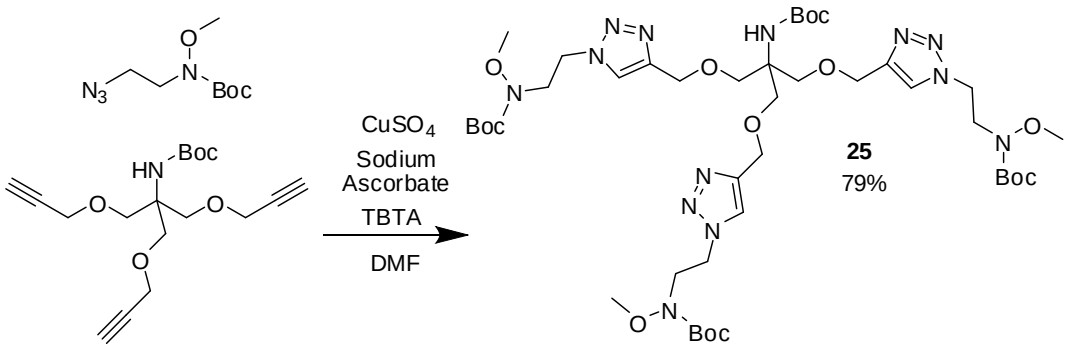


**Scheme 43:** Synthesis of target scaffold **25**

Boc deprotection then gave the desired scaffold (isolated as crude) illustrated below in **Figure 42** subsequent experiments focused on reaction with free sugars and are discussed in the following chapter.

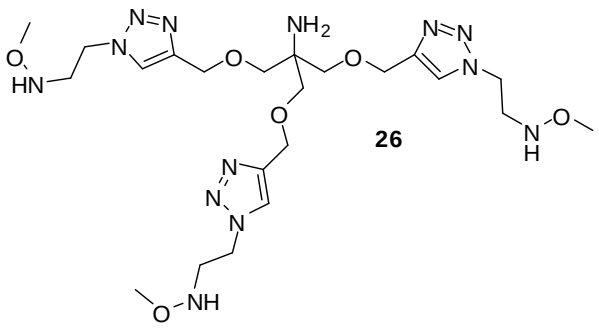


**Figure 42:** Target Tris based scaffold **26** with secondary aminooxy functionality

# 4. Further Investigation of Aminooxy substituted Tris scaffolds and chemoselective ligation

## 4.1 Initial incubation experiments

The Boc deprotected Tris scaffold **26** was synthesised as the hydrochloride salt. Its initial pH in solution, according to pH paper, was ~1. Adjusting the pH to a higher value was deemed preferable. Although reaction between aminooxy moieties and unprotected sugars requires acidic conditions, previous work by Finlay strongly suggested that milder conditions resulted in a higher percentage conversion.[77] Initial experiments were not conducted in the presence of lectins but it was felt that confirming formation of the sugar substituted product (such as the galactose example illustrated in **Scheme 44**) should be done with biologically compatible conditions in mind.

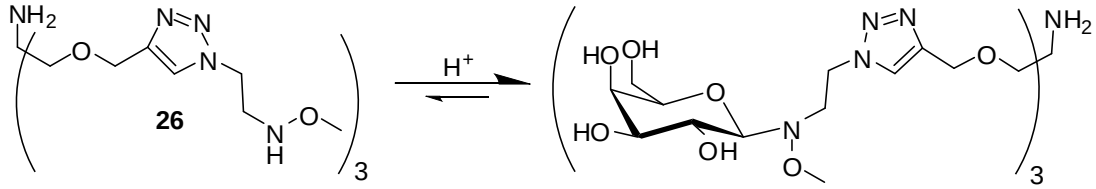


**Scheme 44:** Example of proposed sugar-aminooxy coupling on Tris scaffold **26**, using galactose

The initial investigation was conducted in $D_2O$ to allow detailed periodic monitoring of the mixture by proton NMR. Deprotected scaffold **26** was dissolved in $D_2O$ and the pH*, the observed pH in a deuterated solvent, adjusted by careful addition of 10wt% $NaHCO_3$ in $D_2O$ to ~pH* 5 (monitored using pH paper).

Prior to addition of monosaccharides a proton NMR experiment was performed at the new pH* so that any effect on the chemical shift of proton signals for scaffold **26** could be accounted for in the subsequent measurements.

Four equivalents of galactose (relative to the scaffold, giving 1.3 equivalents of galactose per aminooxy group) were added and the mixture stirred in a sealed vial

for 15hr. HSQC allowed identification of three distinct anomeric environments which are highlighted in the spectrum below, **Figure 43**. This was used in preference to 1D proton NMR alone as scaffold signals for **26** at this pH* were observed in the same region the anomeric protons were expected to appear.

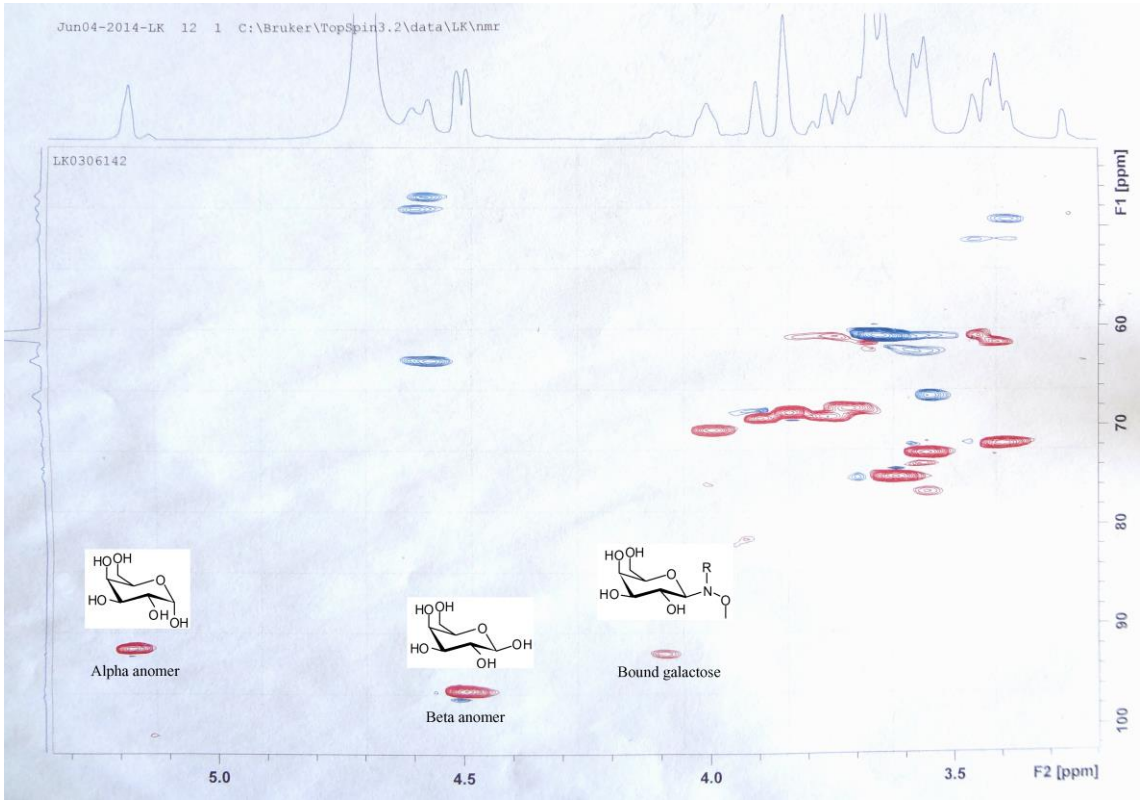


**Figure 43:** HSQC of reaction mixture containing galactose and scaffold **26**, three distinct anomeric environments are highlighted.

Coupling constants confirmed that two of the environments were cyclic β conformation while one was α. Comparison with literature values for galactose anomeric protons and previously synthesised galactose substituted aminooxy compounds made it possible to distinguish free and bound galactose. As the triazole C-H environment was also clearly visible at 7.94 ppm the proportions of free galactose (4.59 ppm for β and 5.27 ppm for α), aminooxy galactoside (4.18 ppm) and core scaffold could be easily compared. Integral values clearly showed that after 15hrs the free galactose predominated, as shown in **Figure 44** below.

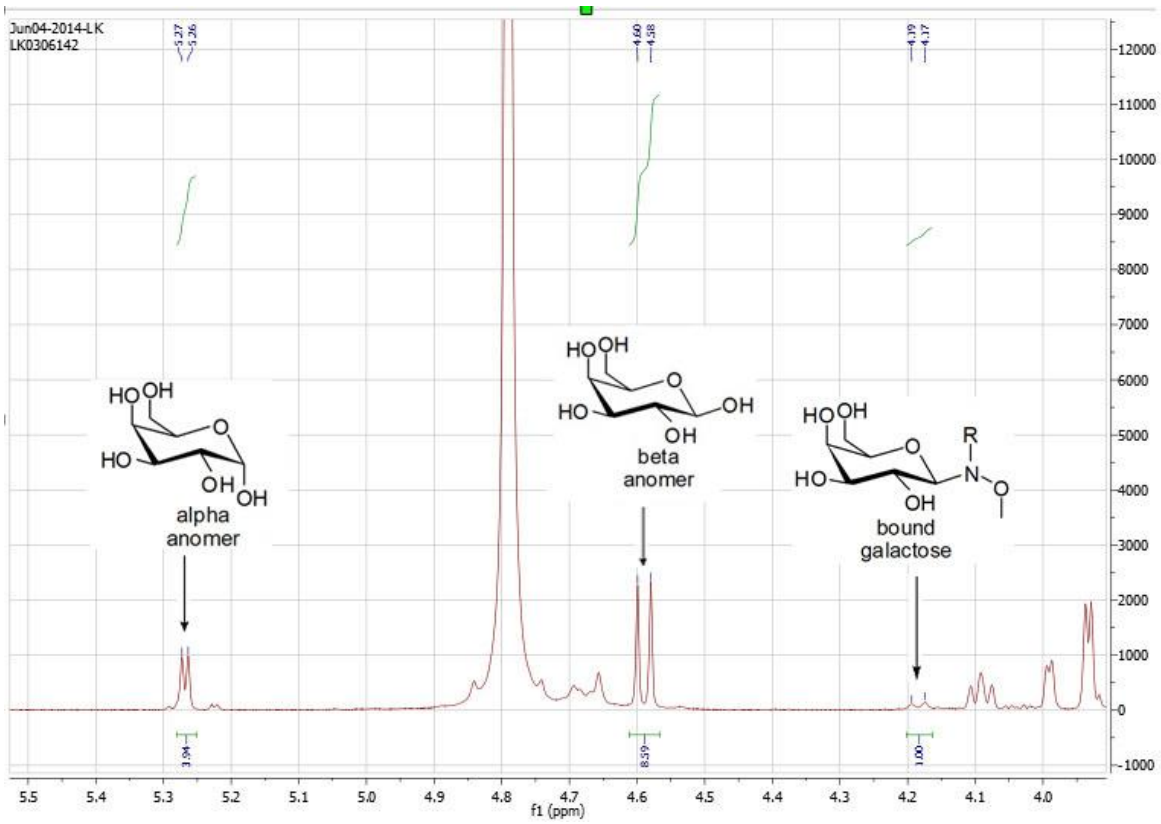


**Figure 44:** Reaction of **26** and galactose after 15hr with free galactose and aminooxy galactoside anomeric protons highlighted. Integration clearly shows the free β galactose predominates

It was estimated that approximately 8% of the galactose present was bound to the scaffold. The mixture was monitored for a further day with little change. This can be seen by comparison of **Figure 44** and **Figure 45.**

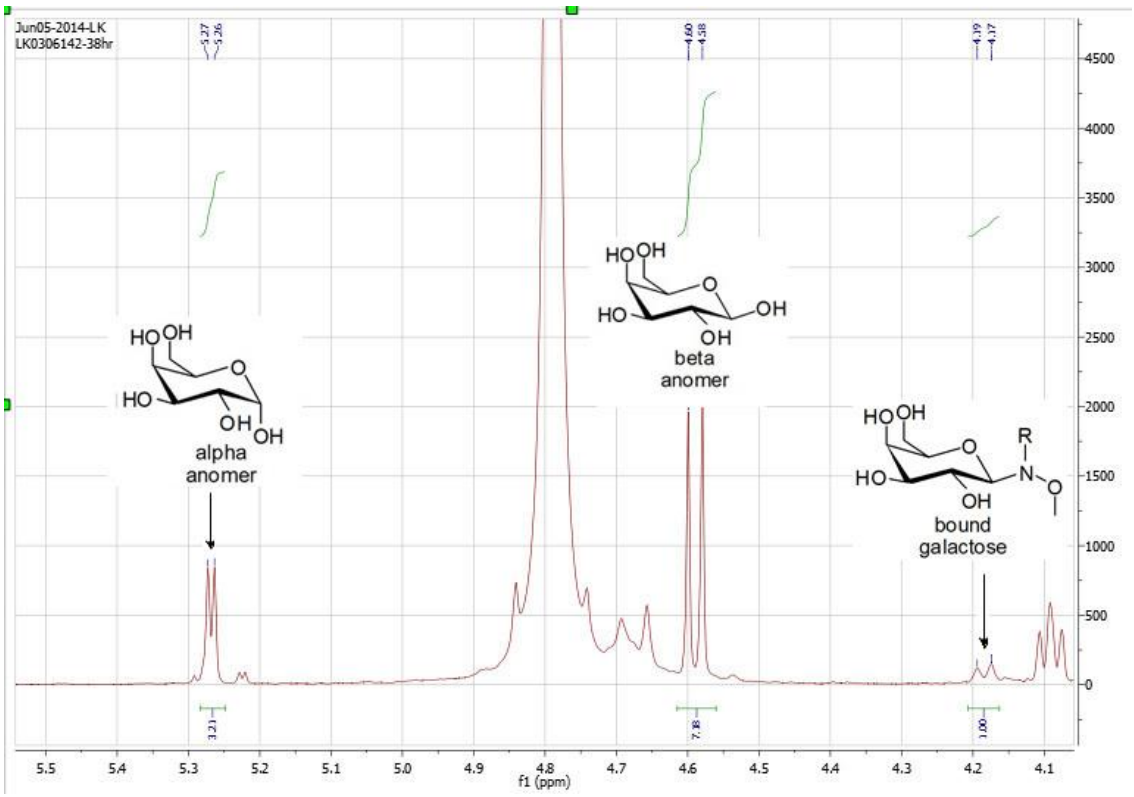


**Figure 45:** Reaction of **26** and galactose after 38hr with free galactose and aminooxy galactoside anomeric protons highlighted. Integration clearly shows the free β galactose predominates as in **Figure 44**

After 38hrs estimation from the integrals suggested approximately 9% of the galactose was bound to the scaffold **26**, an incredibly low proportion of the four equivalents in solution. A further two equivalents of galactose, relative to the scaffold, were added in an attempt to shift the position of equilibrium in favour of the sugar-substituted scaffold. This gave a total of two equivalents of galactose per aminooxy unit. Increasing the equivalents of galactose to a large excess would likely have further encouraged product formation but may have made it difficult to observe by NMR. The mixture was warmed to 30$^{o}$C but as can be seen from **Figure 46** these measures did not produce a marked increase in aminooxy galactoside; suggesting that equilibrium had been reached and in this case it favoured the starting materials over the desired product.

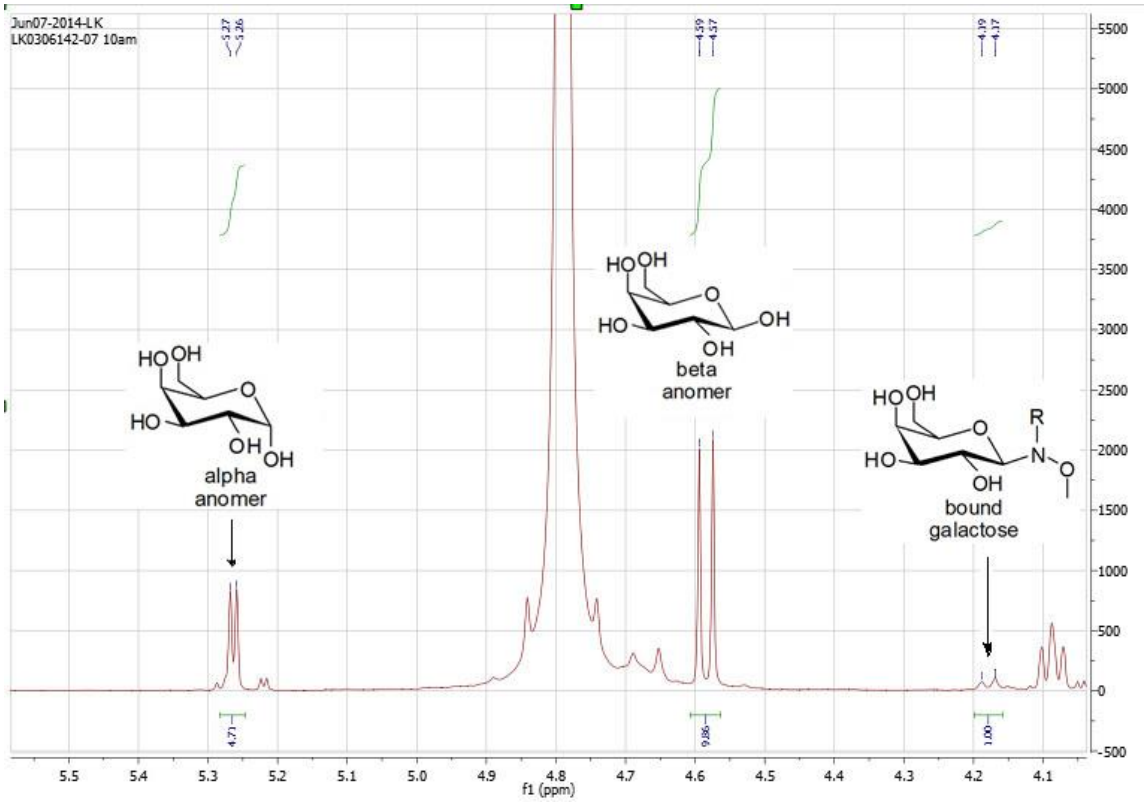


**Figure 46:** Adding 2 more equivalents of galactose did not substantially increase the proportion of aminooxy galactoside

Similar experiments were attempted with glucose and GlcNAc, using nine equivalents of monosaccharide relative to the scaffold (three equivalents per aminooxy) and conducted at 35°C in $D_2O$ at ~pH* 5. While the anomeric protons were not as distinct for these monosaccharides as for galactose the free sugar was similarly seen to predominate. Anomeric signals for the β conformation of free glucose and GlcNAc were significantly closer to the $D_2O$ solvent peak, so similar percentage estimates based on integration would be misleading. As previously the anomeric signals were identified using a combination of HSQC, coupling constants and comparison with the literature. In the case of GlcNAc the doublet corresponding to free β form sugar was entirely masked by the solvent peak. For glucose the β anomeric signal was similarly problematic, coming close to the solvent peak and overlapping with broad scaffold signals at 4.70-4.63 ppm (these were $CH_2$ environments adjacent to the nitrogen of the triazole ring and the quaternary carbon of the triazole ring, pH adjustment significantly shifted many of the proton environments). An NMR of the experiment with glucose, highlighting the anomeric environments and problematic overlap, is shown below in **Figure 47**.

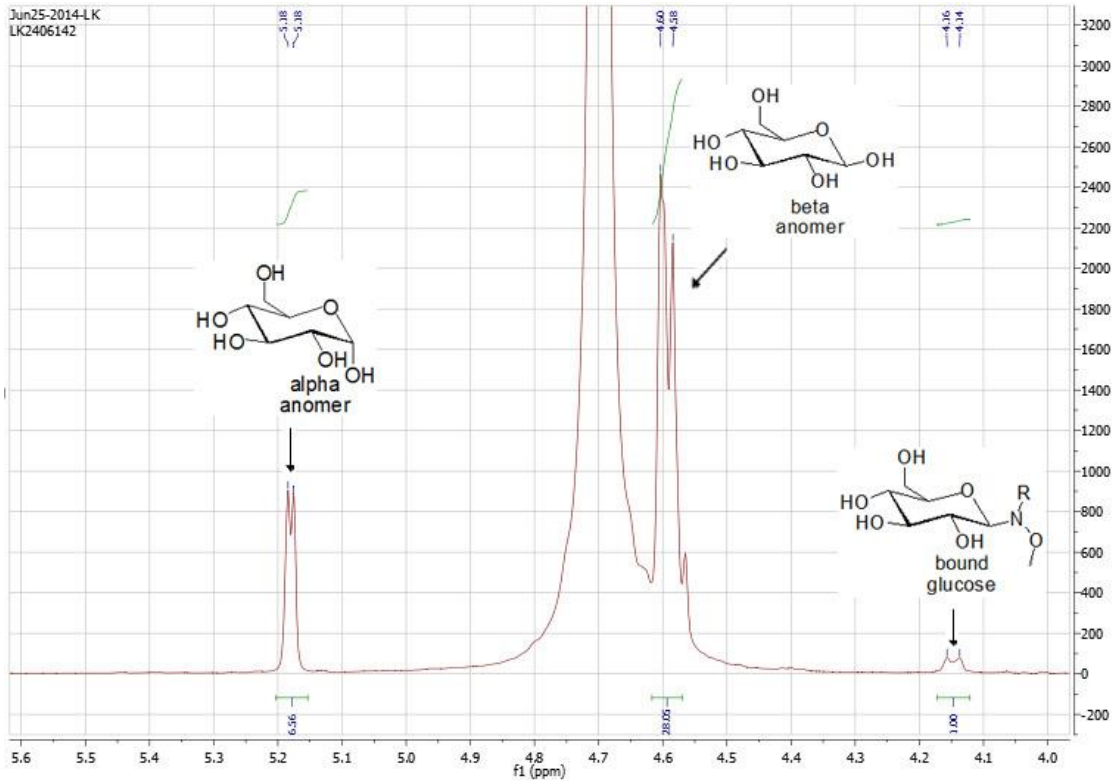


**Figure 47:** Reaction of **26** and glucose after 16hr with free glucose and aminooxy glucoside anomeric protons highlighted. Integration shows the free glucose predominates.

The NMR experiments suggested that the equilibrium under conditions tested was strongly in favour of the free sugar. An attempt was made to monitor the reaction by mass spec using both MALDI and ESI, but Tris scaffold based materials failed to ionise. Separation, while possible, would have required fast removal of solvent from each fraction to prevent equilibrium being re-established and was therefore impractical. A large excess of sugar may have led to product formation, but could also result in a majority of the undesired mono or disubstituted scaffold with interconversion between the two as shown in **Scheme 45.**

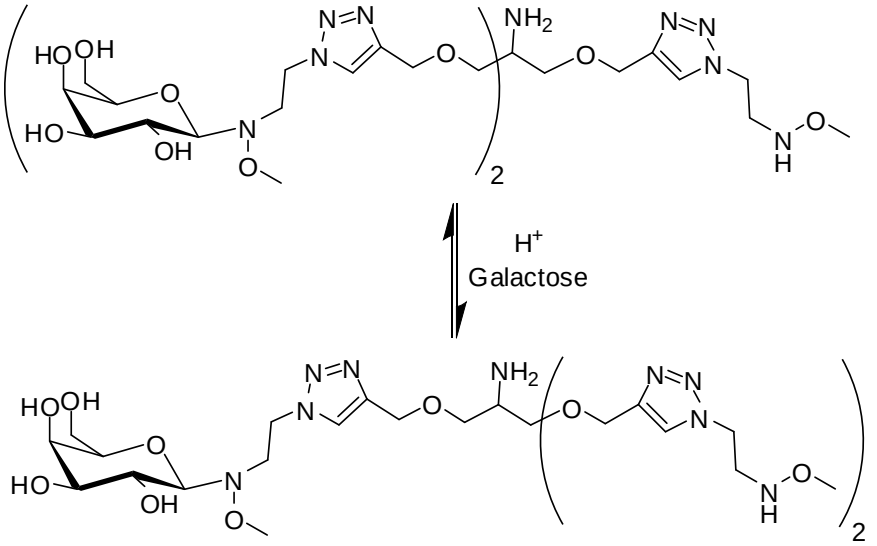


**Scheme 45:** Potential interconversion between di and mono substituted scaffolds makes the ability to monitor product formation important.

A method to monitor reaction progress, which could detect Tris containing fractions even in the presence of vast excess of monosaccharide, was clearly needed. High performance liquid chromatography (HPLC) was considered and separation of small fractions of the equilibrium reactions attempted but these efforts were hampered by the lack of UV absorption for all components. Detection of the scaffold in its current form was difficult but monitoring Tris scaffold containing components was essential for optimising the reaction conditions. As a result an analogue of the core scaffold was synthesised with a chromophore label coupled to the free Tris amine.

## 4.2 Synthesis and properties of UV active Tris scaffold

The Boc protecting group was removed from the tri propargyl Tris scaffold **2** by stirring in 2M hydrochloric methanol giving the salt **27**.

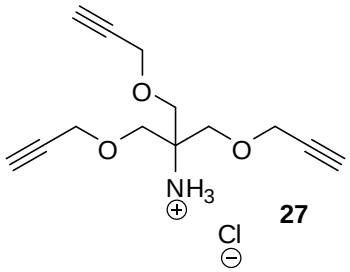


**27**

**Figure 48:** Compound **27**, produced by removing Boc protecting group from Tris core **2.**

The crude salt **27** was fully characterised and product formation confirmed. The IR spectrum showed a peak at 2884 $cm^{-1}$, consistent with an ammonium ion, and still had a peak at 3287 $cm^{-1}$, consistent with a terminal alkyne but the peak at 1711 $cm^{-1}$ in the Boc protected starting material **2** (assigned as the C=O) was absent. Removal of the Boc group was further supported by the mass spec with an intense ion at 236.0 m/z (close to the predicted value for $MH^+$, 236.3 m/z) and by the proton and carbon NMR, which lacked characteristic peaks for the Boc methyl groups (at 1.42 ppm and 28.5 ppm in starting material **2**) and the Boc carbonyl (observed at 154.9 ppm in **2**). This was not purified further and used as crude after removal of the solvent and volatile acid.

With the scaffold amine free the choice of UV active agent was considered. 4-Nitrobenzoyl chloride was chosen as it was relatively small (reducing the likelihood of it blocking binding sites), readily available, and because NMR shifts from this chromophore in both the proton and carbon spectra were unlikely to overlap with signals from saccharide groups or the majority of the scaffold.

4-Nitrobenzoyl chloride was coupled to deprotected Tris core **27** under conditions shown in **Scheme 46**. Yield for the test reaction was a moderate 38% but conducting the reaction on a larger scale resulted in an even lower yield (14%) of compound **28**.

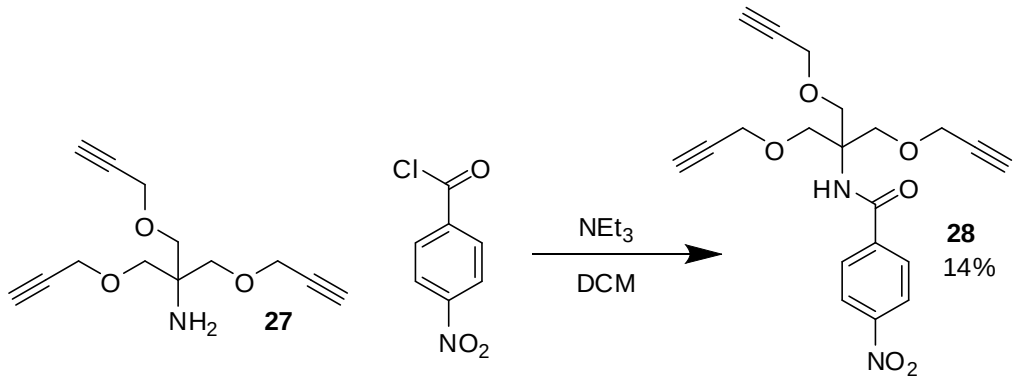


**Scheme 46:** Reaction of deprotected Tris core **27** with 4-nitrobenzoyl chloride giving the UV active Tris core **28**

Changes in the IR spectra going from compound **27** to compound **28** supported product formation; new peaks were observed at 1663 $cm^{-1}$ consistent with a carbonyl group and at 1523 $cm^{-1}$ and 1346 $cm^{-1}$, consistent with an aromatic nitro group, while the peak at 3289 $cm^{-1}$, characteristic of terminal alkynes, was still present. Further support for the synthesis came from the proton and carbon NMR. Although NMRs for starting material **27** and UV active Tris core **28** can't be directly compared (differences in solubility meant different solvents were used) the appearance of new peaks in regions characteristic of aromatic protons and carbons strongly suggested the reaction was successful. Proton NMR of product **28** had two multiplets at 8.28-8.25 ppm and 7.92-7.89 ppm while the carbon NMR showed peaks at 149.7 ppm, 140.9 ppm, 128.3 ppm and 123.9 ppm consistent with the expected aromatic carbons, along with a peak at 165.5 ppm, consistent with the carbonyl of the amide. The structure was confirmed by mass spec, with prominent ions observed at 385.1 m/z and 407.0 m/z, consistent with $MH^+$ and $MNa^+$ respectively.

Click reaction between UV active Tris core **28** and the aminooxy-azide linker **24** (shown in **Scheme 47**) was conducted using copper (I) which was formed *in situ* using copper sulfate and sodium ascorbate.

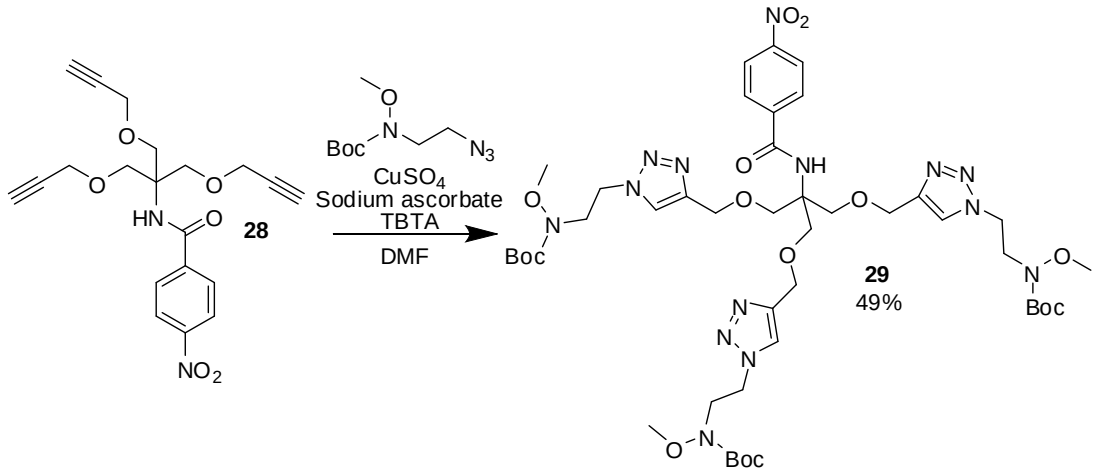


**Scheme 47:** Synthesis of scaffold **29** via click reaction of aminooxy-azide linker **24** and UV active Tris core **28**

The product, UV active Tris scaffold **29,** was purified by silica column chromatography to ensure both the excess azide **24** and any copper salts were removed giving a moderate yield of 49%.

IR supported the formation of **29**, with signals at 3289 $cm^{-1}$ and 2100 $cm^{-1}$, characteristic of the terminal alkynes in Tris core **28** and the azide in linker **24** respectively, absent. Shifts in the proton and carbon NMR spectra also strongly suggested product formation. The triplet at 2.45 ppm in proton spectrum of starting material **28**, characteristic of the terminal alkynes, was absent, which along with the appearance of peaks at 7.50-7.49 ppm suggested the click reaction had occurred, forming the 1,4 triazole as expected. Carbon NMR confirmed the absence of the alkyne and formation of the 1,4 triazole. Characteristic peaks were present at 144.9 ppm and 123.3 ppm (assigned as the quaternary and protonated carbon of the triazole ring, with reference to the HSQC) and a lack of peaks at 79.6 ppm and 75.0 ppm (the quaternary and protonated carbons of the alkyne in starting material **28**). Significant downfield shifts in signals associated with protons from the ethyl linker were also observed on reaction, suggesting product formation. Protons adjacent to the azide in **24** originally appeared at 3.46 ppm but shifted to 4.52-4.48 ppm on reaction while protons adjacent to the aminooxy group appeared at 3.63 ppm in the linker starting material **24** but at 3.93-3.85 ppm in the product **29**.

Low resolution mass spec gave further supporting evidence of product formation, with prominent ions observed at 1033.7 m/z and 1055.6 m/z, consistent with $MH^+$ and $MNa^+$ respectively. Confirmation came from high resolution mass spec which showed an intense peak at 1033.5069 m/z, compared to the calculated value for $M^+$ of 1033.5070 m/z, making it extremely likely the click reaction was successful. Taken together the spectroscopic data confirmed the formation and structure of UV active scaffold **29**.

With **29** available it seemed reasonable to test the scaffold's UV properties to confirm that the chromophore would be detectable at relevant concentrations during HPLC. A UV-Vis spectrum of the compound's absorbance from 220-600 nm was conducted in order to determine $\lambda_{max}$, which was found to be 264 nm ($\varepsilon$ = 9804 $M^{-1}cm^{-1}$).

With the scaffold's UV properties confirmed the aminooxy groups were deprotected by stirring **29** in 2M hydrochloric methanol. The deprotected Tris product **30** (shown

in **Figure 49**) was obtained as the crude hydrochloric salt by removing the methanol solvent and volatile acid but was not purified further.

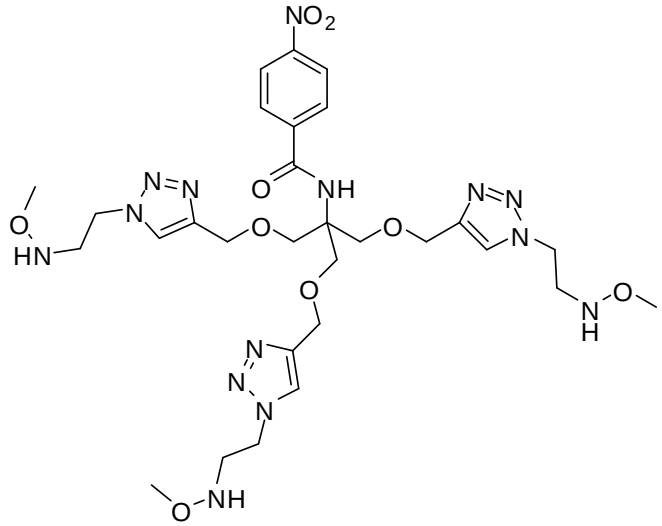

**Figure 49:** Deprotected, UV active Tris scaffold **30**

The Boc deprotection was confirmed by a combination of NMR and mass spec, although an IR spectrum was taken and a peak observed in the starting material **29** at 1701 $cm^{-1}$, consistent with a carbonyl, was absent. Differences in solubility between **29** and product **30** meant that different NMR solvents were used, preventing direct comparison of chemical shifts. However the proton and carbon NMR of deprotected Tris scaffold **30** lacked peaks characteristic of the Boc methyl and carbonyl groups. These were observed at 1.32 ppm for the methyl protons and 155.6 ppm and 28.2 ppm for the carbons of the Boc carbonyl and methyl groups respectively, in the starting material **29**. Further support for the deprotection came from low resolution mass spec, which showed a prominent peak at 755.4 m/z, consistent with $MNa^+$, with final confirmation coming from the high resolution mass spec. This showed an intense peak at 733.3487 m/z, in good agreement with the calculated value (733.3488 m/z) for $M^+$.

As with scaffold **29**, the UV properties of **30** were investigated. An accurately weighed sample was dissolved in water and the pH adjusted to ~pH 6 (measured using pH paper) by addition of saturated sodium hydrogen carbonate solution. Water was used both because **30** was only sparingly soluble in methanol and because future attempts to couple **30** with sugars were likely to be conducted in water. As

previously a UV-Vis spectrum of the compound's absorbance from 220-600 nm was obtained in order to determine $\lambda_{max}$. The $\lambda_{max}$ was 269 nm ($\varepsilon = 4699\ M^{-1}cm^{-1}$), quite similar to the value obtained for the starting material **29**. This suggests that functionality at the linker termini does not have a large affect on the absorption properties of the scaffold, so it is likely that unsubstituted **30** and multiply sugar substituted scaffolds based on **30** could all be detected using the same wavelength.

Having shown that the scaffolds were UV active it seemed likely that HPLC would be a suitable method for monitoring the position of equilibrium and product formation in reactions between **30** and various monosaccharides. With this established, attention turned to creating a suitable HPLC method for monitoring such reactions.

## 4.3 High Performance Liquid Chromatography experiments

In order to draw meaningful conclusions from the planned equilibrium experiments (such as that illustrated in **Scheme 48**) identification and accurate appraisal of the concentration of unsubstituted starting material **30** in HPLC traces of mixtures was necessary. Creating a calibration curve for pure **30** was seen as an essential starting point to meeting this aim.

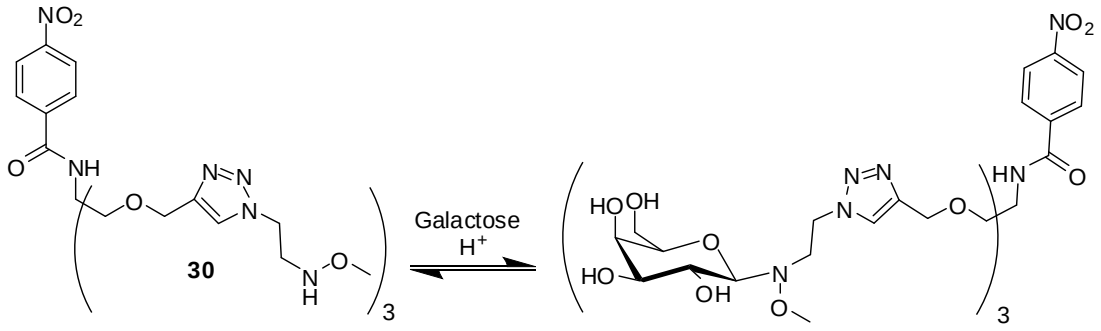


**Scheme 48:** Proposed reaction between Tris scaffold **30** and galactose, showing only tri substituted product and unsubstituted starting material. Mono and disubstituted products are also likely.

In preparation for this a fresh sample of **30** was synthesised. Both pH and concentration of salts in solution are known to affect HPLC retention times in some

cases so these factors were taken into account when preparing solutions of UV active scaffold **30**.[109] Rather than using sodium hydrogen carbonate to neutralise **30** as previously, an excess of ammonium bicarbonate was added. Unlike the sodium hydrogen carbonate, ammonium bicarbonate is volatile and can be removed under vacuum, reducing the overall salt content.

Solutions were then diluted in phosphate buffered $D_2O$ with a buffer concentration of 100 mM. Deuterated solvent was used so that any effect of the buffer on the shifts of proton peaks in **30** could be established at this point. pH* of the buffer was established to be 5.84. Using the pH-pD conversion constant (established to be 0.4) this gave a pD of 6.24 for the buffer.[110] pH* was measured again when **30** was added to ensure it did not break the buffer and was found to be pH* 5.92, giving an acceptable pD of 6.32.

A series of seven solutions of different, known concentrations were then prepared from the stock using ultrapure water. All samples were run using the same method and solvents (methanol and water with 0.05% TFA) with the same volume injected into the HPLC for each run. Peak detection was conducted at 250 and 270 nm throughout.

However a calibration curve could not be produced because HPLC traces of UV active scaffold **30** showed multiple peaks; despite NMR showing that the injected sample of **30** contained no major impurities. Several attempts were made to identify the impurity and its source. An HPLC trace of the Boc protected scaffold **29** also showed two major peaks, both HPLC traces are shown below in **Figure 50.** The two major peaks in the starting material **29** were separated and analysed by mass spec. The peak eluting at 16.1 min was identified as **29**, with prominent peaks for both $MH^+$ (1033.8 m/z) and $MNa^+$ (1055.8 m/z) but the peak eluting at 15.2 min could not be identified.

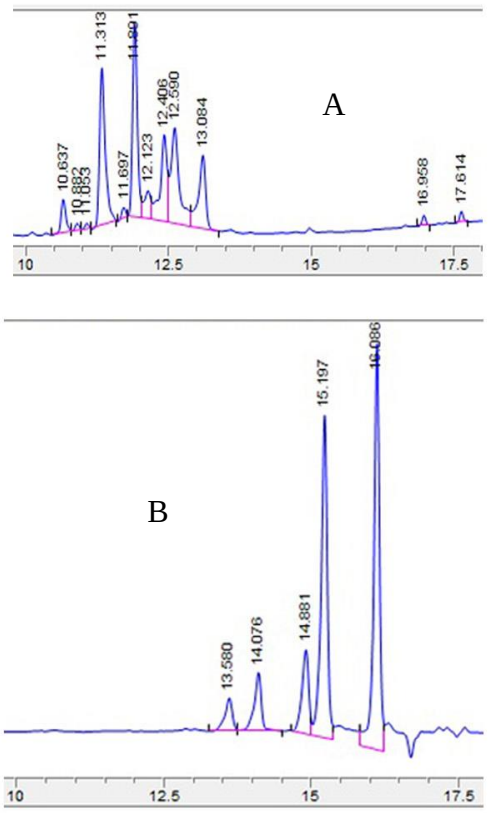


**Figure 50:** HPLC traces for, A: compound **30**, B: compound **29** both detected at 270 nm.

This suggested that the excess peaks in HPLC traces of **30** were caused by an impurity carried over from the starting material. Comparison of mass spec data for **29** and the two peaks present in its HPLC traces confirmed that the impurity was present in the original sample despite previous purification. It was anticipated that some of the impurity peaks in samples of **30** could be caused by *in situ* Boc deprotection of impurities from starting material **29** as the HPLC solvents contained a small amount of TFA. While TFA was not tested as a way of deprotecting **29** it had previously been trialled as a way of removing Boc groups from similar scaffold **25** and had successfully deprotected the compound. In **25** prolonged exposure to TFA caused decomposition but this was not expected to be a problem for **29** due to the lower concentration of TFA and shorter exposure times.

In order to establish their identity two major peaks present in the HPLC trace of UV active tri-aminooxy scaffold **30** were separated and collected. Both purified peaks were then reinjected in order to confirm their purity, note any change in retention

time and show that the peaks had been separated correctly. Major changes were observed in retention time and number of observed peaks on subjecting the samples to a second HPLC run. In both samples the major peak observed was at a different retention time to the peak originally separated with at least one other impurity present; suggesting the situation was more complex than a simple Boc deprotection of one pre-existing impurity. Repeating the procedure with freshly prepared solvents and fresh, concentrated samples confirmed that the samples were not accidentally contaminated and the results were not the product of experimental error. HPLC traces for both purified peaks are shown below in **Figure 51**.

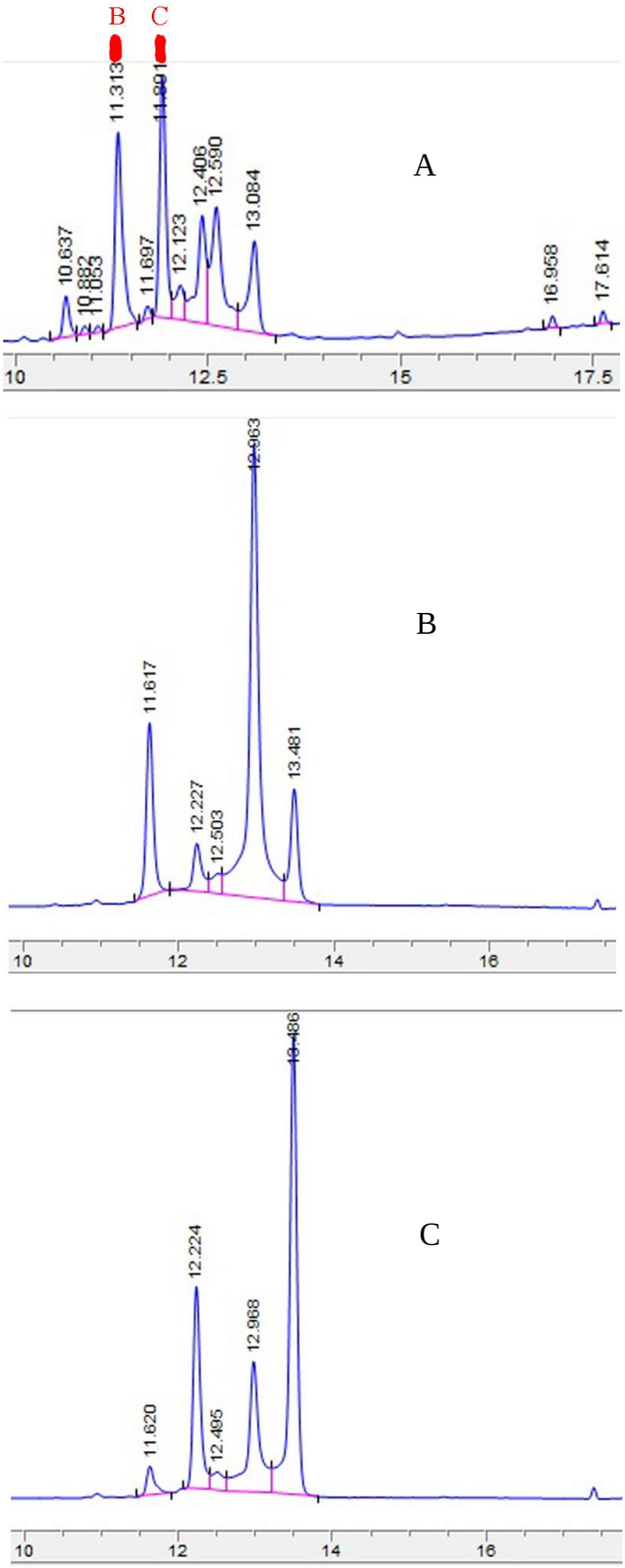


**Figure 51:** HPLC traces for A: compound **30**, B: reinjected peak eluting at 11.3 min, C: reinjected peak eluting at 11.9 min

There were several possible causes for these results. Retention time could have originally been affected by other components in the mixture, giving a 'true' retention time for the purer, separated peaks. Collection of fractions was automated and it was possible that the HPLC was simply collecting too broadly, selecting the wrong peaks or that the dead time for collection had been altered. *In situ* reaction was another possibility, as was decomposition on the column.

In order to test that the HPLC was collecting fractions correctly a stock sample of FmocGlyOH amino acid was prepared and injected. The amino acid was separated and reinjected three times concurrently with no change in retention time, or extra peaks observed. This showed that the HPLC was correctly collecting desired fractions.

The two major peaks in the HPLC trace of **30** were separated and analysed by mass spec. Mass ions corresponding to **30** (previously observed at 733.4 m/z for $MH^+$ and 755.4 m/z for $MNa^+$) were not observed in either sample and the observed mass ions did not correspond to simple Boc deprotection of the impurity seen in the starting material **29**. The impurities could not be identified based on the mass spec. Reaction of **30** with one or more unidentified reagents seemed increasingly likely. The terminal aminooxy groups were chosen for their reactivity towards aldehydes which allows coupling to sugars. Reaction with trace carbonyl containing components in solvents was a possibility.

Further evidence for reaction during the HPLC process came with confirmation that the additional peaks in the separated fractions were truly new. Portions of the original stock solution of **30** were spiked with each separated fraction. If the changing retention time was caused by purifying the initial mixture, removing inter molecular interactions between components, then mixing the original stock and fractions should give HPLC traces identical to the original stock. HPLC traces for mixtures of stock and separated fractions can be seen in **Figures 52**.

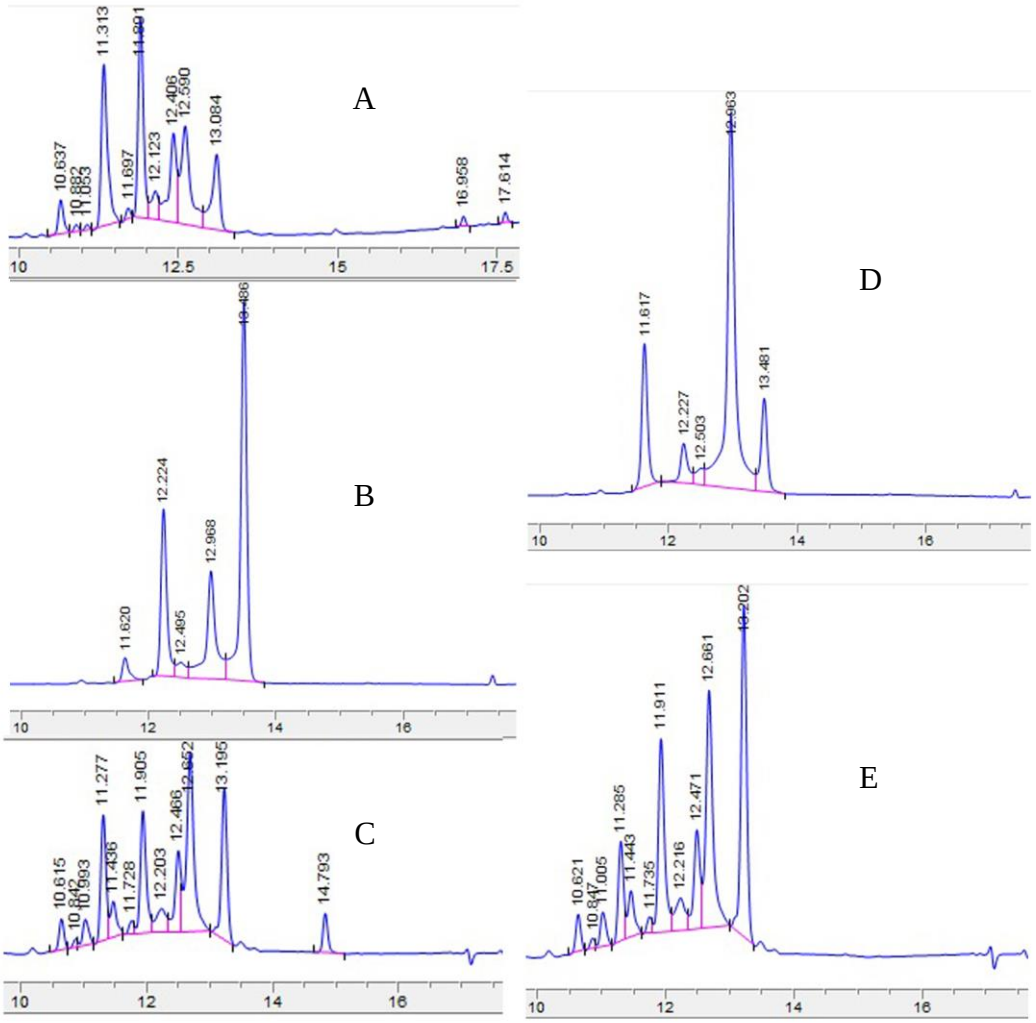


**Figure 52:** HPLC traces of A: compound **30,** B: separated peak eluting at 11.3min, C: solution B spiked with compound **30**, D: separated peak eluting at 11.9min, E: solution D spiked with compound **30**

It became clear that the traces for both solutions showed two distinct peak patterns superimposed, the stock solution and the respective fraction. This gave further support to the idea that the injected material was either reacting or decomposing. Several different solutions were prepared in an attempt to find the cause of this problem.

The HPLC solvents were considered as a possible cause for concern, initially due to the added TFA. As discussed previously TFA had caused decomposition in related scaffold **25**, over a period of time similar to that taken to run an HPLC experiment, collect and re-submit samples. To test whether TFA was causing decomposition a

sample of **30** was prepared in HPLC water (0.05% TFA) left for over an hour and then submitted to the HPLC. Very little difference could be seen between the pattern of peaks prepared in phosphate buffer and HPLC water. This seemed to indicate that TFA was not causing the observed changes in peak pattern and retention time.

We next considered the possibility of the free aminooxy groups reacting with trace contaminants. Reaction with a common solvent, such as acetone which was used to clean all glassware, was thought to be a likely cause as the products were expected to be unstable and might decompose in a number of ways. To investigate this a sample of **30** was dissolved in ultrapure water and spiked with excess acetone. The sample was left overnight before being submitted to the HPLC but the trace appeared the same as the original stock.

Metal chelation by the scaffold **30** was seen as another possible cause of the shift in retention time and peak patterns, either by mediating subsequent unidentified reactions or by a metal exchange process affecting the retention time itself. In order to rule this out as a factor a series of six samples of the same concentration were prepared in ultrapure water. Five were spiked with an excess of common metal salts, sodium chloride, potassium chloride, calcium chloride, magnesium sulfate and copper sulfate, the samples then were run concurrently. These traces also showed no significant differences from traces for the original stock solutions of **30**.

Having ruled out common metal ion contaminants, TFA and acetone as possible factors triggering decomposition we re-examined the experimental method for sources of contamination. Oxidation in air seemed unlikely, as NMR solutions in $D_2O$ did not show any decomposition over a period of weeks while the time between separation and reinjection of collected fractions was in the range of 30 min. Samples of Tris aminooxy scaffold **30** both in solution and as the pure compound, had been left exposed to air in the laboratory at room temperature for several days with no observed decomposition. Both HPLC solvents had been changed repeatedly throughout and the column was flushed with solvent for at least twenty minutes prior to experimental procedures. Blanks were run prior to samples further limiting the possibility of contamination from the column.

In an attempt to recreate the conditions separated fractions were subjected to, a fresh sample of **30** was synthesised and prepared by dissolving in HPLC solvent at roughly eluting proportions (approximately 75% methanol, 25% water). After 30 min this was submitted to the HPLC the trace is shown below in **Figure 53 A**.

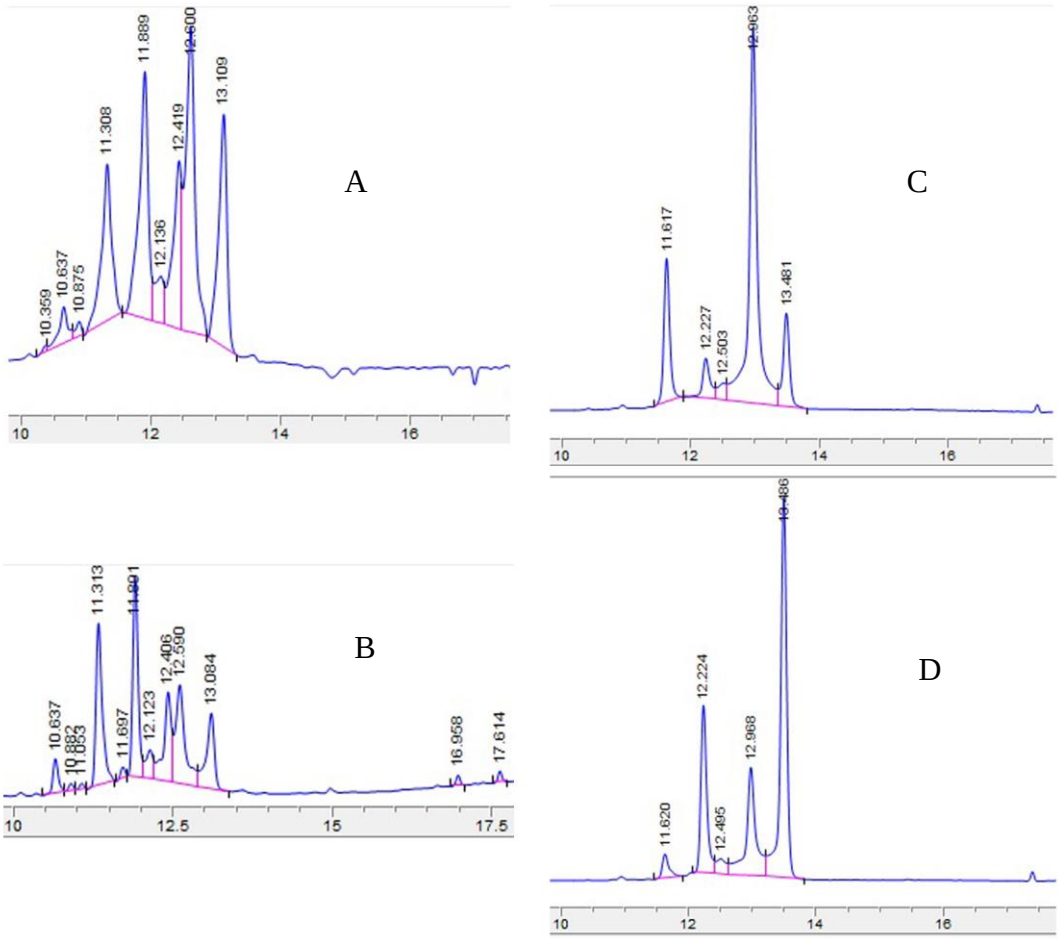


**Figure 53:** HPLC traces of A: compound **30** prepared in 75% HPLC methanol and 25% HPLC water, B: compound **30**, C: separated peak eluting at 11.3 min, D: separated peak eluting at 11.9 min

The peak pattern suggested a combination of the original sample and both separated fractions, with large peaks eluting uncharacteristically late for the stock but significant peaks present earlier that are less intense in the separated fractions. This change in peak pattern seemed to suggest a process of conversion, supporting the idea of reaction or decomposition of UV active tri-aminooxy scaffold **30**.

However it shed no further light on the question of how or why **30** might be reacting; previous exposure to ultrapure water and HPLC water had not produced similar results, suggesting the presence of TFA and water was not the cause. It was tempting to consider the presence of a high proportion of acidic methanol the source of the problem, but synthesis of **30** was conducted in acidic methanol (2M HCl methanol) and the product was fully characterised without incident. Contamination of the HPLC methanol also seemed unlikely as the solvent had been replaced several times over the course of the troubleshooting process.

At this point it seemed clear that the tri-aminooxy scaffold **30** was undergoing multiple reaction or decomposition processes under HPLC conditions used although what products were being formed and how was still unclear. Change in HPLC solvents and conditions may stop the decomposition but it is likely that this instability makes **30** unsuitable as a lectin ligand mimic. However the straightforward synthesis of compounds like **30** should make modifications easier, simplifying the search for more stable analogues.

## 4.4 Chapter Summary

Although tri-aminooxy Tris scaffold **26** was successfully synthesised the compound could not be detected by UV, making it difficult to monitor the progress of reactions with monosaccharides by HPLC. A chromophore bearing analogue was synthesised, starting from the tri propargyl Tris core **2** (**Scheme 49)**.

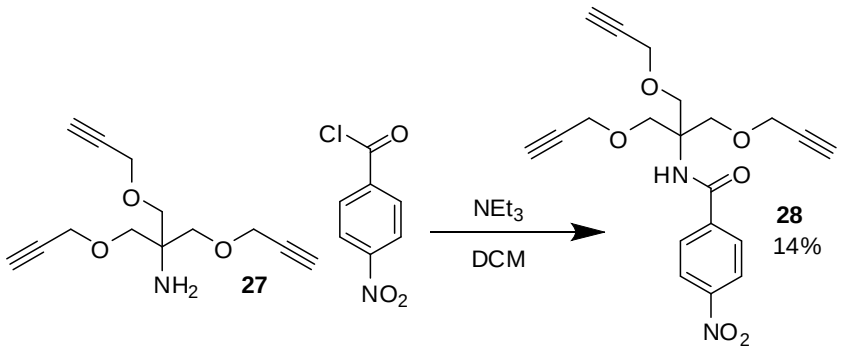


**Scheme 49:** Reaction of Tris core **27** with 4-nitrobenzoyl chloride giving UV active product **28**

Click reaction between UV active Tris core **28** and azide linker **24** gave **29,** a UV active Tris scaffold with protected aminooxy groups (**Scheme 50).**

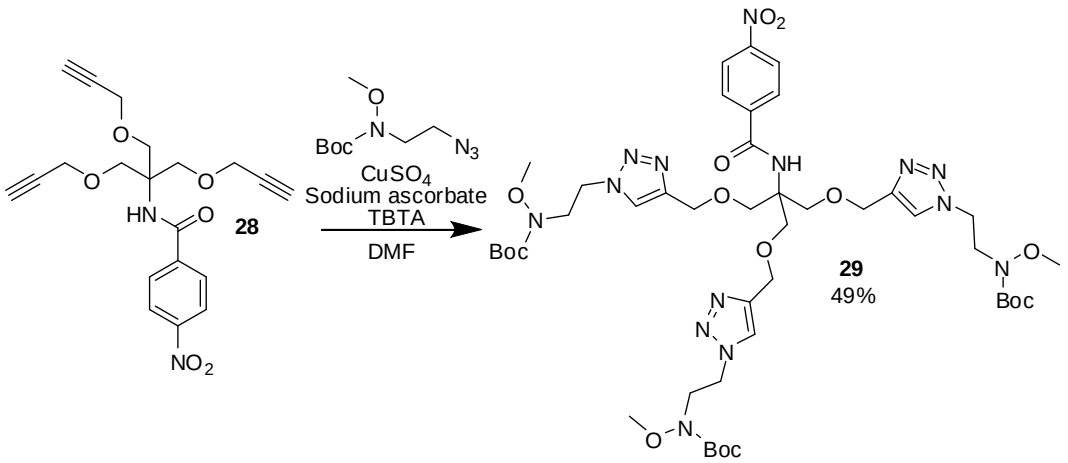


**Scheme 50:** Click reaction between UV active Tris core **28** and azide linker **24** to produce UV active scaffold **29**.

This was subjected to global Boc deprotection using acidic methanol. Deprotected scaffold **30** was used as crude.

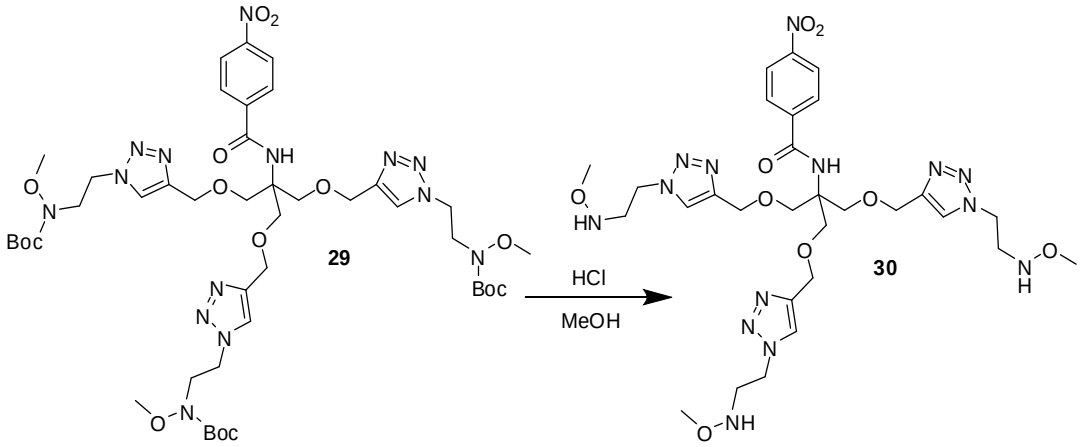


**Scheme 51:** Boc deprotection to produce scaffold **30**

Unfortunately although compound **30** could be detected by UV it proved unstable and decomposed under HPLC conditions, making it unlikely that **30** could be used as a starting point for lectin ligand mimics. However the synthetic route could allow a variety of analogues to made in a straightforward manner and simple changes to the azide linker component or the chromophore may yield a more stable scaffold.

# 5. Initial approaches to Calixarene based scaffolds

## 5.1 An introduction to calixarenes

In order to compare lectin ligand mimics displayed on different scaffolds, synthesis of sugar substituted calix(4)arenes was investigated.

Calixarenes are macrocycles of varying size (4-8 repeated units are common) derived from phenol and formaldehyde.[111] This project concentrates on calix(4)arene which is made up of four phenols connected by methylene bridges.

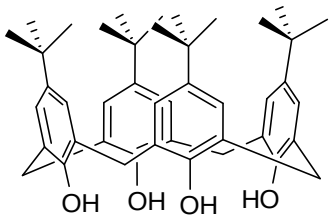


**Figure 54:** A typical calix(4)arene cone structure with tert-butyl groups on the upper rim and phenols at the lower rim

Hydroxy groups make up the narrow lower rim, while the substituents in the para position are the wide upper rim of the calix.[111] Both positions can be functionalised and a range of groups (such as alkyl chains, halides, alkenes, phosphates, peptides and glycosides) have been introduced.[111, 112, 113, 114, 115] The number of available sites for functional groups on the calix upper and lower rim, along with its ability to hold them in a stable but not immobile cone structure makes it an attractive scaffold for ligand mimic design.

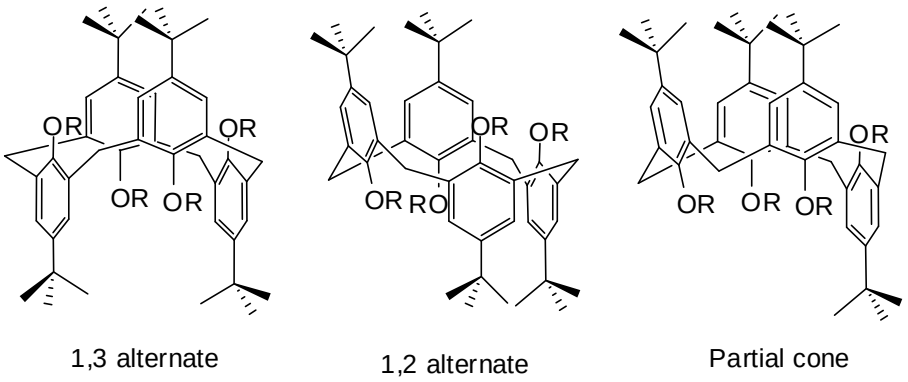


**Figure 55:** Alternate conformations of calixarenes

The position of ligands, the distance between them, the face they're displayed on, and the scaffold can be tailored to the receptor either by reference to crystal structures of the natural receptor-ligand complex or by systematic variation of the scaffold.[116, 117] Using click chemistry to couple glycosides to the calixarenes scaffold allows for a variety of glycocalixes to be synthesised with relative ease.

There are numerous examples of calix based lead compounds displaying multiple active groups. Para-guanidinoethylcalix(4)arene shown in **Figure 56** is one such example.[118]

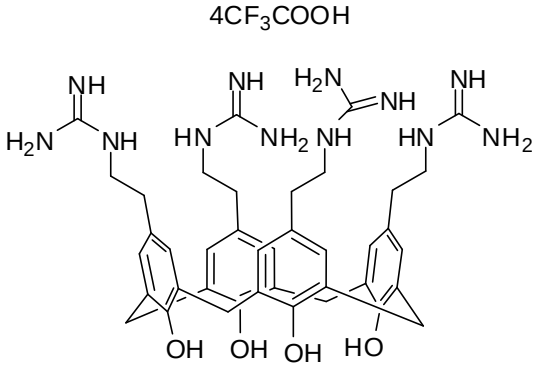


**Figure 56:** Para guanidinoethylcalix(4)arene salt produced by Grare *et al.*[118]

A simple calix(4)arene based compound with four guanidine groups displayed on the upper rim it was intended to mimic the properties of known quaternary ammonium and biguanidine based antiseptic agents.[119] The compound shows broad spectrum activity against both Gram positive and negative bacteria, including some drug-resistant strains. [118, 119] This activity is due to the calixarene structure as studies with

a related phenol-based compound showed no anti-bacterial activity.[120] Interestingly while the antiseptic agents that inspired it are cytotoxic the guanidine-calix has showed low cytotoxicity making it a potential antibiotic.[119, 120]

Calixarene based anti-bacterial, anti-fungal[121] and anti-viral[122] compounds have been produced previously. Harris *et al* described numerous compounds including calixarenes linked to known antibiotics, however when linked to calixarenes the antibiotics do not appear to be as effective as current commercially available anti-bacterials.[123] Calixarenes have also been used as carriers for prodrugs, but have so far shown more limited activity.[124]

Numerous examples of sugar substituted calixarenes also exist in the literature and a wide variety of synthetic strategies are in use.[125] Glycosylation, nucleophilic substitution, the Wittig reaction and amino or thiol based bridges have all been used successfully.[126, 127, 128] Huisgen cycloaddition, also known as click chemistry, is a particularly popular method for introducing sugars and has been utilised on the upper and lower rim using both azido and alkyne based calixes. [43, 129, 130]

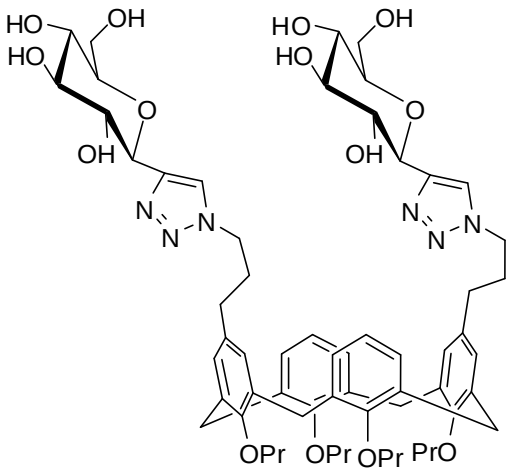


**Figure 57:** Sugar substituted calixarene utilising click chemistry.[129]

Examples of high affinity lectin binding calixarene compounds with biological activity have been developed, the cholera toxin ligand produced by Ungaro *et* al is a prominent example.[116] In designing their cholera toxin binding calixarene they first developed a tri-glycoside-like mimic of the natural ligand shown in **Figure 58**.

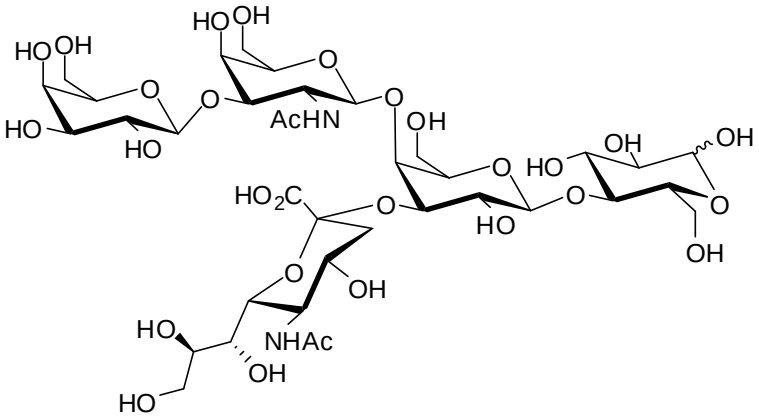


Natural cholera toxin ligand

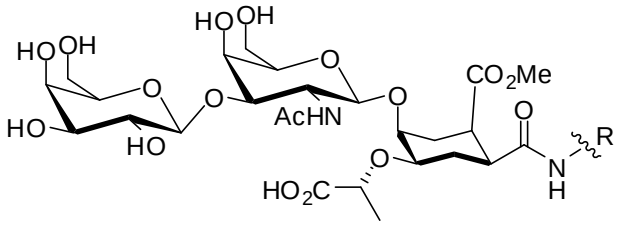


Ligand mimic

**Figure 58:** Natural cholera lectin ligand and mimic, where R is the chosen scaffold.[116]

The eventual calixarene arrangement and the length and rigidity of the linkers used, were then designed with reference to the crystal structure of the lectin so that multiple binding sites were within reach of the displayed glycosides.[116] The result was a 1,3 disubstituted calixarene (shown in **Figure 59**) with significantly stronger binding to the target lectin than the natural ligand (shown in **Figure 58**), recorded $K_d$s were 48 nM and 219 nM respectively.[116]

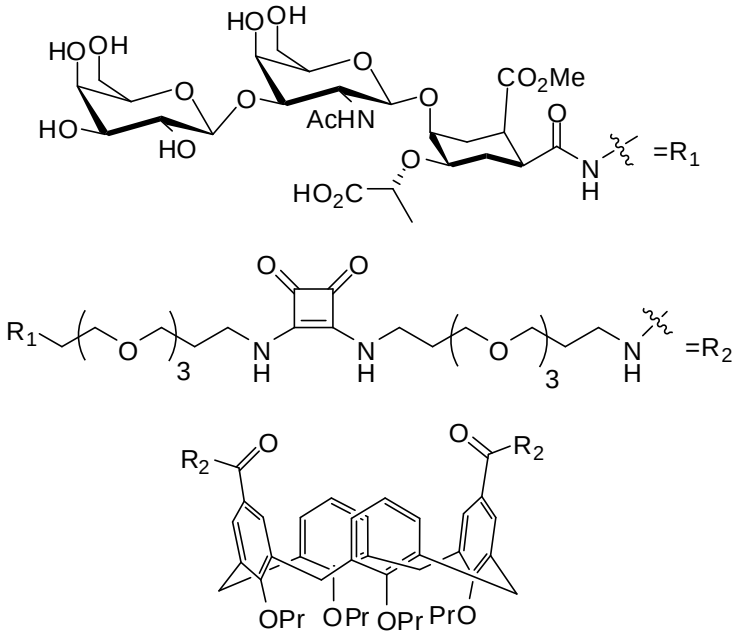


**Figure 59:** 1,3 disubstituted calix developed as a cholera toxin ligand by Ungaro *et al*.[116]

Ungaroi's approach concentrated on the potential for tailoring calixarene scaffolds to a particular target. Cecioni *et al* have successfully used an alternative strategy; utilising differences in calix conformation and the number of sugar substituted sites to produce molecules with different binding strengths.

Cecioni *et al* designed and screened a series of calixarenes with the aim of targeting the galactose-binding PA-IL lectin responsible for the initial stages of *Pseudomonas aeruginosa* infection.[117] The tested series included calixarenes of different conformations and topologies as well as di, tri and tetra galactose substituted derivatives. These variants could be synthesised relatively easily as the same monosaccharides, linkers and coupling strategies were used throughout. The tetra substituted compounds are shown below in **Figure 60**.

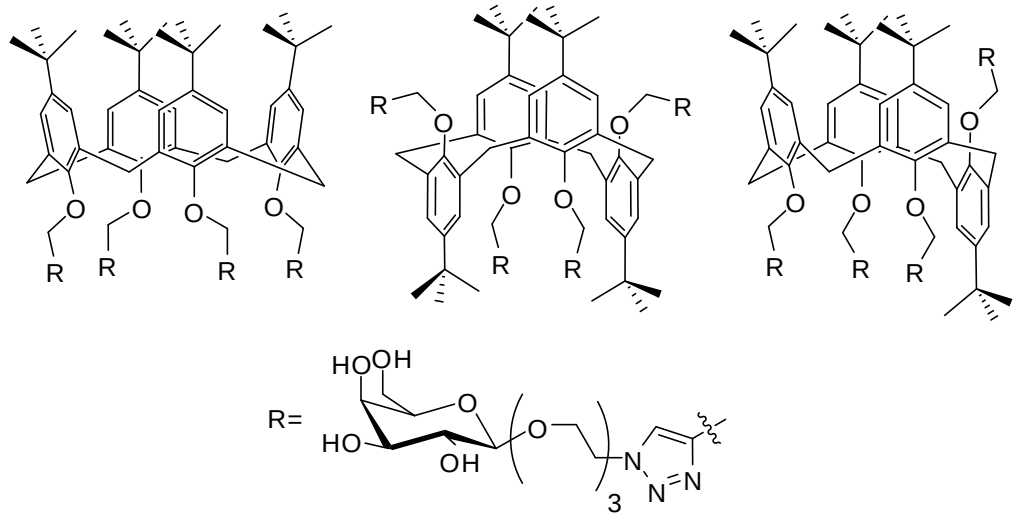


**Figure 60:** PA-IL binding calixarene ligands, illustrating the variety that can be achieved by controlling calix conformation.

While the di substituted derivatives did not bind the expected increase in binding was observed going from the tri to tetra calixarenes. The highest affinity was observed for the tetra substituted, 1,3 alternate example which had the highest known affinity for PA-IL at the time the paper was published, with an $IC_{50}$ of 500 nM.[117]

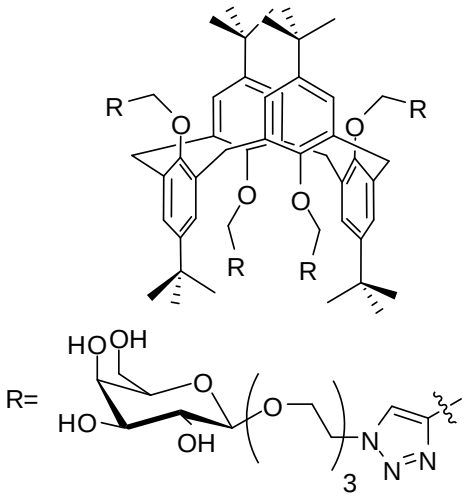


**Figure 61:** High affinity PA-IL ligand based on 1,3 alternate calixarene.[117]

Both examples illustrate advantages particular to the scaffold, with Ungaro *et al* using the cone conformation in order to ensure the binding moieties were correctly spaced and Cecioni *et al* using the possible conformations as a way of producing variation in their screened compounds.[116, 117] These examples show the potential of

calixarenes as scaffolds, highlighting how both simple systematic variations and design based on the structure of the targeted binding sites can yield excellent results.

The synthetic approach Cecioni *et al* took, using click chemistry on the calixarene lower rim, allows straightforward production of analogues with different monosaccharides or different linkers. However the choice to leave t-butyl groups on the upper rim effectively prevents bi-functionalisation of the compounds. In order to preserve calix conformation large groups on both rims are necessary, complicating any adjustments to the synthetic route.[111] Additionally the upper rim t-butyls may necessitate the use of long, hydrophilic linkers to ensure the calixarenes are sufficiently water soluble for biological testing.

Strategies that introduce azides to the calixarene upper rim, such as that used by Baldini *et al* were judged to have more potential for introducing functional handles to both the upper and lower rim.[115]

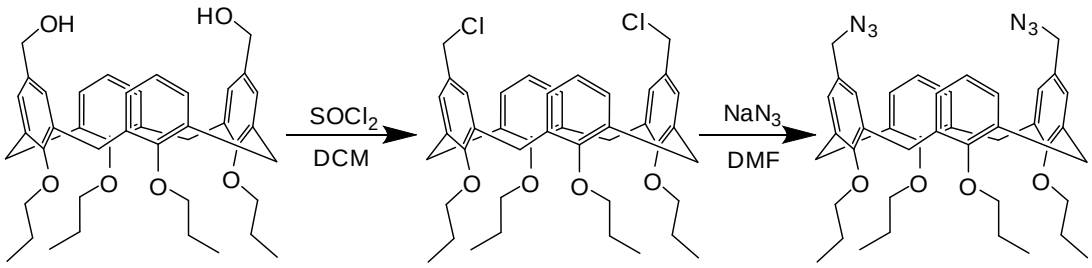


**Scheme 52:** Synthetic route to 1,3 diazido calixarene used by Baldini *et al*.[115]

Synthetic routes from the starting calix(4)arene were longer compared to the Cecioni approach and varying conformation using the Baldini group methods would be complex. However routes to the target azide can utilise the 1,3 dialdehyde calixarene shown below in **Figure 62**.

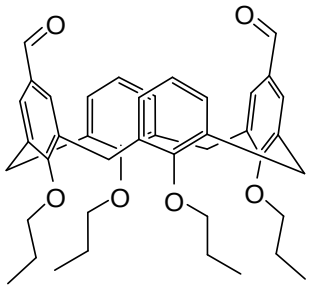

**Figure 62**: 1,3 dialdehyde calixarene, often used to produce the alcohol shown above in **Scheme 52.**

By utilising the bis aldehyde the same synthetic route can potentially be used to access azido and aminooxy substituted calixarenes, giving two methods for attaching sugars to the upper rim.

## 5.2 Synthetic strategies based on 1, 3 disubstituted calixarenes

Inspired by Baldini *et al*[115] successfully synthesising 1,3 disubstituted azido calixarenes and Bew *et al*[131] subsequently producing tetra and dilactose substituted calixarenes via click chemistry we envisioned hybrid systems with sugars coupled to the upper rim and fluorophores coupled to the lower rim as shown below in **Figure 63**. Disubstituted calixarenes were chosen, as opposed to trisubstituted equivalent, due to synthetic expediency.

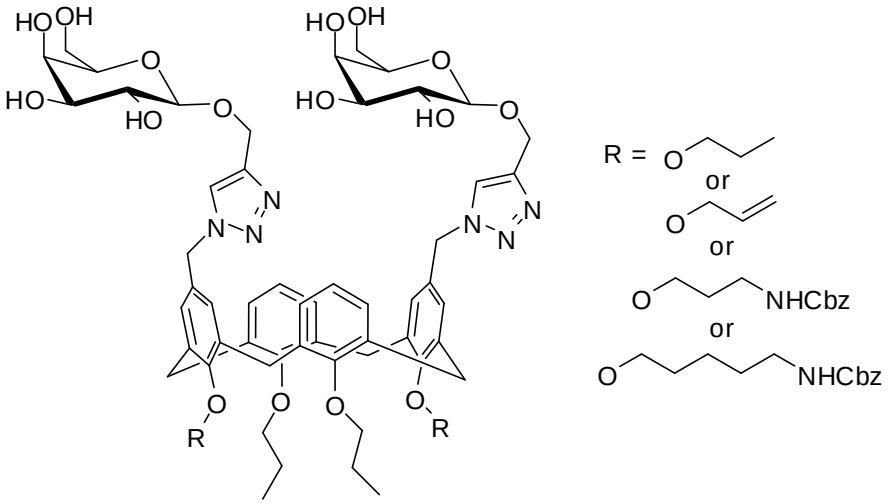


**Figure 63:** Proposed 1,3-disubstituted glycol-calixarene with click linkage where R both locks the conformation and provides a functional handle for attaching fluorophores or chromophores

The aim was to investigate whether the differences in flexibility and display of ligands between Tris and calix based scaffolds would affect their ability to bind lectins. The distance, in terms of bonds, between sugars and between a sugar and the core of the scaffold is similar for both structures. However the calix(4)arene is comparably limited in terms of how attached saccharides can be positioned. Once sufficiently bulky groups are coupled to the upper or lower rim steric hindrance prevents most changes in calix conformation (propyl groups and larger have been shown to be effective).[111] With the conformation locked the number of positions allowing free rotation is vastly reduced compared to Tris based scaffolds such as the one in **Figure 64**.

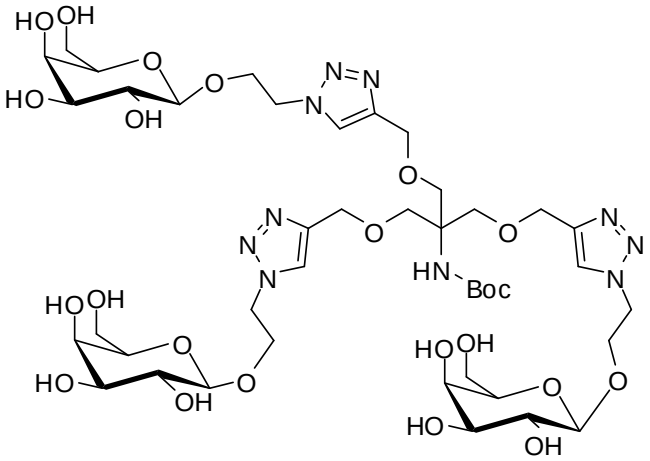


**Figure 64:** Tris based sugar substituted scaffold.

Calixarene based scaffolds, while less flexible than Tris, possess distinct faces allowing binding and non-binding functionality to be positioned so that non-binding structures are less likely to interfere with any sugar-protein interactions. Bulky flourophores positioned away from the binding pocket of a lectin may even act to increase specific binding by blocking the approach of competing molecules.[132] The scaffold's ability to adopt multiple conformers is an additional interesting structural feature which could affect binding. The central calixarene cavity can act as a hydrophobic pocket, mimicking analogous environments in natural proteins and might influence a glycocalix's interactions with lectins. These combined features suggest calixarenes would be extremely interesting ligand mimics, making up for the complex, longer synthetic routes compared to their Tris equivalents.

Synthetic routes to 1,3-bifunctionalised calixes are well established. After referring to the literature two possible routes were investigated simultaneously, both beginning with the steps outlined below in **Scheme 53**.

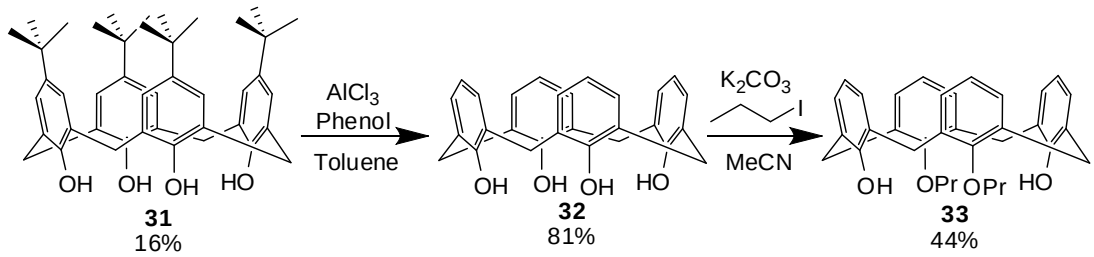


**Scheme 53:** Synthetic route to 1,3-bifunctionalised calixarenes

First calix(4)arene **31** was synthesised from formaldehyde and t-butyl phenol according to well established literature methods.[133] The upper rim t-butyl groups were then removed using a Friedel-Crafts procedure, commonly employed to access the calixarene upper rim, giving calix **32**. Several characteristic changes to the proton NMR confirmed that the reaction was successful: in starting material **31** aromatic protons had appeared as one singlet at 7.19 ppm while in **32** there were two distinct aromatic proton environments, a doublet at 7.06 ppm and a triplet at 6.73 ppm. Additionally the bridging methylene groups changed from a pair of doublets at 4.38 ppm and 3.51 ppm in **31** to a pair of broad signals at 4.26 ppm and 3.55 ppm in calix **32**, the broad signals indicate free rotation of the ring possible once the bulky upper rim t-butyl groups are removed.[111] Reappearance of the methylene doublets (at 4.33 ppm and 3.39 ppm) when **32** reacted with iodopropane to produce **33** indicated the product was once again constrained in the cone structure.[111] Comparison with the literature confirmed that the 1,3 substituted calix **33** had been successfully synthesised and attention turned to the subsequent steps outlined in **Scheme 54** below.

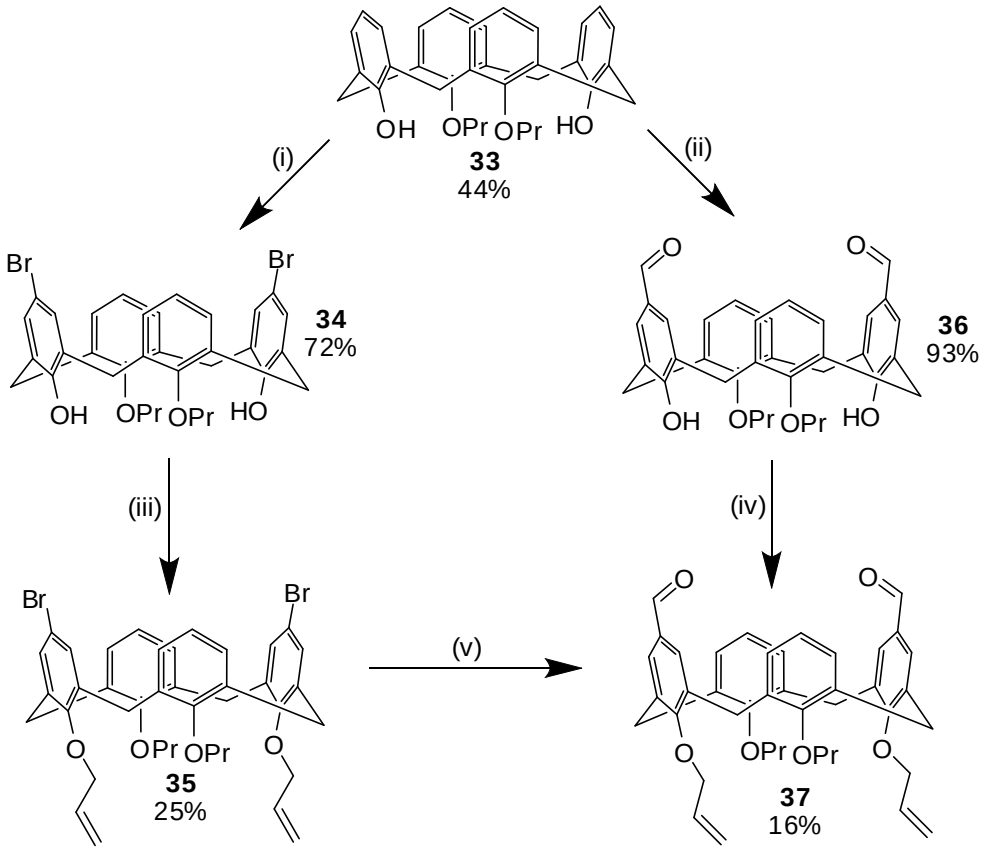


**Scheme 54:** Synthetic routes to 1,3 dialdehyde calixarene **37;** (i) $Br_2$, dry conditions, in DCM (ii) Dichloro methyl methylether, tin (IV) chloride -15$^{o}$C, in $CHCl_3$ (iii) NaH, allyl bromide, in DMF (iv) a) Trimethyl orthoformate, para toluene sulfonic acid, b) NaH, allyl bromide, in DMF (v) DMSO, triethylamine

Using literature procedures both the di bromo calix **34** and the di aldehyde calix **36** were synthesised as detailed above.[134, 135] The di allyl calixarenes **35** and **37** were synthesised from **34** and **36** respectively using procedures based on previously established literature methods (which produced the propyl rather than allyl calixes).

The eventual aim was to synthesis the 1,3 di substituted azido calix shown in **Scheme 55** below, with the proposed synthetic route from di allyl, di aldehyde calix **37** outlined.

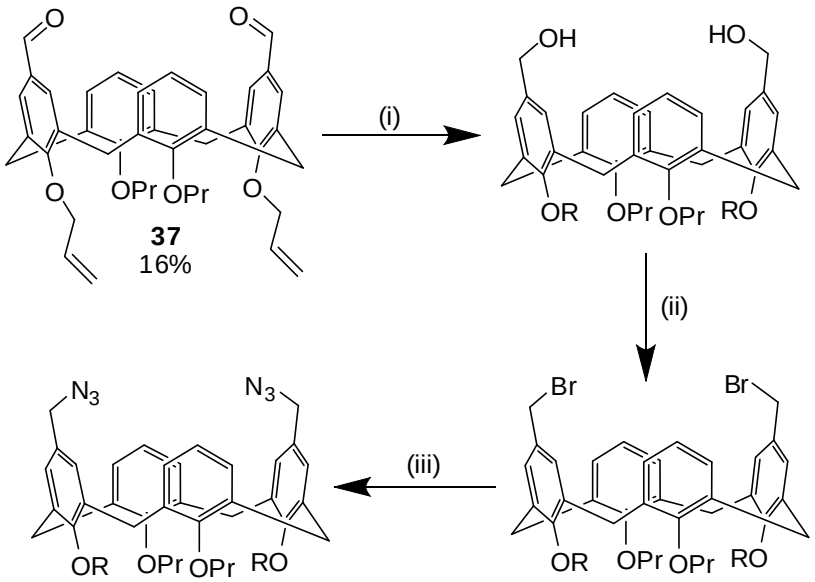


**Scheme 55:** Proposed synthetic routes to diazidocalixarene. (i) $LiAlH_4$, dry conditions, reduced temperature, (ii) $CBr_4$, triphenyl phosphine dry conditions, (iii) $NaN_3$

In both cases the azide would eventually be separated from the upper rim by a methylene group rather than attached directly to the aromatic rings. Previous work (personal communication, Dr Sunil Sharma, UEA) showed that without this spacer click reactions did not occur. Previously both Bew *et al* and Brimage have used the routes described in **Schemes 53-55** to create upper rim substituted calixarenes with propyl groups at the R position to ensure the cone confirmation.[131, 136] If suitably functionalised linkers are attached to the R position (such as those suggested in **Figure 63**) dual functional calixarenes could be produced, with sugars coupled via click chemistry to the upper rim and fluorophores or chromophores at the lower rim.

Several strategies for coupling fluorophores to the lower rim were considered. Propargyl groups have been attached to calix lower rim positions previously[137] but attempting separate click reactions on the upper and lower rim seemed unnecessarily complex. The coupling strategy needed to be high yielding, selective, involving functionality that could be attached to the lower rim in the presence of upper rim substituents and, if possible, biologically compatible. Photoclick reactions of 2,5-diphenyl substituted tetrazoles with terminal alkenes, which produce fluorescent pyrazoles (shown in **Scheme 56**), seemed ideal for this purpose as the strategy met all the relevant criteria and has been successfully conducted in living cells.[138, 139] As

a result allyl groups were chosen as the first potential functional handle to investigate.

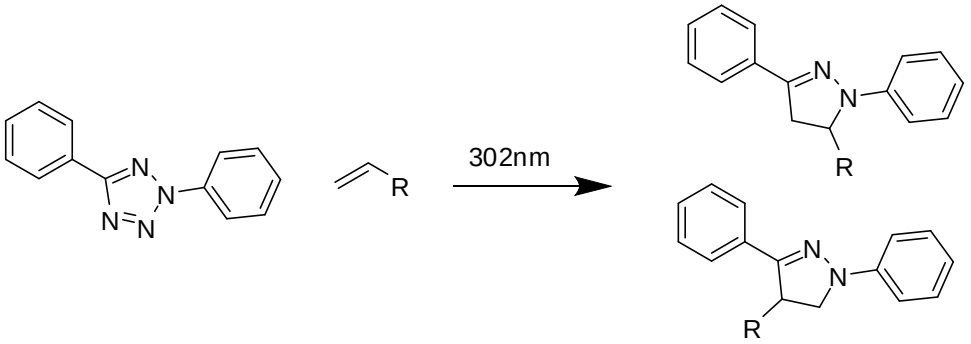


**Scheme 56:** Photoclick reaction of olefin and 2,5-diphenyl tetrazole, where R can be a variety of organic substituents.

Both the di-aldehyde (**36**) and di-bromide (**34)** approach to introducing allyl groups require the same number of synthetic steps as **36** requires protection before any further coupling to the lower rim can proceed.

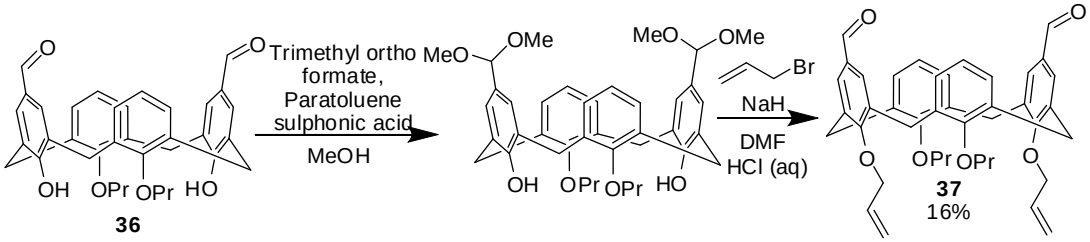


**Scheme 57:** This strategy was previously used (with propyl instead of allyl bromide) to successfully couple propyl groups to the lower rim.[136]

The protected intermediate was used as a crude since it rapidly reformed the starting bisaldehyde **36** in solution. The initial protocol used trimethyl orthoformate in order to temporarily protect upper rim aldehydes, followed by reaction with sodium hydride and allyl bromide as similar conditions had previously been used to successfully attach propyl groups to the lower rim.[136] This is shown in **Scheme 57**.

Yields of **37** were low (highest isolated yield 16%) and this was thought to be due to the protected intermediate reverting to the starting material during work up, the process is illustrated below in **Scheme 58**. Dimethyl acetal protecting groups can be

removed with acid and it was observed that prolonged exposure to magnesium sulfate (which is a mild Lewis acid) during work up led to recovery of the starting dialdehyde **36** and no detectable product. Magnesium sulfate could not be completely eliminated from the procedure; the protected intermediate had to be dried for the reaction with sodium hydride to be effective as sodium hydride reacts spontaneously with water.

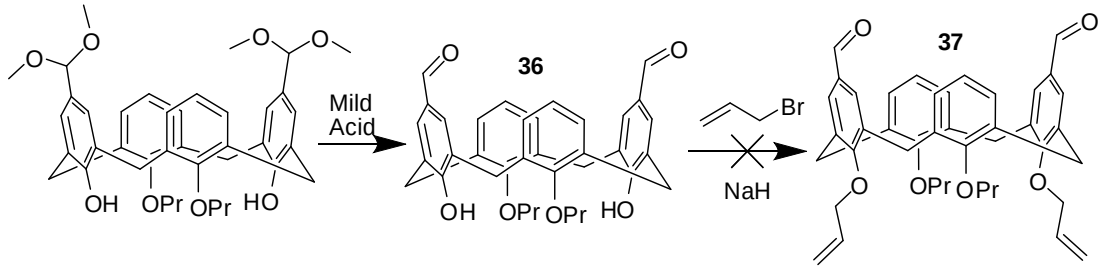


**Scheme 58:** Suggested rational for poor yield of **37** and high recovery of **36.**

When exposure to magnesium sulfate was reduced (by reducing both the quantity of magnesium sulfate used and the length of exposure) the dimethyl acetal calixarene intermediate could be detected by NMR in base-filtered chloroform although this converted back to the starting dialdehyde **36** in solution, preventing complete characterisation. By minimising exposure to magnesium sulfate and using strictly anhydrous conditions for the next step with an excess of sodium hydride the diallyl product, **37**, could be produced and isolated. With these modifications the yield was 16% (over two steps from **36)** with a substantial portion of the starting material recovered.

Initial attempts to attach allyl groups to the dibromo calixarene **34**, using sodium hydride and allyl bromide, appeared to be successful. This route was abandoned in part because the yield was not significantly higher than for the dialdehyde equivalent, **37**. The dibromo di allyl product **35,** was also found to be unstable, storage at room temperature for several days resulted in an insoluble solid which precipitated from NMR solutions. The decomposition product was not characterised and as the dialdehyde based calixarenes **36** and **37** appeared to be stable for long periods of time concentrating on these derivatives seemed reasonable.

With an effective, if low yielding, route to **37** available it seemed reasonable to investigate the photoclick reaction we intended to conduct on the primary alkenes at the calixarene lower rim. Once the optimal photoclick conditions had been found the yield of diallyl calixarene **37** could be improved. As a result tetrazole **39** was synthesised according to literature methods **Scheme 59**.[140]

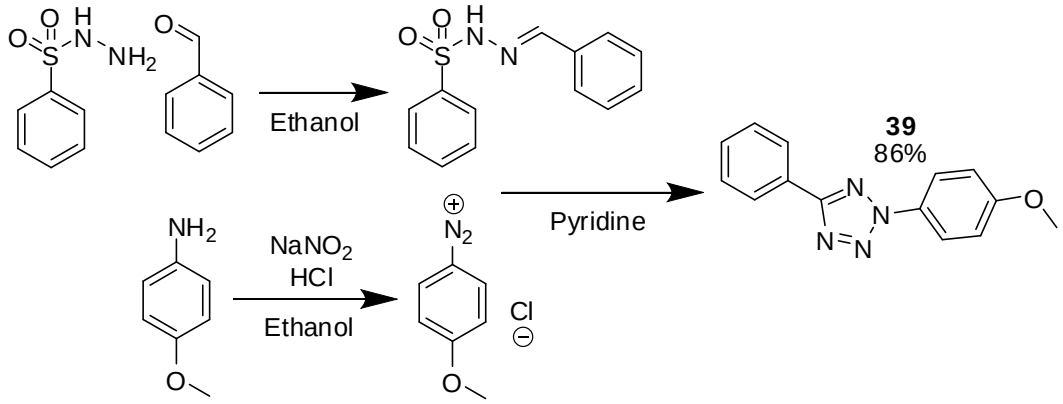


**Scheme 59:** Synthesis of tetrazole **39**, diazonium and hydrazine intermediates were not isolated or characterised.

Comparison with the literature confirmed that tetrazole **39** had been successfully synthesised.

The low yield of diallyl calixarene **37** meant that little material was available, while tetrazole **39** was easily produced in high yield (86%) on a reasonable scale (2.16 g). A series of test reactions to determine the best reaction conditions was planned, using allyl phenol (**38**) in place of the calixarene **37**. These reactions and the results are detailed in the following section.

## 5.3 Tetrazole fluorophores and photo-click test reactions

Tetrazoles are a class of stable heterocyclic compounds compromising a five membered ring with four nitrogen atoms. Compounds with a tetrazole core have been studied as potential explosives, for agricultural and pharmaceutical applications.[141, 142, 143, 144] Tetrazoles decay, when heated or under UV, releasing nitrogen and forming reactive nitrile imines, which undergo concerted 1,3-cycloaddition reactions with olefins giving one major pyrazole product.[145, 146] One

major isomer is produced due to the difference in electron density between the carbons of the alkene in this case. The regioselectivity can be reversed by changing which component is electron rich and which is electron deficient.[147]

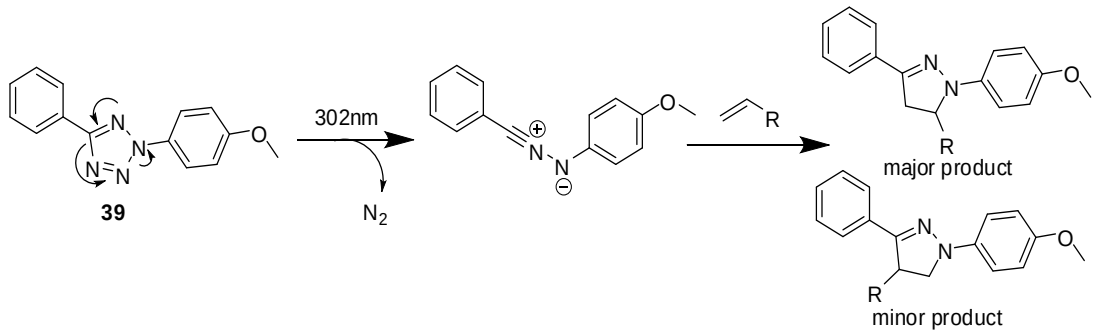


**Scheme 60:** Photoclick reaction between **39** and terminal alkene

Recently biologists have taken advantage of this photochemistry in order to produce a new class of cellular probes based on 2, 5-diphenyl substituted tetrazoles.[139] These probes have several potential advantages. The initial activation and cycloaddition proceed, in a variety of solvents and buffers, making the reaction biologically compatible. The ability to initiate the reaction under mild conditions with spatiotemporal control makes tetrazoles attractive as precursors to fluorescent biological probes. Recent work by Lin *et al* has also shown that tetrazoles can be activated and undergo cycloaddition in living cells without affecting cell mortality.[138, 139]

The initial activation of tetrazole **39** by UV occurs quickly (in fractions of a second), while the subsequent reaction of the activated nitrile imine is relatively slow (in minutes).[138] Optimising the reactions of the nitrile imine can be problematic; as dimerisation and reaction of the activated species with water are common side reactions.[148] Some pyrazole products are also thought to break down under irradiation at similar wavelengths to that required to activate the tetrazole.[148]

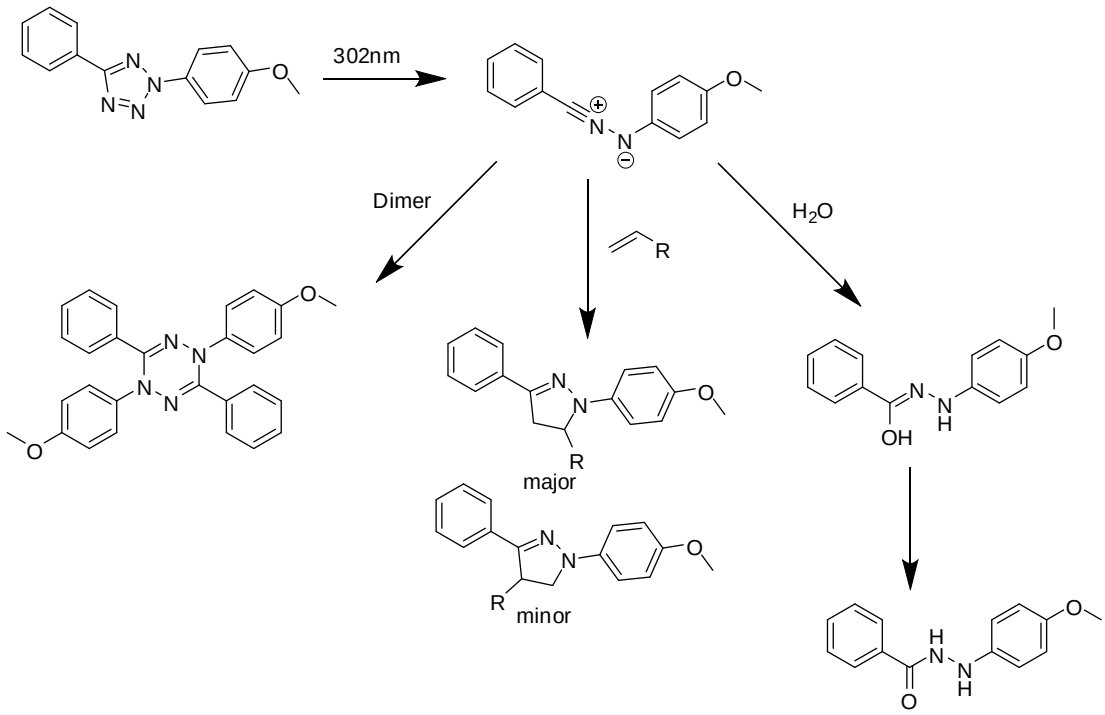


**Scheme 61:** Some of the possible reactions of the activated nitrile imine

Compound **39** was chosen based on work by Wang *et al* who reported high yields in reactions between allyl phenol (**38)** and tetrazole **39** using photoactivation.[149] A series of reactions were then attempted using **38** as a model system in place of diallyl substituted calixarene **37**.

The experiments by Wang *et al* using allyl phenol were conducted in mixtures of aqueous buffer, acetonitrile and DMSO and were aimed at optimising the reaction for use in biological systems and eventually cells. [139, 149] Our aim of using photoclick as a novel method for efficiently attaching fluorophores to the calix lower rim required a different approach. Aqueous buffers were impractical as the diallyl calixarenes were insoluble in water and the high boiling point of DMSO would likely have made extracting the product difficult. Ethyl acetate, DMF and ethanol were used instead as the diallyl calixarenes were known to be soluble in these solvents. Since higher concentrations of both tetrazole and alkene were necessary in order to obtain the product on a chemically relevant scale; the reaction volume was limited by the size of the quartz cuvettes used.

Experiments were also attempted in open plastic petri dishes, as this allowed a greater dilution closer to the concentrations used by Wang *et al*. These experiments were physically difficult to set up; ensuring the entire sample was irradiated evenly was difficult, the solutions could not be stirred as this caused the reaction mixture to splash outside the dish which prevented even mixing.

All experiments described in **Table 5** and **Table 6** were conducted using 302nm UV lamp. All experiments in EtOAc were conducted in quartz cuvettes, the final, low concentration experiment in EtOH was conducted in an open plastic petri dish.

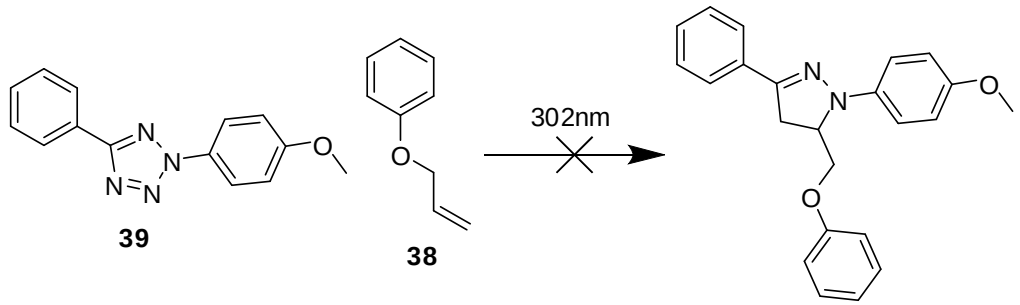


**Scheme 62:** Test reactions between tetrazole (**39)** and allyl phenol (**38)** failed to produce pyrazole

| Time Irradiated min | Equivalents alkene **38** | Solvent | Concentration **39** mM |
|---|---|---|---|
| 20 | 2 | EtOAc | 4.46 |
| 60 | 2 | EtOAc | 9.26 |
| 120 | 2 | EtOAc | 9.26 |
| 120 | 5 | EtOAc | 10.31 |
| 120 | 2 | EtOH | 7.6 |
| 120 | 2 | EtOH | 1.81 |

**Table 5:** Conditions used for attempted photoclick between compounds **38** and **39**

Additionally the reaction was attempted in ethyl acetate, irradiating for two hours and adjusting the concentration of **39** with time by periodically adding set volumes of stock solution. Concentration was changed from 11.50 to 48.21 mM over two hours. It was hoped that this would encourage the activated nitrile imine to react with

allyl phenol. Allyl phenol was stable under the reaction conditions and could not react with any of the components except the activated nitrile imine.

Following irradiation, solvent was removed but no further work up procedures were conducted. All of the reactions were investigated by NMR. However possible product was only detected by NMR when the reaction was carried out at high dilution in ethanol. Under these conditions the percentage conversion, estimated by relative integration of proton NMR peaks, was low (~30%). In each case allyl phenol was clearly visible as a large proportion of the crude.

Direct comparison with literature characterisation data was not possible, different deuterated solvents were employed resulting in significantly different chemical shifts.[149] Minor multiplets at 5.99-5.89 ppm, 5.18-5.15 ppm, 5.14-5.12 ppm, 5.08-5.04 ppm and 5.03-5.02 ppm, downfield of the allyl CH and terminal $CH_2$, were observed in the high dilution reaction. These did not correspond to either starting material or solvent and could suggest a reaction at the allyl group of **38**. However carbon NMR merely showed the expected peaks for **38**, the active nitrile imine of **39** and ethanol, leaving it unclear whether this minority material was the desired pyrazole or one of the many possible decomposition or side products.

This was not investigated further as scaling up the reaction at high dilution was deemed impractical, (reaction scale was 10 mg of **38** in 23 ml of solvent). It was concluded that direct reaction between the diallyl calixarene and tetrazole was unlikely to occur.

The photo-click reaction was next attempted using bromo-heptene and bromo-butene under various conditions. Since it is the pyrazole product that is fluorescent it was presumed that if direct photo-click reaction with calixarenes was impractical it might be possible to couple previously prepared pyrazoles to the calixarenes lower rim instead. Degradation was not observed for either alkene on irradiation in solution for the times and wavelength used. A greater excess of bromo-heptene was used for some experiments as its low boiling point meant it was easily removed and tetrazole based products could therefore be detected even when a vast excess of the alkene was used.

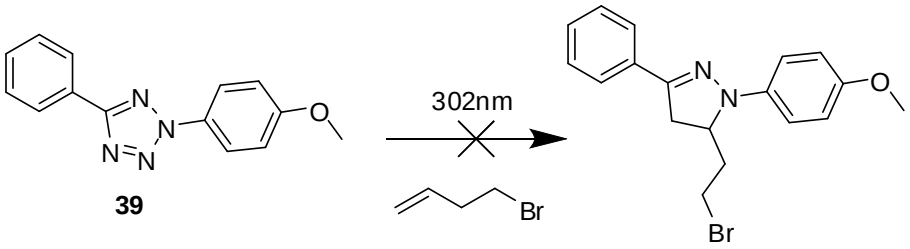


**Scheme 63:** Test reactions between tetrazole **39** and both bromo-alkenes tested were unsuccessful

| | Time Irradiated min | Equivalents alkene | Solvent | Concentration **39** mM |
|---|---|---|---|---|
| Bromo-heptene | 20 | 3 | EtOAc | 7.77 |
| | 120 | 3 | EtOAc | 9.5 |
| | 120 | 320 | EtOAc | 25.06 |
| | 120 | 3 | DMF | 12.84 |
| Bromo-butene | 120 | 3 | EtOAc | 8.72 |
| | 120 | 30 | EtOAc | 4.28 |

**Table 6:** Attempted photoclick between simple primary alkenes and tetrazole **39**

As previously, solvent was removed from the mixtures but they were subjected to no further work up conditions. The mixtures were then investigated by proton NMR. When no pyrazole was detected for these reactions a series of test reactions using bromo-heptene were conducted; attempting to activate the tetrazole by heating in the microwave. Previously tetrazole activation had coincided with an observable colour change in solutions containing tetrazole **39** from a light yellow to dark red. This colour change was not observed during microwave reactions, even after high heating for prolonged periods. Tetrazole activation by irradiation was previously confirmed by NMR, downfield shifts in both the proton and carbon spectra were observed corresponding to both the active nitrile imine and tetrazole based side products. NMR confirmed that under the microwave conditions used the tetrazole **39** was not activated.

As a result alternative methods for coupling fluorophores to the calixarenes lower rim were explored.

## 5.4 Attempts to couple primary amines to the calixarene lower rim

The large variety of commercially available fluorophores and dyes allows an almost limitless choice of functionality for attaching fluorophores to compounds of interest. Primary amines were chosen for several reasons. The proposed linkers could be quickly synthesised from cheap, commercially available materials, standard peptide coupling techniques could be employed if necessary and potentially the same fluorophores could be used for both Tris and calixarene scaffolds.

Primary amines have been coupled to calixarenes lower rims in the past using phthalimides and nitriles.[150] However the harsh conditions needed to deprotect or convert these groups would interfere with functional groups present on the upper rim of the planned calixarenes. Benzyl carbamate protection was seen as an alternative, which could potentially be deprotected at the same time the upper rim aldehydes were reduced to alcohols as shown in **Scheme 64**.

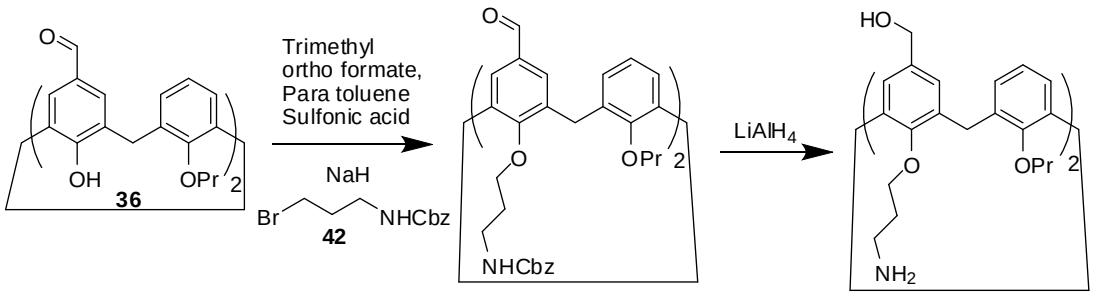


**Scheme 64:** Proposed method for coupling primary amines to calixarene (**36**) lower rim.

Compound **42** (**Scheme 65**) was therefore synthesised with a view to coupling protected amines to the lower rim of **36**.

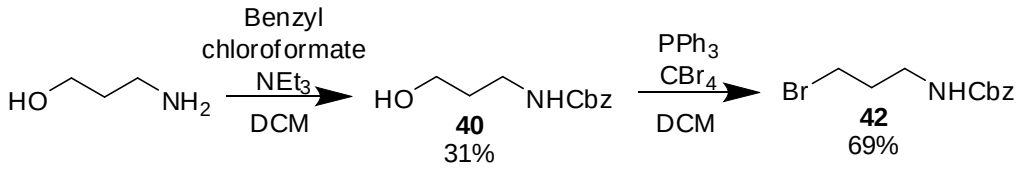


**Scheme 65:** Synthetic pathway to potential benzyl carbamate protected linkers, **40** and **42**

To begin with the reaction was carried out under the same conditions used previously to couple allyl bromide to the lower rim of dialdehyde calixarene **36 (**outlined in **Scheme 57)**. The dialdehyde starting material was recovered but the benzyl carbamate linker **42** was not detected by NMR. Since a large excess of sodium hydride was used it was theorised that the linker was breaking down under the reaction conditions.

This was confirmed by mixing the linker with excess sodium hydride for four hours, quenching and working up as previously. This produced a mixture of yellow oil and insoluble pale semi-solid. The intact linker was not observed by NMR, peaks consistent with polymerisation were detected and the insoluble solid was assumed to be a polymerisation product.

The coupling reaction was repeated using lower equivalents of sodium hydride. Dialdehyde calix **36** was temporarily protected as the dimethyl acetal, promoting reaction at the phenolic groups on the lower rim. But the dimethyl acetal intermediate was previously found to be extremely sensitive, quickly reverting to the less reactive dialdehyde starting material **36** on exposure to mild acid, such as the drying agent magnesium sulfate. Using less sodium hydride was only possible if the dimethyl acetal intermediate was exposed to more magnesium sulfate for longer, encouraging it to revert to **36**. As a result the change in procedure was expected to give a low yield.

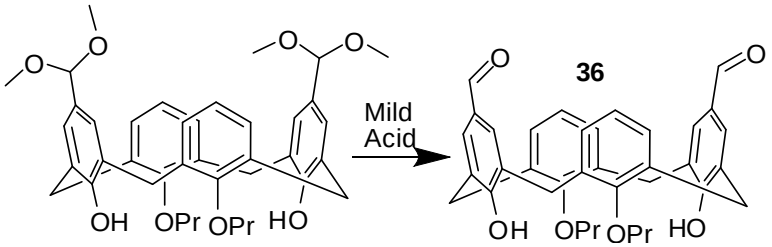


**Scheme 66:** Dimethyl acetal intermediate quickly reverted to the less reactive dialdehyde **36** on exposure to mild acid, such as magnesium sulphate or deuterated chloroform.

Both starting materials were recovered from the mixture but no product was detected. As stated previously similar conditions have led to successful reactions on the lower rim of dialdehyde calix **36** before (and were used to produce diallyl calix **37**), sodium hydride is a sufficiently strong base to initiate reaction.[136] The phenoxide anion may not be sufficiently nucleophilic to react with benzyl carbmate linker **42** or the dimethyl acetal protected intermediate of **36** may be reverting to the less reactive aldehyde under the alternate conditions.

As the linker was unstable more forcing conditions, such as high heat, were not attempted. Instead an alternative method for attaching fluorophores was once again sought.

## 5.5 Towards bifunctionalised aminooxy-click calixarenes

In order to use click chemistry on the lower rim without risking the production of numerous complex impurities a different method to attach sugars to the upper rim would be necessary. As discussed in previous chapters aminooxy chemistry represents an effective and increasingly widely used strategy for coupling unprotected sugars to a variety of molecules. [75, 151, 152] Propargyl groups could be attached to the lower rim using the same strategy as for allyl or propyl groups and the upper rim aldehydes then converted to oxime groups using commercially available aminooxy salts. Aminooxy groups are commonly synthesised via oximes and as a result the reduction step is well known.[97, 98, 153] The mild reduction conditions used should not affect lower rim alkyne groups.

This strategy gives a slightly shorter synthetic route than the analogous click with no synthetic steps on the sugars used, eliminating potentially difficult synthetic and purification procedures. The planned synthetic route to bi-functionalised calixarenes is shown (**Scheme 67**).

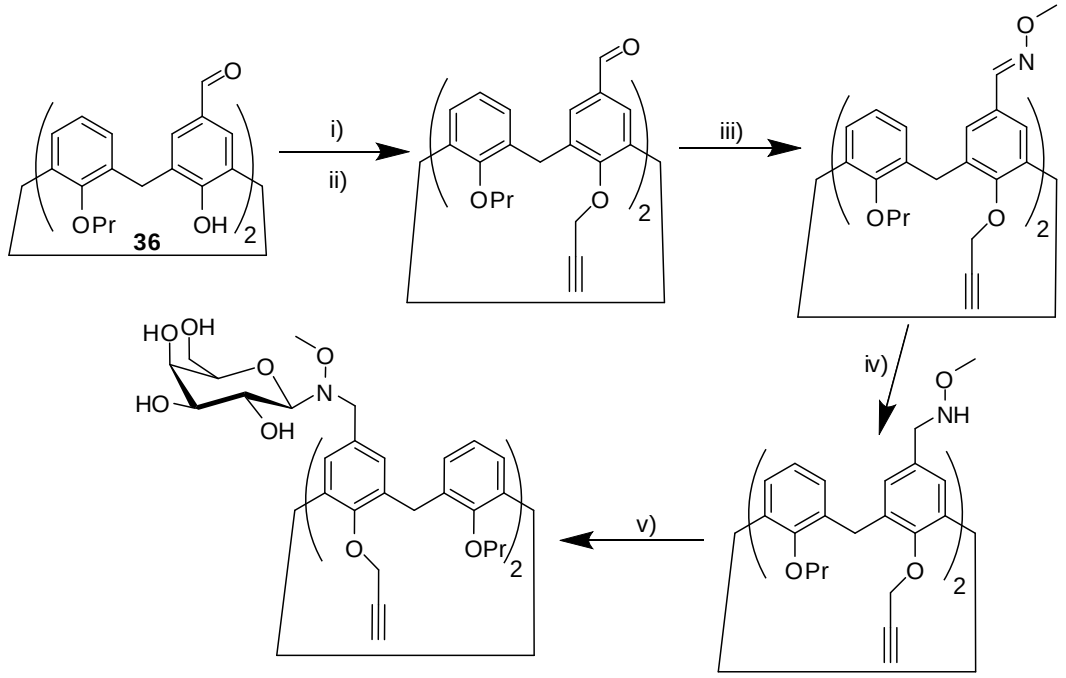


**Scheme 67:** Proposed route to upper rim sugar substituted calix: i) Trimethyl ortho formate, paratoluene sulfonic acid, ii) NaH, propargyl bromide, iii) $H_2NOMe.HCl$, pyridine, iv) $NaBH_3CN$ v) D-galactose, acetic acid, methanol

A series of test reactions were conducted using benzaldehyde in order to confirm the proposed synthetic steps were effective and optimise the conditions if necessary. O-methylbenzaldhyde oxime was isolated in good yield without column chromatography following a standard literature procedure.[153] The following reduction proceeded quickly in moderate yield and sonication with D-galactose yielded the β-anomer (**45**) shown in **Scheme 68** below.[77]

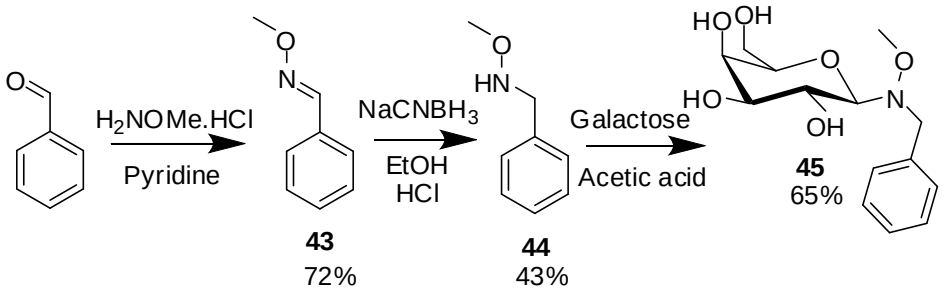


**Scheme 68:** Test reactions using benzaldehyde, compound **43** produced in similar yield to one-pot ozonolysis method shown in Chapter 3, **Scheme 24.**

Using benzaldehyde and its derivatives the chemistry was robust and repeatable. But it has been previously shown that methods which are effective on benzene based systems are not necessarily practical for their calixarene based equivalents. For instance sodium hydride is not generally required to ensure reaction of phenol, but is commonly used to produce calixarenes that are tetra-substituted at the lower rim regardless of upper rim substituents. [117, 126, 154]

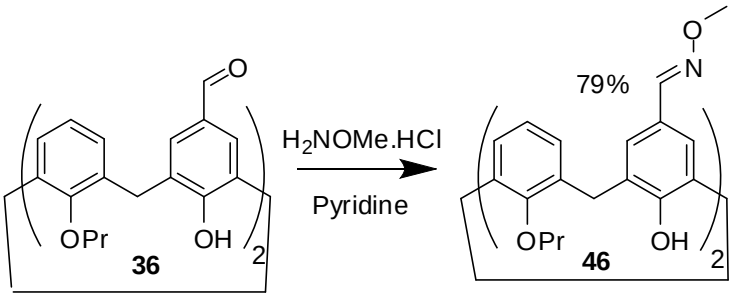


**Scheme 69:** Synthetic route to oxime functionalised calixarene

A small scale test reaction showed that the dioxime calix could be easily synthesised from the dialdehyde in good yield. Although time constraints prevented synthesis of the target sugar substituted calixarenes the results of these test reactions suggest that the strategy is sound and likely to be successful.

## 5.6 Chapter Summary

Calix(4)arene was synthesised according to literature methods and the upper rim t-butyl groups removed. 1,3 Disubstituted calixarenes were chosen as the target due to synthetic expediency and the di-aldehyde derivative **36** was produced (**Scheme 70).**

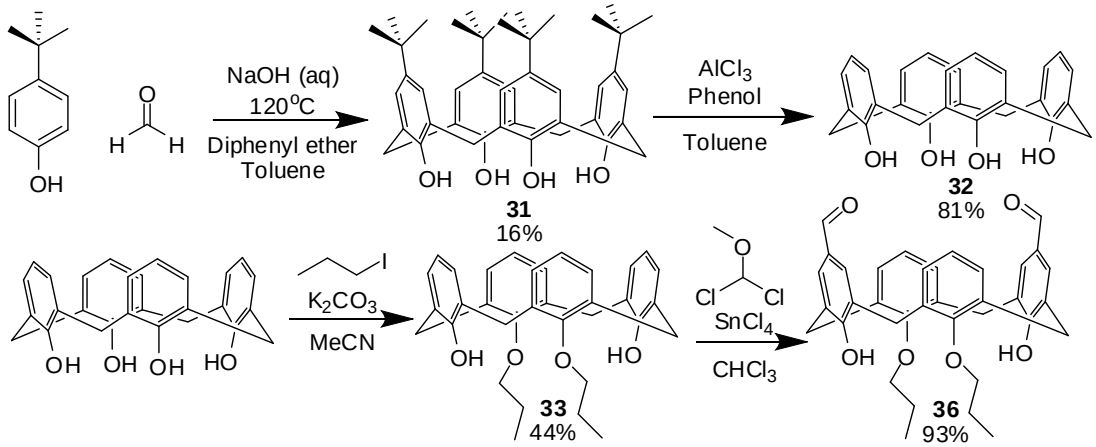


**Scheme 70:** Synthesis of calix(4)arene starting material **32**, and di-aldehyde calix **36**

Allyl groups were introduced to the calixarene lower rim as a functional handle for attaching flourophores, in a two step procedure via a protected dimethyl acetal intermediate. The dimethyl acetal intermediate was used as crude.

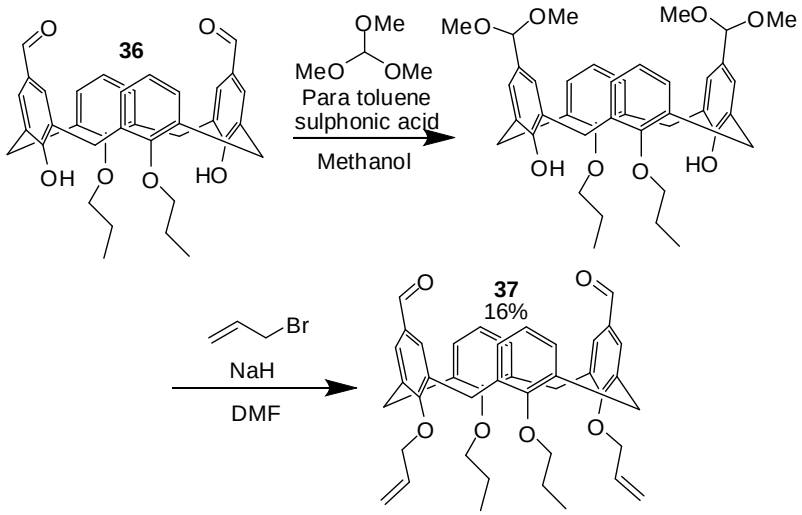


**Scheme 71:** Introducing allyl groups to the lower rim

Tetrazole **39** was then synthesised as photoclick reactions between **39** and alkenes had been demonstrated as a reliable way to produce fluorescent pyrazoles previously. The tetrazole was produced in good yield but test reactions failed to produce significant quantities of pyrazole (**Scheme 72)**.

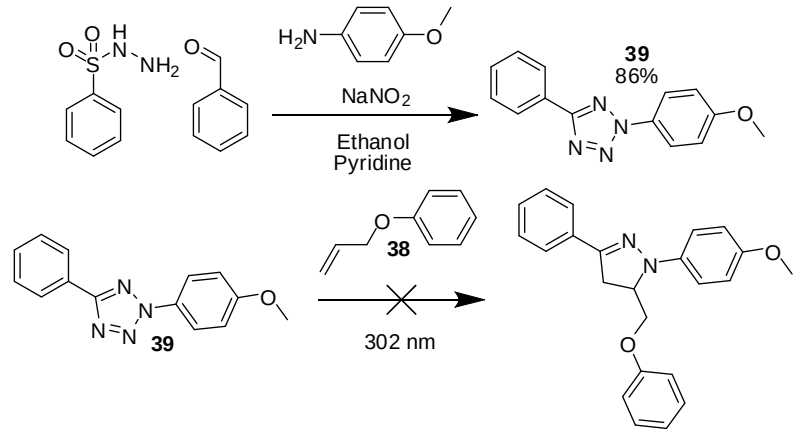


**Scheme 72:** Synthesis of tetrazole **39** was successful but test reactions failed to produce a pyrazole fluorophore

Di-oxime calixarene was produced in good yield as shown below in **Scheme 73,** suggesting that aminooxy functionality (an alternative way to attach saccharides to the upper rim) could be introduced to the calix with relative ease.

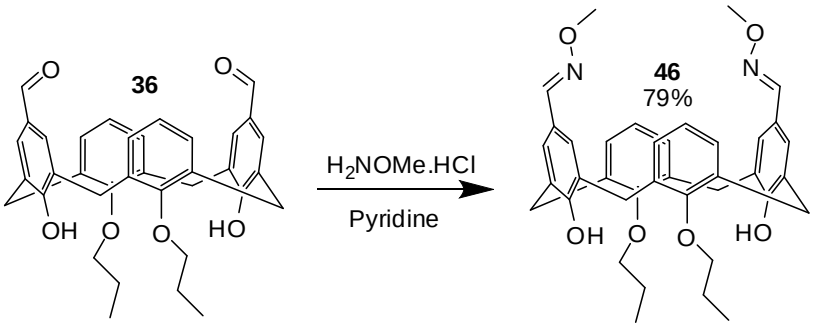


**Scheme 73:** Di-oxime calix **46** was successful synthesised from the di aldehyde **36** in good yield

Some progress has been made towards synthesising calixarene scaffolds with glycoside and fluorescent moieties on opposite faces. While using click chemistry on the upper rim was seen as desirable a complimentary method for attaching fluorophores to the lower rim was not found. The tetrazole based 'photo-click' reaction was found to be inefficient and impractical for large scale synthesis in the test reactions conducted. The alternate strategy of using aminooxy based chemistry to attach glycosides seems, given the results of test reactions, likely to be effective. This would enable the straight-forward use of click chemistry on the lower rim, allowing both the desired groups to be installed and varied with relative ease.

Introducing aminooxy functionality to the calix upper rim and using it to attach unprotected sugars should be the focus of any subsequent experiments.

# 6. Conclusions and Future Work

The aim of this work was to investigate synthetic strategies for straightforward production of lectin ligand mimics. Three potential lectin ligand mimics based on Tris scaffolds were successfully synthesised using click chemistry (**Figure 65**)

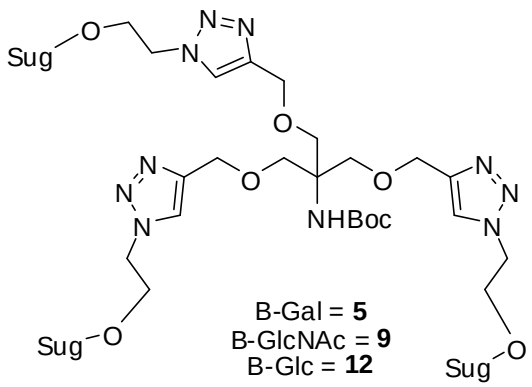


**Figure 65:** Tri-substituted Tris compounds, with acetate protected galactose, GlcNAc and glucose.

These compounds should be deprotected and their binding to relevant lectins, such as human galectins and ficolins, investigated.

Secondary aminooxy Tris scaffolds were successfully synthesised via a convergent route allowing for considerable flexibility and fine tuning of the scaffold structure.

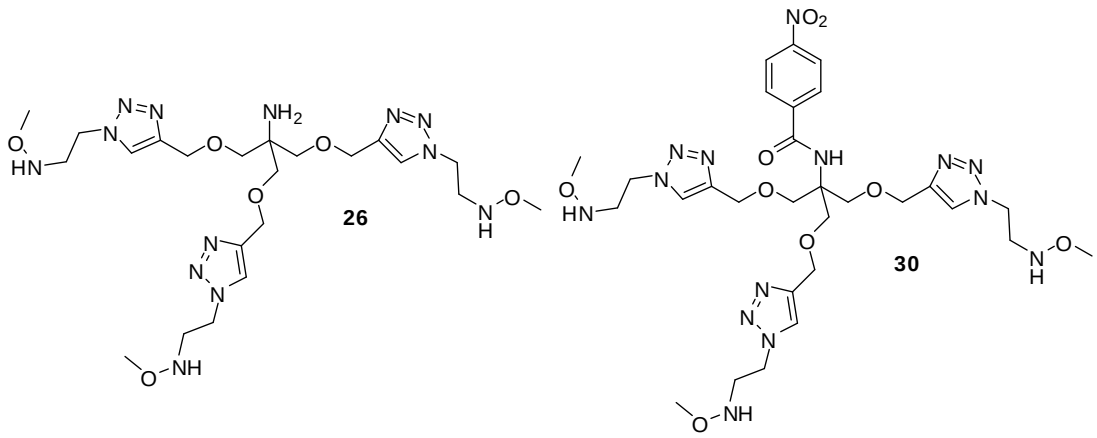


**Figure 66:** Tris based aminooxy scaffolds **26** and **30**

However synthesis of Tris scaffolds with three aminooxy linked sugars and glycocalixes was not completed, in part because complete investigation of both scaffolds was not possible in the time available. Full development of aminooxy appended Tris scaffolds was hampered by difficulties in monitoring the progress of their reactions with simple monosaccharides. While coupling a simple chromophore to the scaffold gave a compound that was easily detected (**30**), observing any of the scaffold's reactions by HPLC proved problematic as the pure scaffold decomposed during chromatography.

Despite extensive investigation of the HPLC conditions used, it was unclear precisely why Tris scaffold **30** –**Figure 66** – was unstable, or what the compound was reacting with or decomposing into.

HPLC experiments performed when compound **30** was prepared in methanol suggested that this might be responsible for the breakdown process, although this could not be confirmed by NMR due to low solubility. Switching the HPLC solvents so that acetonitrile rather than methanol is used may address decomposition issues, allowing the creation of a calibration curve for **30** and subsequent incubation experiments with simple monosaccharides.

If a change of solvent is enough to prevent degradation then work to separate and identify products of the reaction between a selection of simple sugars and **30** should be carried out. Once identified the reaction conditions could be modified to favour the tri-saccharide as far as possible. Binding studies with known lectins could then be carried out with comparison to purely *O*-glycoside products (**Figure 65**)

If however compound **30** continues to decompose after a change in HPLC solvent, systematic synthetic changes to the scaffold may be necessary. Initial investigations of this nature should start by swapping the nitro benzoyl chromophore. If this fails, subsequent investigation should concentrate on adjustments to the aminooxy-azide linker, **24,** used in the scaffold's construction.

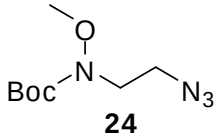


**24**

**Figure 67:** Aminooxy-azide linker, **24**

The direction of future work on related calixarene scaffolds is clearer. Successful synthesis of **46** in high yield (79%) suggests that introducing aminooxy functionality to the calix upper rim is likely to be a simple process comparable to that for its benzene equivalents. A proposed synthetic route is outlined below in **Scheme 74**. A variety of fluorophores or chromophores could be used as outlined and a small library of glycocalixes produced. Binding of these ligand mimics to relevant lectins could then be investigated.

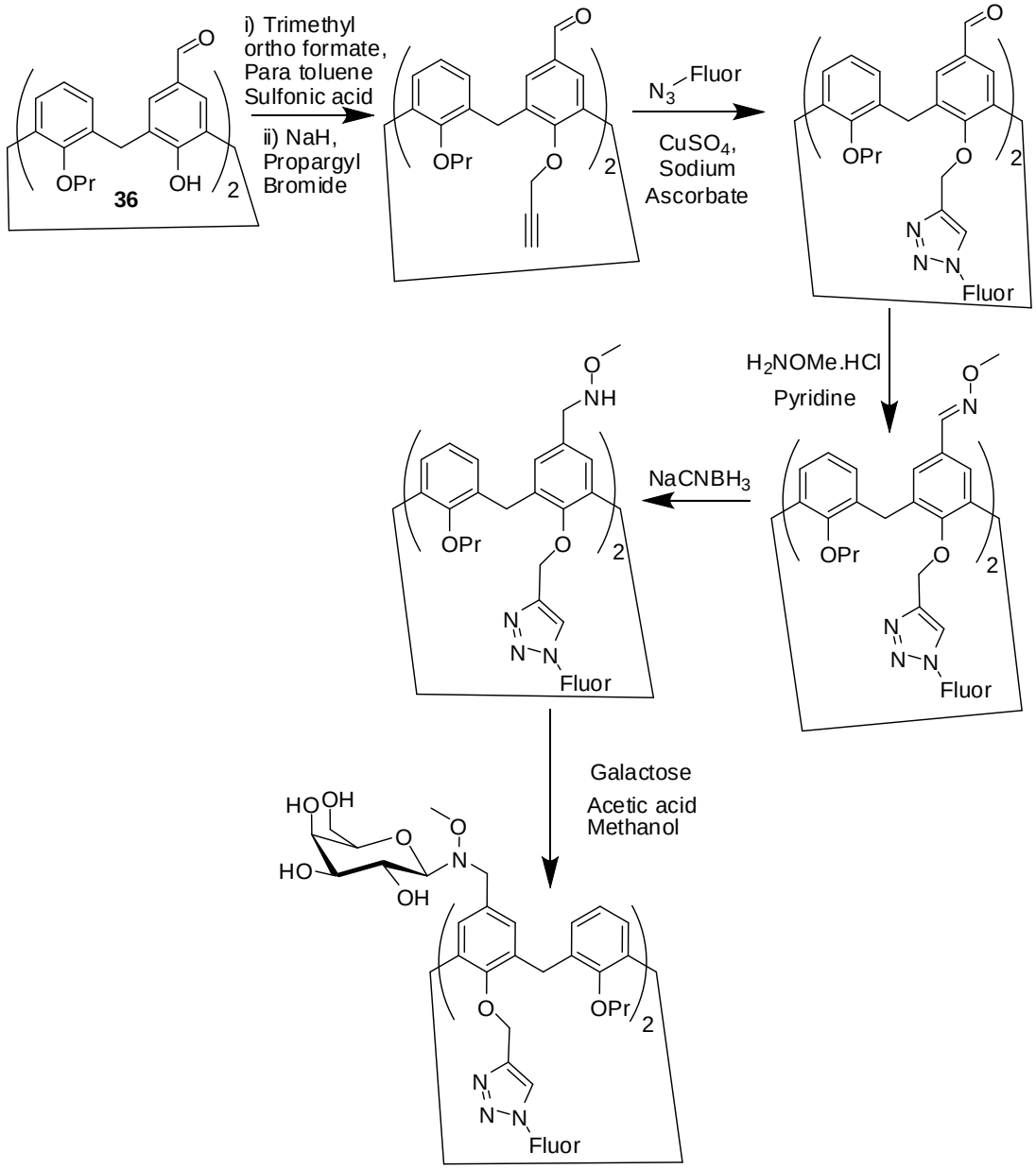


**Scheme 74:** Proposed synthetic route to aminooxy linked glycocalixes with fluorophores or chromophores appended to the lower rim (where Fluor is any suitable fluorophore or chromophore).

Future work should aim to further develop the scaffolds discussed and apply this approach to a wider selection of scaffolds.

# 7. Experimental

## 7.1 General

Proton and $^{13}C$ NMR spectra were recorded using Fourier Transform mode on a Bruker™ Ultrashield PLUS 400 at 400 MHz and 100MHz respectively using Fourier Transform mode. Spectra were analysed and processed using Topspin 3.2 and MestReNova 6.0.2-5475 software. Chemical shifts are recorded in parts per million (δ) with spectra calibrated using $CDCl_3$, MeOD, $D_2O$ and DMSO-$d_6$. Samples in $D_2O$ were spiked with acetonitrile to allow referencing to 1.47 ppm in the carbon spectra. Carbon and hydrogen atoms were assigned using a combination of one dimensional proton and carbon spectra with reference to two dimensional spectra where appropriate ($^1H$-$^1H$ COSY and $^1H$-$^{13}C$ HSQC). Coupling constants (J) are quoted in Hertz (Hz). The following abbreviations are used: s=singlet, d=doublet, t=triplet, dd=doublet of doublets, dt= doublet of triplets, q=quartet, dq=doublet of quartets, ddd= doublet of doublets of doublets, m=multiplet, br=broad peak. IR spectra were recorded as unaltered samples on a Perkin Elmer bx FT-IR system with an ATR (attenuated total reflection) sample stage using Spectrum v5.3.1 software. Electrospray mass spectra were recorded on a LCMS-2010 Shimadzu using methanol as the mobile phase. MALDI spectra were recorded using an Axima-CFR Kratos Analytical model. Accurate molecular masses were obtained by the National Mass Spectrometry Facility at Swansea University. Analytical HPLC was performed on an Agilent 1200 instrument with a UV-Vis diode array detector at 254 nm and 270 nm. Mobile phases used HPLC grade solvents and reagents, mobile phase A was water with 0.05% TFA, mobile phase B was methanol with 0.05% TFA. Separation was performed using an Eclipse XDB-C18 column with the column temperature 40$^oC$. The flow rate was 1 ml/min and the injection volume varied between runs. The gradient started with 5% to 95% B over 15 min, during which all analytes eluted. The column was then returned to 5% B and equilibrated for a further 5 min. pD of solutions prepared in deuterated solvents was calculated using a low volume Jenway 3510 probe and the established conversion factor (0.4).[110] Where deuterated phosphate buffer was used the pD was 6.32 and the concentration 100 mM. UV-Vis spectra and absorbance measurements were taken using a PerkinElmer Lambda 25

uv/vis spectrometer. $\lambda_{max}$ was determined by measuring absorbance over the range 220-600 nm and spectra were analysed using UV winlab software. Solutions of known concentration were prepared using accurate balances and volumetric flasks according to standard procedures. Dilutions were prepared using volumetric flasks and pipettes. Quartz cuvettes were used for all measurements which were performed in methanol for compound **29** and in water at ~pH6 for compound **30.** Optical rotations ($[\alpha]_D$) were obtained using a Perkin-Elmer 241 Polarimeter, at the specified concentration in the specified solvent. Analytical TLC was carried out on aluminium backed Merck TLC Silica gel 60 F254 plates and visualised under UV light or by using basic potassium permanagante as a stain and heating. Flash chromatography was carried out using 60mM silica gel and the solvent systems specified. All chemicals were purchased from Sigma-Aldrich, Acros, Fluka or Alfa-Aesar. Anhydrous chloroform was prepared by drying over oven dried molecular sieves under an atmosphere of nitrogen. Other anhydrous solvents were purchased from Aldrich or Fluka. Petroleum ether refers to the 40-60$^oC$ boiling fraction. Where reactions are reported as being performed in oven dried glassware, under a nitrogen atmosphere standard inert reagent handling techniques were used. Where sonication was employed to aid reactions a Branson 2510 sonic bath operating at a frequency of 40 kHz was used.

## 7.2 Experimental methods

**Tert-butyl 1,3-dihydroxy-2-(hydroxymethyl)propan-2-ylcarbamate, 1:** [155]

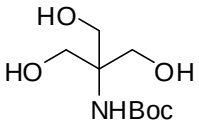


Tris(hydroxymethyl)aminomethane hydrochloride (4.99 g, 31.65 mmol) was suspended in a mixture of dry methanol (90 ml) and triethylamine (10.89 g, 107.6 mmol, 15 ml) A solution of di-tert-butyl carbonate (7.74 g, 35.47 mmol) in dry methanol (45 ml) was added over 15 min. The mixture was stirred at room temperature for 4 hrs before the solvent was removed under vacuum. The resulting solid was extracted with ethyl acetate (400 ml), washed with brine (50 ml) separated and solvent removed giving the product as a white solid (4.54 g, 65%).

mp 142.8-143.1°C (from ethyl acetate); $\upsilon_{max}$ (ATR) 3413 (N-H), 3293 (O-H), 2961 (C-H), 1677 (C=O), 1544 (N-H bend), 1466 (C-H bend), 1292 (C-O), 1257 (C-O); $\delta_H$ (400 MHz, DMSO) 5.75 (1H, s, NH), 4.49 (3H, t, J=5.6, OH), 3.51 (6H, d, J=5.6, $CH_2$), 1.37 (9H, s, Me); $\delta_C$ (100 MHz, DMSO) 155.0 (C=O), 77.8 (C-$Me_3$), 60.4 ($CH_2$), 60.2 (C-NH), 28.2 (Me); Calculated Mass for $C_9H_{19}NO_5$ 221.25 *m/z* ($ES^+$) 244.0 ($MNa^+$)

**Tert-butyl 1,3-bis(prop-2-ynyloxy)-2-((prop-2-ynyloxy)methyl)propan-2-ylcarbamate, 2:** [47]

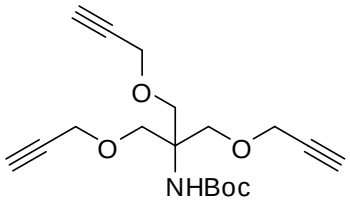


**1** (1.00 g, 4.53 mmol) was dissolved in dry DMF (12 ml) in a round bottomed flask oven dried and cooled under nitrogen. The solution was cooled to -15 °C and propargyl bromide (3 ml, 4.01 g, 33.67 mmol) added. Ground potassium hydroxide (1.51 g, 26.87 mmol) was then added in portions over 15 min. The mixture was allowed to warm to room temperature and then heated to 50°C. The mixture was stirred at 50°C for two days and at room temperature for 24 hrs.

The mixture was extracted with ethyl acetate (250 ml), washed with brine (150 ml, x3), separated, dried over magnesium sulphate, filtered and solvent removed under vacuum giving a brown oil. This was purified by flash column chromatography on silica using petroleum ether and ethyl acetate (17:3) giving the product as a yellow oil (1.05 g, 69%)

$\upsilon_{max}$ (ATR) 3427 (N-H), 3291 (C-H alkyne), 2975 (C-H), 2884 (C-H), 1711 (C=O), 1500 (C-H), 1243 (C-O), 1164 (C-O), 1090 (C-N); $\delta_H$ (400 MHz, $CDCl_3$) 4.92 (1H, s, NH), 4.15 (6H, d, J=2.4, O-$\underline{CH_2}$-CCH), 3.78 (6H, s, NC-$\underline{CH_2}$), 2.42 (3H, t, J=2.4, CH), 1.42 (9H, s, Me); $\delta_C$ (100 MHz, $CDCl_3$) 154.9 (C=O), 79.7 (O-$CH_2$-$\underline{C}$CH), 79.4 (C-$Me_3$), 74.7 (CH), 69.1 (O-$\underline{CH_2}$-CCH), 58.8 (NC-$\underline{CH_2}$), 58.2 (NH-C), 28.5 (Me); Calculated Mass for $C_{18}H_{25}NO_5$ 335.39 *m/z* ($ES^+$) 357.9 ($MNa^+$)

**2 Azidoethanol, 3:** [63]

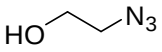


Bromoethanol (2.6 ml, 4.58 g, 36.68 mmol) was dissolved in a mixture of acetone (102 ml) and water (18 ml). Sodium azide (3.48 g, 53.50 mmol) was added and the mixture heated to reflux for 16 hrs then allowed to cool to room temperature.
The mixture was concentrated under vacuum and water added (150 ml). The mixture was extracted with ether (300 ml), separated, dried over magnesium sulphate, filtered and solvent removed under vacuum giving the product as a clear oil (2.70 g, 86%) $\upsilon_{max}$ (ATR) 3354 (O-H), 2934 (C-H), 2877 (C-H), 2092 ($N_3$), 1283 (C-H), 1061 (C-O); $\delta_H$ (400 MHz, $CDCl_3$) 3.81 (2H, t, J=4.8, $\underline{CH_2}$-OH), 3.47 (2H, t, J=4.8, $\underline{CH_2}$-$N_3$), 1.47 (1H, br, OH); $\delta_C$ (100 MHz, $CDCl_3$) 61.6 ($\underline{CH_2}$-OH), 53.7 ($\underline{CH_2}$-$N_3$); Calculated Mass for $C_2H_5N_3O$ 87.08 *m/z* ($ES^+$) 104.9 ($MH_2O^+$)

**2-Azidoethyl 2,3,4,6-tetra *O*-acetyl β-$_D$-galactopyranoside, 4:** [156]

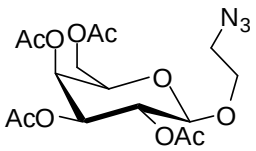


$_D$-Galactose pentacetate (508 mg, 1.3 mmol) and **3** (225 mg, 2.58 mmol) were dissolved in dry DCM (10 ml) in apparatus oven dried and cooled under nitrogen. The mixture was then cooled to 0$^o$C and boron trifluoride diethyl etherate (0.2 ml, 230 mg, 1.62 mmol) was added. The mixture was stirred at 0$^o$C for an hour then allowed to warm to room temperature. The mixture was stirred at room temperature for 20 hrs then diluted with DCM (200 ml). The organic layer was washed with saturated sodium hydrogen carbonate solution (150 ml) and water (150 ml, x3), separated, dried over magnesium sulphate, filtered and solvent removed giving a clear oil.
This was purified by flash column chromatography on silica using petroleum ether and ethyl acetate (1:1) giving the product as a clear oil (289 mg, 53%) $[\alpha]_D^{17.9}$ -19.4 (*c* 1.13, MeOH) (lit.,[157] $[\alpha]_D^{27}$ -11.5 (*c* 1, $CHCl_3$)); $\upsilon_{max}$ (ATR) 2103 ($N_3$), 1741 (C=O), 1367 (C-O), 1211 (C-H); $\delta_H$ (400 MHz, $CDCl_3$) 5.37 (1H, dd, $J_{3-4}$=3.4, $J_{4-5}$=0.8, H-4), 5.21 (1H, dd, $J_{1-2}$=7.8, $J_{2-3}$=10.6, H-2), 5.00 (1H, dd, $J_{2-3}$, $J_{3-4}$, H-3), 4.54 (1H, d, $J_{1-2}$, C-H anomeric), 4.16-4.09 (2H, m, H-6), 4.09-4.04 (1H, m, GalO-$\underline{CH_2}$), 3.91 (1H, dt, $J_{4-5}$, $J_{5-6}$=6.8, H-5), 3.68-3.62 (1H, m, GalO-$\underline{CH_2}$), 3.49-

3.43 (1H, m, $\underline{CH_2}$-$N_3$), 3.29-3.23 (1H, m, $\underline{CH_2}$-$N_3$), 2.13 (3H, s, Me), 2.04 (3H, s, Me), 2.02 (3H, s, Me), 1.96 (3H, s, Me); $\delta_C$ (100 MHz, $CDCl_3$) 170.5 (C=O), 170.3 (C=O), 170.2 (C=O), 169.6 (C=O), 101.2 (C-H anomeric), 71.0 (C-3), 70.9 (C-5), 68.6 (C-2), 68.5 (GalO-$\underline{CH_2}$), 67.1 (C-4), 61.3 (C-6), 50.6 ($\underline{CH_2}$-$N_3$), 20.8 (Me), 20.7 (Me), 20.7 (Me), 20.6 (Me); Calculated Mass for $C_{16}H_{23}N_3O_{10}$ 417.37 *m/z* ($ES^+$) 439.9 ($MNa^+$)

**Tert-butyl 1,3-bis((1-(2-ethyl 2,3,4,6-tetra-O-acetyl-β-$_D$-galactopyranoside)-1H-1,2,3-triazol-4-yl)methoxy)-2-(((1-(2-ethyl 2,3,4,6-tetra-O-acetyl-β-$_D$-galactopyranoside)-1H-1,2,3-triazol-4-yl)methoxy)methyl)propan-2-ylcarbamate, 5:**

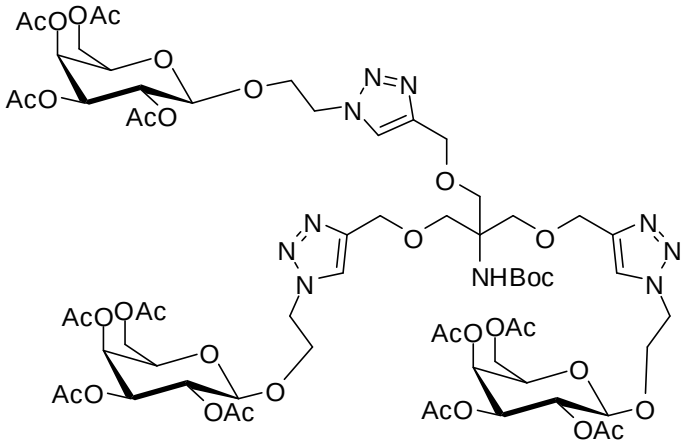


**4** (208 mg, 0.498 mmol) was added to a solution of **2** (52 mg, 0.154mmol) in DMF (4 ml) followed by copper sulphate (39 mg, 0.156 mmol) and sodium ascorbate (27 mg, 0.134 mmol). The mixture was stirred at room temperature for 20 hrs.
The mixture was then extracted with ethyl acetate (200 ml), washed with brine (100 ml, x4), separated, dried over magnesium sulphate, filtered and solvent removed under vacuum giving a pale oil. This was purified by flash column chromatography on silica using ethyl acetate and methanol (19:1) giving the product as a clear oil (161 mg, 66%)
$[\alpha]_D^{18.0}$ -15.4 (*c* 1.19, MeOH); $\upsilon_{max}$ (ATR) 2959 (C-H), 1744 (C=O), 1504 (C-H), 1367 (C-O), 1215 (C-O), 1044 (C-N); $\delta_H$ (400 MHz, $CDCl_3$) 7.62 (3H, s, CH triazole), 5.38 (3H, dd, $J_{3-4}$=3.2, $J_{4-5}$=0.8, H-4), 5.17 (3H, dd, $J_{1-2}$=8, $J_{2-3}$=10.4, H-2), 5.05 (1H, s, NH), 4.98 (3H, dd, $J_{2-3}$, $J_{3-4}$, H-3), 4.64-4.61 (3H, m, N-$\underline{CH_2}$), 4.60 (6H, s, $\underline{CH_2}$-triazole), 4.54 (3H, dd, $J_1$ =8.6, $J_2$=3.8, N-$\underline{CH_2}$), 4.47 (3H, d, $J_{1-2}$, CH

anomeric), 4.26 (3H, dt, $J_1$ =8.6, $J_2$=3.8, GalO-$\underline{CH_2}$), 4.18-4.09 (6H, m, H-6), 3.96-3.90 (6H, m, H-5, GalO-$\underline{CH_2}$), 3.77 (6H, s, $\underline{CH_2}$-CNH), 2.15 (9H, s, O=C-$\underline{Me}$), 2.04 (9H, s, O=C-$\underline{Me}$), 1.97 (9H, s, O=C-$\underline{Me}$), 1.93 (9H, s, O=C-$\underline{Me}$), 1.39 (9H, s, C-$\underline{Me_3}$); $\delta_C$ (100 MHz, $CDCl_3$) 170.5 (C=O, Ac), 170.3 (C=O, Ac), 170.2 (C=O, Ac), 169.6 (C=O, Ac), 154.9 (C=O, Boc), 144.7 (C, triazole), 124.3 (CH, triazole), 101.1 (CH, anomeric), 71.0 (C-5), 70.7 (C-3), 69.5 ($\underline{CH_2}$-CNH), 68.5 (C-2), 67.7 (GalO-$\underline{CH_2}$), 67.0 (C-4), 64.8 ($\underline{CH_2}$-triazole) , 61.3 (C-6), 58.6 (C-NH), 50.2 (N-$\underline{CH_2}$), 28.5 ($\underline{Me}$, Boc), 20.8 ($\underline{Me}$, Ac), 20.8 ($\underline{Me}$, Ac), 20.7 ($\underline{Me}$, Ac); Calculated Mass for $C_{66}H_{94}N_{10}O_{35}$ 1587.5956 *m/z* (MALDI) 1488.92 ($M^+$ -BOC); HRMS ($ES^+$): 1587.5954 ($M^+$)

**N-acetyl 1,3,4,6-tetraacetate α-$_D$-Glucosamine, 6:**

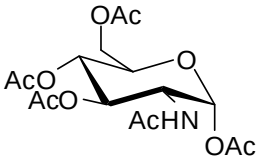


α-$_D$-Glucosamine (2.64 g, 11.94 mmol) was suspended in pyridine (27 ml). Acetic anhydride (5.7 ml, 60.30 mmol) was added and the mixture was stirred for 17 hrs. The mixture was then concentrated and extracted with DCM (300 ml). The organic layer was washed with 1M aqueous HCl (100 ml), saturated copper sulphate solution (100 ml) and brine (150 ml, x4), separated, dried over magnesium sulphate, filtered and solvent removed under vacuum. The resulting concentrated suspension in DCM was left in air overnight to crystallise. This gave **6** as pale crystals (3.87 g, 83%). mp 133.4-136.8$^o$C (from ethyl acetate) (lit.,[67] 134-135$^o$C from ethyl acetate:petroleum ether); $[\alpha]_D^{18.2}$ +89.4 (*c* 1.19, MeOH) (lit.,[67] $[\alpha]_D^{21}$ +94 (*c* 1, $CHCl_3$)); $\upsilon_{max}$ (ATR) 3437 (N-H), 1739 (C=O ester), 1734 (C=O ester), 1672 (C=O amide), 1517 (N-H bend), 1381 (C-H), 1239 (C-O), 1222 (C-O), 1038 (C-N); $\delta_H$ (400 MHz, $CDCl_3$) 6.17 (1H, d, $J_{1\text{-}2}$=3.6, C-H, anomeric), 5.53 (1H, d, $J_{NH\text{-}2}$=9.0, NH), 5.26-5.18 (2H, m, H-3, H-4), 4.51-4.45 (1H, m, H-2), 4.25 (1H, dd, $J_{5\text{-}6a}$=4.0, $J_{6\text{-}6}$=12.4, H-6), 4.06 (1H, dd, $J_{5\text{-}6b}$=2.4, $J_{6\text{-}6}$, H-6), 3.99 (1H, dt, $J_{4\text{-}5}$=9.2, $J_{5\text{-}6a}$, $J_{5\text{-}6b}$, H-5), 2.19 (3H, s, Me), 2.08 (3H, s, Me), 2.06 (3H, s, Me), 2.04 (3H, s, Me), 1.94 (3H, s, NH-$\underline{Ac}$); $\delta_C$ (100 MHz, $CDCl_3$) 171.9 (C=O), 170.8 (C=O), 170.0 (C=O), 169.2 (C=O), 168.7 (C=O), 90.8 (CH, anomeric), 70.8 (C-4 or C-3), 69.9 (C-5), 67.6

(C-4 or C-3), 61.7 (C-6), 51.2 (C-2), 23.2 (NH-Ac), 21.1 (Me), 20.9 (Me), 20.8 (Me), 20.7 (Me); Calculated Mass for $C_{16}H_{23}NO_{10}$ 389.35 *m/z* ($ES^+$) 412.1 ($MNa^+$)

**2-Methyl-(3,4,6-tri-O-acetyl-1,2-dideoxy-α-$_D$-glucopyrano)-[2,1-d]-2-oxazoline, 7:** [65]

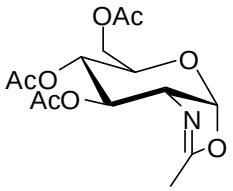


**6** (499 mg, 1.28 mmol) was dissolved in dichloroethane (3 ml) in a round bottomed flask oven dried and cooled under nitrogen. Trimethylsilyl trifluoromethanesulfonate (0.25 ml, 1.38 mmol) was added. The mixture was then heated to 50$^o$C and stirred for 18 hrs.

The mixture was then cooled and diluted with DCM (200 ml). The organic mixture was washed with saturated sodium hydrogen carbonate solution (150 ml, x2) and brine (150 ml, x3), separated, dried over magnesium sulphate, filtered and solvent removed under vacuum giving **7** as a dark oil (401 mg, crude) $[\alpha]_D^{18.4}$ +6.0 (*c* 1.05, MeOH) (lit.,[68] $[\alpha]_D^{18}$ +12.2 (*c* 1, $CHCl_3$)); $\upsilon_{max}$ (ATR) 2961 (C-H), 1737 (C=O), 1672 (C=N), 1368 (C-H bend), 1218 (C-O), 1035 (C-N); $\delta_H$ (400 MHz, $CDCl_3$) 5.96 (1H, d, $J_{1-2}$=7.2, C-H anomeric), 5.26 (1H, t, $J_{2-3}$=2.6, $J_{3-4}$=1.0 H-3), 4.92 (1H, dq, $J_{3-4}$, $J_{4-5}$=9.2, H-4), 4.17-4.16 (2H, m, H-6), 4.14-4.11 (1H, m, H-2), 3.62-3.58 (1H, m H-5), 2.11 (3H, s, Me), 2.09 (3H, s, Me), 2.08 (3H, d, J=1.6, Me-C=N), 2.07 (3H, s, Me); $\delta_C$ (100 MHz, $CDCl_3$) 170.7 (C=O), 169.7 (C=O), 169.3 (C=O), 166.8 (C=N), 99.5 (C-H anomeric), 70.5 (C-3), 68.5 (C-4), 67.7 (C-5), 65.1 (C-2), 63.5 (C-6), 21.1 (Me), 21.0 (Me), 20.9 (Me), 14.1 (Me-C=N); Calculated Mass for $C_{14}H_{19}NO_8$ 329.30 *m/z* ($ES^+$) 330.1 ($MH^+$)

**2-Azidoethyl 2-(acetylamino)-2-deoxy-, 3,4,6-triacetate β-$_D$-glucopyranoside, 8:** [65]

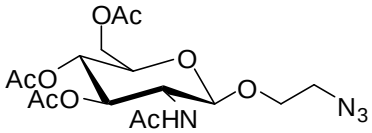


**7** (679 mg, 2.06 mmol) and **3** (368 mg, 4.23 mmol) were dried by co-evaporation with toluene. The reagents were then dissolved in dry DCM (10 ml) and transferred

to apparatus oven dried and cooled under nitrogen. Anhydrous $CuCl_2$ dried under vacuum was then added (300 mg, 2.23 mmol) giving a dark blue mixture. The mixture was heated to reflux, turning dark green.

The mixture was refluxed for 73 hrs then allowed to cool to room temperature. The mixture was diluted with DCM (200 ml) and filtered. The organic mixture was then washed with saturated sodium hydrogen carbonate solution (200 ml) and brine (150 ml, x3), separated, dried over magnesium sulphate, filtered and solvent removed under vacuum giving a pale semi-solid.

This was purified by flash column chromatography on silica using ethyl acetate and methanol (99:1) giving **8** as a white semi-solid (138 mg, 16%) $[\alpha]_D^{23.6}$ -31.0 (*c* 3.66, MeOH) (lit.,[158] $[\alpha]_D^{19\text{-}21}$ -30 (*c* 1, $CHCl_3$)); $\upsilon_{max}$ (ATR) 3251 (N-H), 2111 ($N_3$), 1744 (C=O ester), 1655 (C=O amide), 1570 (N-H bend), 1367 (C-H), 1243 (C-O), 1228 (C-O), 1032 (C-N); $\delta_H$ (400 MHz, $CDCl_3$) 5.58 (1H, d, $J_{NH\text{-}2}$=8.4, NH), 5.36 (1H, dd, $J_{2\text{-}3}$=9.2, $J_{3\text{-}4}$=10.2, H-3), 5.07 (1H, t, $J_{3\text{-}4}$, H-4), 4.83 (1H, d, $J_{1\text{-}2}$=8.4, CH anomeric), 4.25 (1H, dd, $J_{5\text{-}6a}$=4.8, $J_{6\text{-}6}$=12.0, H-6), 4.15 (1H, dd, $J_{5\text{-}6b}$=2.4, $J_{6\text{-}6,}$ H-6), 4.07-4.02 (1H, m, O-$\underline{CH_2}CH_2$), 3.84-3.77 (1H, m, H-2), 3.75-3.68 (2H, m, H-5, O-$\underline{CH_2}$-$CH_2$), 3.54-3.45 (1H, m, $\underline{CH_2}$-$N_3$), 3.29-3.23 (1H, m, $\underline{CH_2}$-$N_3$), 2.08 (3H, s, Me), 2.03 (3H, s, Me), 2.02 (3H, s, Me), 1.95 (3H, s, NH-$\underline{Ac}$); $\delta_C$ (100 MHz, $CDCl_3$) 170.9 (C=O), 170.8 (C=O), 170.6 (C=O), 169.6 (C=O), 100.6 (CH, anomeric), 72.2 (C-5), 72.1 (C-3), 68.7 (C-4), 68.6 (O-$\underline{CH_2}$-$CH_2$), 62.1 (C-6), 55.0 (C-2), 50.8 ($\underline{CH_2}$-$N_3$), 23.5 (NH-$\underline{Ac}$), 20.9 (Me), 20.8 (Me), 20.8 (Me); Calculated Mass for $C_{16}H_{24}N_4O_9$ 416.38 *m/z* ($ES^+$) 417.1 ($MH^+$)

**Tert-butyl 1,3-bis((1-(2-ethyl 2-(acetylamino)-2-deoxy-, 3,4,6-tri-O-acetyl-β-$_D$-glucopyranoside)-1H-1,2,3-triazol-4-yl)methoxy)-2-(((1-(2-ethyl 2-(acetylamino)-2-deoxy-, 3,4,6-tri-O-acetyl-β-$_D$-glucopyranoside)-1H-1,2,3-triazol-4-yl)methoxy)methyl)propan-2-ylcarbamate, 9:**

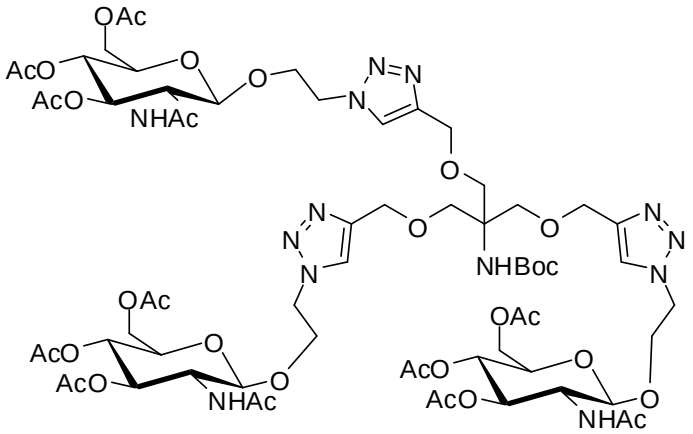


**8** (236 mg, 0.57 mmol) was added to a solution of **2** (58 mg, 0.17 mmol), sodium ascorbate (32 mg, 0.16 mmol) and copper sulphate (43 mg, 0.17 mmol) in DMF (4 ml). The mixture was stirred at room temperature for 22 hrs then extracted with ethyl acetate (300 ml). The organic layer was washed with brine (150 ml, x4), separated, dried over magnesium sulphate, filtered and solvent removed under vacuum giving the crude as a pale oil.

This was purified by flash column chromatography on silica using DCM and methanol (9:1) giving **9** as a white semi-solid (14.6 mg, 5%)

$[\alpha]_D^{23.5}$ -15.7 (*c* 0.89, MeOH); $\upsilon_{max}$ (ATR) 3282 (N-H), 2960 (C-H), 1742 (C=O ester), 1661 (C=O amide), 1532 (N-H bend), 1367 (C-H), 1223 (C-O), 1165 (C-N), 1035 (C-N); $\delta_H$ (400 MHz, $CDCl_3$) 7.70 (3H, s, CH triazole), 7.10 (3H, d, $J_{NH-2}$=8.8, NH, GlcNAc), 5.33-5.28 (3H, m, H-3), 5.05 (3H, t, $J_{4-5}$=9.8, H-4), 4.95 (1H, br, NH, Tris), 4.84 (3H, d, $J_{1-2}$=8.4, CH, anomeric), 4.67-4.61 (3H, m, O-$\underline{CH_2}$-$CH_2$), 4.53 (6H, s, O-$\underline{CH_2}$-triazole), 4.50-4.44 (3H, m, O-$\underline{CH_2}$-$CH_2$), 4.32-4.23 (6H, m, H-6, $CH_2$-N), 4.16 (3H, dd, $J_{5-6a}$=2.4, $J_{6-6}$=12.4, H-6), 3.98 (3H, dd, $J_{NH-2}$, $J_{1-2}$, $J_{2-3}$=10.2, H-2), 3.89-3.83 (3H, m, $\underline{CH_2}$-N), 3.77 (3H, ddd, $J_{4-5}$, $J_{5-6a}$, $J_{5-6b}$=4.6, H-5), 3.61 (6H, s, NHC-$\underline{CH_2}$), 2.09 (9H, s, Me), 2.01 (9H, s, Me), 2.00 (9H, s, Me), 1.91 (9H, s, Me, N-Ac), 1.42 (9H, s, C-$\underline{Me_3}$); $\delta_C$ (100 MHz, $CDCl_3$) 171.0 (C=O, Ac), 170.8 (C=O, Ac), 169.6 (C=O, Ac), 144.4 (C, triazole), 124.5 (CH, triazole), 100.5 (CH, anomeric), 72.4 (C-3), 72.0 (C-5), 69.4 (NHC-$\underline{CH_2}$), 69.0 (C-4), 67.1 ($\underline{CH_2}$-N), 64.3

(O-<u>CH$_2$</u>-triazole), 62.2 (C-6), 54.3 (C-2), 50.2 (O-<u>CH$_2$</u>-CH$_2$), 28.5 (<u>Me</u>, Boc), 23.3 (<u>Me</u>, N-Ac), 20.9 (<u>Me</u>, Ac), 20.8 (<u>Me</u>, Ac), 20.8 (<u>Me</u>, Ac); Calculated Mass for $C_{66}H_{97}N_{13}O_{32}$ 1584.6430 (MALDI) 1486.77 ($M^+$ -BOC), 1608.97 ($MNa^+$); HRMS ($ES^+$): 1584.6428 ($M^+$)

**2-Bromoethyl 2,3,4,6-tetra-O-acetyl β-$_D$-glucopyranoside, 10:** [71]

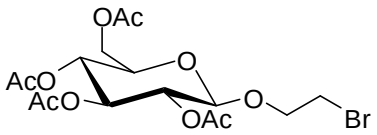


α-D-Glucose pentacetate (507 mg, 1.30 mmol) was dissolved in dry DCM (2 ml) in glassware oven dried and cooled under nitrogen. The solution was cooled to -15$^o$C and bromoethanol (0.1 ml, 176 mg, 1.41 mmol) added followed by boron trifluoride diethyl etherate (0.6 ml, 690 mg, 4.86 mmol). The mixture was stirred for an hour before being allowed to warm to room temperature.

The mixture was stirred for 4 days then diluted with DCM (200 ml). The organic layer was washed with sat sodium hydrogen carbonate solution (150 ml, x2) and brine (150 ml, x3), separated, dried over magnesium sulphate, filtered and solvent removed under vacuum giving the crude as a yellow oil. This was purified by flash column chromatography on silica using ethyl acetate and petroleum ether (2:3) giving a mixture of **10** and glucose pentacetate as a clear oil (201 mg). This was further purified by recrystallizing from petroleum ether:ether (9:1) giving **10** as a white semi-solid (9 mg, 2%)

$[\alpha]_D^{23.6}$ -16.8 (*c* 0.9, MeOH) (lit.,[159] $[\alpha]_D^{25}$ -12.5 (*c* 0.78, $CHCl_3$)); $\upsilon_{max}$ (ATR) 1751 (C=O), 1740 (C=O), 1734 (C=O), 1730 (C=O), 1375 (C-H), 1366 (C-H), 1218 (C-O); $\delta_H$ (400 MHz, $CDCl_3$) 5.22 (1H, t, $J_{3-4}$=9.6, H-3), 5.08 (1H, t, $J_{3-4,}$ H-4), 5.01 (1H, dd, $J_{1-2}$=8.0, $J_{2-3}$=9.6, H-2), 4.57 (1H, d, $J_{1-2}$, C-H anomeric), 4.26 (1H, dd, $J_{5-6a}$=4.8, $J_{6-6}$=12.4, H-6), 4.18-4.12 (2H, m, H-6, O-<u>CH$_2$</u>-CH$_2$), 3.85-3.78 (1H, m, O-<u>CH$_2$</u>-CH$_2$), 3.71 (1H, ddd, $J_{4-5}$=10.0, $J_{5-6a,}$ $J_{5-6b}$=2.4, H-5), 3.48-344 (2H, m, <u>CH$_2$</u>-Br), 2.09 (3H, s, Me), 2.07 (3H, s, Me), 2.02 (3H, s, Me), 2.01 (3H, s, Me); $\delta_C$ (100 MHz, $CDCl_3$) 170.8 (C=O), 170.4 (C=O), 169.6 (C=O), 169.5 (C=O), 101.2 (C-H anomeric), 72.8 (C-3), 72.1 (C-5), 71.2 (C-2), 69.9 (O-<u>CH$_2$</u>-CH$_2$), 68.5 (C-4), 62.0 (C-6), 30.0 (<u>CH$_2$</u>-Br), 20.9 (Me), 20.9 (Me), 20.8 (Me), 20.7 (Me); Calculated Mass for $C_{16}H_{23}BrO_{10}$ 455.25 *m/z* ($ES^+$) 476.9 ($MNa^+$)

**2-Azidoethyl 2,3,4,6-tetra-O-acetyl β-$_D$-glucopyranoside, 11:** [71]

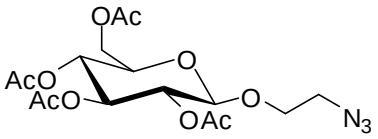


Crude **10** (3.27 g, 7.174 mmol) was dissolved in dry DMF (30 ml) and sodium azide (2.30 g, 35.333 mmol) added. The mixture was heated to 63$^o$C and stirred overnight. The mixture was allowed to cool and extracted with ethyl acetate (200 ml). The mixture was then washed with brine (150 ml, x3), separated, dried over magnesium sulphate, filtered and solvent removed under vacuum giving an orange oil.
This was purified by flash column chromatography on silica using petroleum ether and ethyl acetate (3:2) giving **11** as a white solid (483 mg, 23% over two steps from glucose penta actetate)
mp 98.6-103.8$^o$C (from hexane); $[\alpha]_D^{25.0}$ -48.4 (*c* 1.96, MeOH) (lit.,[72] $[\alpha]_D^{20}$ -31.2 (*c* 1.14, $CH_2Cl_2$)); $\upsilon_{max}$ (ATR) 2950 (C-H), 2105 ($N_3$), 1755 (C=O), 1737 (C=O), 1207 (C-O); $\delta_H$ (400 MHz, $CDCl_3$) 5.21 (1H, t, $J_{3\text{-}4}$=9.4, H-3), 5.10 (1H, dd, $J_{3\text{-}4,}$ $J_{4\text{-}5}$=10.0, H-4), 5.02 (1H, dd, $J_{1\text{-}2}$=8.0, $J_{2\text{-}3}$=9.4, H-2), 4.59 (1H, d, $J_{1\text{-}2}$, C-H anomeric), 4.25 (1H, dd, $J_{5\text{-}6a}$=4.8, $J_{6\text{-}6}$=12.2, H-6), 4.16 (1H, dd, $J_{5\text{-}6b}$=2.4, $J_{6\text{-}6}$=12.2, H-6), 4.03 (1H, dq, $J_1$=10.8, $J_2$=4.8, O-$\underline{CH_2}$-$CH_2$), 3.73-3.66 (2H, m, H-5, O-$\underline{CH_2}$-$CH_2$), 3.52-3.46 (1H, m, $CH_2$-$N_3$), 3.29 (1H, dq, $J_1$=13.6, $J_2$=4.8 $CH_2$-$N_3$), 2.09 (3H, s, Me), 2.05 (3H, s, Me), 2.03 (3H, s, Me), 2.00 (3H, s, Me); $\delta_C$ (100 MHz, $CDCl_3$) 170.8 (C=O), 170.4 (C=O), 169.5 (C=O), 169.5 (C=O), 100.8 (C-H, anomeric), 72.9 (C-3), 72.1 (C-5), 71.2 (C-2), 68.7 (C-4), 68.5 (O-$\underline{CH_2}$-$CH_2$), 62.0 (C-6), 50.7 ($CH_2$-$N_3$), 20.9 (Me), 20.8 (Me), 20.7 (Me); Calculated Mass for $C_{16}H_{23}N_3O_{10}$ 417.37 *m/z* ($ES^+$) 440.1 ($MNa^+$)

**Tert-butyl 1,3-bis((1-(2-ethyl 2,3,4,6-tetra-O-acetyl-β-$_D$-glucopyranoside)-1H-1,2,3-triazol-4-yl)methoxy)-2-(((1-(2-ethyl 2,3,4,6-tetra-O-acetyl-β-$_D$-glucopyranoside)-1H-1,2,3-triazol-4-yl)methoxy)methyl)propan-2-ylcarbamate, 12:**

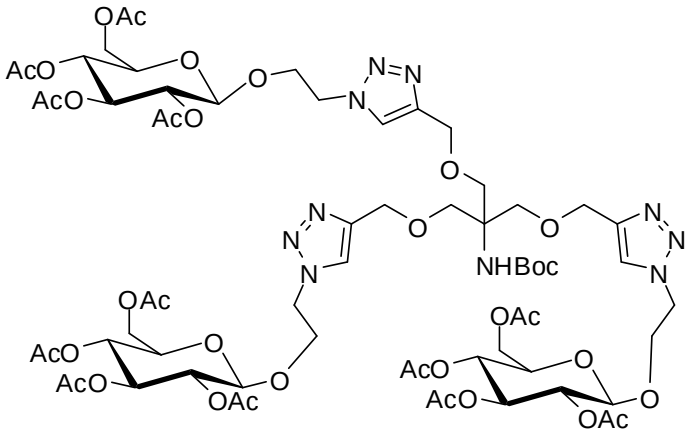


**11** (415 mg, 0.994 mmol) was added to **2** (104 mg, 0.31 mmol) as a solution in DMF (5 ml). Sodium ascorbate (49 mg, 0.247 mmol) and copper sulphate (85 mg, 0.340 mmol) were then added followed by catalytic TBTA. The mixture was stirred at room temperature for 5 days then extracted with DCM (300 ml). The organic layer was washed with water (150 ml, x4), separated, dried over magnesium sulphate, filtered and solvent removed under vacuum giving the crude as an orange oil. This was purified by flash column chromatography on silica using ethyl acetate and methanol (9:1) giving **12** as a clear oil (170 mg, 35%)

$[\alpha]_D^{25.0}$ -18.3 (*c* 1.74, MeOH); $\upsilon_{max}$ (ATR) 1744 (C=O), 1215 (C-O); $\delta_H$ (400 MHz, $CDCl_3$) 7.60 (3H, s, C-H triazole), 5.17 (3H, t, $J_{H3-H4}$=9.6, H-3), 5.05 (3H, t, $J_{H4-H5}$=9.6, H-4), 5.01 (1H, br, N-H), 5.00-4.95 (3H, dd, $J_{H1-H2}$=8, $J_{H2-H3}$=9.6, H-2), 4.62-4.56 (9H, m, N-$\underline{CH_2}$-$CH_2$, O-$\underline{CH_2}$-triazole), 4.74-4.54 (6H, m, CH anomeric, N-$\underline{CH_2}$-$CH_2$), 4.27-4.21 (6H, m, O-$\underline{CH_2}$-$CH_2$, H-6), 4.14-4.10 (3H, m, H-6), 3.97-3.91 (3H, m, O-$\underline{CH_2}$-$CH_2$), 3.75 (6H, s, HNC-($\underline{CH_2}$)$_3$), 3.72-3.68 (3H, m, H-5), 2.08 (9H, s, Me), 2.01 (9H, s, Me), 1.98 (9H, s, Me), 1.93 (9H, s, Me), 1.39 (9H, s, C-$\underline{Me_3}$); $\delta_C$ (100 MHz, $CDCl_3$) 170.7 (C=O, Ac), 170.2 (C=O, Ac), 169.5 (C=O, Ac), 169.4 (C=O, Ac), 154.9 (C=O, Boc), 145.0 (C, triazole), 124.0 (CH, triazole), 100.7 (CH, anomeric), 72.6 (C-3), 72.1 (C-5), 71.0 (C-2), 69.5 (HN-C-($\underline{CH_2}$)$_3$), 68.4 (C-4), 67.9 (O-$\underline{CH_2}$-$CH_2$), 64.9 (O-$\underline{CH_2}$-triazole), 61.9 (C-6), 58.6 (HN-$\underline{C}$-($CH_2$)$_3$), 50.0 (N-$\underline{CH_2}$-$CH_2$), 28.5 ($\underline{Me}$, Boc), 20.9 ($\underline{Me}$, Ac), 20.7 ($\underline{Me}$, Ac), 20.7 ($\underline{Me}$, Ac); Calculated

Mass for $C_{66}H_{94}N_{10}O_{35}$ 1587.5937 *m/z* MALDI 1611.31 ($MNa^+$); HRMS ($ES^+$): 1587.5938 ($M^+$)

**(2-(2-Cyanoethoxy)-1,1-bis((2-cyanoethoxy)methyl)ethyl)amine; Tris(2-cyanoethoxymethyl)aminomethane, 13:** [99]

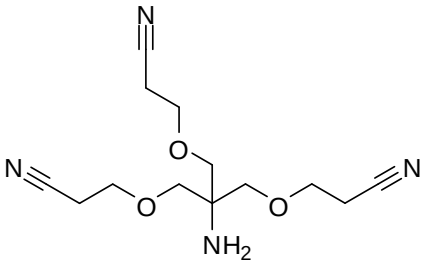


Tris(hydroxymethyl)aminomethane hydrochloride (3.03 g, 19.213 mmol) was suspended in tetrahydrofuran (50 ml) and potassium hydroxide (3.21 g, 57.209 mmol) added as an aqueous 40wt% solution. The mixture was stirred for 15 min and acrylonitrile (7.6 ml, 6.156g, 114.587 mmol) added. The mixture was stirred overnight then concentrated before extracting with DCM (200 ml). This was washed the water (150 ml) and the aqueous layer extracted with further portions of DCM (100 ml, x2). The organic fractions were combined, dried over magnesium sulphate, filtered and solvent removed giving a yellow oil. This was purified by flash column chromatography on silica using DCM and methanol (9:1) giving the product as a yellow oil (2.55 g, 48%)

$\upsilon_{max}$ (ATR) 3378 (N-H), 2874 (C-H), 2251 (CN), 1587 (N-H), 1465 (C-H), 1270 (C-O), 1105 (C-$NH_2$), 733 (C-H); $\delta_H$ (400 MHz, $CDCl_3$) 3.67 (6H, t, J=6.0, O-$\underline{CH_2}$-$CH_2$), 3.44 (6H, s, C-$\underline{CH_2}$-O), 2.60 (6H, t, J=6.0, $CH_2$-CN), 2.54 (2H, br, $NH_2$); $\delta_C$ (100 MHz, $CDCl_3$) 118.1 (CN), 72.4 (C-$\underline{CH_2}$-O), 65.8 (O-$\underline{CH_2}$-$CH_2$), 56.3 (C-$NH_2$), 18.9 ($\underline{CH_2}$-CN); Calculated Mass for $C_{13}H_{20}N_4O_3$ 280.32 *m/z* ($ES^+$) 302.9 ($MNa^+$)

**Carbamic acid, N-[2-(2-cyanoethoxy)-1,1-bis[(2-cyanoethoxy)methyl]ethyl]-, 1, 1-dimethylethyl ester, 14:** [99]

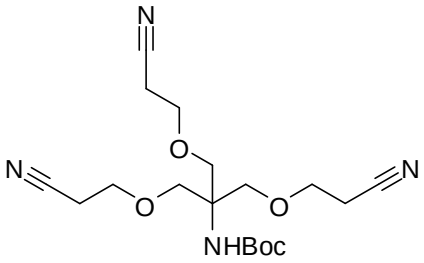


**13** (497 mg, 1.773 mmol), was dissolved in tetrahydrofuran (5 ml) and cooled to $0^{o}$C. A solution of di-tert-butyl dicarbonate (494 mg, 2.263 mmol) in tetrahydrofuran (1 ml) was then added followed by triethylamine (0.3 ml, 2.152 mmol). The mixture was allowed to warm to room temperature and stirred for 6 hrs. The mixture was extracted with ethyl acetate (100 ml), washed with brine (100 ml, x3), separated, dried over magnesium sulphate, filtered and solvent removed giving a pale oil. This was purified by flash column chromatography on silica using DCM and methanol (49:1) giving **14** as a yellow oil (606 mg, 89%).

$\upsilon_{max}$ (ATR) 3426 (N-H), 2975 (C-H), 2933 (C-H), 2882 (C-H), 2251 (CN), 1708 (C=O), 1500 (N-H), 1269 (C-O), 1245 (C-O), 1108 (C-NH); $\delta_H$ (400 MHz, $CDCl_3$) 4.86 (1H, br, NH), 3.77 (6H, s, C-$\underline{CH_2}$-O), 3.69 (6H, t, J=6.0, O-$\underline{CH_2}$-$CH_2$), 2.60 (6H, t, J=6.0, $CH_2$-CN), 1.42 (9H, s, Me); $\delta_C$ (100 MHz, $CDCl_3$) 154.9 (C=O), 118.0 (CN), 79.8 ($\underline{C}$-$Me_3$), 69.5 (C-$\underline{CH_2}$-O), 65.9 (O-$\underline{CH_2}$-$CH_2$), 58.6 ($\underline{C}$-NH), 28.4 (Me), 18.9 ($\underline{CH_2}$-CN); Calculated Mass for $C_{18}H_{28}N_4O_5$ 380.44 *m/z* ($ES^+$) 403.0 ($MNa^+$)

**Carbamic acid, [2-(2-propenyloxy)-1,1-bis[(2-propenyloxy)methyl]ethyl]-, 1,1-dimethylethyl ester, 15:** [160]

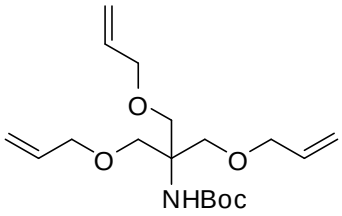


**1** (1.00 g, 4.520 mmol) was suspended in dry DMF (10 ml) in glassware oven dried under $N_2$. Allyl bromide (2.4 ml, 3.36 g, 27.734 mmol) was added and the mixture cooled to $0^{o}$C. Ground potassium hydroxide (991 mg, 17.662 mmol) was then added in portions over 15 min. The mixture was allowed to warm to room temperature and stirred overnight. The mixture was extracted with ethyl acetate (200 ml), washed

with brine (150 ml, x3), separated, dried over magnesium sulphate, filtered and solvent removed giving a yellow oil. This was purified by flash column chromatography on silica using petroleum ether and ethyl acetate (9:1) giving the product as a clear oil (393 mg, 25%)

$\upsilon_{max}$ (ATR) 3447 (N-H), 3079 (C-H, alkene), 2977 (C-H), 2929 (C-H), 2871 (C-H), 1716 (C=O), 1647 (C-C, alkene), 1497 (C-H), 1243 (C-O), 1167 (C-O), 1089 (C-N), 990 (C-H, alkene), 921 (C-H, alkene); $\delta_H$ (400 MHz, $CDCl_3$) 5.93-5.83 (3H, m, CH), 5.28-5.14 (6H, m, $CH_2CH$-$\underline{CH_2}$), 4.96 (1H, br, NH), 3.98 (6H, dt, $J_1$=5.6, $J_2$=1.2, O-$\underline{CH_2}CH$), 3.70 (6H, s, C-$CH_2$), 1.42 (9H, s, Me); $\delta_C$ (100 MHz, $CDCl_3$) 155.0 (C=O), 134.9 (CH), 116.9 ($CH_2CH$-$\underline{CH_2}$), 79.1 ($\underline{C}$-$Me_3$), 72.4 ($\underline{CH_2}$-$CHCH_2$), 69.3 (C-$\underline{CH_2}$), 58.7 (C-NH), 28.5 (Me); Calculated Mass for $C_{18}H_{31}NO_5$ 341.44 *m/z* ($ES^+$) 364.0 ($MNa^+$)

**2-Azidoethyl tosylate, 16:** [161]

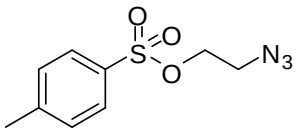


Azidoethanol **3** (1.02 g, 11.656 mmol) was dissolved in dry chloroform (5 ml) in glassware previously oven dried and cooled under nitrogen. Dry pyridine (0.95 ml, 11.746 mmol) was added and the mixture cooled to 0$^o$C. Para tosyl chloride (2.21 g, 11.581 mmol) was dissolved in dry chloroform (20 ml) and this was added dropwise to the cooled mixture. Following addition the mixture was allowed to warm to room temperature and stirred overnight. The mixture was diluted with chloroform (200 ml), washed with sat sodium hydrogen carbonate solution (150 ml) and water (150 ml, x3), separated, dried over magnesium sulphate, filtered and solvent removed giving a yellow oil. This was purified by flash column chromatography on silica using petroleum ether and ethyl acetate (7:3) giving **16** as a yellow oil (264 mg, 9%).

$\upsilon_{max}$ (ATR) 2928 (C-H), 2109 ($N_3$), 1597 (C=C), 1495 (C=C), 1441 (C=C), 1360 (S=O), 911 (S-O); $\delta_H$ (400 MHz, $CDCl_3$) 7.84 (2H, d, J=8.0, Ar), 7.37 (2H, d, J=8.0, Ar), 4.17 (2H, t, J=5.2, O-$CH_2$), 3.49 (2H, t, J=5.2, $CH_2$-$N_3$), 2.46 (3H, s, Me); $\delta_C$ (100 MHz, $CDCl_3$) 145.4 (Ar-$SO_3$), 132.8 ($\underline{Ar}$-Me), 130.1 (Ar), 128.1 (Ar), 68.2 (O-$CH_2$), 49.7 ($CH_2$-$N_3$), 21.8 (Me)

**2-(methoxyamino) ethanol, 17:** [162]

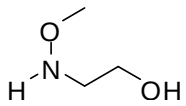

O-methylhydroxyamine was produced from the hydrochorlic salt by stirring with sodium hydroxide in dry THF for 3 days. The solution was filtered and the concentration of free amine determined by quantitive NMR using toluene as a reference. O-methylhydroxyamine solution (3.4 ml, 600 mg, 12.75 mmol) was mixed with bromoethanol (0.3 ml, 529mg, 4.233 mmol). The mixture was warmed to 45$^{o}$C and stirred overnight, then heated to reflux and stirred for a further day. Solvent was removed giving an orange oil which was purified by flash column chromatography on silica using DCM and methanol (9:1) giving **17** as a pale oil (66 mg, 17%)

$\upsilon_{max}$ (ATR) 3365 (O-H), 2945 (C-H), 1464 ($CH_2$), 1048 (C-N); $\delta_H$ (400 MHz, $CD_3OD$) 3.66 (2H, t, J=5.6, $\underline{CH_2}$-OH), 3.51 (3H, s, Me), 2.97 (2H, t, J=5.6, $\underline{CH_2}$-N); $\delta_C$ (100 MHz, $CD_3OD$) 61.5 (OMe), 59.4 ($\underline{CH_2}$-OH), 54.2 ($\underline{CH_2}$-N); Calculated Mass for $C_3H_9NO_2$ 91.11 *m/z* ($ES^+$) 91.9 ($MH^+$)

**N-Boc-O-methyl hydroxylamine, 18:** [163]

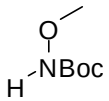

Ditertbutyl dicarbonate (14.79 g, 67.766 mmol) was dissolved in DCM (80 ml) and a solution of sodium carbonate (16.35 g, 195.773 mmol) in water (70 ml) was added. This was followed by addition of a solution of O-methylhydroxylammonium chloride (20.18 g, 190.386 mmol) in water (70 ml). A gas was evolved and the mixture stirred overnight. The mixture was then diluted with DCM (300 ml), washed with water (150 ml, x2), dried over magnesium sulphate, filtered and solvent removed giving **18** as a clear oil (8.43 g, 84%)

$\upsilon_{max}$ (ATR) 3283 (N-H), 2978 (C-H), 1715 (C=O), 1367 (C-H bend), 1250 (C-H), 1165 (C-N); $\delta_H$ (400 MHz, $CDCl_3$) 3.71 (3H, s, O-Me), 1.48 (9H, s, $Me_3$); $\delta_C$ (100 MHz, $CDCl_3$) 157.0 (C=O), 81.7 ($\underline{C}$-$Me_3$), 64.5 (O-Me), 28.3 (Me)

**2-Bromoethyl acetate, 19:**

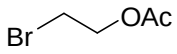


Bromoethanol (5.6 ml, 9.87g, 78.963 mmol) was dissolved in dry DCM (25 ml) and cooled to 0$^{o}$C. Acetic anhydride (7.6 ml, 8.21g, 80.4 mmol) was then added. The mixture was allowed to warm to room temperature and stirred in the dark overnight. The mixture was then diluted with DCM (250 ml), washed with water (200 ml, x3), separated, dried over magnesium sulphate, filtered and solvent removed giving the product as a pale oil (11.79 g, 89%)

$\upsilon_{max}$ (ATR) 2971 (C-H), 1737 (C=O), 1215 (C-H); $\delta_H$ (400 MHz, $CDCl_3$) 4.37 (2H, t, J=6.0, $CH_2$-OAc), 3.50 (2H, t, J=6.0, $CH_2$-Br), 2.09 (3H, s, Me); $\delta_C$ (100 MHz, $CDCl_3$) 170.7 (C=O), 63.9 ($CH_2$-OAc), 28.8 ($CH_2$-Br), 20.9 (Me)

**2-(tert-butoxycarbonyl(methoxy)amino)ethyl acetate, 20:**

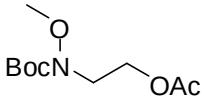


**18** (511 mg, 3.449 mmol) was dissolved in dry DMF (5 ml) and cooled to 0$^{o}$C. Concurrently **19** (0.6 ml, 908mg, 5.440 mmol) was mixed with sodium iodide (65 mg, 0.434 mmol). Sodium hydride (267 mg, 6.675 mmol) was added to the solution of **18** and a gas evolved. The mixture of **19** and sodium iodide was then added dropwise. The reaction was allowed to warm to room temperature and stirred overnight in the dark. The mixture was quenched with water and extracted with DCM (200 ml). The mixture was then washed with water (100 ml, x4), separated, dried over magnesium sulphate, filtered and solvent removed giving a yellow oil (975 mg crude).

$\upsilon_{max}$ (ATR) 2934 (C-H), 1740 (C=O), 1675 (C=O), 1367 (C-H bend), 1229 (C-H), 1166 (C-O), 1137 (C-O); $\delta_H$ (400 MHz, $CDCl_3$) 4.23 (2H, t, J=5.8, O-$CH_2$), 3.71-3.68 (5H, m, O-Me, $CH_2$-N), 2.05 (3H, s, Me, Ac), 1.50 (9H, s, Me, Boc); $\delta_C$ (100 MHz, $CDCl_3$) 170.9 (C=O, Ac), 156.3 (C=O, Boc), 81.6 (C-$Me_3$), 62.5 (O-Me), 60.7 (O-$CH_2$), 47.9 ($CH_2$-N), 28.3 (Me, Boc), 20.9 (Me, Ac); Calculated Mass for $C_{10}H_{19}NO_5$ 233.26 *m/z* ($ES^+$) 255.9 ($MNa^+$)

**Tert-butyl 2-hydroxyethyl(methoxy)carbamate, 21:**

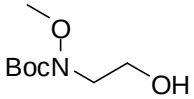


**20** (2.34 g, 10.010 mmol) was dissolved in dry methanol (15 ml) and cooled to 0$^{o}$C. Sodium methoxide (281 mg, 5.202 mmol) was then added and the mixture stirred for 3 hrs.

The mixture was then diluted with methanol and filtered through protonated ion exchange resin. Solvent was removed giving **21** as a yellow oil (1.50 g, 47% over two steps from **18** and **19**)

$\upsilon_{max}$ (ATR) 3435 (O-H), 2976 (C-H), 2935 (C-H), 1698 (C=O), 1366 (C-H bend), 1161 (C-O), 1113 (C-O); $\delta_H$ (400 MHz, $CDCl_3$) 3.77 (2H, t, J=5.2, $\underline{CH_2}$-OH), 3.68 (3H, s, O-Me), 3.60 (2H, t, J=5.2, $CH_2$-N), 2.46 (1H, br, OH), 1.48 (9H, s, Me); $\delta_C$ (100 MHz, $CDCl_3$) 157.0 (C=O), 81.9 ($\underline{C}Me_3$), 62.5 (O-Me), 60.5 ($CH_2$-OH), 51.8 ($CH_2$-N), 28.4 (Me, Boc); Calculated Mass for $C_8H_{17}NO_4$ 191.22 *m/z* ($ES^+$) 213.9 ($MNa^+$)

**Tert-butyl 2-(diphenoxyphosphoryloxy)ethyl(methoxy)carbamate, 22:**

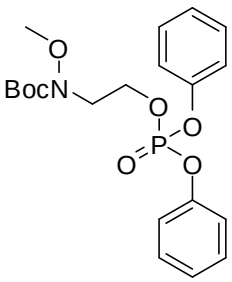


**21** (51 mg, 0.267 mmol) was dissolved in dry toluene (3 ml) in a round bottomed flask oven dried and cooled under nitrogen. The solution was cooled to 0$^{o}$C. Diphenyl phosporyl azide (0.2 ml, 255mg, 0.928 mmol) was added followed by DBU (0.1 ml, 102mg, 0.669 mmol). The mixture was stirred at 0$^{o}$C for 3 hrs and sodium azide (52 mg, 0.800 mmol) added. The mixture was allowed to warm to room temperature and stirred overnight. The mixture was quenched with 1M aqueous HCl (4 ml) and extracted with chloroform (50 ml). It was then washed with water (30 ml, x2), separated, dried over magnesium sulphate, filtered and solvent removed giving a brown oil. This was purified by flash column chromatography on silica using DCM and methanol (50:1) giving **22** as a clear oil (56 mg, 50%)

$\upsilon_{max}$ (ATR) 2975 (C-H), 1701 (C=O), 1589 (C=C), 1488 (C=C), 1187 (P=O), 946 (P-O); $\delta_H$ (400 MHz, $CDCl_3$) 7.36-7.32 (4H, m, Ar), 7.24-7.18 (6H, m, Ar), 4.41-4.37 (2H, m, O-$\underline{CH_2}$), 3.75 (2H, dt, $J_1$=5.6, $J_2$=1.2, N-$\underline{CH_2}$), 3.66 (3H, s, O-$\underline{Me}$), 1.48 (9H, s, Me); $\delta_C$ (100 MHz, $CDCl_3$) 156.3 (C=O), 150.6 (d, J=7.1, Ar, ipso), 129.9 (d, J=0.4, Ar, meta), 125.5 (d, J=1.1, Ar, para), 120.2 (d, J=4.9, Ar ortho), 82.0 ($\underline{C}$-$Me_3$), 65.2 (d, J=6.2, O-$\underline{CH_2}$), 62.8 (O-$\underline{Me}$), 49.7 (d, J=8.0, N-$\underline{CH_2}$), 28.3 (Me); $\delta_P$ (162 MHz, $CDCl_3$) -12.0 (P); Calculated Mass for $C_{20}H_{26}NO_7P$ 423.40 *m/z* ($ES^+$) 446.1 ($MNa^+$)

**2-(tert-butoxycarbonyl(methoxy)amino)ethyl methanesulfonate, 23:**

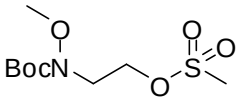


**21** (722 mg, 3.776 mmol) was dissolved in DCM (15 ml) and triethylamine added (1.3 ml, 944mg, 9.327 mmol). The mixture was cooled to 0$^o$C and mesyl chloride (0.75 ml, 1.11g, 9.690 mmol) added. The mixture was allowed to warm to room temperature, stirred for 1½hrs then quenched by stirring with excess sat sodium hydrogen carbonate solution. The mixture was extracted with dichloromethane (150 ml), washed with sat sodium hydrogen carbonate solution (100 ml) and brine (100 ml, x3), separated, dried over magnesium sulphate, filtered and solvent removed giving the product as a yellow oil (488 mg, 48%)

$\upsilon_{max}$ (ATR) 2977 (C-H), 1701 (C=O), 1350 ($SO_2OR$), 1171 ($SO_2OR$), 1121 (C-O); $\delta_H$ (400 MHz, $CDCl_3$) 4.36 (2H, t, J=5.6, O-$\underline{CH_2}$), 3.78 (2H, t, J=5.6, N-$\underline{CH_2}$), 3.71 (3H, s, O-$\underline{Me}$), 3.02 (3H, s, S-$\underline{Me}$), 1.50 (9H, s, Me); $\delta_C$ (100 MHz, $CDCl_3$) 156.3 (C=O), 82.3 ($\underline{C}$-$Me_3$), 65.7 (O-Me), 62.7 (O-$CH_2$), 48.5 (N-$CH_2$), 37.7 (S-Me), 28.3 (C-$\underline{Me_3}$); Calculated Mass for $C_9H_{19}NO_6S$ 269.32 *m/z* ($ES^+$) 292.1 ($MNa^+$)

**Tert-butyl 2-azidoethyl(methoxy)carbamate, 24:**

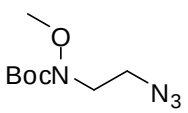


**23** (488 mg, 1.812 mmol) was dissolved in dry DMF (4 ml) and sodium azide (381 mg, 5.853 mmol) added. The mixture was heated to 50$^o$C and stirred overnight. The mixture was allowed to cool to room temperature and extracted with chloroform (150 ml). The mixture was washed with brine (100 ml, x3), separated, dried over

magnesium sulphate, filtered and solvent removed giving the product as a yellow oil (327 mg, 83%)

$\upsilon_{max}$ (ATR) 2977 (C-H), 2935 (C-H), 2100 ($N_3$), 1701 (C=O), 1366 (C-H bend), 1162 (C-O), 1111 (C-O); $\delta_H$ (400 MHz, $CDCl_3$) 3.71 (3H, s, O-Me), 3.63 (2H, t, J=6.0, N-$CH_2$), 3.46 (2H, t, J=6.0, $N_3$-$CH_2$), 1.51 (9H, s, Me); $\delta_C$ (100 MHz, $CDCl_3$) 156.3 (C=O), 82.1 (<u>C</u>-$Me_3$), 62.7 (O-Me), 48.5 ($N_3$-$CH_2$), 48.3 (N-$CH_2$), 28.4 (C-<u>$Me_3$</u>)

**Tert-butyl 2-tri((1-(2-(tert-butoxycarbonyl(methoxy)amino)ethyl)-1H-1,2,3-triazol-4-yl)methoxy)ethylcarbamate, 25:**

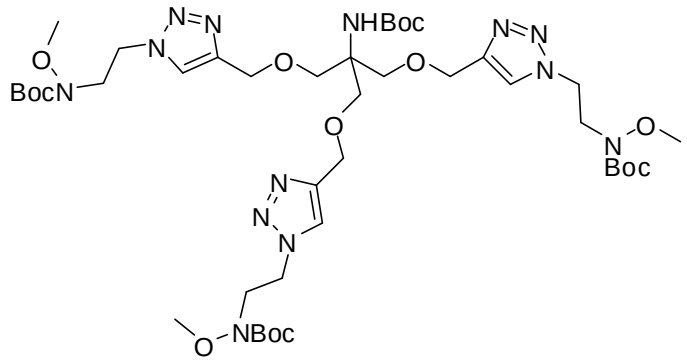


Tripropargyl Tris core **2** (79 mg, 0.236 mmol) was added to a solution of **24** (200 mg, 0.925 mmol) in DMF (3 ml). Sodium ascorbate (36 mg, 0.182 mmol) and copper sulphate (143 mg, 0.573 mmol) were then added followed by catalytic TBTA. The mixture was stirred at room temperature for 3 days then extracted with chloroform (150 ml). The organic layer was washed with water (100 ml, x4) , separated, dried over magnesium sulphate, filtered and solvent removed under vacuum giving the crude as a green oil.

This was purified by flash column chromatography on silica using DCM and methanol (19:1) giving **25** as a clear oil (182 mg, 79%)

$\upsilon_{max}$ (ATR) 2977 (C-H), 1707 (C=O), 1672 (C=O); $\delta_H$ (400 MHz, $CDCl_3$) 7.60 (3H, s, CH triazole), 4.93 (1H, s, NH), 4.59-4.56 (12H, m, O-$CH_2$, N-$CH_2$ triazole), 3.94 (6H, t, J=6.0, MeON-<u>$CH_2$</u>), 3.73 (6H, s, HNC-<u>$CH_2$</u>), 3.64 (9H, s, O-Me), 1.40 (27H, s, Me Boc aminoxy), 1.40 (9H, s, Me Boc amine); $\delta_C$ (100 MHz, $CDCl_3$) 155.7 (C=O), 154.9 (C=O), 145.1 (C, triazole), 123.5 (CH, triazole), 82.2 (<u>C</u>-$Me_3$), 82.2 (<u>C</u>-$Me_3$), 69.5 (HNC-<u>$CH_2$</u>), 65.0 (O-<u>$CH_2$</u>-triazole), 62.5 (O-Me) , 58.5 (HN<u>C</u>-$CH_2$), 49.1 (MeON-<u>$CH_2$</u>), 47.3 (N-$CH_2$ triazole), 28.5 (Me, Boc amine), 28.2 (Me, Boc

aminoxy); Calculated Mass for $C_{42}H_{73}N_{13}O_{14}$ 984.5473 *m/z* (MALDI) 1007.22 ($MNa^+$), 1047.23 ($MCu^+$); HRMS ($ES^+$) 984.5460 ($MH^+$)

**Mono(1,3-bis((1-(2-(methoxyammonio)ethyl)-1H-1,2,3-triazol-4-yl)methoxy)-2-(((1-(2-(methoxyammonio)ethyl)-1H-1,2,3-triazol-4-yl)methoxy)methyl)propan-2-aminium) monochloride, 26:**

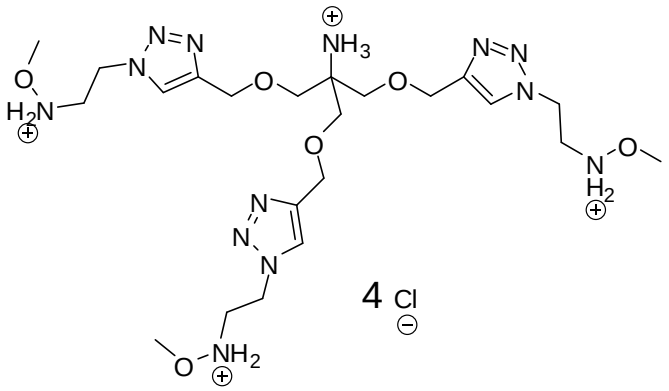


**25** (35 mg, 0.036 mmol) was dissolved in 2M hydrochloric methanol (10 ml) and stirred for 30 min. The solvent was then removed under vacuum giving the product as a pale oil (32 mg, crude)

$\upsilon_{max}$ (ATR) 2439 (N-H ammonium), 1147 (C-N), 1095 (C-O); $\delta_H$ (400 MHz, $D_2O$) 8.09 (3H, s, C-H triazole), 4.84 (6H, t, J=5.6, N-$\underline{CH_2}$ triazole), 4.59 (6H, s, O-$CH_2$ triazole), 3.89 (6H, t, J=5.6, MeONH-$\underline{CH_2}$), 3.80 (9H, s, OMe), 3.58 (6H, s, $H_2NC$-($\underline{CH_2}$)$_3$); $\delta_C$ (100 MHz, $D_2O$) 144.1 (C triazole), 126.4 (C-H triazole), 67.8 ($H_2NC$-($\underline{CH_2}$)$_3$), 63.8 (O-$CH_2$ triazole), 62.2 (O-Me), 59.7 ($H_2N\underline{C}$-$(CH_2)_3$), 48.2 (MeONH-$\underline{CH_2}$), 44.9 (N-$\underline{CH_2}$ triazole); Calculated Mass for $C_{22}H_{41}N_{13}O_6$ 583.64 *m/z* ($ES^+$) 584.3 ($MH^+$), 606.3 ($MNa^+$)

**1,3-bis(prop-2-ynyloxy)-2-((prop-2-ynyloxy)methyl)propan-2-aminium chloride, 27:**

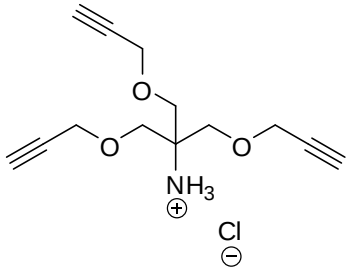


Tri propargyl Tris core **2** (98 mg, 0.292 mmol) was dissolved in 2M hydrochloric methanol (3 ml) and stirred for 3 hrs. The solvent was removed under vacuum giving

the crude as a brown oil. This was washed with cold ether (10 ml, x2), giving the product as a yellow oil (40 mg, 51%)

$\upsilon_{max}$ (ATR) 3287 (C-H alkyne), 2884 (N-H ammonium), 2114 (C≡C alkyne); $\delta_H$ (400 MHz, $CD_3OD$) 4.26 (6H, d, J=2.4, O-$CH_2$C), 3.73 (6H, s, NC($\underline{CH_2}$)$_3$), 2.97 (3H, t, J=2.4, C-H); $\delta_C$ (100 MHz, $CD_3OD$) 79.6 (O-$CH_2\underline{C}$), 77.1 (CH), 68.8 (O-$\underline{CH_2}$C), 60.1 (NH-C), 59.6 (NC($\underline{CH_2}$)$_3$); Calculated Mass for $C_{13}H_{17}NO_3$ 236.1281 *m/z* ($ES^+$) 236.0 ($M^+$); HRMS ($ES^+$): 236.1282 ($M^+$)

**N-(1,3-bis(prop-2-ynyloxy)-2-((prop-2-ynyloxy)methyl)propan-2-yl)-4-nitrobenzamide, 28:**

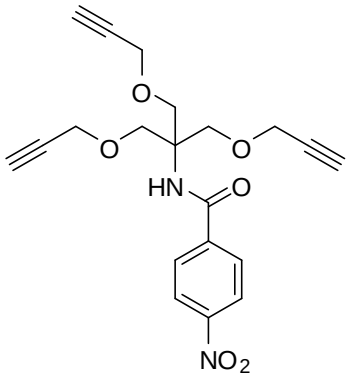


**27** (40 mg, 0.148 mmol) was dissolved in a 1:1 mixture of DCM and triethylamine (2 ml). 4-Nitrobenzoyl chloride was added (35 mg, 0.189 mmol) and the mixture stirred for 3 hrs. A further 3 ml of triethylamine was then added and the mixture stirred overnight.

The mixture was extracted with DCM (50 ml) washed with water (40 ml, x3), separated, dried over magnesium sulphate, filtered and solvent removed under vacuum giving the crude as a yellow oil.

This was purified by flash column chromatography on silica using petroleum ether and ethyl acetate (3:2) giving the product as a clear oil (22 mg, 38%)

$\upsilon_{max}$ (ATR) 3289 (C-H alkyne), 2854 (C-H), 2116 (C≡C), 1663 (C=O), 1602 (C=C), 1523 (N-O), 1346 (N-O); $\delta_H$ (400 MHz, $CDCl_3$) 8.28-8.25 (2H, m, Ar-H ortho nitro), 7.92-7.89 (2H, m, Ar-H ortho C=O), 6.50 (1H, s, NH), 4.19 (6H, d, J=2.4, O-$\underline{CH_2}$-CCH), 3.97 (6H, s, HNC($\underline{CH_2}$)$_3$), 2.45 (3H, t, J=2.4, C-H); $\delta_C$ (100 MHz, $CDCl_3$) 165.5 (C=O), 149.7 (Ar, ipso C=O), 140.9 (Ar, ipso nitro), 128.3 (Ar ortho C=O), 123.9 (Ar, ortho nitro), 79.6 ($\underline{C}$-CH), 75.0 (C-H), 68.5 (O-$\underline{CH_2}$-CCH), 60.0 (HN-

C($CH_2$)$_3$), 58.9 (HN-C(C$H_2$)$_3$); Calculated Mass for $C_{20}H_{20}N_2O_6$ 385.1394 *m/z* ($ES^+$) 385.1 ($MH^+$), 407.0 ($MNa^+$); HRMS ($ES^+$): 385.1394 ($MH^+$)

**Tert-butyl N-(1,3-bis((1-(2-(methoxyamino)ethyl)-1H-1,2,3-triazol-4-yl)methoxy)-2-(((1-(2-(methoxyamino)ethyl)-1H-1,2,3-triazol-4-yl)methoxy)methyl)propan-2-yl)-4-nitrobenzamide carbamate, 29:**

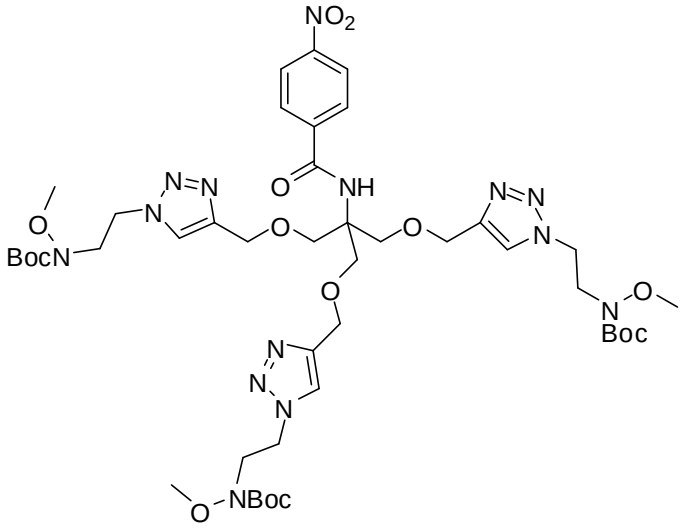


**28** (508 mg, 1.322 mmol) was dissolved in DMF (21 ml) with **24** (1.13 g, 5.224 mmol). Copper sulphate (310 mg, 1.242 mmol), sodium ascorbate (238 mg, 1.201 mmol) and catalytic TBTA were then added and the mixture stirred overnight. The mixture was extracted with chloroform (250 ml) washed with water (200 ml, x4), separated, dried over magnesium sulphate, filtered and solvent removed under vacuum giving the crude as a green oil.

This was purified by flash column chromatography on silica using DCM and methanol (19:1) giving the product as a yellow oil (675 mg, 49%) $\lambda_{max}$(MeOH)/nm 264 (ε/dm3 $mol^{-1}$ $cm^{-1}$ 9800); $\upsilon_{max}$ (ATR) 2936 (C-H), 1701 (C=O), 1663 (C=O), 1602 (C=C), 1525 (N-O, nitro), 1346 (N-O, nitro); $\delta_H$ (400 MHz, $CDCl_3$) 8.24-8.20 (2H, m, Ar ortho nitro), 8.02-7.98 (2H, m, Ar meta nitro), 7.50-7.49 (3H, m, CH triazole), 7.35 (1H, d, J=4.4, N-H), 4.56 (6H, s, O-$CH_2$ triazole), 4.52-4.48 (6H, m, N-$CH_2$ triazole), 3.93-3.85 (12H, m, HNC-C$H_2$, MeON-C$H_2$), 3.58 (9H, s, O-Me), 1.32 (24H, s, Me, Boc); $\delta_C$ (100 MHz, $CDCl_3$) 165.6 (C=O, amide), 155.6 (C=O, Boc), 149.6 (Ar, ipso nitro), 144.9 (C, triazole), 140.8 (Ar, ipso amide), 128.7 (Ar, meta nitro), 123.8 (Ar, ortho nitro), 123.3 (CH, triazole), 82.2 (C-$Me_3$), 69.0 (HNC-C$H_2$), 64.8 (O-$CH_2$ triazole), 62.5 (O-Me), 60.7 (HNC-$CH_2$), 48.9 (MeON-C$H_2$), 47.2 (N-$CH_2$ triazole), 28.2 (Me, Boc); Calculated Mass for

$C_{44}H_{68}N_{14}O_{15}$ 1033.5070 *m/z* ($ES^+$) 1033.7 ($MH^+$), 1055.6 ($MNa^+$); HRMS ($ES^+$): 1033.5069 ($M^+$)

**N-(1,3-bis((1-(2-(methoxyamino)ethyl)-1H-1,2,3-triazol-4-yl)methoxy)-2-(((1-(2-(methoxyamino)ethyl)-1H-1,2,3-triazol-4-yl)methoxy)methyl)propan-2-yl)-4-nitrobenzamide, 30:**

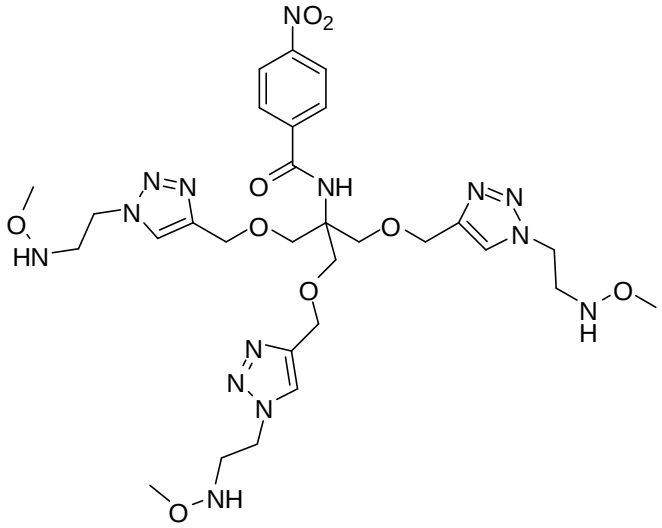

**29** (51 mg, 0.049 mmol) was dissolved in 2M hydrochloric methanol (5 ml) and stirred for 3½hrs. The solvent was then removed under vacuum, giving the protonated product as a pale oil (47 mg).

This was then dissolved in $D_2O$ and neutralised by addition of excess ammonium bicarbonate. Repeated co-evaporations with $D_2O$ gave the neutral product as a pale semi-solid (40 mg, crude)

$\lambda_{max}$($H_2O$ pH 6)/nm 269 (ε/dm3 $mol^{-1}$ $cm^{-1}$ 4700); $\upsilon_{max}$ (ATR) 3361 ($D_2O$), 1646 (C=O amide), 1600 (C=C, aromatic), 1525 (N-O nitro), 1448 (C=C aromatic), 1348 (N-O nitro); $\delta_H$ (400 MHz, $D_2O$) At pH6, 8.32 (2H, d, J=8.8, Ar, ortho nitro), 8.01 (3H, s, CH triazole), 7.81-7.77 (2H, m, Ar, meta nitro), 4.64 (6H, s, O-$\underline{CH_2}$ triazole), 4.56 (6H, t, J=5.8, MeON-$CH_2$-$\underline{CH_2}$), 3.85 (6H, s, HNC-$\underline{CH_2}$), 3.46 (9H, s, O-Me), 3.35 (6H, t, J=5.8, MeON-$\underline{CH_2}$-$CH_2$); $\delta_C$ (100 MHz, $D_2O$) At pH 6 reference to acetonitrile 1.47, 169.2 (C=O), 158.4 (Ar, ipso nitro), 150.0 (Ar, ipso amide), 144.5 (C, triazole) , 129.0 (Ar, meta nitro), 126.0 (CH, triazole), 124.4 (Ar, ortho nitro), 67.8 (HNC-$\underline{CH_2}$), 64.0 (O-$\underline{CH_2}$ triazole), 61.4 (O-Me), 61.2 (HN$\underline{C}$-$CH_2$), 50.3 (MeON-$\underline{CH_2}$-$CH_2$-N), 48.2 (MeON-$CH_2$-$\underline{CH_2}$-N); Calculated Mass for $C_{29}H_{44}N_{14}O_9$ 733.3488 *m/z* ($ES^+$) 755.4 ($MNa^+$); HRMS ($ES^+$): 733.3487 ($MH^+$)

**P-tert-butylcalix(4)arene, 31:** [133]

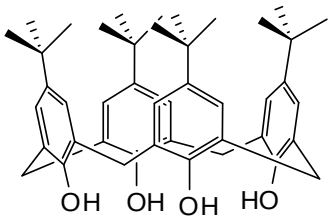


Ground t-butyl phenol (50 g, 0.333 mol), and 31 ml formaldehyde solution (38% aq) was added to 1M aqueous sodium hydroxide (6 ml). The mixture was heated to 120$^{o}$C under a stream of nitrogen for 5½ hrs, until a thick foam was formed. This was allowed to cool to room temperature and left overnight.

Diphenyl ether (400 ml) and toluene (20 ml) were then added to the foam and the mixture heated to reflux for 4½ hrs. It was then allowed to cool to room temperature over 24 hrs. Ethyl acetate (300 ml) was then added to precipitate the product, which was left for 5 days before filtering and washing with acetone (500 ml) giving product as a white solid (34.06 g, 16%).

$\upsilon_{max}$ (ATR) 3221 (O-H), 2950 (C-H), 1582 (C=C), 1486 (C=C), 1454 (C=C), 1237 (C-O), 1201 (C-O); $\delta_H$ (400 MHz, $CDCl_3$) 9.63 (4H, s, OH) , 7.19 (8H, s, Ar), 4.38 (4H, d, J=13.2, $CH_2$), 3.51 (4H, d, J=13.2 $CH_2$), 1.26 (36H, s, $CH_3$); $\delta_C$ (100 MHz, $CDCl_3$) 146.8 (Ar-OH), 144.9 (Ar-tButyl), 128.9 (Ar), 125.7 (Ar-$CH_2$), 34.2 (C-$CH_3$), 32.5 ($CH_2$), 31.6 ($CH_3$)

**Calix(4)arene, 32:** [164]

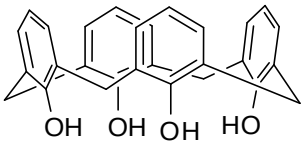


Aluminium chloride (13.01 g, 97.752 mmol) was added to a solution of **31** (10.22 g, 15.767 mmol) and phenol (7.06 g, 36.263 mmol) in toluene (100 ml). The mixture was stirred for 1½ hrs then quenched with ice, giving a dark orange mixture.

The reaction mixture was diluted with DCM. The aqueous layer was washed with portions of DCM (100 ml, x4) and the combined organic layer washed with water (100 ml). The organic layer was then separated, dried over magnesium sulphate, filtered and concentrated under reduced pressure. Methanol (200 ml) was then added, the product precipitated as a white powder (5.41 g, 81%).

$\upsilon_{max}$ (ATR) 3139 (O-H), 2933 (C-H), 1594 (C=C); $\delta_H$ (400 MHz, $CDCl_3$) 10.20 (4H, s, OH), 7.06 (8H, d, J=7.2 Ar), 6.73 (4H, t, J=7.2 Ar), 4.26 (4H, br, $CH_2$), 3.55 (4H, br, $CH_2$); $\delta_C$ (100 MHz, $CDCl_3$) 148.9 (Ar-OH), 129.1 (Ar), 128.4 (Ar-$CH_2$), 122.4 (Ar, para OH), 31.8 ($CH_2$); Calculated Mass for $C_{28}H_{24}O_4$ 424.49 *m/z* ($ES^-$) 423 (M – H)

**26,28-dipropoxypentacyclo[19.3.1.1^3,7 .1^9,13 .1^15,19]octacosa-1(25),3,5,7(28),9(27),10,12,15(26),16,18,21,23-dodecaene-25,27-diol, 33:** [165]

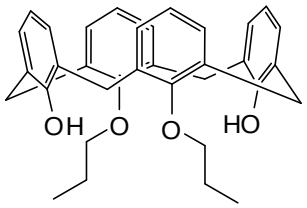


**32** (2.50 g, 5.89 mmol) and potassium carbonate (2.04 g, 14.72 mmol) were suspended in acetonitrile (40 ml) and stirred for 5 min. Iodopropane (1.45 ml, 2.50 g, 14.72 mmol) was then added and the mixture heated to reflux. After 16 hrs the mixture was cooled and white precipitate filtered off. Solvent was removed under vacuum giving a white solid and both portions were worked up separately as follows. The solid was dissolved in DCM (200 ml), washed with 1M aqueous HCl (150 ml, x2), and with distilled water (150 ml, x2). The organic layer was separated, dried over magnesium sulphate, filtered and solvent removed under vacuum.
The precipitated solid gave the product as a white solid (1.32 g, 44%). The residue gave a mixture of product and starting material as a yellow solid (852 mg).
$\upsilon_{max}$ (ATR) 3260 (O-H), 2958 (C-H), 2925 (C-H), 2875 (C-H), 1592 (C=C); $\delta_H$ (400 MHz, $CDCl_3$) 8.31 (2H, s, OH), 7.06 (4H, d, J=7.6, Ar), 6.93 (4H, d, J=7.6, Ar), 6.75 (2H, t, J=7.6, Ar), 6.65 (2H, t, J=7.6, Ar), 4.33 (4H, d, J=12.8, $CH_2$), 3.99 (4H, t, J=6.6, O-$\underline{CH_2}$-$CH_2$), 3.39 (4H, d, J=12.8, $CH_2$), 2.08 (4H, sextet, $J_1$=7.4, $J_2$=6.6, O-$CH_2$-$\underline{CH_2}$), 1.32 (6H, t, J=7.4, $CH_3$); $\delta_C$ (100 MHz, $CDCl_3$) 153.5 (Ar-OPr), 152.0 (Ar-OH), 133.6 (Ar), 129.1 (Ar), 128.6 (Ar), 128.3 (Ar), 125.4 (Ar), 119.1 (Ar, para OPr), 78.5 (O-$\underline{CH_2}$-$CH_2$), 77.4 (O-$\underline{CH_2}$-$CH_2$), 31.6 ($CH_2$), 23.7 (O-$CH_2$-$\underline{CH_2}$), 11.1 ($CH_3$); Calculated Mass for $C_{34}H_{36}O_4$ 508.65 *m/z* ($ES^+$) 509 ($MH^+$)

**11,23-dibromo-26,28-dipropoxypentacyclo[19.3.1.1^3,7 .1^9,13 .1^15,19]octacosa-1(25),3,5,7(28),9(27),10,12,15(26),16,18,21,23-dodecaene-25,27-diol, 34:** [134]

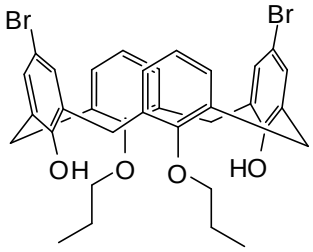


**33** (506 mg, 0.995 mmol) was dissolved in dry DCM (25 ml) in a round bottomed flask oven dried and cooled under nitrogen. Bromine (0.13 ml, 393 mg, 2.46 mmol) was added and the mixture stirred at room temperature for 45 min.
The mixture was then filtered and the precipitate washed with DCM (10 ml, x3). This gave the product as a pale yellow solid (477 mg, 72%)
$\upsilon_{max}$ (ATR) 3221 (O-H), 2960 (C-H), 2934 (C-H), 2876 (C-H), 1576 (C=C); $\delta_H$ (400 MHz, $CDCl_3$) 8.36 (2H, s, OH), 7.17 (4H, s, Ar), 6.95-6.93 (4H, m, Ar), 6.81 (2H, br, Ar), 4.25 (4H, d, J=13.0, $CH_2$), 3.95 (4H, br, O-$CH_2$), 3.32 (4H, d, J=13.0, $CH_2$), 2.04 (4H, br, $CH_2$-$\underline{CH_2}$), 1.31-1.27 (6H, m, $CH_3$)

**5,17-dibromo-26,28-bis(prop-2-en-1-yloxy)-25,27-dipropoxypentacyclo[19.3.1.1^3,7 .1^9,13 .1^15,19]octacosa-1(25),3,5,7(28),9(27),10,12,15(26),16,18,21,23-dodecaene, 35:**

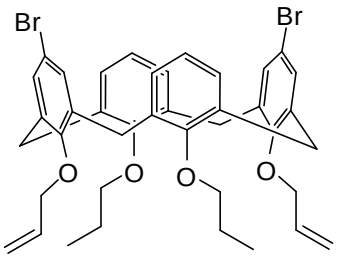


**34** (207 mg, 0.31 mmol) was added to dry DMF (10 ml) in a round bottomed flask oven dried and cooled under nitrogen. Sodium hydride (34 mg, 0.855 mmol) was added and the mixture stirred for 30 min before allyl bromide (0.07 ml, 91 mg, 0.75 mmol) was added. The mixture was stirred at room temperature for 28 hrs. The mixture was then quenched with distilled water giving a cloudy white mixture. This was extracted with ether (150 ml), washed with distilled water (100 ml, x3), separated, dried over magnesium sulphate, filtered and the solvent removed under vacuum. This gave the crude as a pale yellow solid (190 mg)

Washing with petroleum ether (50 ml, x3) gave the product as a white solid (58 mg, 25%)

$\delta_H$ (400 MHz, $CDCl_3$) 7.16 (4H, s, Ar), 6.45-6.34 (4H, m, Ar, para OPr, CH), 6.29 (4H, d, J=7.6, Ar), 5.17-5.16 (2H, m, CH=$\underline{CH_2}$), 5.15-5.12 (2H, m, CH=$\underline{CH_2}$), 4.59 (4H, d, J=6.6, O-$\underline{CH_2}$-CH), 4.37 (4H, d, J=13.4, $CH_2$), 3.71 (4H, t, J=6.6, O-$\underline{CH_2}$-$CH_2$), 3.11 (4H, d, J=13.4, $CH_2$), 1.90 (4H, sextet, J=7.4, $CH_2$-$\underline{CH_2}$), 1.07 (6H, t, J=7.4, $CH_3$); $\delta_C$ (100 MHz, $CDCl_3$) 156.0 (Ar-O), 155.6 (Ar-O), 139.2 ($\underline{Ar}$-$CH_2$), 135.7 (CH), 132.9 ($\underline{Ar}$-$CH_2$), 131.3 (Ar), 127.9 (Ar), 122.5 (Ar-H, para O), 117.4 (CH=$\underline{CH_2}$), 115.0 (Ar-Br), 77.3 (O-$CH_2$), 75.9 (O-$CH_2$), 31.2 ($CH_2$), 23.6 ($CH_2$-$\underline{CH_2}$), 10.8 (Me)

**26,28-dihydroxy-25,27-dipropoxypentacyclo[19.3.1.1^3,7 .1^9,13 .1^15,19]octacosa-1(25),3,5,7(28),9(27),10,12,15(26),16,18,21,23-dodecaene-5,17-dicarbaldehyde, 36:** [135]

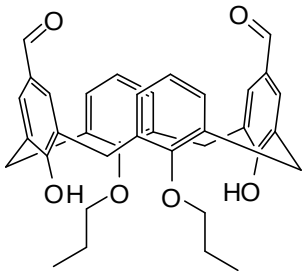


**33** (452 mg, 0.889 mmol) was dissolved in dry chloroform (15 ml) and cooled to -15$^oC$ in a round bottomed flask flushed with nitrogen. Tin (IV) chloride (1.1 ml, 2.32 g, 8.886 mmol) was added followed by dichloro methyl methylether (0.2 ml, 255 mg, 2.222 mmol). The mixture was allowed to warm to room temperature and stirred for 1¼ hrs before quenching with distilled water. The mixture was diluted with chloroform (250 ml), washed with distilled water (200 ml, x3), separated and filtered to remove a pink solid that was insoluble in both chloroform and water. The organic layer was then dried over magnesium sulphate, filtered and solvent removed under vacuum. This gave a pale pink solid, which was washed with methanol (50 ml), giving the product as a pale pink solid (467 mg, 93%)

$\upsilon_{max}$ (ATR) 3171 (O-H), 2924 (C-H), 1671 (C=O), 1583 (C=C); $\delta_H$ (400 MHz, $CDCl_3$) 9.79 (2H, s, O=$\underline{CH}$), 9.26 (2H, s, OH), 7.64 (4H, s, Ar), 6.98 (4H, d, J=7.4 Ar), 6.81 (2H, t, J=7.4, Ar), 4.31 (4H, d, J=13.2, $CH_2$), 4.02 (4H, t, J=6.4, O-$\underline{CH_2}$-$CH_2$), 3.51 (4H, d, J=13.2, $CH_2$), 2.09 (4H, sextet, $J_1$=7.6, $J_2$=6.4, O-$CH_2$-$\underline{CH_2}$), 1.33

(6H, t, J=7.6, $CH_3$); $\delta_C$ (100 MHz, $CDCl_3$) 191.0 (C=O), 159.8 (Ar-OH), 151.8 (Ar-OPr), 132.5 (Ar, ortho C=O), 131.1 (Ar, meta O-Pr), 129.6 (Ar), 128.7 (Ar), 128.7 (Ar), 125.8 (Ar, para O-Pr), 78.7 (O-$CH_2$-$CH_2$), 77.3 (O-$CH_2$-$CH_2$), 31.4 ($CH_2$), 23.6 (O-$CH_2$-$CH_2$), 11.0 (Me); Calculated Mass for $C_{36}H_{36}O_6$ 564.67, *m/z* ($ES^+$) 1130 (2M)

**26,28-bis(prop-2-en-1-yloxy)-25,27-dipropoxypentacyclo[19.3.1.1^3,7 .1^9,13 .1^15,19]octacosa-1(25),3,5,7(28),9(27),10,12,15(26),16,18,21,23-dodecaene-5,17-dicarbaldehyde, 37:**

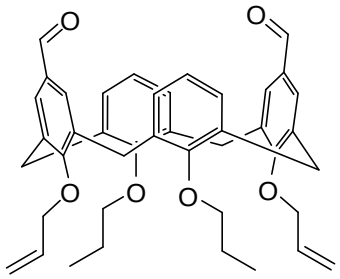

**36** (467 mg, 0.827 mmol) was dissolved in dry methanol (40 ml) and trimethyl orthoformate (1.55 ml, 1.50 g, 14.17 mmol) and paratoluene sulphonic acid (40 mg, 2.1 mmol) added under nitrogen. The mixture was heated to reflux for 4 hrs, then allowed to cool and quenched with saturated sodium hydrogen carbonate solution. The mixture was extracted with DCM (200 ml), washed with distilled water (100 ml), separated, dried over magnesium sulphate, filtered and solvent removed under vacuum giving the crude brown semi-solid.

This was dissolved in dry DMF (25ml) and transferred to a round bottomed flask oven dried and cooled under nitrogen. Sodium hydride (1.00 g, 25. 3 mmol) was then added and stirred for 15 min (a gas was evolved) before allyl bromide (0.36 ml, 503 mg, 4.16 mmol) was added. The mixture was stirred at room temperature for 19 hrs then quenched by slow addition of 1M aqueous hydrochloric acid (35 ml), producing a gas. The mixture was extracted with ether (250 ml), washed with saturated sodium thiosulphate solution (200 ml) and distilled water (200 ml, x3), separated, dried over magnesium sulphate, filtered and solvent removed under vacuum. This gave the crude as a yellow tacky solid (364 mg)

This was washed with petroleum ether (70 ml, x3) giving the product as a white solid (82 mg, 16%)

$\upsilon_{max}$ (ATR) 2922 (C-H), 2853 (C-H, aldehyde), 1694 (C=O), 1596 (C=C, aromatic), 1456 (C=C, aromatic), 1127 (C-O), 988 (C-H, alkene), 760 (C-H); $\delta_H$ (400 MHz, $CDCl_3$) 9.82 (2H, s, O=CH), 7.48 (4H, s, Ar), 6.41-6.37 (4H, m, Ar, CH-$CH_2$), 6.31 (4H, d, J=7.6 Ar), 5.20-5.15 (4H, m, CH-$CH_2$), 4.68 (4H, d, J=6.4, O-$CH_2$-CH), 4.45 (4H, d, J=13.6, $CH_2$), 3.76 (4H, t, J=7.4, O-$CH_2$-$CH_2$), 3.27 (4H, d, J=13.6, $CH_2$), 1.91 (4H, sextet, J=7.4, O-$CH_2$-$CH_2$), 1.07 (9H, t, J=7.4, $CH_3$); $\delta_C$ (100 MHz, $CDCl_3$) 191.9 (C=O), 162.5 (Ar-O), 155.8 (Ar-O), 137.9 (Ar-C=O), 135.1 (CH-$CH_2$), 133.2 (Ar-$CH_2$), 131.4 (Ar-$CH_2$), 130.6 (Ar), 128.2 (Ar), 122.7 (Ar, para O), 118.0 (CH-$CH_2$), 77.4 (O-$CH_2$), 76.1 (O-$CH_2$), 32.1 ($CH_2$), 23.6 (O-$CH_2$-$CH_2$), 10.8 (Me); Calculated Mass for $C_{42}H_{44}O_6$ 645.3202, MALDI 702.98 ($MNaCl^+$); HRMS ($ES^+$) 645.3205 ($M^+$), 662.3472 ($MH_2O^+$)

**Allyl phenyl ether, 38:** [166]

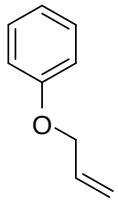


Phenol (494 mg, 5.25 mmol) was dissolved in DMF (5 ml) and potassium carbonate (1.48 g, 10.74 mmol) added. The mixture was stirred for 10 min before allyl bromide was added (0.92 ml, 1.29g, 10.63 mmol). The mixture was stirred overnight then quenched with water. The mixture was extracted with ether (150 ml), washed with distilled water (100 ml, x3), separated, dried over magnesium sulphate, filtered and solvent removed under vacuum giving the product as a yellow oil (531 mg, 75%) $\upsilon_{max}$ (ATR) 2959 (C-H vinyl), 1455 (C=C aromatic), 1007 (C-H aromatic); $\delta_H$ (400 MHz, $CDCl_3$) 7.32 (2H, dd, J=7.6, Ar), 6.99-6.94 (3H, m, Ar), 6.13-6.04 (1H, m, CH), 5.47-5.41 (1H, m, CH-$CH_2$), 5.33-5.29 (1H, m, CH-$CH_2$), 4.58 (2H, dt, $J_1$=5.2, $J_2$=1.2, O-$CH_2$); $\delta_C$ (100 MHz, $CDCl_3$) 158.7 (Ar-O), 133.5 (CH), 129.6 (Ar meta), 121.0 (Ar para), 117.8 (CH-$CH_2$), 114.9 (Ar ortho), 68.9 (O-$CH_2$)

**2-(4-Methoxyphenyl)-5-phenyl-2H-tetrazole, 39:** [140]

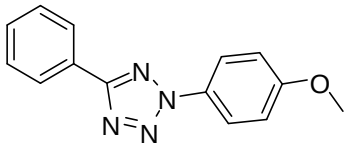

Benzaldehyde (1.02 ml, 1.065g, 10.03 mmol) was dissolved in ethanol (60 ml) and benzenesulfonohydrazide (1.72 g, 9.99 mmol) was added slowly. The mixture was stirred for an hour and 20 min before quenching with ice water (200 ml). This gave a milky precipitate which was centrifuged and the solvent decanted. The solid was further dried by vacuum filtering then stored at –18$^{o}$C overnight. This was then dissolved in pyridine (70 ml) and cooled to 0$^{o}$C.

P-anisidine (1.25 g, 10.17 mmol) was then dissolved in ethanol (8 ml), 8.1M HCl (aq, 10.6 ml) was added and the mixture cooled to 0$^{o}$C. A solution of sodium nitrite (697 mg, 10.11 mmol) in water (4 ml) was added to the p-anisidine solution dropwise over 20 min.

This mixture was then slowly added to the previously prepared pyridine solution which became red. The mixture was stirred for an hour before extracting with chloroform (250 ml). The organic layer was washed with water (200 ml, x3), separated, dried over magnesium sulphate, filtered and solvent removed giving the crude as a tacky red solid.

This was purified by flash column chromatography on silica using ethyl acetate and petroleum ether (1:9) giving the product as a brown solid (2.16 g, 86%)

$\upsilon_{max}$ (ATR) 3016 (C-H aromatic), 1596 (C=N), 1530 (C=C), 1514 (C=C), 1466 (C=C), 1450 (C=C), 1436 (C=C), 1257 (C-H methyl); $\delta_H$ (400 MHz, $CDCl_3$) 8.25-8.23 (2H, m, ortho Ar-C), 8.11-8.07 (2H, m, ortho Ar-N), 7.54-7.48 (3H, m, Ar-C, para meta-tetrazole), 7.06-7.02 (2H, m, ortho Ar-OMe), 3.86 (3H, s, Me); $\delta_C$ (100 MHz, $CDCl_3$) 165.1 (C=N), 160.6 (Ar-OMe), 130.5 (Ar), 129.0 (Ar), 127.4 (Ar-C=N), 127.1 (Ar), 121.5 (Ar), 114.8 (Ar), 55.7 (Me); Calculated Mass for $C_{14}H_{12}N_4O$ 252.27 *m/z* ($ES^+$) 253 ($MH^+$)

**Benzyl 3-hydroxypropylcarbamate, 40:** [167]

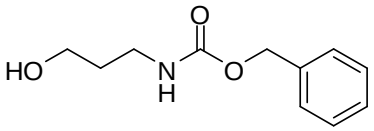

3-Amino-1-propanol (5 ml, 4.91 g, 65.37 mmol) was dissolved in DCM (50 ml) and cooled to 0°C. Triethylamine (7.6 ml, 5.52 g, 54.53 mmol) was then added. A solution of benzylchloroformate (7.8 ml, 9.32 g, 54.64 mmol) in DCM (5 ml) was added dropwise over 30 min. The mixture was stirred at 0°C for a further 30 min before being allowed to warm to room temperature. The mixture was stirred at room temperature for 1½ hrs, water (100 ml) and ether (100 ml) were then added. The aqueous layer was extracted with further ether (100 ml) and the combined organic fractions were washed with water (150 ml) and brine (150 ml, x2), separated, dried over magnesium sulphate, filtered and the solvent removed under vacuum giving a clear oil.

This was purified by flash column chromatography on silica using petroleum ether and ethyl acetate (3:7) giving the product as a white solid (3.57 g, 31%).

$\upsilon_{max}$ (ATR) 3323 (O-H), 2954 (C-H), 2884 (C-H), 1683 (C=O), 1530 (C=C), 1485 (C=C), 1453 (C=C), 1255 (C-O ester), 1059 (C-OH); $\delta_H$ (400 MHz, $CDCl_3$) 7.36-7.29 (5H, m, Ar), 5.10 (2H, s, $\underline{CH_2}$-Ar), 3.67 (2H, t, J=6.0, HO-$\underline{CH_2}$), 3.34 (2H, t, J=6.0, HN-$\underline{CH_2}$), 2.42 (1H, br, OH), 1.69 (2H, quintet, J=6.0, $CH_2$); $\delta_C$ (100 MHz, $CDCl_3$) 157.4 (O=C), 136.6 (ipso Ar), 128.7 (Ar), 128.3 (Ar), 128.2 (Ar), 67.0 ($\underline{CH_2}$-Ar), 59.7 (HO-$\underline{CH_2}$), 37.9 (HN-$\underline{CH_2}$), 32.7 ($CH_2$); Calculated Mass for $C_{11}H_{15}NO_3$ 209.24 *m/z* ($ES^+$) 231.9 ($MNa^+$)

**Benzyl 5-hydroxypentylcarbamate, 41:** [168]

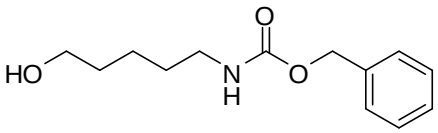

5-Amino-1-pentanol (5 ml, 4.75 g, 45.997 mmol) and triethylamine (5.2 ml, 3.78 g, 37.308 mmol) were dissolved in DCM (50 ml) and the mixture chilled to 0°C. Benzylchloroformate (5.5 ml, 6.57 g, 38.528 mmol) was then added dropwise over 15 min. The mixture was stirred at 0°C for 30 min then allowed to warm to room temperature and stirred overnight. The mixture was filtered to remove precipitate and extracted with ether (250 ml). The organic layer was washed with brine (200 ml, x2)

and water (200 ml), separated, dried over magnesium sulphate, filtered, and solvent removed under vacuum giving an opaque oil.

This was purified by flash column chromatography on silica using petroleum ether and ethyl acetate (3:7) giving the product as a white solid (2.83 g, 31%)

$\upsilon_{max}$ (ATR) 3391 (O-H), 3330 (N-H), 3061 (C-H aromatic), 2942 (C-H), 2862 (C-H), 1682 (C=O), 1531 (C=C), 1453 (C=C), 1254 (C-O ester), 1020 (C-O); $\delta_H$ (400 MHz, $CDCl_3$) 7.35-7.30 (5H, m, Ar), 5.08 (2H, s, $\underline{CH_2}$-Ar), 4.90 (1H, br, NH), 3.61 (2H, t, J=6.4, HO-$\underline{CH_2}$), 3.19 (2H, q, J=6.4, HN-$\underline{CH_2}$), 1.60-1.48 (4H, m, HO-$CH_2$-$\underline{CH_2}$, HN-$CH_2$-$\underline{CH_2}$), 1.42-1.34 (2H, m, $CH_2$-$CH_2$-$\underline{CH_2}$); $\delta_C$ (100 MHz, $CDCl_3$) 156.6 (C=O), 136.7 (Ar ipso), 128.6 (Ar), 128.2 (Ar), 66.7 ($\underline{CH_2}$-Ar), 62.6 (HO-$CH_2$), 41.0 (HN-$CH_2$), 32.3 (HN-$CH_2$-$\underline{CH_2}$), 29.8 (HO-$CH_2$-$\underline{CH_2}$), 23.0 ($CH_2$-$CH_2$-$\underline{CH_2}$); Calculated Mass for $C_{13}H_{19}NO_3$ 237.29 *m/z* ($ES^+$) 259.9 ($MNa^+$)

**Benzyl 3-bromopropylcarbamate, 42:**

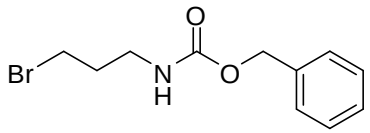


**40** (484 mg, 2.31 mmol) was dissolved in dry DCM (14 ml) in a round bottomed flask oven dried and cooled under nitrogen and the solution cooled to 0°C. Triphenylphosphine (926 mg, 3.53 mmol) and carbon tetrabromide (1.19 g, 3.59 mmol) were then added. The mixture was stirred for 20 min at 0°C, allowed to warm to room temperature and stirred for a further 1½ hrs in the dark. The mixture was then quenched with water and diluted with DCM (75 ml). The organic layer was washed with water (100 ml) and brine (100 ml, x2), separated, dried over magnesium sulphate, filtered and solvent removed under vacuum. This gave a brown semisolid (2.03 g) which was purified by flash column chromatography on silica using petroleum ether and ethyl acetate (4:1) giving the product as a clear oil (434 mg, 69%)

$\upsilon_{max}$ (ATR) 3330 (N-H), 2945 (C-H), 1692 (C=O), 1521 (C=C), 1454 (C=C), 1244 (C-O ester); $\delta_H$ (400 MHz, $CDCl_3$) 7.36-7.31 (5H, m, Ar), 5.09 (2H, s, $\underline{CH_2}$-Ar), 5.02 (1H, br, NH), 3.42 (2H, t, J=6.2, Br-$CH_2$) 3.34 (2H, q, J=6.2, HN-$\underline{CH_2}$), 2.06 (2H, quintet, J=6.2, $CH_2$); $\delta_C$ (100 MHz, $CDCl_3$) 156.6 (O=C), 136.5 (ipso Ar), 128.6 (Ar), 128.2 (Ar), 128.2 (Ar), 66.8 ($\underline{CH_2}$-Ar), 39.5 (HN-$\underline{CH_2}$), 32.5 ($CH_2$), 30.7 (Br-$\underline{CH_2}$); Calculated Mass for $C_{11}H_{14}BrNO_2$ 272.14 *m/z* ($ES^+$) 293.7 ($MNa^+$)

**O-Methylbenzaldehyde oxime, 43:** [97]

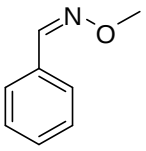

Benzaldehyde (0.95 ml, 992 mg, 9.35 mmol) was suspended in pyridine (29 ml) and O-methylhydroxylamine hydrochloride (1.01 g, 12.14 mmol) was added. The mixture was stirred for 22 hrs at room temperature, the solvent was then removed under vacuum.

The resulting solid was extracted with ethyl acetate (150 ml). The solution was then washed with saturated copper sulphate solution (100 ml portions) until the copper-pyridine complex was no longer visible and water (100 ml, x2). It was then separated, dried over magnesium sulphate, filtered through Celite and the solvent removed under vacuum giving the product as a clear oil (915 mg, 72%)

$\upsilon_{max}$ (ATR) 3062 (C-H aromatic), 2936 (C-H methyl), 2898 (C-H methyl), 2817 (C-H), 1693 (C=N), 1490 (C-H), 1447 (C-H), 1212 (C-O), 1182 (C-O), 946 (N-O), 754 (C-H aromatic), 691 (C-H aromatic); $\delta_H$ (400 MHz, $CDCl_3$) 8.07 (1H, s, HC=N), 7.59-7.57 (2H, m, Ar ortho), 7.38-7.36 (3H, m, Ar meta and para), 3.98 (3H, s, Me); $\delta_C$ (100 MHz, $CDCl_3$) 148.7 (C=N), 132.4 (Ar ipso), 129.9 (Ar para), 128.8 (Ar ortho), 127.1 (Ar meta), 62.1 (O-Me); Calculated Mass for $C_8H_8NO$ 135.16 *m/z* ($ES^+$) 135.8 ($M^+$)

**N-Benzyl-O-methylhydroxylamine, 44:** [98]

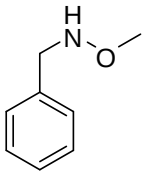

**43** (989 mg, 7.31 mmol) was dissolved in ethanol (5 ml) and cooled to 0$^o$C. Sodium cyanoborohydride (1.40 g, 22.28 mmol) was added and the mixture stirred for 15 min. 15% hydrochloric acid in ethanol (6 ml) was then added and a gas evolved. The mixture was stirred at 0$^o$C for 15 min then allowed to warm to room temperature and stirred for 2¼ hrs. The mixture was quenched with excess potassium carbonate. The mixture was left open in a fumehood to allow cyanide gas to disperse, then concentrated under vacuum. The mixture was extracted with dichloromethane (150

ml), washed with saturated sodium hydrogen carbonate solution (100 ml, x2), dried over magnesium sulphate, filtered and solvent removed under vacuum to give a clear oil. This was purified by flash column chromatography on silica using petroleum ether and ethyl acetate (9:1) giving the product as a clear oil (436 mg, 43%) $\upsilon_{max}$ (ATR) 3251 (N-H), 3062 (C-H Ar), 3029 (C-H Ar), 2979 (C-H), 2934 (C-H), 2893 (C-H), 2806 (C-H), 1603 (C=C), 1495 (C=C), 1453 (C-H), 1247 (C-O), 1058 (C-N), 993 (N-O), 744 (C-H Ar), 696 (C-H Ar); $\delta_H$ (400 MHz, $CDCl_3$) 7.38-7.30 (5H, m, Ar), 4.06 (2H, s, $CH_2$), 3.53 (3H, s, OMe); $\delta_C$ (100 MHz, $CDCl_3$) 137.7 (Ar ipso), 129.0 (Ar), 128.6 (Ar), 127.6 (Ar para), 62.0 (OMe), 56.3 ($CH_2$-NH); Calculated Mass for $C_8H_{11}NO$ 137.18 *m/z* ($ES^+$) 137.9 ($M^+$)

**Benzyl methoxyamine β-$_D$-galactopyranoside, 45:** [77]

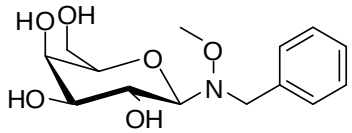


$_D$-Galactose (164 mg, 0.911 mmol) was suspended in a mixture of methanol (6 ml) and glacial acetic acid (2 ml). **44** (49 mg, 0.358 mmol) was then added as a solution in methanol (0.2 ml). The mixture was sonicated for 5 hrs without pause, allowing the mixture to warm up.

The mixture was then purified by flash column chromatography on silica using ethyl acetate and methanol (9:1) giving the product as a white solid (70 mg, 65%) mp 147.3-149.5$^o$C (from methanol); $[\alpha]_D^{17.8}$ -5.0 (*c* 0.8, MeOH) (lit.,[74] $[\alpha]_D^{22}$ -10.3 (*c* 1.0, MeOH); $\upsilon_{max}$ (ATR) 3364 (O-H), 2949 (C-H), 1498 (C=C), 1456 (C=C), 1383 (C-H), 1145 (C-O), 1069 (C-O), 1028 (C-N), 998 (N-O), 735 (C-H Ar); $\delta_H$ (400 MHz, $CD_3OD$) 7.46-7.43 (2H, m, Ar), 7.33-7.29 (2H, m, Ar), 7.28-7.25 (1H, m, Ar para), 4.11 (2H, dd, J=51.6, N-$CH_2$), 3.93 (1H, d, $J_{1\text{-}2}$=8.8, CH anomeric), 3.85-3.79 (3H, m, H-2, H-6), 3.73 (1H, dd, $J_{2\text{-}3}$=11.2, $J_{3\text{-}4}$=6, H-3), 3.45-3.42 (2H, m, H-4, H-5), 3.40 (3H, s, O-Me); $\delta_C$ (100 MHz, $CD_3OD$) 138.8 (Ar, ipso), 131.1 (Ar), 129.2 (Ar), 128.3 (Ar, para), 94.0 (CH Anomeric), 78.5 (C-4 or C-5), 76.4 (C-4 or C-5), 70.6 (C-2 or C-3), 69.1 (C-2 or C-3), 62.7 (C-6), 62.3 (O-Me), 57.2 (N-$CH_2$); Calculated Mass for $C_{14}H_{21}NO_6$ 299.32 *m/z* ($ES^+$) 322.1 ($MNa^+$)

**26,28-Dihydroxy-25,27-dipropoxycalix[4]arene-5,17-dicarbaldehyde, O-methyl oxime, 46:**

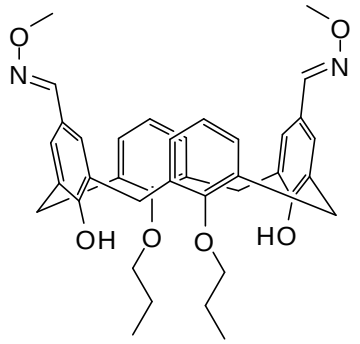


**36** (196 mg, 0.346 mmol) was suspended in pyridine (3 ml) and O-methylhydroxylamine hydrochloride (90 mg, 1.080 mmol) was added. The mixture was stirred overnight at room temperature, the solvent was then removed under vacuum. The resulting concentrated solution was extracted with chloroform (100 ml). The solution was then washed with saturated copper sulphate solution (70 ml portions) until the copper-pyridine complex was no longer visible and water (100 ml, x2). It was then separated, dried over magnesium sulphate, filtered and the solvent removed under vacuum giving the product as a pink solid (173 mg, 79%) $\upsilon_{max}$ (ATR) 3245 (O-H), 2961 (C-H), 1735 (C=N), 1603 (C=C), 1258 (C-H); $\delta_H$ (400 MHz, $CDCl_3$) 8.64 (2H, s, HC=N), 7.97 (2H, s, OH), 7.32 (4H, s, Ar), 6.94 (4H, d, J=7.6, Ar), 6.75 (2H, t, J=7.6, Ar), 4.29 (2H, d, J=12.8, $CH_2$), 3.99 (4H, t, J=6.2, O-$CH_2$), 3.96 (6H, s, O-Me), 3.42 (4H, d, J=12.8, $CH_2$), 2.07 (4H, m, $J_1$=7.2, $J_2$=6.2, $CH_2$-$\underline{CH_2}$-$CH_3$), 1.32 (6H, t, J=7.2, $CH_2$-$\underline{CH_3}$); $\delta_C$ (100 MHz, $CDCl_3$) 155.5 ($\underline{Ar}$-OPr), 152.0 ($\underline{Ar}$-OH), 149.0 (C=N), 133.0 ($\underline{Ar}$-C=N), 129.3 (Ar), 128.6 (Ar), 127.6 (Ar), 125.5 (Ar), 123.1 (Ar), 78.5 (O-$CH_2$), 61.8 (O-Me), 31.4 ($CH_2$), 23.6 ($CH_2$-$\underline{CH_2}$-$CH_3$), 11.0 ($CH_2$-$\underline{CH_3}$); Calculated Mass for $C_{38}H_{42}N_2O_6$ 623.3107 *m/z* MALDI 646.67 ($MNa^+$); HRMS ($ES^+$): 623.3107 ($M^+$)

# Abbreviations

Ac- Acetyl

Boc- Tert-butyl carbamate

Calix- Calix(4)arene

COSY- Correlation Spectroscopy

Cbz- Benzyl carbamate

DBU- 1,8-Diazabicyclo[5.4.0]undec-7-ene

DC-SIGN- Dendritic Cell-Specific Intercellular adhesion molecule-3-Grabbing Non-integrin

DCM- Dichloromethane

DIBAL- Diisobutylaluminium hydride

DMF- Dimethylformamide

DMSO- Dimethyl sulfoxide

DPPA- Diphenylphosphoryl azide

EDTA- Ethylenediaminetetraacetic acid

ELISA- Enzyme-linked immunosorbent assay

Equiv- Equivalents

ESI- Elcectrospray Ionisation

Etc- Etcetera

Fmoc- 9-Fluorenylmethyl carbamate

FmocGlyOH- 9-Fluorenylmethyl carbamate protected glycine

GlcNAc- N-Acetyl-D-glucosamine

HPLC- High Performance Liquid Chromatography

HSQC-Heteronuclear Single Quantum Correlation experiment

Hrs- hours

IR- Infrared

L-SIGN- Liver-Specific Intracellular adhesion molecules-3-Grabbing Non-integrin

MALDI-Matrix-assisted laser desorption ionisation

Mass spec- Mass spectroscopy

Me- Methyl

min- minutes

MRI- Magnetic resonance imaging

NMR- Nuclear Magnetic Resonance spectroscopy

Ph- Phenyl

ppm- parts per million

Pr- Propyl

Rf- Retention factor

RT- Room temperature

SN2- Bimolecular nucleophilic substitution reaction

STD-NMR- Saturation-Transfer Difference Nuclear Magnetic Resonance experiment

TBTA- Tris(benzyltriazolylmethyl)amine

Temp- Temperature

TFA- Trifluoroacetic acid

THF- Tetrahydrofuran

TLC- Thin layer chromatography

TMSOTf- Trimethylsilyl trifluoromethane sulfonate

Tris- Tris(hydroxymethyl)aminomethane, also Trizma base

UV- Ultraviolet

UV-Vis- Ultraviolet-visible

# References


(1) Y M Chabre, R Roy *Design and Creativity in Synthesis of Multivalent Neoglycoconjugates*; Elsevier B.V. , 2010; Vol. 63.

(2) Y C Lee, R T Lee *Accounts of Chemical Research* **1995**, *28*, 321.

(3) W B Turnbull, J F Stoddart *Reviews in Molecular Biotechnology* **2002**, *90*, 231.

(4) D Page, R Roy *Bioconjugate Chemistry* **1997**, *8*, 714.

(5) J D Badjic, A Nelson, S J Cantrill, W B Turnbull, J F Stoddart *Accounts of Chemical Research* **2005**, *38*, 723.

(6) T R Branson, W B Turnbull *Chemical Society Reviews* **2013**, *42*, 4613.

(7) R Sharma, I Zhang, L Abbassi, R Rej, D Maysinger, R Roy *Polymer Chemistry* **2015**, *6*, 1436.

(8) N P Pera, R J Pieters *MedChemComm* **2014**, *5*, 1027.

(9) C St-Pierre, M Ouellet, D Giguere, R Ohtake, R Roy, S Sato, M J Tremblay *Antimicrobial Agents and Chemotherapy* **2011**, *55*, 154.

(10) Y Liu, J Liu, X Pang, T Liu, Z Ning, G Cheng *Molecules* **2015**, *20*, 2272.

(11) A Imberty, M Wimmerova, C Sabin, E P Mitchell In *Protein-Carbohydrate Interactions in Infectious Diseases*; Bewley, C. A., Ed.; The Royal Society of Chemistry: 2006, p 30.

(12) W B Turnbull, B L Precious, S W Homans *Journal of the American Chemical Society* **2004**, *126*, 1047.

(13) D Arosio, S Baretti, S Cattaldo, D Potenza, A Bernardi *Bioorganic & Medicinal Chemistry Letters* **2003**, *13*, 3831.

(14) H Ling, A Boodhoo, B Hazes, M D Cummings, G D Armstrong, J L Brunton, R J Raed *Biochemistry* **1998**, *37*, 1777.

(15) P I Kitov, J M Sadowska, G Mulvey, G D Armstrong, H Ling, N S Pannu, R J Read, D R Bundle *Nature* **2000**, *403*, 669.

(16) V Wittmann, R J Pieters *Chemical Society Reviews* **2013**, *42*, 4492.

(17) G L Mulvey, P Marcato, P I Kitov, J Sadowska, D R Bundle, G D Armstrong *The Journal of Infectious Diseases* **2003**, *187*, 640.

(18) K Nishikawa, K Matsuoka, E Kita, N Okabe, M Mizuguchi, K Hino, S Miyazawa, C Yamasaki, J Aoki, S Takashima, Y Yamakawa, M Nishijima, D Terunuma, H Kuzuhara, Y Natori *Proceedings of the National Academy of Sciences of the United States of America* **2002**, *99*, 7669.

(19) K Nishikawa, K Matsuoka, M Watanabe, K Igai, K Hino, K Hatano, A Yamada, N Abe, D Terunuma, H Kuzuhara, Y Natori *Journal of Infectious Diseases* **2005**, *191*, 2097.

(20) A Yamada, K Hatano, K Matsuoka, T Koyama, Y Esumi, H Koshino, K Hino, K Nishikawa, Y Natori, D Terunuma *Tetrahedron* **2006**, *62*, 5074.

(21) I R Nabi, J Shankar, J W Dennis *Journal of Cell Science* **2015**, *128*, 2213.

(22) I Iurisci, A Cumashi, A A Sherman, Y E Tsvetkov, N Tinari, E Piccolo, M D'Egidio, V Adamo, C Natoli, G A Rabinovich, S Iacobelli, N E Nifantiev *Anticancer Research* **2009**, *29*, 403.

(23) R D Cummings, F T Liu In *Essentials of Glycobiology*; 2 ed.; A Varki, R. D. C., J D Esko, H H Freeze, P Stanley, C R Bertozzi, G W Hart, M E Etzler, Ed.; Cold Spring Harbor Laboratory Press: 2009.

(24) H van Hattum, H M Branderhorst, E E Moret, U J Nilsson, H Leffler, R J Pieters *Journal of Medicinal Chemistry* **2013**, *56*, 1350.

(25) W Yao, M Xia, X Meng, Q Li, Z Li *Organic & Biomolecular Chemistry* **2014**, *12*, 8180.

(26) Matsushita, M *Journal of Innate Immunity* **2010**, *2*, 24.

(27) T Hummelshoj, N M Thielens, H O Madsen, G J Arlaud, R B Sim, P Garred *Molecular Immunology* **2007**, *44*, 401.

(28) V Garlatti, L Martin, M Lacroix, E Gout, G J Arlaud, N M Thielens, C Gaboriaud *Journal of Innate Immunity* **2010**, *2*, 17.

(29) M L Jensen, C Honore, T Hummelshoj, B E Hansen, H O Madsen, P Garred *Molecular Immunology* **2007**, *44*, 856.

(30) R M Zacho, L Jensen, R Terp, J C Jensenius, S Thiel *The Journal of Biological Chemistry* **2012**, *287*, 8071.

(31) R Sugimoto, Y Yae, M Akaiwa, S Kitajima, Y Shibata, H Sato, J Hirata, K Okochi, K Izuhara, N Hamasaki *The Journal of Biological Chemistry* **1998**, *273*, 20721.

(32) M Matsushita, Y Endo, S Taira, Y Sato, T Fujita, N Ichikawa, M Nakata, T Mizuochi *The Journal of Biological Chemistry* **1996**, *271*, 2448.

(33) N J Lynch, S Roscher, T Hartung, S Morath, M Matsushita, D N Maennal, M Kuraya, T Fujita, W J Schwaeble *Journal of Immunology* **2004**, *172*, 1198.

(34) Q Pan, H Chen, F Wang, V T Jeza, W Hou, Y Zhao, T Xiang, Y Zhu, Y Endo, T Fujita, X L Zhang *Journal of Innate Immunity* **2012**, *4*, 312.

(35) J Liu, M A M Ali, Y Shi, Y Zhao, F Luo, J Yu, T Xiang, J Tang, D Li, Q Hu, W Ho, X Zhang *Cellular and Molecular Immunology* **2009**, *6*, 235.

(36) S Bidula, H Kenawy, Y M Ali, D Sexton, W J Schwaeble, S Schelenz *Infection and Immunity* **2013**, *81*, 1730.

(37) A Verma, M White, V Vathipadiekal, S Tripathi, J Mbianda, M Ieong, L Qi, J K Taubenberger, K Takahashi, J C Jensenius, S Thiel, K L Hartshorn *The Journal of Immunology* **2012**, *189*, 2478.

(38) A Krarup, U B S Sorensen, M Matsushita, J C Jensenius, S Thiel *Infection and Immunity* **2005**, *73*, 1052.

(39) Y Liu, Y Endo, D Iwaki, M Nakata, M Matsushita, I Wada, K Inoue, M Munakata, T Fujita *The Journal of Immunology* **2005**, *175*, 3150.

(40) A L Favier, E Gout, O Reynard, O Ferraris, J P Kleman, V Volchkov, C Peyrefitte, N M Thielens *Journal of Virology* **2016**.

(41) S K Yang, X Shi, S Park, T Ha, S C Zimmerman *Nature Chemistry* **2013**, *5*, 692.

(42) S J Son, M A Brimble, S Yang, P W R Harris, T Reddingius, B W Muir, O E Hutt, L Waddington, J Guan, G P Savage *Australian Journal of Chemistry* **2013**, *66*, 23.

(43) S Cecioni, J P Praly, S E Matthews, M Wimmerova, A Imberty, S Vidal *Chemistry - A European Journal* **2012**, *18*, 6250.

(44) E Fan, Z Zhang, W E Minke, Z Hou, C L M J Verlinde, W G J Hol *Journal of the American Chemical Society* **2000**, *122*, 2663.

(45) K H Schlick, J R Morgan, J J Weiel, M S Kelsey, M J Cloninger *Bioorganic & Medicinal Chemistry Letters* **2011**, *21*, 5078.

(46) E A L Biessen, D M Beuting, H C P F Roelen, G A van de Marel, J H van Boom, T J C van Berkel *Journal of Medicinal Chemistry* **1995**, *38*, 1538.
(47) Y M Chabre, C Contino-Pepin, V Placide, T C Shiao, R Roy *Journal of Organic Chemistry* **2008**, *73*, 5602.
(48) X E Wells, V J Bender, C L Francis, H M He-Williams, M K Manthey, M J Moghaddam, W G Reilly, R G Whittaker *Drug Development Research* **1999**, *46*, 302.
(49) P R Ashton, E F Hounsell, N Jayaraman, T M Nilsen, N Spencer, J F Stoddart, M Young *Journal of Organic Chemistry* **1998**, *63*, 3429.
(50) Y M Chabre, D Giguere, B Blanchard, J Rodrigue, S Rocheleau, M Neault, S Rauthu, A Papadopoulos, A A Arnold, A Imberty, R Roy *Chemistry - A European Journal* **2011**, *17*, 6545.
(51) R Kikkeri, X Liu, A Adibekian, Y H Tsai, P H Seeberger *Chemical Communications (Cambridge, United Kingdom)* **2010**, *46*, 2197.
(52) R Kikkeri, I Garcia-Rubio, P H Seeberger *Chemical communications* **2009**, 235.
(53) G R Newkome, C Shreiner *Chemical Reviews (Washington, DC, United States)* **2010**, *110*, 6338.
(54) H C Kolb, M G Finn, K B Sharpless *Angewandte Chemie International Edition* **2001**, *40*, 2004.
(55) R Lallana, R Riguera, E Fernandez-Megia *Angewandte Chemie, International Edition* **2011**, *50*, 8794.
(56) P H Elchinger, P A Faugeras, B Boens, F Brouillette, D Montplaisir, R Zerrouki, R Lucas *Polymers (Basel, Switzerland)* **2011**, *3*, 1607.
(57) S W Millward, H D Agnew, B Lai, S S Lee, J Lim, A Nag, S Pitram, R Rohde, J R Heath *Integrative Biology* **2013**, *5*, 87.
(58) G Franc, A K Kakkar *Chemical Society Reviews* **2010**, *39*, 1536.
(59) H C Kolb, K B Sharpless *Drug Discovery Today* **2003**, *8*, 1128.
(60) F Himo, T Lovell, R Hilgraf, V V Rostovtsev, L Noodleman, K B Sharpless, V V Fokin *Journal of the American Chemical Society* **2005**, *127*, 210.
(61) N Berthet, B Thomas, I Bossu, E Dufour, E Gillion, J Garcia, N Spinelli, A Imberty, P Dumy, O Renaudet *Bioconjugate Chemistry* **2013**, *24*, 1598.
(62) K N Shetty, V L Latha, R N Rao, S K Nadimpalli, K Suguna *IUBMB Life* **2013**, *65*, 634.
(63) P Pan, W Ooi, K Sudesh, T Takarada, A Goto, M Maeda, M Fujita *Polymer* **2011**, *52*, 895.
(64) Z Chen, X Cai, Y Yang, G Wu, Y Liu, F Chen, X Li *Pharmaceutical Research* **2012**, *29*, 471.
(65) W Wang, C Jin, L Guo, Y Liu, Y Wan, X Wang, L Li, W Zhao, P G Wang *Chemical Communications (Cambridge, United Kingdom)* **2011**, *47*, 11240.
(66) B G Davis, A J Fairbanks *Carbohydrate Chemistry*; Oxford University Press, 2002.
(67) D H Leaback, P G Walker *Journal of the Chemical Society* **1957**, 4754.
(68) G J L Bernardes, R Kikkeri, M Maglinao, P Laurino, M Collot, S Y Hong, B Lepenies, P H Seeberger *Organic & Biomolecular Chemistry* **2010**, *8*, 4987.
(69) O Norberg, L Deng, T Aastrup, M Yan, O Ramstrom *Analytical Chemistry (Washington, DC, United States)* **2011**, *83*, 1000.

(70) C Hoebartner, P I Pradeepkumar, S K Silverman *Chemical Communications (Cambridge, United Kingdom)* **2007**, 2255.

(71) S M Paterson, J Clark, K A Stubbs, T V Chirila, M V Baker *Journal of Polymer Science, Part A: Polymer Chemistry* **2011**, *49*, 4312.

(72) R Liu, A Wei *Journal of Carbohydrate Chemistry* **2012**, *31*, 384.

(73) F Peri, P Dumy, M Mutter *Tetrahedron* **1998**, *54*, 12269.

(74) A Iqbal, H Chibli, C J Hamilton *Carbohydrate Research* **2013**, *377*, 1.

(75) J M Langenhan, M M Endo, J M Engle, L L Fukumoto, D R Rogalsky, L K Slevin, L R Fay, R W Lucker, J R Rohlfing, K R Smith, A E Tjaden, H M Werner *Carbohydrate Research* **2011**, *346*, 2663.

(76) R D Goff, J S Thorson *Medicinal Chemistry Communications* **2014**, *5*, 1036.

(77) Finlay, R M J, The Queen's University of Belfast, 2009.

(78) L Cipolla, F Peri *Mini-Reviews in Medicinal Chemistry* **2011**, *11*, 39.

(79) A K V Iyer, M Zhou, N Azad, H Elbaz, L Wang, D K Rogalsky, Y Rojanasakul, G A O'Doherty, J M Langenhan *ACS Medicinal Chemistry Letters* **2010**, *1*, 326.

(80) I Ohtsuka, Y Sadakane, M Higuchi, N Hada, J Hada, N Kakiuchi, A Sakushima *Bioorganic & Medicinal Chemistry* **2011**, *19*, 894.

(81) I Ohtsuka, Y Sadakane, M Higuchi, N Hada, T Atsumi, N Kakiuchi *Bioorganic & Medicinal Chemistry* **2014**, *22*, 3829.

(82) Y Liu, T Feizi, M A Campanero-Rhodes, R A Childs, Y Zhang, B Mulloy, P G Evans, H M I Osborn, D Otto, P R Crocker, W Chai *Chemistry & Biology* **2007**, *14*, 847.

(83) T K Styslinger, N Zhang, V S Bhatt, N Pettit, A F Palmer, P G Wang *Journal of the American Chemical Society* **2012**, *134*, 7507.

(84) T Mori, T Ohtsuka, Y Okahata *Langmuir* **2010**, *26*, 14118.

(85) M B Thygesen, J Sauer, K J Jensen *Chemistry - A European Journal* **2009**, *15*, 1649.

(86) A Streit, C T Yuen, R W Loveless, A M Lawson, J Finne, B Schmitz, T Feizi, C D Stern *Journal of Neurochemistry* **1996**, *66*, 834.

(87) H Attrill, A Imamura, R S Sharma, M Kiso, P R Crocker, D M F van Aalten *Journal of Biological Chemistry* **2006**, *281*, 32774.

(88) J Zhang, L V Ponomareva, K Marchillo, M Zhou, D R Andes, J S Thorson *Journal of Natural Products* **2013**, *76*, 1627.

(89) W Li, J Li, Y Wu, N Fuller, M A Markus *Journal of Organic Chemistry* **2010**, *75*, 1077.

(90) I Kosiova, O Simak, N Panova, M Budesinsky, M Petrova, D Rejman, R Liboska, O Pav, I Rosenberg *European Journal of Medicinal Chemistry* **2014**, *74*, 145.

(91) D Pappo, S Shimony, Y Kashman *Journal of Organic Chemistry* **2005**, *70*, 199.

(92) S Huang, J Qing, S Wang, H Wang, L Zhang, Y Tang *Organic & Biomolecular Chemistry* **2014**, *12*, 2344.

(93) M P Dwyer, K Paruch, C Alvarez, D J Doll, K Keertikar, J Duca, T O Fischmann, A Hruza, V Madison, E Lees, D Parry, W Seghezzi, N Sgambellone, F Shanahan, D Wiswell, T J Guzi *Bioorganic & Medicinal Chemistry Letters* **2007**, *17*, 6216.

(94) I Taniguchi, W A Kuhlman, A M Mayes, L G Griffith *Polymer International* **2006**, *55*, 1385.
(95) J G Ray, Z Zhang, C Szabo, J Siekmann, R Scheinecker, S Haider, H Rottensteiner, P Kosma In *PCT Int. Appl.*; Baxter International Inc., USA; Baxter Healthcare SA USA, 2013; Vol. WO 2013173557, p 235.
(96) F Peri, A Deutman, B La Ferla, F Nicotra *Chemical Communications* **2002**, 1504.
(97) J S Thorson, R W Gantt, P M J Peltier-Pain In *U.S. Pat. Appl. Publ.*; Wisconsin Alumni Research Foundation, USA USA, 2013, p 80.
(98) R W Gantt, P Peltier-Pain, W J Cournoyer, J S Thorson *Nature Chemical Biology* **2011**, *7*, 685.
(99) N Avlonitis, M Debunne, T Aslam, N McDonald, C Haslett, K Dhaliwal, M Bradley *Organic & Biomolecular Chemistry* **2013**, *11*, 4414.
(100) J d M Munoz, J Alcazar, A de la Hoz, A Diaz-Ortiz *Tetrahedron Letters* **2011**, *52*, 6058.
(101) R Willand-Charnley, T J Fisher, B M Johnson, P H Dussault *Organic Letters* **2012**, *14*, 2242.
(102) Y Iwama, K Okano, K Sugimoto, H Tokuyama *Chemistry - A European Journal* **2013**, *19*, 9325.
(103) L L Klein, M D Tufano *Tetrahedron Letters* **2013**, *54*, 1008.
(104) E A Shalamova, Y Lee, G Chung, A N Semakin, J Oh, A Y Sukhorukov, D E Arkhipov, S L Ioffe, S E Semenov *Tetrahedron Letters* **2014**, *55*, 1222.
(105) N Chandan, A L Thompson, M G Moloney *Organic & Biomolecular Chemistry* **2012**, *10*, 7863.
(106) A S Thompson, G R Humphrey, A M DeMarco, D J Mathre, E J J Grabowski *Journal of Organic Chemistry* **1993**, *58*, 5886.
(107) L Rokhum, G Bez *Journal of Chemical Sciences (Bangalore, India)* **2012**, *124*, 687.
(108) T C Bissot, R W Parry, D H Campbell *Journal of the American Chemical Society* **1957**, *79*, 796.
(109) Riley, C M *High Performance Liquid Chromatography*; 2 ed.; Blackie Academic & Professional: London, 1997.
(110) A Krezel, W Bal *Journal of Inorganic Biochemistry* **2004**, *98*, 161.
(111) Gutsche, C D *Calixarenes*; The Royal Society of Chemistry, 1989; Vol. 1.
(112) *Calixarenes 2001*; 1 ed.; Z Asfari, V Bohmer, J Harrowfield, J Vicens, Ed.; Kluwer Academic Publishers, 2001; Vol. 1.
(113) *Calixarenes in Action*; L Mandolini, R Ungaro, Ed.; Imperial College Press, 2000; Vol. 1.
(114) F Sansone, L Baldini, A Casnati, R Ungaro *New Journal of Chemistry* **2010**, *34*, 2715.
(115) L Baldini, F Sansone, A Casnati, F Ugozzoli, R Ungaro *Journal of Supramolecular Chemistry* **2002**, *2*, 219.
(116) D Arosio, M Fontanella, L Baldini, L Mauri, A Bernardi, A Casnati, F Sansone, R Ungaro *Journal of the American Chemical Society* **2005**, *127*, 3660.
(117) S Cecioni, R Lalor, B Blanchard, J P Praly, A Imberty, S E Matthews, S Vidal *Chemistry - A European Journal* **2009**, *15*, 13232.
(118) M Grare, M Mourer, J B Regnouf de Vains, C Finance, R E Duval *Pathologie Biologie* **2006**, *54*, 470.

(119) M Grare, M H Dibama, S Lafosse, A Ribon, M Mourer, J B Regnouf-de-Vains, C Finance, R E Duval *Clinical Microbiology and Infection* **2010**, *16*, 432.

(120) M Grare, M Mourer, S Fontanay, J B Regnouf-de-Vains, C Finance, R E Duval *Journal of Antimicrobial Chemotherapy* **2007**, *60*, 575.

(121) M B Patel, N R Modi, J P Raval, S K Menon *Organic & Biomolecular Chemistry* **2012**, *10*, 1785.

(122) C Geller, S Fontanay, M Mourer, H M Dibama, J B Regnouf-de-Vains, C Finance, R E Duval *Antiviral Research* **2010**, *88*, 343.

(123) Harris, S J 1995, p 149.

(124) H M Dibama, I Clarot, S Fontanay, A B Salem, M Mourer, C Finance, R E Duval, J B Regnouf de Vains *Bioorganic & Medicinal Chemistry Letters* **2009**, *19*, 2679.

(125) D V Titov, M L Gening, Yu E Tsvetkov, N E Nifantiev *Russian Chemical Bulletin, International Edition* **2013**, *62*, 577.

(126) A Dondoni, M Kleban, X Hu, A Marra, H D Banks *Journal of Organic Chemistry* **2002**, *67*, 4722.

(127) M Gingras, Y M Chabre, M Roy, R Roy *Chemical Society Reviews* **2013**, *42*, 4823.

(128) U Schaedel, F Sansone, A Casnati, R Ungaro *Tetrahedron* **2005**, *61*, 1149.

(129) A Dondoni, A Marra *Journal of Organic Chemistry* **2006**, *71*, 7546.

(130) F G Calvo-Flores, J Isac-Garcia, F Hernandez-Mateo, F Perez-Balderas, J A Calvo-Asin, E Sanchez-Vaquero, F Santoyo-Gonzalez *Organic Letters* **2000**, *2*, 2499.

(131) S P Bew, R A Brimage, N L'Hermite, S V Sharma *Organic Letters* **2007**, *9*, 3713.

(132) D Ponader, P Maffre, J Artez, D Pussak, N M Ninnemann, S Schmidt, P H Seeberger, C Rademacher, G U Nienhaus, L Hartmann *Journal of the American Chemical Society* **2014**, *136*, 2008.

(133) J Park, J H Lee, J Jaworski, S Shinkai, J H Jung *Inorganic Chemistry* **2014**, *53*, 7181.

(134) V Stastny, P Lhotak, V Michlova, I Stibor, J Sykora *Tetrahedron* **2002**, *58*, 7207.

(135) A Arduini, M Fabbi, M Mantovani, L Mirone, A Pochini, A Secchi, R Ungaro *Journal of Organic Chemistry* **1995**, *60*, 1454.

(136) Brimage, R A, Univeristy of East Anglia, 2006.

(137) W Xu, J J Vittal, R J Puddephatt *Canadian Journal of Chemistry* **1996**, *74*, 766.

(138) R K V Lim, Q Lin *Accounts of Chemical Research* **2011**, *44*, 828.

(139) W Song, Y Wang, J Qu, Q Lin *Journal of the American Chemical Society* **2008**, *130*, 9654.

(140) S Ito, Y Tanaka, A Kakehi, K Kondo *Bulletin of the Chemical Society of Japan* **1976**, *49*, 1920.

(141) R P Singh, H Gao, D T Meshri, J M Shreeve *Structure and Bonding (Berlin, Germany)* **2007**, *125*, 35.

(142) Z Fan, D Wang, J Huang, S Wang, D Guo, H Zhao, Y Li, Z Fang, X Ji, X Hua, R Fan In *Faming Zhuanli Shenqing* China, 2011.

(143) P B Mohite, V H Bhaskar *International Journal of PharmTech Research* **2011**, *3*, 1557.

(144) M M V Ramana, S C Nitesh, S V Rathod In *Indian Pat. Appl.* India, 2011.

(145) N H Toubro, A Holm *Journal of the American Chemical Society* **1980**, *102*, 2093.

(146) Scheiner, P; Mobil Oil Corp. : USA, 1970.

(147) K N Houk, J Sims, C R Watts, L J Luskus *Journal of the American Chemical Society* **1973**, *95*, 7301.

(148) C S Angadiyavar, M V George *Journal of Organic Chemistry* **1971**, *36*, 1589.

(149) Y Wang, W Song, W J Hu, Q Lin *Angewandte Chemie International Edition* **2009**, *48*, 5330.

(150) A P Luk'yanenko, E A Alekseeva, S S Basok, A V Mazepa, A I Gren *Russian Journal of Organic Chemistry* **2011**, *47*, 527.

(151) Y Takekawa, S Matsunaga, R W M von Soest, N Fusetani *Journal of Natural Products* **2006**, *69*, 1503.

(152) R D Goff, J S Thorson *Organic Letters* **2012**, *14*, 2454.

(153) F Peri, J Jimenez-Barbero, V Garcia-Aparicio, I Tvaroska, F Nicotra *Chemistry - A European Journal* **2004**, *10*, 1433.

(154) W Hueggenberg, A Seper, I M Oppel, G Dyker *European Journal of Organic Chemistry* **2010**, 6786.

(155) J Kang, H Chung, S Y Kim, Y Kim, J Lee, N E Lewin, L V Pearce, P M Blumberg, V E Marquez *Bioorganic & Medicinal Chemistry* **2003**, *11*, 2529.

(156) L M Artner, L Merkel, N Bohlke, F Beceren-Braun, C Weise, J Dernedde, N Budisa, C P R Hackenberger *Chemical Communications (Cambridge, United Kingdom)* **2012**, *48*, 522.

(157) A Sasaki, N Murahashi, H Yamada, A Morikawa *Biological and Pharmaceutical Bulletin* **1995**, *18*, 740.

(158) E V Sukhova, A V Dubrovskii, Y E Tsvetkov, N E Nifantiev *Russian Chemical Bulletin* **2007**, *56*, 1655.

(159) P Quagliotto, G Viscardi, C Barolo, D D'Angelo, E Barni, C Compari, E Duce, E Fisicaro *Journal of Organic Chemistry* **2005**, *70*, 9857.

(160) K M G O'Connell, M Diaz-Gavilan, W R J D Galloway, D R Spring *Beilstein Journal of Organic Chemistry* **2012**, *8*, 850.

(161) P S Sane, B V Tawade, D V Palaskar, S K Menon, P P Wadgaonkar *Reactive & Functional Polymers* **2012**, *72*, 713.

(162) Jacques Perronnet, Andre Teche; Offen., G., Ed.; Roussel-UCLAF: Germany, 1974, p 29.

(163) M Kawase, T Kitamura, Y Kikugawa *Journal of Organic Chemistry* **1989**, *54*, 3394.

(164) L U Khan, H F Brito, J Holsa, K R Pirota, D Muraca, M C F C Felinto, E E S Teotonio, O L Malta *Inorganic Chemistry* **2014**, *53*, 12902.

(165) S K Nayak, M K Choudhary *Tetrahedron Letters* **2012**, *53*, 141.

(166) J Schlueter, M Blazejak, L Hintermann *ChemCatChem* **2013**, *5*, 3309.

(167) J Lee, E Park, S Y Kang, Y Kong, J Lee, H J Kim, M E Jung, K Lee, J Kim, A N Pae, W Park; Green Cross Corporation, S. Korea 2011; Vol. WO 2011059207.

(168) K Okano, M Hashimoto, T Kodama, M Iwata, C Migihashi, D Tanaka; Dainippon Sumitomo Pharma Co., Ltd., Japan Japan, 2008.